Russian Academy of Science
Fersman Mineralogical Museum

Volume 39

New Data on Minerals

Founded in 1907

Moscow
Ocean Pictures Ltd.
2004

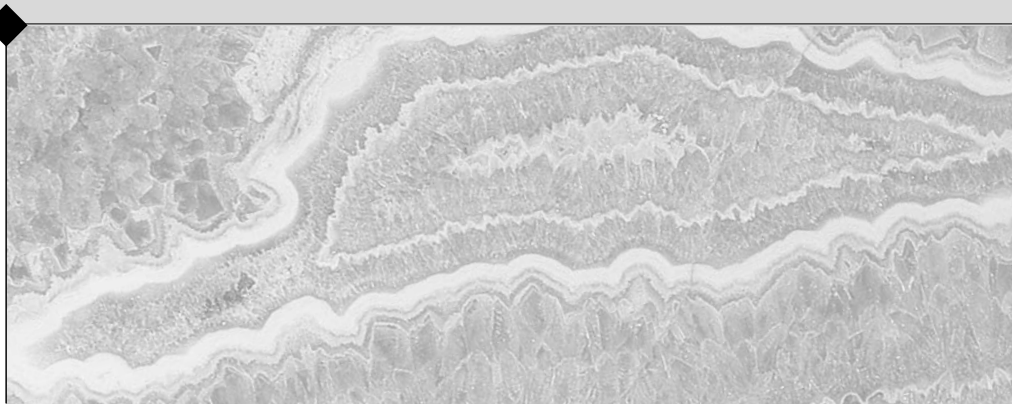

ISBN 5-900395-62-6
UDC 549

New Data on Minerals. Moscow.: Ocean Pictures, 2004. volume 39, 172 pages, 92 color images. Editor-in-Chief Margarita I. Novgorodova. Publication of Fersman Mineralogical Museum, Russian Academy of Science.

Articles of the volume give a new data on komarovite series minerals, jarandolite, kalsilite from Khibiny massif, presents a description of a new occurrence of nikelalumite, followed by articles on gemnetic mineralogy of lamprophyllite - barytolamprophyllite series minerals from Iuja-Vrite-malignite complex of burbankite group and mineral composition of rare-metal-uranium, berrillium with emerald deposits in Kuu granite massif of Central Kazakhstan.
Another group of article dwells on crystal chemistry and chemical properties of minerals: stacking disorder of zinc sulfide crystals from Black Smoker chimneys, silver forms in galena from Dalnegorsk, tetragonal $Cu_{21}S$ in recent hydrothermal ores of Mid-Atlantic Ridge, ontogeny of spiral-split pyrite crystals from Kursk magnetic Anomaly.
Museum collection section of the volume consist of articles devoted to Faberge lapidary and nephrite caved sculptures from Fersman Mineralogical Museum.
The volume is of interest for mineralogists, geochemists, geologists, and to museum curators, collectors and amateurs of minerals.

LIBRARY OF CONGRESS CATALOGING-IN PUBLICATION DATA

Authorized for printing by the Fersman Mineralogical Museum of the Russian Academy of Science

Published by:
Fersman Mineralogical Museum RAS
Bld. 18/2 Leninsky Prospekt,
Moscow, 117071, Russia
phone (7-095) 952-00-67;
fax (7-095) 952-48-50
e-mail: mineral@fmm.ru
web-site: www.fmm.ru

Ocean Pictures Ltd
4871 S. Dudley St., Littleton
CO 80123, USA
phone/fax (303) 904-2726
phone/fax (7-095) 203-3574
e-mail: minbooks@online.ru
web-site: www.minbook.com

Printed in Russia

CONTENTS

New Minerals and Their Varieeties: New Finds of Rare Minerals, Mineral Paragenesis

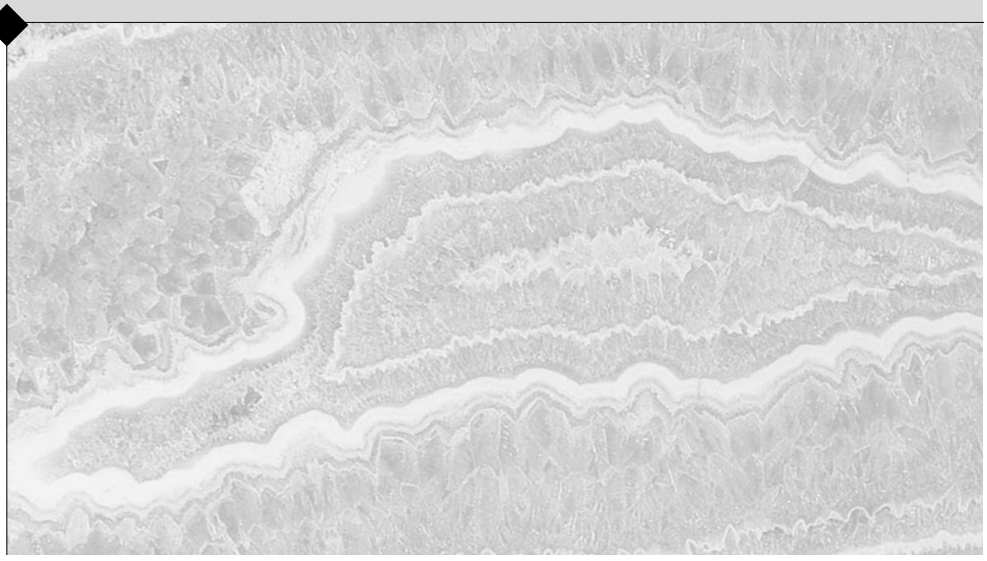

UDC 549.66

NEW DATA ON KOMAROVITE SERIES MINERALS

Igor V. Pekov
Geological Faculty, Lomonosov Moscow State University, Moscow mineral@geol.msu.ru

Yulia V. Azarova
Institute of Geology, Petrography, and Mineralogy of Ore Deposits, RAS, Moscow

Nikita V. Chukanov
Institute of Problems of Chemical Physics RAS, Chernogolovka, Moscow Oblast, chukanov@icp.ac.ru

The complex (electron microprobe, X-ray diffraction, IR-spectroscopy etc.) research was accomplished for representative collection of samples of komarovite series minerals, occurred in pseudomorphs after vuonnemite from Lovozero and Khibiny alkaline massifs (Kola Peninsula), representations about their cation composition are much extended. New and earlier published materials on these minerals are critically considered and generalized. In light of their strongly pronounced zeolite-like structure, the schemes of isomorphism and decationization are discussed. Ideal general formula for komarovite series members: $(Na,M)_{6-x}Ca(Nb,Ti)_6[Si_4O_{12}](O,OH)_{14}(F,OH)_2 \cdot nH_2O$ where M = Ca, Sr, Ba, K, Pb, REE, Th etc. In this series, it is propesed to distinguish two mineral species: **komarovite** (decationized, corresponds to original komarovite, with $x > 3$) and **natrokomarovite** (cation-saturated, with $x < 3$). Within the limits of the modern nomenclature the latter term is represented more correct than earlier used for this mineral name «Na-komarovite». Komarovite and natrokomarovite strongly differ in chemical composition but are close on X-ray powder diagrams and IR-spectra. In chemical relation, oxosilicates of the komarovite series occupies an intermediate position between oxides of the pyrochlore group and silicates of the labuntsovite group. That causes a place of natrokomarovite in general scheme of evolution of niobium mineralization in differentiates of alkaline complexes: it appears as an intermediate product at fluctuations of the activity of silica in pegmatitic-hydrothermal systems. Komarovite is a typical transformational mineral species formed by solid-state transformation (decationization, ion exchange, additional hydration) of natrokomarovite under late hydrothermal and probably in hypergene conditions.
3 tables, 2 figures, and 18 references

Komarovite series minerals occur in derivatives of agpaitic rocks from three high-alkali massifs: Lovozero and Khibiny at Kola Peninsula, and Ilimaussaq in South Greenland. Proper komarovite, hydrous niobosilicate of calcium and manganese, was characterized as a new mineral from Lovozero (Portnov *et al.*, 1971). Two years earlier E.I. Semenov (1969) has described a «white Nb-silicate» from Ilimaussaq, its proximity to komarovite was shown later (Krivokoneva *et al.*, 1979). This mineral differed from specimen from Lovozero by high content of sodium (Na >> Ca) was not voted by the IMA Commission on New Minerals and Mineral Names. Nevertheless it has come in a number of mineralogical handbooks (Gaines *et al.*, 1997; Mandarino, 1999) with the name «Na-komarovite» proposed by G.K. Krivokoneva with co-authors (1979). Insufficiently studied mineral from Khibiny described as M53 (Khomyakov, 1990) is very close to «Na-komarovite».

Already at the analysis of the first X-ray powder patterns the relationship of Greenland «white Nb-silicate» with pyrochlore has discovered, and the homological relations of these minerals were continued (Semenov, 1969). G.K. Krivokoneva with co-authors considered komarovite as a «silificated pyrochlore»: in opinion of these researchers, its crystal structure consists of oxide (pyrochlore) and silicate modules (Krivokoneva *et al.*, 1979). Fine-grained structure of aggregates, significant variations of the chemical composition, and presence of other mineral admixtures strongly complicate the study of komarovite and its high-sodic analogue. Because of that, until recently their major characteristics, not only crystal structure and correct formulae, but even the symmetry and unit cell parameters remained debatable.

The find of «Na-komarovite» single crystals in Ilimaussaq has allowed to T. Balic'-Zunic' with co-authors (2002) to solve its crystal structure, appearing unique. The assumptions of E.I. Semenov (1969) and G.K. Krivokoneva with co-authors (1979) have basically proved to be true: the pyrochlore type blocks connected by Si, O- groups underlie in a basis of komarovite structural type. The mineral is orthorhombic, space group *Cmmm*, unit cell parameters: $a = 7.310$, $b = 24.588$, $c = 7.402$ Å (Balic'-Zunic' *et al.*, 2002). We shall note, M. Dano obtained the same dimensions of the orthorhombic unit cell ($a = 7.411$, $b = 24.612$, $c = 7.318$ Å) for Greenland «white Nb-silicate» from the X-ray powder data (Semenov, 1969). Pyrochlore layers (blocks) are oriented in such a manner that axes *a* and *c* in komarovite are parallel directions <110> in pyrochlore; unit cell parameters

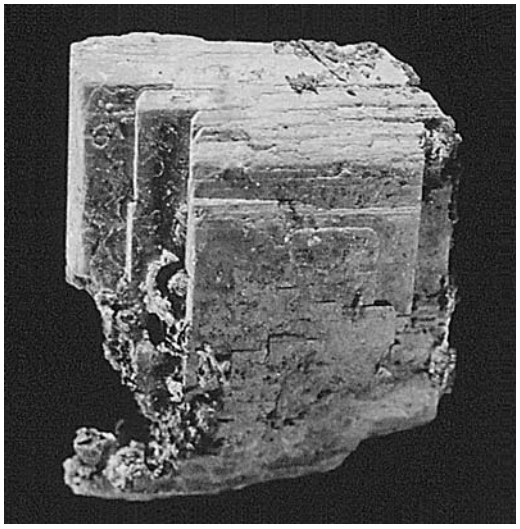

FIG. 1. Komarovite pseudomorph after cluster of vuonnemite crystals (specimen 2.5 x 2 cm) from the Komarovitovoe pegmatite, Kukisvumchorr Mt., Khibiny massif. A.S. Podlesnyi collection. Photo: N.A. Pekova

a and *c* of komarovite (7.3−7.4 Å) represent half of diagonals of pyrochlore cubic unit cell (~10.4 Å). Pyrochlore block is formed by (Nb,Ti)-octahedra and eight-vertex polyhedra of large cations (Na, Ca, etc.). F sites in crystal structures of pyrochlore and komarovite are analogous except that in the latter molecules of H_2O on the block surface replace the F atoms. In the crystal structure of komarovite the pyrochlore fragments are «interlaid» with isolated four-membered Si, O-rings, $[Si_4O_{12}]$ (of labuntsovite type), lying in the plane parallel (001). Between these rings and pyrochlore blocks, there are channels parallel [100], inside which additional Na atoms (in ten-vertex polyhedra) and H_2O molecules are localized (Balic'-Zunic' *et al.*, 2002). Thus, the structural type of komarovite has turned out to be the striking representative of the plesiotype family of oxysalts (Makovicky, 1997) with pyrochlore oxide modulus. The ideal formula for studied crystal is $Na_6CaNb_6Si_4O_{26}F_2{\cdot}4H_2O$, and general crystallochemical formula for minerals of komarovite type was proposed as $(Na,K)Na_{5+x-y}Ca_{1-2x+y}REE_xTi_yNb_{6-y}Si_4O_{26}F_2{\cdot}4H_2O$ (Balic'-Zunic' *et al.*, 2002). X-ray powder diagram of komarovite-like minerals is absolutely individual and allows making the undoubtful diagnostics of them. Thus, belonging of komarovite from Lovozero and A.P. Khomyakov's phase M53 to structural type of Greenland mineral is not raise doubts.

T. Balic'-Zunic' with co-authors (2002) has proposed to unite the minerals from Lovozero and Ilimaussaq under the general name *komarovite*, in spite of sufficient difference in their chemical composition. On the contrary, we are represented expedient to consider low-sodium and high-sodium phases as two different mineral species, the members of the solid solution series. Thus the original name **komarovite** should be kept for a low-sodium mineral, which was given by A.M. Portnov with co-authors (1971), and high-sodium mineral we propose to name as **natrokomarovite** (especially as the name «Na-komarovite» did not accept by the IMA CNMMN). The data obtained within the present work on samples from Lovozero and Khibiny allow essentially extending conception about cation composition and isomorphism in the komarovite series. Using both published and new materials, we have tried to show dependence of chemical composition of these minerals from formation conditions, and also the place of komarovite series members in general scheme of niobium mineralization evolution in derivatives of agpaitic complexes.

Occurrences

In Ilimaussaq, natrokomarovite («white Nb-silicate») was first found in hydrothermalites of naujaites from North Slope of Mt. Nakalaq, in pseudomorphs after epistolite plates, reached 5 x 3 x 1 sm in size, an also as independent segregations among analcime. It forms white fine-grained aggregates and usually occurs in close intergrowths with neptunite (Semenov, 1969). The second finding of natrokomarovite in Ilimaussaq provided a material for crystal structure study was made in albitite at Kvanefjeld plateau. Here it forms yellowish transparent crystals up to 0.4 x 0.04 x 0.02 mm in size, flattened on {010} and elongated on [100]. These crystals form segregations (probably pseudomorphs after vuonnemite) in aegirine-albite rock with neptunite, epistolite, analcime, tugtupite etc. (Balic'-Zunic' *et al.*, 2002).

In Lovozero massif, komarovite was found only in core of hydrothermally altered pegmatite № 61 (according to E.I. Semenov's numeration) at North Slope of Mt. Karnasurt where it occurs in significant amounts. It is included in polycomponent pseudomorphs after large (up to 10 cm in size) tabular crystals of vuonnemite. These pale-pink pseudomorphs usually located among natrolite are composed by fine-grained aggregates of komarovite, labuntsovite group minerals (mainly it is the members of organovaite and kuzmenkoite series), and strontiopyrochlore. Albite, microcline, ae-

girine, yofortierite, mangan-neptunite, leifite, epididymite, lorenzenite, catapleiite, elpidite, nontronite, oxides of Mn etc. are associated with them. Here there are perfectly shaped lamellae-pseudomorphs up to 3 x 2.5 cm in size, consist mainly of komarovite. Their shape does not give up doubts that vuonnemite was the protomineral (Portnov *et al.*, 1971; Pekov, 2000; Azarova *et al.*, 2002).

In Khibiny, both natrokomarovite and komarovite are determined. They are found in several hydrothermally altered pegmatites uncovered by underground minings of Kirovskii mine at Mt. Kukisvumchorr. For the first time natrokomarovite («phase M53») was found here as pale-pink rectangular lamellae up to 5 x 3 x 1 cm in size with strong vitreous lustre in selvages of natrolite veinlets (Khomyakov, 1990). The similar pseudomorphs with lilac to pink colour, reached to 16 cm across and to 4 cm thick were determined by us in axial natrolite zone of the «Belovitovoye» pegmatite. The largest their intergrowth consisting of five crystals of replaced vuonnemite has the sizes 25 x 12 cm. The main components of pseudomorphs are natrokomarovite and apatite forming fine-grained aggregates. Komarovite (the product of alteration of natrokomarovite), nenadkevichite and X-ray amorphous hydrous oxide of Nb and Ti, close to gerasimovskite, are present in subordinate amounts. Microcline, aegirine, lamprophyllite, gaidonnayite, belovite-(La), belovite-(Ce), neotocite, ancylite-(Ce), sulfides etc. are associated with these pseudomorphs. We have found proper komarovite in hydrothermal parageneses yet of two pegmatites, one of them was named «Komarovitovoye». Here pink, cream, brown-grey and dark-grey pseudomorphs (Fig. 1) after well-shaped tabular crystals of vuonnemite up to 7 cm in diameter grow on the wall of large cavity. They consist of fine-grained aggregates of komarovite, nenadkevichite, pyrochlore, and apatite; in association with them there are natrolite, calcite, fluorite, aegirine, magnesio-arfvedsonite, murmanite, lamprophyllite, eudialyte, lorenzenite, catapleiite, tsepinite-Na, tainiolite, sphalerite etc. In cavities of closely located small pegmatite, komarovite containing significant amounts of lead and titanium form pink fine-grained pseudomorphs after well-shaped crystals of vuonnemite associated with natrolite.

X-ray and IR-spectroscopic data

Pseudomorphs after vuonnemite containing komarovite series minerals from Lovozero

Table 1. X-ray powder data of komarovite series minerals

1		*2*		*3*		*4*		
I	*d, Å*	*I*	*d, Å*	*I*	*d, Å*	*I*	*d, Å*	*hkl*
90	12.364	73	12.3	100	12.36	100	12.15	020
75	7.034	25	7.00	14	7.00	8	6.97	110
75	6.359	30	6.30	25	6.35	4	6.37	021
20	6.170	10	6.15	12	6.17	19	6.04	040
90	5.464	30	5.43	13	5.45	8	5.41	130
5	5.104							111
30	4.739	15	4.75	10	4.73			041
75	3.278	20	3.26	6	3.28	37	3.204	112
100	3.174	100	3.170	24	3.16	5	3.175	042
100	3.149	40	3.128	10	3.13	5	3.106	240
5	3.079							080
25	3.066			8	3.063	8	3.057	132
10	2.895							241
20	2.841	17	2.840	8	2.840	5	2.810	081
75	2.749	25	2.748	11	2.751			062
75	2.732	25	2.718			4	2.715	260
60	2.604	20	2.589	4	2.592	4	2.586	202
5	2.563							261
5	2.547							222
10	2.461	3	2.456			3	2.429	0.10.0
5	2.408			4	2.389			172
5	2.354							280
5	2.337							330
5	2.197							262
5	2.139							1.11.0
10	2.115	7	2.110			2	2.068	063
5	2.097							351
5	2.052							0.12.0
5	2.042							2.10.0
5	2.019			3	2.010			223
30	1.986	17	1.983					282
5	1.977							332
30	1.852	9	1.850			2	1.842	004
30	1.829	8	1.825			2	1.816	400
5	1.810							420
75	1.788	45	1.783	5	1.786	8	1.781	2.10.2

Note:
1 — natrokomarovite, Ilimaussaq: Guinier camera, analyst M. Dano (Semenov, 1969); 2 — komarovite, Lovozero: diffractometer, analyst G.K. Krivokoneva (Portnov et al., 1971); 3-4 our data (diffractometer DRON UM-1, Cu Ka radiation, Ni filter, analyst V.G. Shlykov): 3 — komarovite, Lovozero; 4 — PbTi-variety of komarovite, Khibiny.
hkl indices are given on (Balic'-Zunic' *et al.*, 2002).

Table 2. Wavenumbers (cm^{-1}) of absorption bands in the IR-spectra of komarovite and natrokomarovite

Komarovite, Lovozero	*Natrokomarovite, Khibiny*	*Band assignment*
3380	3400	ν(O-H)
3240 sh	3265 sh	
1795 w		$\delta(H_3O)$
1720 w		
1637	Recovered	$\delta(H_2O)$
	by bands of	
	admixed phases	
	1593	Admixture
	1420 w	of organic matter?
	1353 w	
1136	1130 sh	ν(Si-O-Si)
1099	1090 sh	
1020 sh	1020 sh	ν(Si-O)
992		
939	940	
842	810	Mixed vibrations of
750	840	(Nb,Ti)Si-framework
658	650	ν(Nb,Ti-O)
585	580 sh	
543	540 sh	
	520	
439	445	δ(O-Si-O)
390 sh	385	

Note:
ν — stretching vibrations; ; δ — bending vibrations; sh — shoulder; w — weak line

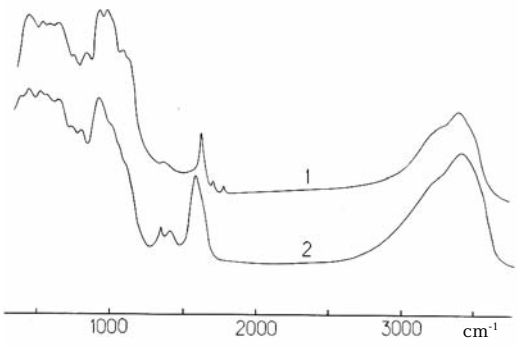

FIG. 2. The IR spectra of komarovite from Lovozero (1) and natrokomarovite from Khibiny

and Khibiny were studied in present work by electron microprobe analysis method, X-ray powder diffraction, IR-spectroscopy, optic and electron microscopy.

X-ray powder diffraction is a most effective method for precise determination of mineral belonging to komarovite series, including mixtures. As already was mentioned, these minerals have absolutely individual X-ray powder diagram (Table 1). As a main diagnostic feature it is possible to propose the pair of intensive reflections in small angle ($d > 3$ Å) region, with interplanar distances ~12.3 and ~5.45 Å. Other intensive reflections obtained in the X-ray powder diagrams of komarovite series members (regions ~7.0, 6.30 – 6.36, 3.12 – 3.17 Å) can overlap with strong reflexes of the labuntsovite group minerals which often compose pseudomorphs after vuonnemite together with komarovites (Azarova *et al.*, 2002; Chukanov *et al.*, 2003). Komarovite series members do not practically differ among each other on X-ray diagrams, the reason of that is discussed below.

The IR-spectroscopy as well as X-ray diffraction can be used as reliable method of identification of komarovite series members. The IR-spectra of these minerals (Fig. 2, Table 2) were obtained by spectrophotometer Specord 75 IR for powder samples pressed in KBr; the frequencies of bands were measured with accuracy ±1 cm^{-1} (standards: polystyrene and gaseous ammonia). The spectra of komarovite and natrokomarovite are close among each other. In contrast to majority of other cyclosilicates, these minerals are characterized by high coefficients of extinction in the range of wavenumbers 500 – 660 cm^{-1}, that is caused by the absorption of IR-radiation by pyrochlore-like blocks. The main difference of the IR-spectrum of natrokomarovite from Khibiny (№ 8 in Table 3) from the spectrum of komarovite from Lovozero is an absence of the strong band with maximum at 992 cm^{-1} in the first one that results in decrease of medium-weighted frequency of Si-O-stretching vibrations. More often this frequency decrease is caused by the reduction of degree of condensation of silica-oxide tetrahedra in the mineral structure (Chukanov, 1995). Moreover, the band of mixed vibrations of komarovite framework at 842 cm^{-1} is shifted up to 810 cm^{-1} in case of natrokomarovite. The frequencies of other bands on komarovite and natrokomarovite spectra are close, but differ in the intensities, that means similarity of structural motif, but also different character of spatial allocation of charge in frameworks of these minerals.

Komarovite and natrokomarovite both con-

Table 3. Chemical composition of komarovite series minerals

	1	*2*	*3*	*4*	*5*	*6*	*7*	*8*	*9*
					wt %				
Na_2O	12.26	13.71	0.85	0.84	0.67	0.76	12.2	6.32	0.15
K_2O	0.15		0.30	0.85	0.67	0.74	1.6	0.36	0.21
CaO	3.36	5.30	4.70	3.95	3.22	3.39	4.8	7.95	7.65
SrO				4.31	4.22	4.35	0.4	2.68	0.38
BaO				1.10	1.09	1.01	0.6	5.75	3.61
PbO				n.d.	n.d.	n.d.		bdl	12.03
MnO			5.00	0.30	0.69	0.11	0.1	0.83	1.09
REE_2O_3	1.68*	0.46		n.d.	n.d.	n.d.		bdl	bdl
Fe_2O_3	0.18**	0.48	1.50	0.24	1.04	0.49	0.1	0.13	0.71
Al_2O_3		1.38	1.00	1.20	1.83	1.33	0.2	0.14	bdl
SiO_2	17.50	16.46	23.50	15.68	15.93	16.71	18.7	15.01	15.54
ThO_2				n.d.	n.d.	n.d.		4.02	bdl
TiO_2	3.34	5.27	2.50	2.79	3.64	3.44	6.8	9.95	14.90
Nb_2O_5	53.98	50.23	47.00	47.32	50.72	52.94	46.1	33.39	26.91
Ta_2O_5				n.d.	n.d.	n.d.	0.4	bdl	bdl
H_2O	n.d.	4.64	12.00	n.d.	n.d.	n.d.	6.0	n.d.	n.d.
F	3.03	2.50	1.21	n.d.	n.d.	n.d.	2.0	n.d.	2.57
$-O=F_2$	-1.28	-1.05	-0.51				-0.8		-1.08
Total	94.20	99.38	99.05	78.58	83.72	85.27	99.2	86.53	84.67
					Formula calculated on Si + Al = 4				
Na	5.43	5.88	0.27	0.38	0.29	0.32	5.00	3.23	0.07
K	0.04		0.06	0.25	0.19	0.21	0.43	0.12	0.07
Ca	0.82	1.26	0.82	0.99	0.76	0.79	1.09	2.24	2.11
Sr				0.58	0.54	0.55	0.05	0.41	0.06
Ba				0.10	0.09	0.09	0.05	0.59	0.36
Pb									0.83
Mn			0.69	0.06	0.13	0.02	0.02	0.19	0.24
Fe	0.03	0.08	0.18	0.04	0.17	0.08	0.02	0.03	0.14
REE	0.14	0.04							
Al		0.36	0.19	0.33	0.48	0.34	0.05	0.04	
Si	4.00	3.64	3.81	3.67	3.52	3.66	3.95	3.96	4.00
Th								0.24	
Ti	0.57	0.88	0.30	0.49	0.61	0.57	1.08	1.97	2.88
Nb	5.58	5.02	3.44	5.01	5.07	5.24	4.40	3.98	3.13
Ta							0.02		
F	2.19	1.75	0.62				1.34		2.09
H_2O		3.42	6.49				4.23		
Σoct.	6.18	5.98	3.92	5.54	5.85	5.89	5.52	5.98	6.15
Σe.f.c.	6.43	7.18	1.84	2.36	2.00	1.98	6.64	7.02	3.74

Note:
1-2, 7-8 — natrokomarovite; 3-6, 9 — komarovite.
1 — Kvanefjeld, Ilimaussaq; 2 — Nakalaq, Ilimaussaq; 3-6 — Karnasurt, Lovozero; 7-9 — Kukisvumchorr, Khibiny.
References: 1 — Balic-Zunic *et al.,* 2002; 2 — Semenov, 1969; 3 — Portnov *et al.,* 1971; 7 — Khomyakov, 1990; 4,5,6,8,9 — our electron microprobe data (analysts N.N. Korotaeva and A.N. Nekrasov).
Σoct. — sum of octahedral cations: Nb + Ta + Ti + Fe; Σe.f.c. — sum of extra-framework cations: Na + K + Ca + Sr + Ba + Pb + Mn + REE + Th.
* — La_2O_3 0.57, Ce_2O_3 1.11 wt %; ** — recalculated from 0.16 FeO; n.d. — not detected; bdl — below detection limits

tain large amount of weakly connected water molecules, giving in the IR-spectra the strong wide bands at 3380 – 3400 cm^{-1}. Komarovite from Lovozero apparently contains also small amount of hydronium ions $(H_3O)^+$, about than it is possible to judge on presence of weak bands at 1795 and 1720 cm^{-1} in its IR-spectrum. In the range 1350 – 1593 cm^{-1} of the spectrum of natrokomarovite from Khibiny there are bands, which by their positions and intensities ratios, probably, are caused by mechanical admixture of organic matter.

Chemical composition

The study of samples from Lovozero and Khibiny by means of optic and electron microscopy has shown the mineral individuals of komarovite series as a rule are flattened and have submicrometer size. Usually the pseudomorphs after vuonnemite are heterogeneous, and grains of other minerals in them are comparable in size with particles of komarovite. That strongly complicates the obtaining of correct chemical data of our minerals, including electron microprobe method. During present work, more then twenty samples of pseudomorphs after vuonnemite from Lovozero and Khibiny, in which previously X-ray and IR-spectroscopic methods have obtained the significant contents of komarovite-like phases, were studied by microprobe instruments Camebax-MBX equipped by energy-dispersive spectrometer LINK AN 10000 and Camebax SX 50 (WDS method). Only some from more than fifty analyses were carried out from homogeneous (or nearly homogeneous) minerals of the komarovite series. The typical chemical compositions are presented in Table 3; the formulae, according to crystal structural data, were calculated on (Si + Al) = 4, the same method was used for calculation of earlier published analyses. The sum of octahedral cations (Nb,Ta,Ti,Fe) for correct analyses are close to 6 (the limits of fluctuations are from 5.5 to 6.2, Table 2). Only in the first chemical analysis of komarovite (№ 3 in Table 3), carried out by wet chemical method (Portnov *et al.*, 1971), the significant greater amount of strontium than in all other analyses and abnormally high contents of manganese and iron are observed. It is impossible to exclude that the sample was polluted, for example, by fine fibres of yofortierite, $(Mn,Fe)_5Si_8O_{20}(OH)_2 \cdot 8-9H_2O$, which is closely associated with komarovite.

Table 3 shows that both samples from Ilimaussaq are characterized by high content of sodium and contain admixtures of rare-earth elements, whereas some appreciable amounts of potassium, strontium, barium, and manganese are absent in them. The samples from Kola Peninsula usually contain much potassium, strontium, barium, and manganese, and in some cases also lead and thorium. In Lovozero only komarovite with $Na_2O < 1$ wt % was detected, and in Khibiny there are natrokomarovite (both typical high-sodian with 12.2% Na_2O and with slightly decreased content of sodium: 6.3% Na_2O) and komarovite (0.15% Na_2O). In all studied samples from Khibiny there is not enough aluminium. They are strongly enriched by titanium and depleted by niobium in comparison with samples from Lovozero and Ilimaussaq.

Discussion

Komarovite series minerals have complicated and variable chemical composition, especially in large cation part. As it is shown in the Table 3, they contain: Na_2O 0.1 – 13.7 wt%; K_2O 0.1 – 1.6%; CaO 3.2 – 8.0%; SrO 0.0 – 4.4%; BaO 0.0 – 5.8%; PbO 0 – 12%; REE_2O_3 0.0 – 1.7%; ThO_2 0 – 4%. At so wide isomorphism, their X-ray powder diagrams vary a little (Table 1). It is connected to that komarovite series minerals have pronounced zeolite-like structures and can be considered as niobosilicate analogues of zeolites with mixed framework formed by vertex-connected Si-tetrahedra and (Nb,Ti)-octahedra. That explains many peculiarities of chemical composition and properties of discussed minerals. In particular, total amount and ratios of large cations, and also degree of hydration do not practically influence values of interplanar distances. As well as in other zeolites, not only in aluminosilicate ones, but also in their rare-metal-bearing analogues with mixed tetrahedral-octahedral framework the unit cell parameters and, accordingly, the interplanar distances in komarovites significantly depend on composition of framework and slightly on variations in extra-framework sites. Probably the main factor determining unit cell parameters of komarovite is a value of Nb/Ti-ratio as well as for labuntsovite group minerals (Chukanov *et al.*, 2003). It is shown in Table 1 that X-ray diagrams of cation-saturated natrokomarovite form Greenland and strongly decationized komarovite from Lovozero are practically indistinguishable, whereas high-titanium komarovite from Khibiny (№ 8 in Table 3) have decreased values of majority of interplanar distances in spite of its enrichment by large out-of-framework atoms (Pb, Ba).

Isomorphism in komarovites is complicated; no doubts these replacements take place simultaneously on some schemes. T. Balic'-Zunic' with co-authors suggest the isomorphous scheme $Na^{+}Nb^{5+} \leftrightarrow Ca^{2+}Ti^{4+}$ with hypothetical end members with compositions: $Na_6CaNb_6Si_4O_{26}F_2{\cdot}4H_2O$ and $Ca_7Ti_6Si_4O_{26}F_2{\cdot}4H_2O$ (Balic'-Zunic' *et al.*, 2002). The increased content of calcium in most rich in titanium samples from Khibiny (№№ 8–9 in Table 3) can be evidence of that scheme is realized at some degree in nature. Our data show that isomorphism between niobium and titanium in komarovite series takes place in wide range and, probably, is continuous as well as in minerals of pyrochlore and labuntsovite groups. The charge balance can be achieved, for example, by typical for these groups way: $Nb^{5+} + O^{2-} \leftrightarrow Ti^{4+} + OH^{-}$.

The substitutions with participation of vacancies in extra-framework cation positions play very important role in komarovite series minerals. It is shown in Table 3 that the sum of large cations varies in widest limits: from 1.8 to 7.2 *atoms per formula units* (*apfu*). Most cation-saturated samples are characterized by highest content of sodium, whereas in significant vacant ones the role of divalent cations increases, i. e. the isomorphous scheme $2M^{+} \leftrightarrow M^{2+} + \square$ where M^{+} = Na, K; M^{2+} = Ca, Sr, Ba, Pb is realized. Location of significant part of O-atoms on bridge and «pendent» vertices of (Nb,Ti)-octahedra in pyrochlore module allows their protonization ($O^{2-} \rightarrow OH^{-}$) that permits to achieve yet greater degree of vacancity of extra-framework cation sites. That is assisted by substitution $F^{-} \rightarrow H_2O$, noted by T. Balic'-Zunic' with co-authors (2002). The IR-spectroscopic data (Fig. 2, Table 2) are shown that in komarovite from Lovozero there is small amount of hydronium $(H_3O)^{+}$. The content of large cations (Na, K, H_3O, Ca, Sr, Ba, Pb, REE, Th) in komarovites and pyrochlore group minerals are practically identical. Both are characterized by wide variations in ratios of these cations and in degree of vacancity of their sites. For komarovite series minerals, the majority of substitutions with participation of large cations takes place within the pyrochlore module. The presence of additional wide channels in places where between pyrochlore-like blocks there are «spreaders» in the form of $[Si_4O_{12}]$ rings strengthens zeolite character. The framework density of komarovite series minerals is 15.0–15.6 atoms per 1000 Å^3 that falls into interval of values for most broad-porous natural aluminosilicate zeolites.

Komarovite from Lovozero is the most strongly decationized member of the series; the sum of large (extra-framework) cations in it varies in limits 1.8–2.4 *apfu* (Table 3). As the same time, this mineral is not different from cation-saturated natrokomarovite by value of Nb/Ti-ratio. All data evidence that komarovite is a product of natrokomarovite alteration (leaching of sodium and additional hydration) and forms at late hydrothermal stages under alkalinity decrease. The similar phenomenon resulting in transition from some species to others is well known for many high-sodic minerals from hyperagpaitic assemblages, first of all for representatives of the lomonosovite group (lomonosovite → murmanite; vuonnemite → epistolite), the lovozerite group (zirsinalite → lovozerite; kazakovite → tisinalite; kapustinite → litvinskite), the keldyshite series (parakeldyshite → keldyshite) (Khomyakov, 1990; Pekov *et al.*, 2003). Significantly vacant members of the pyrochlore group, which was formed by leaching of sodium and calcium from full-cationic analogues, are also spread in nature. Products of successive stages of natrokomarovite alteration containing different amounts of sodium were observed by us in the «Belovitovoye» pegmatite at Mt. Kukisvumchorr (Khibiny). All that allows thing the process of decationization of natrokomarovite in water medium (under late hydrothermal and hypergene conditions) proceed easily.

Zeolite-like structure of komarovite series minerals permits the presence of strong ion exchange properties at them, similarly to the pyrochlore group members (Nechelyustov, Chistyakova, 1986). It is very probably that observed ratios of extra-framework cations in proper komarovite are achieved by natural ion exchange at late hydrothermal stages: replacement of Na^{+} by larger and/or high-valent cations (Ca, Sr, Ba, Pb, REE, Th, H_3O) easily realizes in reactions of this type. The example of high-lead komarovite from Khibiny is very bright. The saturation of this mineral by lead, freeing by dissolving of galena from pegmatite at late hydrothermal stage, can realize only after the leaching of sodium or simultaneously with it. As a whole, the content of large cations in komarovite reflects the geochemical speciality of latest stages of hydrothermal process: the samples from Lovozero are more enriched by strontium, and ones from Khibiny — by barium and calcium.

The independent crystallization of komarovite, zeolite-like mineral with strong cation deficiency, from solution is seemed extremely improbable. From the experimental data it is known (Barrer, 1985) that phases with such open-worked structures can arise only at par-

ticipation of large cations, which the framework forms around; the same cations neutralize its surplus negative charge (the theory of this phenomenon are discussed by N.V. Belov in his «Second Chapter of Silicate Crystal Chemistry», see for example: Belov, 1976). Thus, by A.P. Khomyakov's terminology, komarovite seems to be the typical transformational mineral species, i.e. incapable to heterogeneous origin, but forming only by solid-state transformation of the mineral-predecessor, full-cationic natrokomarovite. It fall into the same genetic group as murmanite, epistolite, lovozerite, tisinalite, litvinskite, keldyshite, kalipyrochlore, and a number of other minerals formed by decationization and hydration of corresponding proto-phases. That is the additional argument in favour of that komarovite and natrokomarovite are considered as different mineral species. The ideal general formula for komarovite series members can be write down as $(Na,M)_{6-x}Ca(Nb,Ti)_6[Si_4O_{12}](O,OH)_{14}(F,OH)_2 \cdot nH_2O$ where M = Ca, Sr, Ba, K, Pb, REE, Th etc. according to data of T. Balic'-Zunic' with co-authors (2002) and our results. The formal border between komarovite and natrokomarovite can be proposed on chemical composition with $x = 3$, taking in account «the rule 50%»: the series members with $x < 3$ will concern to natrokomarovite, and with $x > 3$, i. e. with prevalence of vacancies in sodium positions, to komarovite. The name *natrokomarovite* seems to be more correct than *Na-komarovite*, because the latter does not correspond the rules of modern nomenclature, according which the symbol of chemical element must not be stand as a prefix of mineral species name and be separate from it by hyphen (*Na-komarovite* is only such case: Mandarino, 1999).

Practically all finds of komarovite series minerals are made in pseudomorphs after vuonnemite, which is not accidentally. Niobium and titanium are ordered in the crystal structure of vuonnemite (Drozdov *et al.*, 1974; Ercit *et al.*, 1998) that caused the stable ratio Nb:Tic ≈ 2. This feature of the vuonnemite crystal structure allows to niobium to accumulate in hyperagpaitic pegmatites separating from close in properties, but significant more widespread titanium. Vuonnemite is an anhydrous hypersodic mineral crystallized in significant amounts at «dry» hyperagpaitic stage of pegmatite formation. At alkalinity decrease and water activity increase, it becomes unstable and easily replaced by numerous other niobium minerals, superseding each other depending of conditions. In general, they are immediate part of pseudomorphs after vuonnemite that is connected to low mobility of Nb^{5+} in relatively low-alkaline hydrothermal solutions (Azarova *et al.*, 2002). Natrokomarovite is one of these minerals. This is a zeolite-like hydrous phase, and it is represented the most probable to crystallize under temperatures not above 200 − 250°C. Thus, komarovite, being the product of decationization of natrokomarovite, must be yet more low-temperature; most likely, it can form under hypergene conditions.

The study of mineral relations in pseudomorphs after vuonnemite from Lovozero by means of electron microscope has shown that komarovite was formed after labuntsovite group minerals and, in its turn, replaced by strontiopyrochlore. On the contrary, in the samples from Khibiny there are late veinlets of nenadkevichite in pseudomorphs after vuonnemite consisting of natrokomarovite, Nb,Ti-oxides, and apatite (probably the latter inherits phosphorus from vuonnemite).

Komarovite series members are concerned to oxosilicates, been characterized by intermediate content of SiO_2 (15 − 19 wt %) between (Nb,Ti)-silicates of the labuntsovite group (35 − 45% SiO_2) and (Nb,Ti)-oxides (pyrochlore group minerals, gerasimovskite — not more than 3 − 5% SiO_2). The place of natrokomarovite in general scheme of the evolution of niobium mineralization in high-alkali pegmatitic-hydrothermal systems, most likely, are caused by following: it arises as an intermediate (and, to all appearances, relatively unstable) product under fluctuations of silica activity in hydrothermalites. The changing of niobium minerals takes place in accordance with the direction of evolution of solutions chemistry. At gradual decrease of activity of SiO_2 the following scheme is realized: niobium members of the labuntsovite group → natrokomarovite → komarovite → oxides (the members of the pyrochlore group, gerasimovskite) as well as under the increase of silica activity there is an inverse order: oxides → natrokomarovite → labuntsovite group minerals. It is not except that presence of silicon in many analyses of pyrochlore, including electron microprobe ones, was caused exactly by presence of komarovite-like fragments.

In conclusion we shall note that easiness of replacement of komarovite series members by minerals of labuntsovite and pyrochlore groups has also structural presuppositions. Natrokomarovite and komarovite contain prepared «construction elements» of these minerals, pyrochlore blocks and silica-oxide rings of labuntsovite type, i. e. the komarovite series is a original «intermediate unit» between pyroc-

hlore and labuntsovite groups not only in chemical but also in structural relation. That gives doubtless energetic advantage at corresponding reactions: in order to transform komarovite into pyrochlore or into labuntsovite-like mineral it is enough to «disassemble» its crystal construction not on «bricks» (atoms), but only on blocks. Perhaps the «decay» of natrokomarovite and komarovite on silicate and oxide minerals, labuntsovite-like mineral and pyrochlore, takes place in nature. The rarity of komarovite series members is most likely explained by easiness of such transformations.

The authors are grateful to A.S. Podlesnyi for providing of samples from Khibiny for study, and also to A.E. Zadov, N.N. Korotaeva, A.N. Nekrasov, V.G. Shlykov, and N.A. Pekova for the help in this work.

References

Azarova Yu.V., Pekov I.V., Chukanov N.V., Zadov A.E. Products and processes of alteration of vuonnemite under low-temperature transformations in hyperagpaitic pegmatites // Zapiski VMO. **2002.** № 5. P. 112–121. (Rus.)

Balic'-Zunic' T., Petersen O.V., Bernhardt H.-J. & Micheelsen H.I. The crystal structure and mineralogical description of a Na-dominant komarovite from the Ilimaussaq alkaline complex South Greenland // N. Jb. Miner. Mh. **2002.** № 11. P. 497–514.

Barrer R. Hydrothermal Chemistry of Zeolites. (Gidrotermal'naya Khimiya Tseolitov). Moscow, Mir. **1985.** 420 pp. (Rus.)

Belov N.V. Essays on Structural Mineralogy. (Ocherki po Strukturnoi Mineralogii). Moscow, Nedra. **1976.** 344 pp. (Rus.)

Chukanov N.V. IR-spectra of silicates and aluminosilicates // Zapiski VMO. **1995.** № 3. P. 80–85. (Rus.)

Chukanov N.V., Pekov I.V., Zadov A.E., Voloshin A.V., Subbotin V.V., Sorokhtina N.V., Rastsvetaeva R.K., Krivovichev S.V. Minerals of the Labuntsovite Group. (Mineraly Gruppy Labuntsovita). Moscow, Nauka. **2003.** 323 pp. (Rus.)

Drozdov Yu.N., Batalieva N.G., Voronkov A.A., Kuz'min E.A. Crystal structure of $Na_{11}Nb_2TiSi_4P_2O_{25}F$ // Dokl. Akad. Nauk SSSR. **1974.** V. 216. №1. P. 78–81. (Rus.)

Ercit T.S., Cooper M.A., Hawthorne F.C. The crystal structure of vuonnemite, $Na_{11}TiNb_2(Si_2O_7)_2(PO_4)_2O_3(F,OH)$, a phosphate — bearing sorosilicate of the lomonosovite group // Can. Miner. **1998.** Vol. 36. P. 1311–1320.

Gaines R.V., Skinner H.C.W., Foord E.E., Mason B., Rosenzweig A. Dana's New Mineralogy. 8th Ed. **1997.** John Wiley & Sons Inc., New York. 1819 pp.

Khomyakov A.P. Mineralogy of Hyperagpaitic Alkaline Rocks. (Mineralogiya Ultraagpaitovykh Shchelochnykh Porod). Moscow. 1990. 196 pp. (Rus.)

Krivokoneva G.K., Portnov A.V., Semenov E.I., Dubakina L.S. Komarovite: silificated pyrochlore // Dokl. Akad. Nauk SSSR. **1979.** V. 248. №2. P. 443–447. (Rus.)

Makovicky E. Modularity — different types and approaches // Modular Aspects of Minerals (ed. by S.Merlino). Eur. Miner. Union, Notes in Miner. Budapest. **1997.** P. 315–343.

Mandarino J.A. Fleischer's Glossary of Mineral Species. Tucson. **1999.** 225 pp.

Nechelyustov G.N., Chistyakova N.I. Ion exchange in natural samples of pyrochlore // Miner. Zhurnal. **1986.** V. 8. № 4. P. 57–64. (Rus.)

Pekov I.V. Lovozero Massif: History, Pegmatites, Minerals. Moscow, OP, **2000.** 480 pp.

Pekov I.V., Chukanov N.V., Yamnova N.A., Egorov-Tismenko Yu.K., Zadov A.E. A new mineral kapustinite, $Na_{5.5}Mn_{0.25}ZrSi_6O_{16}(OH)_2$, from Lovozero massif (Kola Peninsula) and new data on genetic crystallochemistry of the lovozerite group // Zapiski VMO. **2003.** № 6. P. 1–14. (Rus.)

Portnov A.M., Krivokoneva G.K., Stolyarova T.I. Komarovite, a new niobosilicate of calcium and manganese // Zapiski VMO. **1971.** № 5. P. 599–602. (Rus.)

Semenov E.I. Mineralogy of Ilimaussaq Alka-

UDC 549.657.42

ARAPOVITE, $(U,Th)(Ca,Na)_2(K_{1-x}\square_x)Si_8O_{20}\cdot H_2O$ — NEW MINERAL

Atali A. Agakhanov
Fersman Mineralogical Museum RAS, Moscow, atali@fmm.ru

Leonid A. Pautov
Fersman Mineralogical Museum RAS, Moscow, pla@fmm.ru

Yulia A. Uvarova
Geological Department, Manitoba University, Winnipeg, Canada

Elena V. Sokolova
Geological Department, Manitoba University, Winnipeg, Canada

Frank C. Hawthorne
Geological Department, Manitoba University, Winnipeg, Canada

Vladimir Yu. Karpenko
Fersman Mineralogical Museum RAS, Moscow

Vyacheslav D. Dusmatov
Fersman Mineralogical Museum RAS, Moscow

Eugenii I. Semenov
Fersman Mineralogical Museum RAS, Moscow

New mineral, uranium analogue of turkestanite, arapovite, was found among alkaline rocks of Dara-i-Pioz (Tajikistan). The mineral is represented by zonal areas 0.1-0.3 mm width in turkestanite crystals from polylithionite-aegirine-microcline rock. It is associated with stillwellite-(Ce), sogdianite, zektzerite, pyrochlore, hyalotekite, tazhikite group minerals, albite, and quartz. The mineral has dark-green color; it is transparent in the thin sections. The hardness is 5.5-6.0 on Mohs' scale, Dexp.= 3.43(2), Dcalc.=3.414 g/cm^3. The mineral is optically uniaxial, negative, no=1.615(2); ne=1.610(2). It is partially metamict. Crystal structure was studied by single-crystal method. The mineral is tetragonal, sp. gr. P4/mcc. Unit cell parameters are following: a=7.6506(4), c=14.9318(9)Å, V=873.9(1)Å^3, Z=2. Crystal structure refinement was made on annealed material by 528 independent reflexes with R1= 2.9%. Unit cell parameters of annealed mineral are following: a=7.5505(4), c= 14.7104(4)Å, V=838.6(1)Å. The main lines on powder X-ray diagram are [d, Å, (I, %), (hkl)]: 7.57 (14) (010), 7.39 (12) (002), 5.34(23) (100), 5.28 (38) (012), 3.37 (100) (120), 3.31 (58) (014), 2.640 (64) (024), 2.161(45) (224). Chemical composition (electron microprobe method, wt %, H_2O — Penfield method) is following: SiO_2 53.99, UO_2 16.63, ThO_2 10.57, Ce_2O_3 0.55, La_2O_3 0.14, Pr_2O_3 0.05, Nd_2O_3 0.62, Sm_2O_3 0.11, Eu_2O_3 0.14, Gd_2O_3 0.03, Dy_2O_3 0.13, PbO 0.82, CaO 8.11, Na_2O 2.54, K_2O 4.52, H_2O^+ 1.80, total 100.76. The empiric formula of arapovite is $(U_{0.55}Th_{0.36}Pb_{0.03}Ce_{0.03}Nd_{0.03}La_{0.01}Sm_{0.01}Eu_{0.01}Dy_{0.01})_{1.04}(Ca_{1.29}Na_{0.73})_{2.02}(K_{0.85}\ \square_{0.15})_{1.00}Si_8O_{20.06}\cdot 0.89H_2O$. The ideal formula is $(U,Th)(Ca,Na)_2(K_{1-x}\square_x)Si_8O_{20}\cdot H_2O$. The IR-spectrum is given. The mineral was named after Yu.A. Arapov, geologist, petrographer, worked at Turkestan-Alay Range.
3 tables, 3 figures, 7 references

In the alkaline rocks of Verkhnii Dara-i-Pioz massif (Tajikistan), silicates with twinned sixfold, fourfold, and recently discovered threefold silica-oxide rings are widespread. In 1965 the thorium mineral was described among representatives with fourfold rings under the name «alkali-enriched crystalline ekanite» (Ginzburg *et al.*, 1965), which was finished studying later and was named turkestanite (Pautov *et al.*, 1997). Moreover, in the rocks of this massif silicate with similar properties, with prevalence of uranium and thorium, containing large amount of water and described under the name «uranium hydrate variety of ekanite — UH-ekanite» (Semenov, Dusmatov, 1975) was found. One more uranium-thorium silicate similar to «UH-ekanite» but differed by significant small content of water and different amount of alkalis was found by authors during subsequent study of Dara-i-Pioz massif. The further study of the mineral allows distinguishing it as independent mineral species, uranium analogue of turkestanite. The mineral was named in honor of Yu.A. Arapov (1907—1988), famous geologist, participant of Pamirs-Tajik expedition firstly noted green thorium silicate on Dara-i-Pioz, author of numerous works on geochemistry, mineralogy, petrography of Middle Asia.

Occurrence and mineral assemblage

Arapovite was found during study of alkaline rocks of Verkhnii Dara-i-Pioz massif, which were collected by authors (L.A. Pautov, A.A. Agakhanov, V.Yu. Karpenko) together with P.V. Khvorov in the moraine of Dara-i-Pioz

[1]It was considered by the RMS KNMMN and approved by the IMA KNMMN on November 3, 2003

glacier (Garm Region, Tajikistan).

The mineralogy of the massif was considered in a number of publications (Dusmatov, 1968, 1971, etc.). Arapovite was found in the samples of rock composed mainly by microcline with subordinate amount of aegirine, polylithionite, bad-shaped crystals of stillwellite and turkestanite, small segregations of sogdianite and zektzerite replaced it. Rarely pyrochlore, hyalotekite, tazhikite group minerals, albite, and quartz were noted in this rock.

Arapovite was found in the form of small (0.1−0.3 mm) zones in large (up to 1 cm) bad-shaped crystals of turkestanite. Arapovite is spread both in central, and in edge zones of the crystals.

Physical properties

Arapovite has dark-green color; it is transparent in thin sections. In contrast to turkestanite arapovite has more deep green color connected to larger content of uranium. The luster is vitreous, pitchy. The cleavage and jointing are absent. The fracture is conchoidal. The hardness is 5.5−6 on Mohs' scale. Micro-indentation, VHN = 707 kgs/mm^2 (average value by 12 measurements with fluctuation of single measure from 682 to 766 kgs/mm^2) at load 100 g. The micro-indentation was measured by PMT-3 instrument calibrated on NaCl. The density of the mineral was determined by balancing of mineral grains in Clerichi solution; it is equal 3.43(2) g/cm^3. Arapovite is optically uniaxial, negative. Refractive indexes were measured by central screening method on rotated needle: n_o =1.615(2); n_e = 1.610(2) (λ = 589 nm). The IR-spectrum of the mineral (Fig. 1) obtained by Specord-75IR (the sample was suspension on KBr base) has the following absorption bands: 3460, 1091 (shoulder), 1043, 797, 778, 590, 491 cm^{-1}; it is close to the IR-spectrum of turkestanite.

X-ray data

X-ray powder diagram of arapovite obtained by photomethod has small amount of diffusive lines (Tabl. 1) that is evidence of partially metamict state of the mineral. The following parameters of tetragonal unit cell were obtained by single-crystal study: a=7.6506(4), c= 14.9318(9)Å, V=873.9(1)Å^3, sp. gr. P4/*mcc, Z=2.* The mineral was annealed at 900°C during 3 hours in argon current for obtaining more detail X-ray powder diagram; after that the mineral gave clear X-ray diffractogram containing a lot of lines (Tabl. 1). X-ray powder diagram of arapovite is very close to data of turkestanite and steacyite by set of lines and their intensities.

The refinement of arapovite crystal structure was made on annealed material because of its partial metamict properties. The unit cell parameters of annealed mineral were decreased slightly; they are following: a= 7.5505(4), c= 14.7104(4)Å, V=838.6(1)Å^3. The study was made with single-crystal diffractometer Bruker P4 (MoKα radiation, CCD detector). The crystal structure was refined with R_1= 2.9% by 528 independent reflexes [$F_o > 4\sigma F_0$]. In the crystal structure of arapovite there is one tetrahedral site occupied entirely by Si with distance <Si−O> = 1.617 Å. Also there are two [8]-coordinated sites, A and B, occupied by

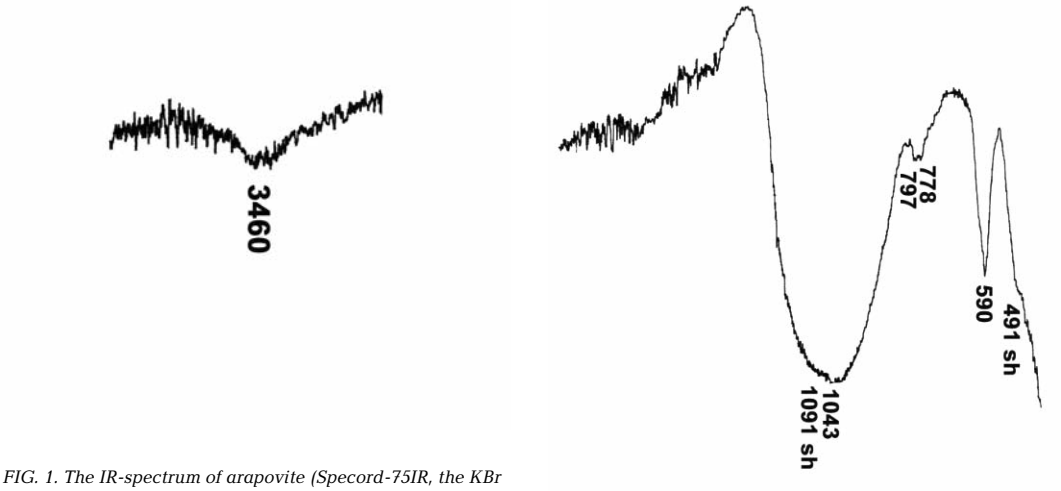

FIG. 1. The IR-spectrum of arapovite (Specord-75IR, the KBr tablet with mineral). Analyst Atali A. Agakhanov

Table 1. X-ray powder data of arapovite

1		2				
$I_{exp.}$	$d_{exp.}$	$I_{exp.}$	$d_{exp.}$	$I_{calc.}$	$d_{calc.}$	*hkl*
7	7.76	14	7.57	33	7.551	0 1 0
		12	7.39	58	7.355	0 0 2
8	5.40	23	5.34	26	5.339	1 0 0
		38	5.28	67	5.269	0 1 2
		3	4.33	10	4.321	1 1 2
10	3.41	100	3.37	100	3.372	1 2 0
8	3.37	58	3.31	80	3.306	0 1 4
3	3.10	9	3.07	15	3.069	1 2 2
		8	3.03	8	3.029	1 1 4
		15	2.672	16	2.670	2 2 0
9	2.67	64	2.640	55	2.634	0 2 4
2	2.56	21	2.515	18	2.517	0 3 0
1	2.52	15	2.493	13	2.487	1 2 4
		4	2.391	5	2.388	1 3 0
		1	2.334	3	2.332	0 1 6
		1	2.227	1	2.228	1 1 6
2	2.189	45	2.161	34	2.160	2 2 4
		11	2.080	10	2.077	2 3 1
		6	2.063	8	2.056	0 2 6
1	2.02	29	2.016	23	2.014	2 3 2
1	2.00	14	1.989	17	1.984	1 2 4
		8	1.888	13	1.888	0 4 0
		5	1.841	12	1.838	0 0 8
1	1.829	21	1.821	20	1.820	2 3 4
		11	1.808	13	1.806	2 2 6
		6	1.781	8	1.7770	1 4 2
		7	1.761	8	1.756	0 3 6
		16	1.689	11	1.688	2 4 0
1	1.647	30	1.644	19	1.646	2 4 2
		18	1.618	13	1.615	1 2 8
		4	1.537	14	1.534	2 4 4
		11	1.514	4	1.514	2 2 8
		7	1.483	14	1.485	0 3 8
		2	1.443	8	1.444	0 1 10
				6	1.440	3 3 6
		12	1.400	5	1.402	2 5 0
				3	1.397	0 5 4
		7	1.373	2	1.371	0 2 10

Note:
1 — non-annealed arapovite. URS-50IM, FeKa, Mn filter, RKD 57.3 camera, the lines on the debayegram are diffusive; 2 — annealed arapovite, diffractometer DRON-4, CuKa, the counter speed is 1 grad/min, graphite monochromator, quartz was the inner standard. Analyst A.A. Agakhanov

(U,Th) and (Ca,Na) with distances $<A-O> = 2.403$ Å and $<B-O> = 2.489$ Å. Moreover, in the crystal structure of arapovite there is [12]-coordinated C-site occupied partially by potassium with distance $<C-O> = 3.103$Å. In the crystal structure of arapovite SiO_4 tetrahedra form twinned fourfold rings $[Si_8O_{20}]^{8-}$. The [8]-coordinated A- and B-polyhedra with mutual edges form the layers (001). These layers are joined in framework by $[Si_8O_{20}]$ groups (Fig. 3). The C atoms are located in the large holes of the framework. The topology of arapovite crystal structure is identical to that of turkestanite, $Th(Ca,Na)_2(K_{1-x}\square_x)Si_8O_{20}\cdot nH_2O$ (Kabalov *et al.*, 1988) and steacyite, $Th(Na,Ca)_2(K_{1-x}\square_x)Si_8O_{20}$ (Richard and Perrault, 1972).

Chemical composition

The chemical composition of arapovite was performed by electron microprobe instrument JCXA-50A (JEOL) equipped by energy-dispersive spectrometer under accelerating voltage 20 kV and electron microprobe current 3 nA. The standards were following: microcline USNM143966 (Si, K), synthetic UO_2 (U), synthetic ThO_2 (Th), $LaPO_4$ (La), $CePO_4$ (Ce), NdP_5O_{14} (Nd), PrP_5O_{14} (Pr), SmP_5O_{14} (Sm), EuP_5O_{14} (Eu), $GdPO_4$ (Gd), Dy_2O (Dy), crocoite (Pb), anorthite USNM137041 (Ca), omphacite USNM110607 (Na). The concentrations were calculated with use of ZAF-correction. Six mineral grains were analyzed (Fig. 2). The water was determined by Penfield method from micro-weight (20 mg). The results of analyses are in the Tabl. 2. The empiric formula of arapovite calculated on 8 atoms of Si by analyses results is following: $(U_{0.55}Th_{0.36}Pb_{0.03}Ce_{0.03}Nd_{0.03}La_{0.01}Sm_{0.01}Eu_{0.01}Dy_{0.01})_{1.04}(Ca_{1.29}Na_{0.73})_{2.02}(K_{0.85}\square_{0.15})_{1.00}Si_8O_{20.06}\cdot 0.89H_2O$. The ideal formula of arapovite is: $(U,Th)(Ca,Na)_2(K_{1-x}\square_x)Si_8O_{20}\cdot H_2O$. The coincidence index is $(1-K_p/K_c) = 0.031$ (excellent).

Comparison with similar minerals

Arapovite, $(U,Th)(Ca,Na)_2(K_{1-x}\square_x)Si_8O_{20}\cdot H_2O$, is U^{4+}-analogue of turkestanite, $Th(Ca,Na)_2(K_{1-x}\square_x)Si_8O_{20}\cdot nH_2O$, and U^{4+}-Ca-analoge of steacyite, $Th(Na,Ca)_2(K_{1-x}\square_x)Si_8O_{20}$ (Tabl. 3). There is the continual isomorphous series between arapovite and turkestanite. Apparently, the presence of isomorphous series between arapovite, steacyite, and iraqite is possible, however, the intermediate phases weren't found in these series. The existence of arapovite as phase where C-site occupied predominantly by potassium is caused (according to valence balance) by that A-site of 4-valent cations is also occupied by some amount of

Table 2. Chemical composition of arapovite and «uranium hydrate ekanite (UH-ekanite)»

	*Arapovite**							*«UH-ekanite»***
	1	*2*	*3*	*4*	*5*	*6*	*average*	
SiO_2	54.25	53.62	54.27	53.86	54.10	53.86	53.99	48.00
UO_2	20.49	14.64	17.33	16.66	16.31	14.37	16.63	22.80
ThO_2	4.98	14.26	9.46	9.36	13.40	11.99	10.57	5.50
Ce_2O_3	0.71	0.19	0.56	0.80	0.22	0.83	0.55	
La_2O_3	0.20	0.10	0.14	0.13	0.06	0.18	0.14	
Pr_2O_3	0.00	0.13	0.19	0.00	0.00	0.00	0.05	
Nd_2O_3	0.76	0.45	0.92	0.73	0.32	0.55	0.62	
Sm_2O_3	0.19	0.05	0.23	0.05	0.12	0.01	0.11	
Eu_2O_3	0.47	0.06	0.00	0.28	0.00	0.00	0.14	
Gd_2O_3	0.03	0.00	0.00	0.14	0.00	0.00	0.03	
Dy_2O_3	0.13	0.29	0.35	0.00	0.01	0.02	0.13	
PbO	0.72	0.70	0.70	0.78	1.04	0.98	0.82	
CaO	8.48	8.11	8.45	8.09	7.31	8.21	8.11	8.24
Na_2O	2.29	2.24	2.52	3.24	2.49	2.47	2.54	0.70
K_2O	4.87	4.30	4.66	4.28	4.56	4.43	4.52	1.50
H_2O^+	1.80	1.80	1.80	1.80	1.80	1.80	1.80	13.76
Total	100.38	100.95	101.57	100.20	101.74	99.70	100.76	100.50
Formula calculated on Si = 8								
Si^{+4}	8.00	8.00	8.00	8.00	8.00	8.00	8.00	8.00
U^{+4}	0.67	0.49	0.57	0.55	0.54	0.47	0.55	0.85
Th^{+4}	0.17	0.48	0.32	0.32	0.45	0.41	0.36	0.21
Ce^{+3}	0.04	0.01	0.03	0.04	0.01	0.05	0.03	
La^{+3}	0.01	0.01	0.01	0.01	0.00	0.01	0.01	
Pr^{+3}	0.00	0.00	0.01	0.00	0.00	0.00	0.00	
Nd^{+3}	0.04	0.02	0.05	0.04	0.02	0.03	0.03	
Sm^{+3}	0.01	0.00	0.01	0.00	0.01	0.00	0.01	
Eu^{+3}	0.02	0.00	0.00	0.01	0.00	0.00	0.01	
Gd^{+3}	0.00	0.00	0.00	0.01	0.00	0.00	0.00	
Dy^{+3}	0.01	0.01	0.02	0.00	0.00	0.00	0.01	
Pb^{+2}	0.03	0.03	0.03	0.03	0.04	0.04	0.03	
Ca^{+2}	1.34	1.30	1.33	1.29	1.16	1.31	1.29	1.47
Na^{+1}	0.66	0.65	0.72	0.93	0.71	0.71	0.73	0.23
K^{+1}	0.92	0.82	0.88	0.81	0.86	0.84	0.85	0.32
H^{+1}	1.77	1.79	1.77	1.78	1.78	1.78	1.78	15.30
O^{-2}	20.65	21.00	21.01	20.99	20.91	20.90	20.95	27.50

Note:

* — electron microprobe analyses. H_2O — Penfield method (analysts A.A. Agakhanov, V.Yu. Karpenko).

** — wet chemistry method. Analyst A.V. Bykova (the total 99.50 was given in the original) (Semenov, Dusmatov, 1975).

Table 3. Comparative description of arapovite, turkestanite, steacyite

	Arapovite	*Turkestanite*	*Steacyite*
Chemical formula	$(U,Th)(Ca,Na)_2(K_{1-x}\square_x)Si_8O_{20}\cdot H_2O$	$Th(Ca,Na_2(K_{1-x}\square_x)\ Si_8O_{20}\cdot nH_2O$	$Th(Na,Ca)_2(K_{1-x}\square_x)Si_8O_{20}$
Space group	*P4/mcc*	*P4/mcc*	*P4/mcc*
a, Å	7.65	7.59	7.58
c, Å	14.93	14.82	14.77
Z	2	2	2
The strong lines of X-ray powder diagram: $d_{exp.}(I)$	7.57(14) 7.39(12) 5.34(23) 5.28(38) 3.37(100) 3.31(58) 2.6(64) 2.161(45)	7.59(23) 7.40(20) 5.36(40) 5.31(70) 3.40(100) 3.34(65) 2.65(59) 2.175(25)	7.60(14) 7.42(11) 5.37(15) 5.3(45) 3.38(100) 3.32(55) 2.64(41) 2.00(26)
Density, g/cm^3	3.43	3.36	302
Optic characteristics	uniaxial (-)	uniaxial (-)	uniaxial (-)
n_o	1.615	1.611	1.573
n_e	1.610	1.606	1.572

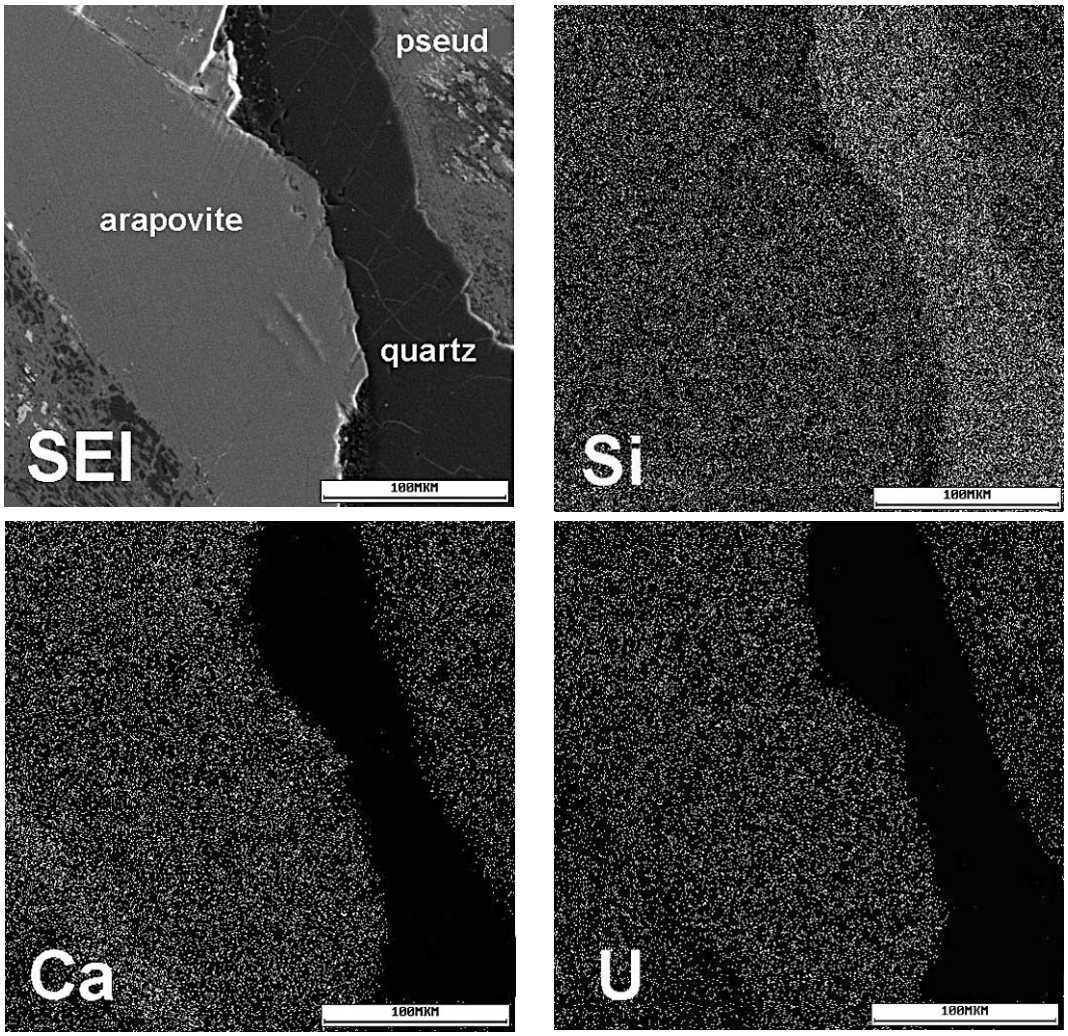

FIG. 2. The intergrowth of arapovite with quartz and the pseudomorph after arapovite. The image in SEI regime and in X-ray characteristic radiation of mentioned elements

UDC 549.657.42

ZERAVSHANITE, $Cs_4Na_2Zr_3(Si_{18}O_{45})(H_2O)_2$, NEW CESIUM MINERAL FROM DARA–I–PIOZ MASSIF (TAJIKISTAN)

Leonid A. Pautov
Fersman Mineralogical Museum RAS, Moscow, pla@fmm.ru

Atali A. Agakhanov
Fersman Mineralogical Museum RAS, Moscow, atali@fmm.ru

Yulia A. Uvarova
Geological Department, Manitoba University, Winnipeg, Canada

Elena V. Sokolova
Geological Department, Manitoba University, Winnipeg, Canada

Frank C. Hawthorne
Geological Department, Manitoba University, Winnipeg, Canada

New cesium mineral zeravshanite with formula $Cs_4Na_2Zr_3(Si_{18}O_{45})(H_2O)_2$ (monoclinic system, sp. group *C2/c*, $a = 26{,}3511(8)$Å, $b = 7.5464(3)$ Å, $c = 22.9769(8)$Å, $\beta = 107.237(1)°$, $V = 4363.9(4)$Å^3, $Z = 4$) was found in the moraine of Dara-i-Pioz glacier located at the joint of Zeravshan, Turkestan and Alay Ranges (Tajikistan). The mineral was named after *type locality*. Zeravshanite forms of grains (from 0.02 up to 0.2 mm in size) in the quartz rock with aegirine, polylithionite, pectolite, reedmergnerite, sogdianite, leucosphenite, stillwellite-(Ce), microcline, baratovite, fluorite, galena, turkestanite, minerals of tazhikite and eudialyte groups, neptunite, pekovite, cesium analogue of polylithionite etc. Zeravshanite is colorless, transparent. Hardness is 6 on Mohs' scale. Micro-indentation, VHN = 838 kgs/mm^2. Density is 3.09(5) (exp.), 3.17 (calc.) g/cm^3. Zeravshanite is biaxial, optical negative. 2V (calc.) = — 63°. Optic angle dispersion is medium, v>r. $n_p = 1.582(2)$, $n_m = 1.598(2)$, $n_g = 1.603(2)$. The IR-spectrum (strong absorption bands) is following: 1089, 1045, 978, 709, 662, 585, 538 cm^{-1}. The chemical composition (wt %, average on 6 electron microprobe analyses) is: SiO_2 — 52.20, TiO_2 — 0.43, ZrO_2 — 16.41, SnO_2 — 0.46, Fe_2O_3 — 0.21, Na_2O — 3.06, K_2O — 0.09, Cs_2O — 26.58, H_2O (calc.) — 1.74, total — 101.18. The strong lines of X-ray powder diagram are following (d, I): 6.32(5); 3.65(5); 3.35(10); 3.25(4); 2.82(5); 2.62(7); 1.946(4); 1.891(4); 1.865(4). Crystal structure is determined with R = 2.8%. The sample with new mineral is kept in the Fersman Mineralogical Museum RAS (Moscow, Russia). 2 tables, 4 figures, 4 references

New cesium mineral with formula $Cs_4Na_2Zr_3(Si_{18}O_{45})(H_2O)_2$ (monoclinic system, sp. group *C2/c*, $a = 26{,}3511(8)$ Å, $b = 7.5464(3)$ Å, $c = 22.9769(8)$Å, $\beta = 107.237(1)°$, $V = 4363.9(4)$Å^3, $Z = 4$) was found in the moraine of Dara-i-Pioz glacier located at the joint of Zeravshan, Turkestan and Alay Ranges (Tajikistan) in essentially quartz rock with polylithionite, pectolite, reedmergnerite, aegirine, leucosphenite etc. The mineral was named zeravshanite* after *type locality*.

Locality and mineral assemblage

Zeravshanite was found during studying of rock samples from Verkhnii Dara-i-Pioz massif collected by L.A. Pautov and A.A. Agakhanov together with V.Yu. Karpenko and P.V. Khvorov at the moraine of Dara-i-Pioz glacier (Harm Region, Tajikistan). Dara-i-Pioz massif is located at the upper coarse of the same name river (left tributary of Yarkhych River), and glaciers cover significant area of the massif. The uncovered parts of massif are difficult of access, because of that the most part of mineralogical and petrographical observations were made on rock blocks in moraine material of Dara-i-Pioz glacier. Geology and mineralogy of the massif were considered in a number of publications (Dusmatov, 1968, 1971, Belakovskiy, 1991, etc.). The bright mineralogical peculiarity of Dara-i-Pioz alkaline massif is the presence of proper minerals of cesium in it. These are cesium kupletskite, telyushenkoite discovered at Dara-i-Pioz, and now zeravshanite. Apparently, the list of cesium minerals from Dara-i-Pioz isn't finished on that: recently cesium micas and a number of undetermined cesium silicates were found, and now they are studied.

Zeravshanite was found in the samples of rock composed mainly by quartz with subordinate amount of aegirine, polylithionite, reedmergnerite, pectolite, and a whole number of other accessory minerals. This rock occurs rarely in the moraine of Dara-i-Pioz glacier. All its findings are represented by blocks with different degree of roundness and with sizes up to half-meter, very rarely lager. Unfortunately, the authors never found the contacts of this quartz rock with any other rock that doesn't allow judging with some validity about form of

* It was considered by the RMS KNMMN and approved by the IMA KNMMN on September 21, 2003

bodies composed by this rock and about its genesis. Some researchers consider it as quartz cores of pegmatites, others are inclined to see in it the fragments of proper silicite veined bodies. The appearance and mineral composition of this rock is very exotic, and it is difficult to give the simple interpretation and name in the limits of existed rock classification. As it was mentioned, quartz is the main mineral of the rock. Quartz has ice-like appearance, more often absolutely transparent, but it looks white because of inter-grain borders and cracks. The structure is inequigranular, from medium-grained to coarse-grained, and rarely up to gigantic-grained. Very often the equimedium-grained parts without strong borders are observed, which are composed by isometric polyhedra, quartz granules. The well-shaped black tabular crystals of aegirine (up to 5 cm in size), large lamellae of polylithionite (up to 20 cm in size), semitransparent grass-green crystals of leucosphenite, lentil-shaped crystals of stillwellite-(Ce), the nests of coarse-grained reedmergnerite, single crystals and intergrowths of white microcline, pink to violet tabular segregations of sogdianite-sugilite series mineral (up to 20 cm in size), columnar to needle-shaped crystals of dark-green hydrated high-uranium turkestanite are sporadically impregnated in quartz. Rarely pyrochlore, neptunite, galena, calcite, kapitsaite-(Y), berezanskite, tienshanite, darapiosite, dusmatovite, tazhikite group minerals, baratovite, native bismuth, sphalerite, fluorite, fluorapatite, and fluorapophyllite are noted in this rock. The distribution of mentioned minerals in the rock is extremely uneven, without some orientation of individuals of accessory minerals. The typical peculiarity of described rock is the brown polymineral aggregates (up to 25 cm in size) with strong borders, which occur only in this rock and are composed predominantly by pectolite with subordinated amount of aegirine, fluorite, quartz, polylithionite, neptunite, very rare by pekovite and cesium analogue of polylithionite. For the first time zeravshanite was found in the edge zone of pectolite aggregate at the border with quartz in the form of unshaped grains (0.02 – 0.1 mm in size) and intergrowths or tabular individuals up to 0.2 mm in the largest dimension (Fig. 3) in intergrowth with pectolite and undetermined silicate of cesium and calcium. Zeravshanite occurs very rare, it was found only in single samples from many tens of micro-sections of pectolite aggregates. Other findings of zeravshanite were made also in described quartz rock, but without apparent connection with pectolite aggregates. In the

Table 1. The results of calculation of zeravshanite debayegram

I	$d_{exp.}$	$d_{calc.}$	*hkl*
2	7.31	7.271	202
5	6.32	6.327	-402
		6.292	400
1	5.43	5.453	-312
1	4.57	4.561	-114
2	4.24	4.279	-512
		4.201	114
1	4.18	4.195	600
5	3.65	3.658	006
		3.636	404
10	3.35	3.367	-712
		3.356	-223
		3.349	222
4	3.25	3.263	206
		3.246	710
		3.241	-422
9	3.14	3.144	-224
1	2.89	2.907	224
5	2.82	2.833	-716
		2.820	406
7	2.62	2.626	026
		2.622	910
		2.608	-518
3	2.517	2.517	10 0 0
		2.514	714
1	2.478	2.483	-916
		2.481	-822
		2.468	226
2	2.276	2.279	-2.0.10
		2.279	-334
		2.264	-532
1	2.227	2.230	-918
2	2.185	2.187	-12.0.4
3	2.146	2.149	532
2	2.095	2.097	12.0.0
		2.094	10.2.0
1	2.071	2.072	518
4	1.946	1.951	-2.2.10
		1.942	-736
4	1.891	1.892	-12.2.4
4	1.865	1.865	-538
		1.864	-14.0.2
3	1.829	1.830	734
		1.829	0.0.12
3	1.816	1.818	-936
		1.814	-7.1.12
1	1.786	1.784	044
1	1.764	1.762	-14.0.8
1	1.736	1.737	12.22
2	1.674	1.677	046
		1.672	-14.2.2
1	1.649	1.650	10.2.6
		1.646	0.2.12
1	1.632	1.633	246
		1.631	-16.0.6
1	1.546	1.547	14.2.2
1	1.534	1.534	13.3.0
3	1.500	1.500	-7.3.12
2	1.454	1.454	14.2.4
		1.453	-2.4.10

Note:
RKD 114, Fe anod, Mn filter, URS-50IM.
Analyst L.A. Pautov

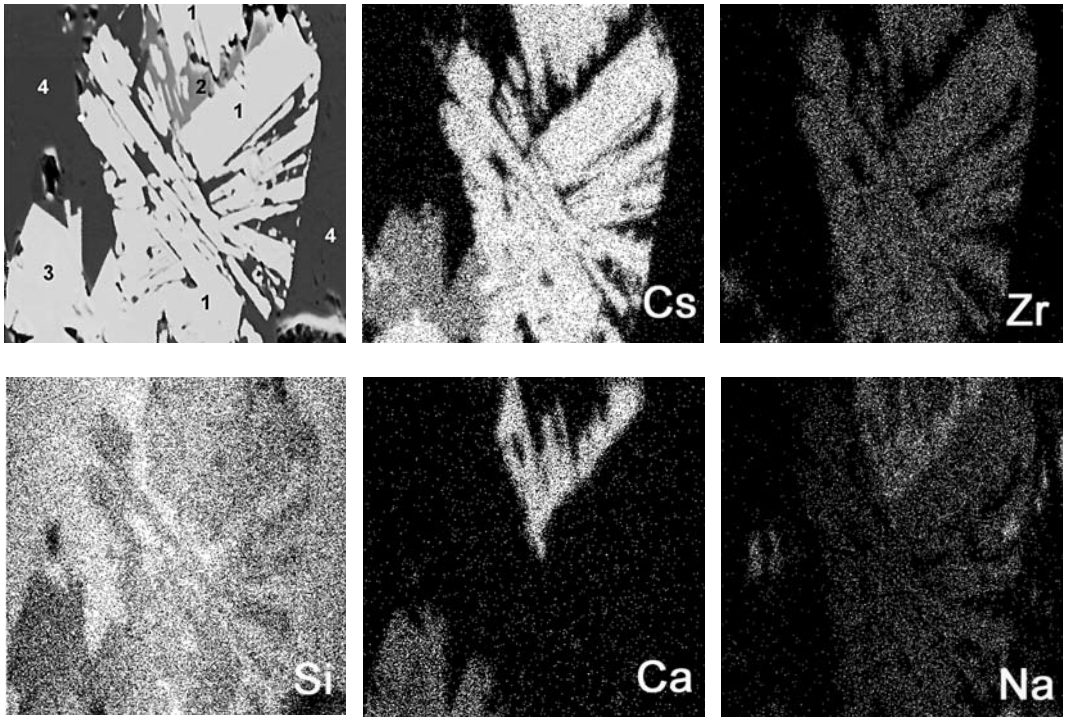

FIG. 3. The intergrowth of lamella grains of zeravshanite (1) with pectolite (2) and undetermined Cs-Ca silicate (3) in quartz (4). The image in COMPO regime and characteristic X-ray radiation of mentioned elements. Field of vision width is 200 mkm

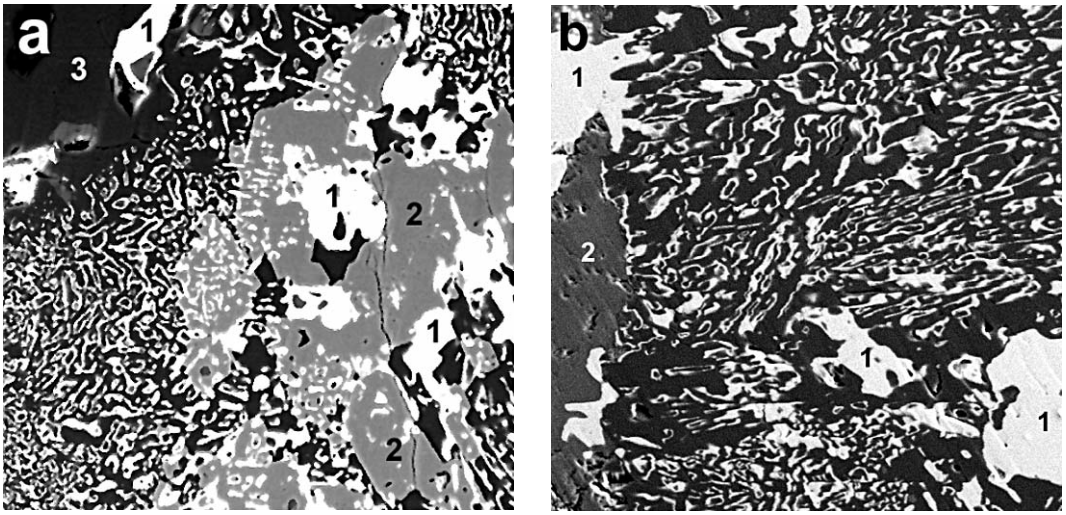

a *b*

FIG. 4. a) Graphic intergrowths of zeravshanite (1) with quartz (black) and aegirine (2). Field of vision width is 100 mkm. b) Graphic intergrowths of zeravshanite (1) with quartz (black). The dark-gray is pectolite (2). Field of vision width is 60 mkm

latter case zeravshanite is represented by grains with indented outlines and graphic intergrowths with quartz, aegirine, arfvedsonite, and rarely with pectolite (Fig. 4).

Physical properties

Zeravshanite is absolutely colorless, water-transparent mineral. It is practically indistinct from quartz by its appearance. The luster is vitreous, slightly stronger than the luster of quartz. The mineral hasn't luminescence in the short-wave and long-wave ultraviolet light. The hardness is 6 on Mohs' scale. Micro-indentation, VHN = 838 kgs/mm^2 (the average value by 12 measures with fluctuation of single measures from 805 up to 880 kgs/mm^2) at the load 50 g. The micro-indention was obtained by PMT-3 instrument, calibrated by NaCl. The density of the mineral was determined by balancing of mineral grains in Clerichi solution, it is equal 3.09(5) g/cm^3. The observation was made at vertical position of microscope table in the glass with hole, in which mineral grains and solution were placed. The single gas-liquid inclusions were observed in all grains that, undoubtedly, resulted in some understatement of measured density in comparison with calculated density, 3.17 g/cm^3. Zeravshanite is optical negative, biaxial mineral. 2V (calc.) = — 63°. Optic angle dispersion is medium, v>r. Refractive indexes were measured on rotated needle, n_p = 1.585(2); n_m = 1.598(2); n_g. = 1.603(2) (for light with wave length 589 nm). Very insignificant amount of new mineral wasn't allowed obtaining the exhaustive optic constants. It wasn't succeeding study of its optic orientation and measure the value of angle 2V. The cleavage in one direction was observed on single grains in immersion preparations. The grains lain in preparation on cleavage plane gave in conoscope the section close to that perpendicular to obtuse bisector. The elongation of elongated fragments is negative. The IR-spectrum of the mineral obtained by Specord-75IR (the sample was micro-tablet of the mineral in KBr) has the following most strong absorption bands: 1089, 1045, 978, 709, 662, 585, 538 cm^{-1}.

X-ray data

X-ray powder diagram of the mineral (Table 1) was obtained by photomethod in RKU 114 mm camera on Fe radiation with Mn filter. Silicon was used as inner standard. The debayegram is individual and doesn't coincide with any known mineral or synthetic compound. Crystal structure of zeravshanite (Uvarova *et al.*, 2004) with ideal formula $Cs_4Na_2Zr_3(Si_{18}O_{45})(H_2O)_2$ (monoclinic system, unit cell parameters are following: a = 26.3511(8), b = 7.5464(3), c = 22.9769(8)Å, β = 107.237(1)°, V = 4363.9(4)Å^3, sp. group $C2/c$, Z = 4), was solved by direct method and refined with R_1 = 2.8% on 4508 independent reflexes [$F_o > 4\sigma I F I$] with diffractometer Bruker $P4$ (Mo$K\alpha$ radiation, CCD detector). In the crystal structure of the mineral there are 9 tetrahedral *Si*-sites (<*Si*-O> = 1.614 Å); two [6]-coordinated *M*-sites occupied by Zr with small amounts of Ti, Fe^{3+}, and Sn (<*M*-O> = 2.067 Å); one [5]-coordinated *Na*-site (<*Na*-O, H_2O> = 2.406 Å); two *A*-sites occupied predominantly by Cs (with small amounts of Na and K), from which *A*(1)-site is [12]-coordinated and *A*(2)-site is [11]-coordinated (<*A*(1)-O, H_2O> = 3.371 и <*A*(2)-O> = 3.396 Å). In the crystal structure of zeravshanite Si-tetrahedra form the layers $\{Si_{18}O_{45}\}^{18-}$ consisting of 5- and 8-membered Si-O rings (Fig. 1). The topology of the layers can be described as connected wollastonite-like chains $\{Si_3O_9\}^6$. The tetrahedra of (10−1) Si-O layers and *M*- and *Na*-polyhedra equally divide the mutual vertices forming mixed construction $\{Na_2 Zr_3 (Si_{18}O_{45}) (H_2O)_2\}$ with holes containing *A* atoms (Fig. 2). The square *Na*-pyramids jointed by mutual vertices form zigzag chains along [010]. Each *Na*-pyramid has mutual edge with *M*(2)-octahedron at that the *cys*-decoration of chain of *Na*-pyramids by *M*(2)-octahedra is realized. Also there is the entirely occupied (H_2O)-site. Atoms of H are determined. (H_2O) groups form ligands with *Na* and *A*(1) with weak O-H bonds (~ 2.9 Å) in the limits of mixed construction.

Chemical composition

The chemical composition of zeravshanite was studied by electron microprobe instrument JCXA-50A (JEOL) equipped by modernized energy-dispersive spectrometer LINK and by three wave spectrometers. The analyses on all elements were made on EDS under accelerating voltage 20 kV and electron microprobe current 3 nA. The standards were following: anorthite USNM 137041 (Si), ilmenite USNM 96189 (Ti, Fe), synthetic jadeite (Na), microcline USNM 143966 (K), synthetic ZrO_2 (Zr), synthetic SnO_2 (Sn), synthetic $CsTb(PO_3)_4$ (Cs). Six mineral grains were analyzed. The distribution of main components of zeravshanite was studied by wave spectrometers; any heterogeneity or zoning wasn't discovered. The concentra-

Table 2. Chemical composition of zeravshanite (wt %)

Constituent	*1*	*2*	*3*	*4*	*5*	*6*	*Average*
SiO_2	52.50	52.47	52.35	52.39	51.32	52.18	52.20
TiO_2	0.23	0.51	0.95	0.88	0.02	0.00	0.43
ZrO_2	17.16	16.98	15.53	14.82	16.72	17.23	16.41
SnO_2	0.02	0.04	0.74	1.93	0.00	0.00	0.46
Fe_2O_3	0.22	0.26	0.26	0.00	0.022	0.33	0.21
Na_2O	3.08	3.35	3.03	3.01	2.97	2.94	3.06
K_2O	0.01	0.07	0.01	0.38	0.00	0.07	0.09
Cs_2O	26.50	25.65	27.25	25.61	27.02	27.47	26.58
H_2O calc.	1.74	1.74	1.74	1.74	1.74	1.74	1.74
Total	101.46	101.07	101.86	100.76	100.01	101.96	101.18
Formula calculated on 18 atoms of Si							
Si	18.00	18.00	18.00	18.00	18.00	18.00	18.00
Ti	0.06	0.13	0.25	0.23	0.01	0.00	0.11
Zr	2.87	2.84	2.60	2.48	2.86	2.90	2.76
Sn	0.00	0.01	0.10	0.26	0.00	0.00	0.06
Fe	0.06	0.07	0.07	0.00	0.06	0.09	0.06
Na	2.05	2.23	2.02	2.01	2.02	1.97	2.05
K	0.00	0.03	0.00	0.017	0.00	0.03	0.04
Cs	3.87	3.75	4.00	3.75	4.04	4.04	3.91
H_2O calc.	2	2	2	2	2	2	2
O	44.91	45.06	45.01	44.91	44.85	44.95	44.95

Note: analysts L.A. Pautov, A.A. Agakhanov

tions were calculated with use of ZAF-correction. The results of analyses are given in the Table 2. Unfortunately, it was impossible to determine the amount of water by direct method because of extremely small amount of new mineral; and so in the Table 2 the amount of water is given by data of crystal structure study. Chemical formula of zeravshanite calculated on 18 atoms of Si by results of electron microprobe analyses is following: $(Cs_{3.91} Na_{0.05} K_{0.04})_{4.00} Na_{2.00}(Zr_{2.76}Ti_{0.11} Fe^{3+}_{0.06}Sn_{0.06})_{2.99}(Si_{18}O_{44.92}) (H_2O)_2$. The chemical formula of the mineral by results of crystal structure study is quite close to the formula calculated by chemical analysis: $(Cs_{3.80} Na_{0.18} K_{0.02})_{4.00} Na_{2.00}(Zr_{2.73} Ti_{0.19} Fe^{3+}_{0.04} Sn_{0.04})_{3.00} (Si_{18}O_{45}) (H_2O)_2$. The ideal formula of zeravshanite is $Cs_4Na_2Zr_3(Si_{18}O_{45})(H_2O)_2$. The coincidence index is $(1\text{-}K_p/K_c) = 0.004$ (superior).

Zeravshanite doesn't have analogues among minerals of inorganic synthetic compounds.

The sample with zeravshanite was given to the Fersman Mineralogical Museum RAS (Moscow).

Acknowledgments

The authors thank Vladimir Yu. Karpenko, Pavel V. Khvorov for help in carrying out of field works at the moraine of Dara-i-Pioz glacier and in laboratory studies, and Vyacheslav D. Dusmatov, Igor V. Pekov, and Dmitrii I. Belakovskiy for valuable advices.

The work was supported by the grant of Russian Foundation for Basic Research (04-05-64118).

References

Belakovskiy D.I. Die seltenen Mineralien von Dara-i-Pioz im Hochgebirge Tadshikistans. Lapis. **1991.** 16. № 12. p. 42–48.

Dusmatov V.D. To mineralogy of one of the alkaline rocks massifs. // In book: Alkaline Rocks of Kirgizia and Kazakhstan. (Shchelochnye Porody Kirgizii i Kazakhstana). Frunze. **1968.** P. 134–135. (Rus.).

Dusmatov V.D. Mineralogy of Dara-i-Pioz Alkaline Massive (South Tyan-Shan). (Mineralogiya Shchelochnogo Massiva Dara-i-Pioz (Yuzhnyi Tyan'-Shan')). PhD Thesis. M. **1971.** 18 p. (Rus.).

UDC 549.072, 549.02

JARANDOLITE $Ca[B_3O_4(OH)_3]$, CALCIUM BORATE FROM SERBIA: NEW NAME AND NEW DATA[1]

Svetlana V. Malinko
All-Russian Scientific-Research Institute of Mineral Resources (VIMS), Moscow

S. Anic'ic'
Geofactory «Non-metals», Serbia

D. Joksimovic'
Geofactory «Non-metals», Serbia

A.E. Lisitsyn
All-Russian Scientific-Research Institute of Mineral Resources (VIMS), Moscow

V.V. Rudnev
All-Russian Scientific-Research Institute of Mineral Resources (VIMS), Moscow, vims@df.ru

G.I. Dorokhova,
Lomonosov Moscow State University, Moscow

N.A. Yamnova
Lomonosov Moscow State University, Moscow

V.V. Vlasov
Central Scientific-Research Institute of Geology of Non-Metallic Raw Materials (TsNIIGeolnerud), Kazan

A.A. Ozol
Central Scientific-Research Institute of Geology of Non-Metallic Raw Materials (TsNIIGeolnerud), Kazan

Nikita V. Chukanov
Institute of Problems of Chemical Physics RAS, Chernogolovka, Moscow Region, chukanov@icp.ac.ru

The new data are given on calcium borate jarandolite from Jarandol basin (Serbia) which short description has been published earlier (Stojanovic' 1992, Stojanovic' *et al.* 1993) under the tentative name «srbianite». Jarandolite forms columnar aggregates of flattened individuals up to 1.5 cm in length and associates with colemanite, howlite, ulexite, veatchite, studenitsite, pentahydroborite, and montmorillonite. The mineral is colourless, semi-transparent. The lustre is vitreous, cleavage is highly perfect on (001). Micro-indentation hardness is $H_{average}$ = 645 kg/mm^2 (approximately 5 on Mohs' scale). Density (exp): 2.49 (2) g/cm^3, density (calc) = 2.57 g/cm^3 (from empirical formula); 2.57 g/cm^3 (from structural data). The mineral is optically biaxial, positive. $2V = 60(2)^\circ$, $n_p = 1.573(2)$, $n_m = 1.586(2)$, $n_g = 1.626(2)$. Dispersion of optical axes is medium, $r > v$. Elongation is positive. Orientation is following: $Np = c$, $Nm = b$, $aNg = +8^\bullet$. Pleochroism is absent. The simple forms {001}, {011}, and {11} are observed. Micro-twinning is on (001). IR-spectrum and thermogram are given. Chemical composition (wet analysis, wt %) is: Na_2O 0.05, K_2O 0.07, CaO 30.56, MgO 0.02, MnO 0.01, Fe_2O_3 0.20, Al_2O_3 0.03, SiO_2 0.20, B_2O_3 55.44, Cl 0.21, H_2O 13.36, $-O=Cl_2$ −0.05, total 100.10. The empirical formula of jarandolite is: $Ca_{1.02}(B_{2.99}Si_{0.01})O_{4.125}(OH)_{2.79}Cl_{0.01}$. The spiral-screwed chains of colemanite type underlie in the base of crystal structure of jarandolite, which has been studied on monocrystal (R = 0.035). The mineral is monoclinic, the space group $P2_1/a$, $a = 8.386(3)$, $b = 8.142(4)$, $c = 7.249(3)$ Å, $\beta = 98.33(3)^\circ$, $V = 489.7$ Å^3. The strongest lines of X-ray powder diagram are following [*d*, Å (*I*, %) (*hkl*)]: 4.32 (57) (111), 3.39 (100) (201), 3.13 (50) (211), 2.93 (23) (−202), 2.606 (25) (221), 1.849 (25) (−421, 420).
1 table, 5 figures, and 8 references.

New hydrous calcium borate, jarandolite, with chemical composition $2CaO{\cdot}3B_2O_3{\cdot}3H_2O$ was found by geologist of geofactory «Non-metals», Belgrade, Stoyan Anic'ic' in volcano-sedimentary boron deposits Pobrdjski Potok and Piskanja approximately 280 km southward from Belgrade (Fig. 1), nearby small mountainous town Balevats on the shore of Jbar River. The mineral study, which results are given in this article, was made in All-Russian Scientific-Research Institute of Mineral Resources (VIMS), Moscow; Lomonosov Moscow State University, and Central Scientific-Research Institute of Geology of Non-Metallic Raw Materials (TsNIIGeolnerud), Kazan. Borate is named jarandolite after occurrence of its segregations in volcano-sedimentary rock mass of Jarandol basin of Miocene age in Serbia.

First information on borate with close chemical composition, which was determined by data of microprobe analyses, but without data on crystal structure and with some inexact optical constants, was published earlier in the theses of reports of conference of Serbian Crystallographic Association (Stojanovic', 1992; Djuric' *et al.*, 1993) and Yugoslavian Mineralogical Association (Stojanovic' *et al.*, 1993). The authors give the name srbianite to studied borate, after the find place in Serbia. Already after publication of data on new borate the applica-

[1] Is approved by Commission on New Minerals and Mineral Names of International Mineralogical Association on September 2, 2003

tion (registration № MMA 95–020, see Can. Mineral., 1996) was handed in Commission on New Minerals and Mineral Names IMA (IMA CNMMN). However, approved new mineral, Commission did not affirm suggested name, and longstanding (up to 2003 year) debates on this question have not brought to its positive solution.

At the same period (1992–1994 years) parallel to work of D. Stojanovic' with collogues we also studied early-unknown borates from volcano-sedimentary boron deposits Pobrdjski Potok and Piskanja. Firstly the new sodium-calcium borate, studenitsite $NaCa_2[B_9O_{14}(OH)_4]\cdot 2H_2O$, was studied and described (Yamnova *et al.*, 1993; Malinko *et al.*, 1995), this mineral was approved by the IMA CNMMN in 1994 year. At the same time, in 1995 year, S.V. Malinko with co-authors gave the application on new mineral, jarandolite, in the IMA CNMMN, however, this application was received by Commission later than analogous application from Serbian authors. Because of that, admitted the priority of D. Stojanovic' with co-authors, the authors of present article have postponed publication of their researches, waiting for the solution of the IMA CNMMN on application 95–020.

The Chairman of the IMA CNMMN E.A.J. Burke gave the detailed information about consideration of application 95–020 on new borate and permitted to use the text of his comments in this publication.

Comment of the Chairman of the IMA CNMMN

The history of proposal 95–020 is a long, sad, and unique one in the history of the CNMMN! The initial data for this mineral were mailed by Dobrica R. Stojanovic' to Joe Mandarino, Chairman of the CNMMN, on 25 November 1992, but this letter never arrived in Toronto. A new letter was mailed on 16 June 1993, it was received on 27 July 1993, and answered on 28 July 1993: more information was needed on some data. Stojanovic' replied to this letter, without the data, on 28 December 1994, but the letter was forwarded to Joel Grice who had meanwhile taken over as CNMMN chairman. Joel Grice asked for the same additional info as Joe Mandarino in a letter of 23 March 1995, and got these data in April 1995. The proposal for the new mineral with the name srbianite (95–020) was mailed to the CNMMN members on 31 May 1995. From this proposal it was evident that the name srbianite had already been published, *without CNMMN approval*, in Serbian journals in 1992 and 1993.

The voting results of proposal 95–020 were published in CNMMN Memorandum Vol. 21 No. 8 of 30 August 1995: the mineral was approved, but the name 'srbianite' was suspended because of a lack of the requested majority of 'yes' votes. Joel Grice suggested to choose a more specific name for a second voting, but Stojanovic' requested that the name 'srbianite' would be submitted again. This was sent to CNMMN on 31 January, and the results appeared in Memorandum Vol. 22 No. 4 of 30 April 1996. The name was suspended for the second time, and Joel

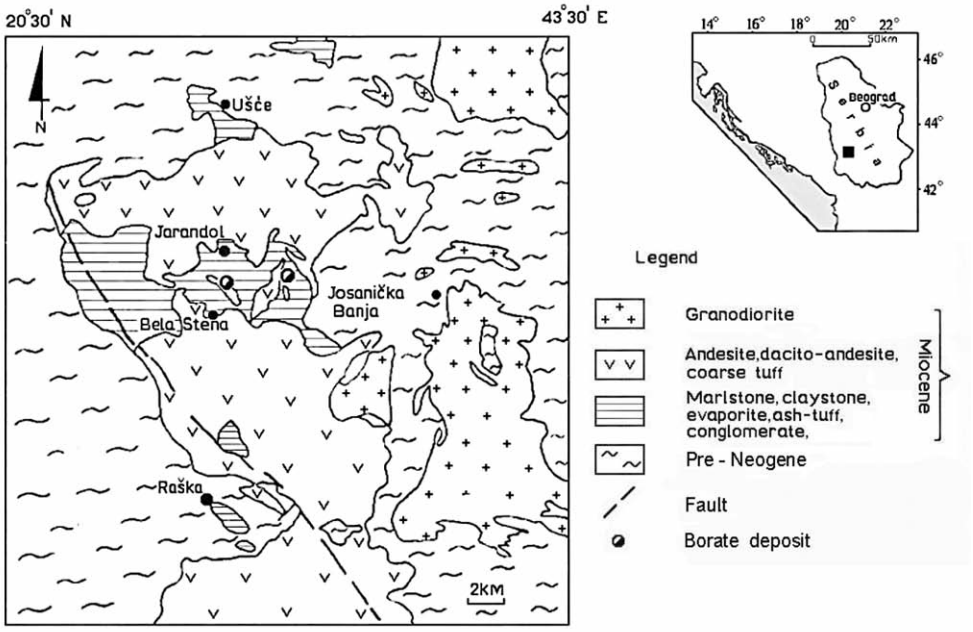

FIG. 1. The location of boron deposits in Jarandol volcano-sedimentary basin (Obradovic' J. et al., 1992)

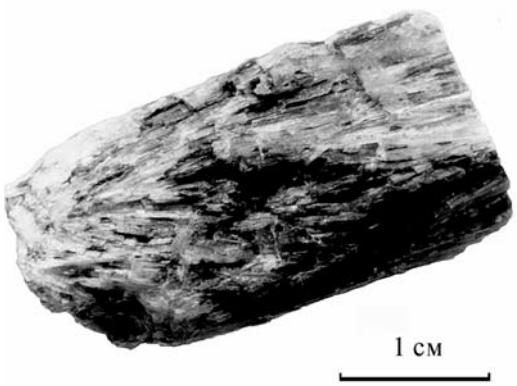

FIG. 2. The fragment of jarandolite crystals intergrowth from the core of borehole

suggested again a more site-specific name. In spite of this, Stojanovic' asked for a third vote, but now on the name 'serbianite'. This name was submitted to CNMMN on 29 August 1997, and the result of the voting appeared in Memorandum Vol. 23 No. 11 of 26 November 1997: the name was rejected with an overwhelming majority. Joel Grice was then very lenient in proposing Stojanovic' to choose a different name for a fourth voting.

Stojanovic' did not reply to this offer from Joel Grice until June 2002, asking indeed for a fourth vote, but again on the names 'srbianite' or 'serbianite'. Joel Grice consulted his fellow CNMMN officers and the new Chairman-elect, but did not reply to this letter. Next step: Stojanovic' sent a copy of his June 2002 letter to Ernst Burke (3rd CNMMN chairman involved) in February 2003. He made it clear in his answer (12 February 2003) to Stojanovic' that his wish was impossible: we had three CNMMN votings on these names, and all three were negative. Allowing a fourth vote on these names would be against all rules, and accepting one of these names would be a very significant, but inadmissible precedent for all authors wishing to circumvent CNMMN procedures.

In order to save the results of this new (and unique) borate mineral, Ernst Burke offered two alternatives to Stojanovic': 1) propose a new name, like Joel Grice had already suggested three times; this could have been done easily, because the Serbian literature with the name 'srbianite' was apparently so obscure that it was never mentioned in GeoRef or Web of Science; 2) cooperate with a Russian team that had proposed the same mineral (from the same locality as 95−020) in March 1995, just after Joel Grice received the borate dossier from Joe Mandarino. In view of the previous gap of almost 5 years, Ernst Burke demanded from Stojanovic' that he would answer him before 11 April 2003; if he did not receive the reply by that date he would lift the priority for the mineral.

In the first week of April 2003 Ernst Burke received an answer from Stojanovic' on his proposals. The latter repeated his wish of June 2002 / February 2003 to have a fourth vote on the names 'srbianite' or 'serbianite'. Ernst Burke consulted two members of the IMA Council (the past-president and the secretary), who backed his intention to stick by the CNMMN rules after having been lenient towards Stojanovic' twice (allowing a third voting on 'serbianite', and proposing a fourth vote on another name). Ernst Burke decided then to give the Russian team the opportunity to name the mineral, as Stojanovic' obviously refuses to follow the CNMMN voting results.

The present publication is the result of this long procedure to give a name for this borate mineral. Because the type locality is the same as in the original proposal 95−020, there is no problem there. Only the holotype material will of course be different. The decision to approve the mineral was already published (without the name, as usual) in the yearly list of new minerals, e. g., in Canadian Mineralogist, 34 (1996), 687. The outcome of the CNMMN vote on jarandolite was published in Memorandum Vol. 29, Nr. 9; votes for the mineral: 25 yes, 1 no, 0 abstain; votes for the name: 24 yes, 2 no, 0 abstain.

The authors of the jarandolite proposal have communicated to the CNMMN chairman that their main goal is to publish an extended set of data on this mineral under an approved name. In their paper they will mention the previous work of the team of Stojanovic', and corresponding references will also be given. This has to be considered as a very honourable attitude from the Russian team.

E.A.J. Burke, chairman of the IMA CNMMN

Occurrence

Deposits, in which ores the new calcium borate was determined, are located in Sought-West Serbia and confined to the chain of continental sedimentary basins, situated along Balkan Peninsula at the East of Mediterranean Sea region, which was formed as a result of intensive Oligocene-Pliocene tectonogenesis. One of them is Jarandol Miocene lacustrine basin with area up to 200 km^2, in which borate deposits was found. Magnesite deposits, containing borate layers and coal intercalations, alternating with analcime-enriched tufogenic rocks, clays, and marls, compose this sedimentary basin. Subsequent Oligocene-Pliocene volcanism and tectonic activity have formed here the lacustrine facies of Neogene volcano-sedimentary formations with thickness 850−1500 m. As a result of extremely diverse conditions of sedimentation in Jarandol basin the volcano-sedimentary series, consisting of argillaceous rocks, which contain different amounts of tufogenic and carbonaceous sediments, coaly, magnesite, and borate lens, was formed (Obradovic' *et al.*, 1992).

Borate deposits mainly occur in tufogenic and argillaceous rocks at different depth from day surface and have thickness from 1 to 12 m

(average is 4 m). Main boron minerals in them are colemanite, howlite, ulexite, and veatchite. In earlier studied by us new borate from these ores, studenitsite $NaCa_2[B_9O_{14}(OH)_4]\cdot 2H_2O$, the veinlets of pentahydroborite are determined firstly for this deposit. In single cases in volcano-sedimentary rocks of Jarandol basin there were the finds of searlesite and lü neburgite, filling the cracks in magnesite deposits. The distribution of montmorillonite in assemblage with borates is typical.

Morphology and physical properties.

The studied samples of new borate from 1.5×3.0 to 2.0×3.5 cm in size, which was colleted from the core of hole at the depth nearly 100 m from day surface, are presented by the fragments of aggregate of jarandolite crystals, intergrowing along elongation, with tabular habit (Fig. 2). The size of separate individuals varies within the limits from first millimeters to 1.5 cm in length at the thickness from a fraction of millimeter to 1−2 mm. The mineral is colourless, semitransparent in mass and transparent in small fragments. The colour in powder is white. In some samples there are the smectite segregations, which tincture the neighboring jarandolite crystals in light brown colour. The lustre is vitreous, cleavage is highly perfect on (001). The micro-indentation of the mineral was measured by E.G. Ryabova on apparatus PMT−3, calibrated on rock salt at load 50 g, exposition 15 sec.; average value is calculated by five imprints: $H_{average}$ = 645 kg/mm^2 (H_0 = 6.0); H_{min} = 616 kg/mm^2 (H_0 = 6.0); H_{max} = 669 kg/mm^2 (H_0 = 6.1). The imprint is correct; the mineral is brittle. The density, measured with hydrostatic weighing, is 2.49(2) g/cm^3. The density, calculated from empirical formula, is 2.57 g/cm^3. The mineral does not interact with water, slowly dissolves in diluted HCl and H_2SO_4. In cathode and ultraviolet rays the mineral does not luminance.

The mineral is optically biaxial, positive. $2V_{exp}$ = 60(2)°; $2V_{calc}$ = 59°23?. Refractive indexes measured by immersion method in white light are: n_p = 1.573(2), n_m = 1.586(2), n_g = 1.626(2). Dispersion of optical axes is medium, *r* > *v*. Elongation is positive. Orientation is following: *Np* = *c*, *Nm* = *b*, *aNg* = +8° Pleochroism is absent.

The seven samples of crystal fragments with traces of faces were measured on two-circle reflected goniometer GD−1. On the six crystals there are only two simple forms: pinacoid {001} and orthorhombic prism {110}. On the seventh crystal the traces of two faces of orthorhombic prism {11} are noted. The quality of faces is bad, all signals of goniometer was fixed only by reflections (from here there is a precision of measuring ~ 1°). The surface of all faces is imperfect: the pinacoid is slightly curved; on the prism faces there are the traces of dissolution. For goniometric measuring the crystals are regulated by faces of zone [100]. The transition to standard mineralogical setting (c_{001} = 8.33°) was made with Wulf net. The theoretical values of spherical faces coordinates was calculated by values of unit cell parameters of the mineral: for {110} $-\varphi_{exp.}$ ~10°, $\varphi_{calc.}$ = 9.31°, $\rho_{exp.}$ ~43°, $\rho_{calc.}$ = 42.08°, for {-111} $\varphi_{exp.}$ ~ −34°, $\varphi_{calc.}$ = −33.21°, $\rho_{exp.}$ ~47°, $s_{calc.}$ = 46.67°. The crystal appearance is tabular (elongation along [100], flattening on [001]). The habit is pinacoid-orthorhombic (Fig. 3).

The simple twins are observed in polished sections. The measured value of orientation of normal to plane of composition face, DN_g ~ 83°, corresponds well to theoretical angle 81.67° = 90° (cN_g) — 8.33° (c_{001}) for penetration twin on (001).

In IR-spectrum of jarandolite the wave numbers for maximums of absorption bands (Fig. 4) are following (cm^{-1}; s — strong band, w − weak band, sh — shoulder): 3550 s, 3115, 2980, 1447, 1402 s, 1369, 1300 s, 1226, 1135 sh,

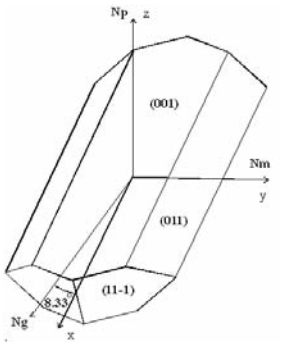

FIG. 3. The appearance of jarandolite crystal

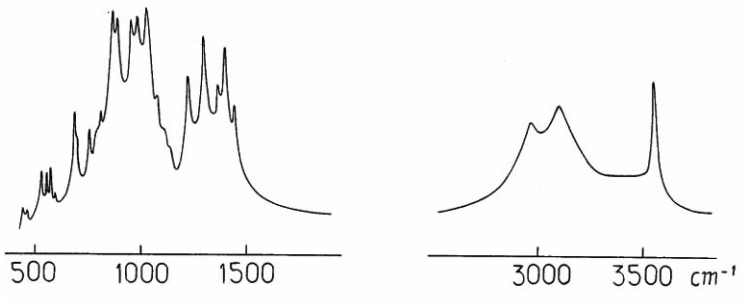

FIG. 4. IR-spectrum of jarandolite

Table 1. Data of calculation of X-ray powder diagram of jarandolite (Co radiation, DRON UM-1)

I_{obs}, %	d_{obs}, Å	d_{calc}, Å	*hkl*
2	4.77	4.76	-111
57	4.32	4.31	111
5	4.16	4.15	200
5	4.08	4.07	020
4	3.54	3.54	021
5	3.48	3.47	-211
100	3.39	3.385	201
13	3.18	3.18	121
50	3.13	3.13	211
23	2.93	2.93	-202
8	2.795	2.793	221
5	2.758	2.758	-212
14	2.690	2.691	022
25	2.606	2.603	221
17	2.360	2.358	311
19	2.287	2.288	320
6	2.212	2.215	-203
12	2.155	2.153	222
10	2.115	2.117	231
11	2.074	2.074	-401, 400
12	2.061	2.062	-123, 023
3	2.033	2.035	040
3	2.009	2.010	-411, 410
4	1.975	1.977	140
7	1.951	1.953	203
5	1.944	1.945	123
11	1.921	1.920	-402
3	1.867	1.869	-412, 411
25	1.849	1.848	-421, 420
1	1.826	1.827	240
1	1.782	1.782	-332
7	1.756	1.757	-142
4	1.736	1.737	-422, 421
5	1.693	1.693	-403, 402
5	1.658	1.658	-413
5	1.627	1.626	510
2	1.323	1.323	601
		1.322	-161
2	1.309	1.309	620

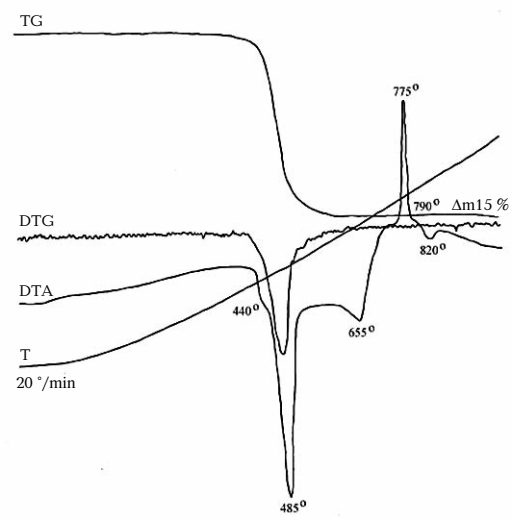

FIG. 5. Derivatogram of jarandolite. Thermoanalyzer «Thermoflex», preparation mass is 30 mg, T_{max} ~1000°C

1110 sh, 1075, 1026 s, 983 s, 953 s, 889 s, 867 s, 810, 795 sh, 756, 695 sh, 687, 597 w, 577, 560, 533, 444 w, 419 w. Two groups of bands in the ranges 850 – 1050 cm^{-1} (most intensive) and 1220 – 1450 cm^{-1} (less intensive) correspond to stretching vibrations with participation of the bonds $^{IV}B-O$ (in tetrahedrons $BO_2(OH)_2$ and $BO_3(OH)$) and $^{III}B-O$ (in triangles BO_3) respectively. The bands at 2980 and 3115 cm^{-1} are caused by O – H-valent oscillations of two OH-groups, forming very strong hydrogen bonds. The narrow band at 3550 cm^{-1} corresponds to almost free (non forming hydrogen bonds) OH-group. It is obvious that only the latter OH-group can replace Cl without significant energy expenses, which would be necessary for break of hydrogen bonds. The absence of bands in the range 1500 – 1700 cm^{-1} is evident of the absence of molecules H_2O in crystal structure of jarandolite.

On thermogram of jarandolite (thermal analysis was made by R.N. Yudin, the rate of heating is 20°/min (Fig. 5), three endothermic effects are distinctly displayed; the first effect is connected to double peak with two non-equivalent maximums: less significant at 440°C and more strong at 485°C; this reaction is accompanied by conformed minimum on DTG curve, and also large ledge on thermogravimetric curve, which fixes approximately 15% loss of mass. The second endothermic peak is the less pronounced endothermic reaction, characterized by flattened peak with maximum at 655°C on DTA curve; it is not accompanied by the loss of mass. The third endothermic effect has the maximum at 820°C. Apparently, the first, most strongly pronounced endothermic reaction is connected to dehydroxylization. The total loss of mass during thermal analysis (approximately 15%) is completely concern to this endothermic reaction and close to content of H_2O in the mineral, which was determined by chemical analysis (13.36%). The endothermic reaction, characterized by flattened peak with maximum at 655°C, apparently, is caused by some crystal structural changes of the mineral, whereas the endothermic peak at 820°C fixes its melting. In addition to endothermic reactions, on thermogram of jarandolite the exothermic reaction with maximum at 775°C is strongly pronounced, evidently, it is connected to so-called borate regrouping, i. e. reconstruction of crystal structure, which is peculiar to most of hydrous borates under increased temperatures.

Chemical composition

Chemical composition of jarandolite was

studied by method of wet chemistry (analyst S.P. Purusova) from the sample, which was preventively studied by physical, optical, and X-ray methods. The contents of main components are following (wt %): Na_2O 0.05, K_2O 0.07, CaO 30.56, MgO 0.02, MnO 0.01, Fe_2O_3 0.20, Al_2O_3 0.03, SiO_2 0.20, B_2O_3 55.44, Cl 0.21, H_2O 13.36, $-O=Cl_2$ −0.05, total 100.10. The empirical formula of jarandolite, calculated on 3 atoms (B + Si) is $Ca_{1.02}(B_{2.99}Si_{0.01})O_{4.125}(OH)_{2.79}Cl_{0.01}$ (taking in account only components with content >0.005 *atoms per formula unit*). The ideal formula is $Ca(B_3O_4)(OH)_3$. The compatibility by Gladstone-Dale criterion is good: $1 - (K_p/K_c) = -0.003$ («Superior») for D_{calc}; $1 - (K_p/K_c) = -0.037$ («Excellent») for D_{exp}.

X-ray and structural studies

X-ray and structural studies of jarandolite was made by N.A. Yamnova, Yu.K. Egorov-Tismenko, and D.Yu. Pushcharovskii (1994). For X-ray structural analysis the monocrystal with line sizes 0.450×0.300×0.250 mm was selected. The parameters and symmetry of monoclinic (Laue class 2/*m*) unit cell of jarandolite are following: $a = 8.386(3)$, $b = 8.142(4)$, $c = 7.249(3)$ Å, $\beta = 98.33(3)°$, $V = 489.7$ Å^3, these values have been determined by Laue swing method and refined by automatic diffractometer P Syntex (Mo_K radiation, flat graphite monochromator). Space group is $P2_1/a$. The X-ray powder diagram (Tabl. 3) is good indiced with the obtained unit cell parameters.

Crystal structure of this mineral was solved by direct method with the program MULTAN up to R-factor 0.035 and entirely is considered in the article (Yamnova *et al.*, 1994). The formula of jarandolite $Ca[B_3O_4(OH)_3]$ (Z = 4, X-ray density 2.54 g/cm^3) corresponds to this structure.

The parallel (001) goffered layers-walls of centrosymmetric pairs of Ca-polyhedra, united on mutual O-vertexes, compose the base of crystal structure of jarandolite. The walls are interlaid by boron-oxygen bands of colemanite type $[B_3O_4(OH)_3]$, which are elongated along *b* axis of unit cell and formed by tetrahedra of two types, $BO_2(OH)_2$ and $BO_3(OH)$, and triangle BO_3 groups. However, in contrast to colemanite, in crystal structure of jarandolite the rings are as if curled around spiral axis 2_1. The structure of cationic constructions is also different: in colemanite the bands of centrosymmetric pears of eight-vertex Ca-polyhedra are endless along the *a* axis of unit cell whereas in jarandolite these bands are united in the layer-walls. As it is above-mentioned, two out of three hydroxyl groups form strong hydrogen bonds.

Jarandolite is structurally and chemically close to colemanite $Ca[B_3O_4(OH)_3]\cdot H_2O$ ($P2_1/a$, $a = 8.743$, $b = 11.264$, $c = 6.102$ Å, $\beta = 110.115°$, $Z = 4$), which is distinguished from jarandolite by optical constants ($n_p = 1.586$, $n_m = 1.592$, $n_g = 1.614$, $2V = 125°$), optical sign, density (D = 2.54 g/cm^3), and other characteristics.

The standard sample of jarandolite is deposited in Fersman Mineralogical Museum RAS, Moscow (registration № 1538/1).

The authors take an opportunity to express their thanks to S.P. Purusova, E.G. Ryabeva, R.N. Yudin, G.K. Krivokoneva, E.I. Varfalomeeva for participation in study of new borate, and also E.A. Obradovic' for kind assistance in this research.

The leading role in the study of new borate played an outstanding specialist in mineralogy of boron deposits S.V. Malinko (1927−2002), and we devote the conclusion of this work to her memory.

References

Malinko S.V., Anic'ic' S., Joksimovic' D., Lisitsyn A.E., Dorokhova G.I., Yamnova N.A., Vlasov V.V., Ozol A.A. Studenitsite $NaCa_2[B_9O_{14}(OH)_4]\cdot 2H_2O$, the new borate from Serbia, Yugoslavia // ZVMO. **1995.** P. 3. P. 57−64. (Rus.)

Yamnova N.A., Egorov-Tismenko Yu.K., Malinko S.V., Pushcharovskii D.Yu., Dorokhova G.I. Crystal structure of new natural calcium hydroborate $Ca[B_3O_4(OH)_3]$ // Kristallografiya. **1994.** V. 39. P. 6. P. 991−993. (Rus.)

Yamnova N.A., Egorov-Tismenko Yu.K., Pushcharovskii D.Yu., Malinko S.V., Dorokhova G.I. Crystal structure of new natural Na,Ca-hydroborate $NaCa_2[B_9O_{14}(OH)_4]\cdot 2H_2O$ // Kristallografiya. **1993.** V. 38. P. 6. P. 71−76 (Rus.)

Canadian Mineralogist. **1996**. Vol. 34. № 3. P. 687.

Djuric', S., Tanuic', P., Stojanovic', D., Potkonjak, B, Radukic', G. Crystallographic data for Srbianite, new boron mineral from Ibar Valley, Serbia, Yugoslavia //II Conference of the Serbian Crystallographic Society, Sep. 1993, Abstracts II. — Beograde. **1993**. P. 46 (in Serbian and English).

Obradovic' J., Stamatakis M.G., Aniuic' S., Economou G.S. Borate and borosilicate deposits in the miocene Jarandol basin, Serbia, Yugoslavia //Econ. Geol. **1992**. Vol.87. P.2169−2174.

Stojanovic' D. Srbijanite — novi kalcijum borat hidroksid, $CaB_3O_4(OH)_3$ // I Conf. of the Serbian Crystallographic Soc. Abstracts I. − Beog-

UDC 549.6

NEW OCCURENCE OF NICKELALUMITE ON KARA–CHAGYR, SOUTH KIRGIZIA

Vladimir Yu. Karpenko
Fersman Mineralogical Museum RAS, Moscow, pla@fmm.ru

Atali A. Agakhanov
Fersman Mineralogical Museum RAS, Moscow, pla@fmm.ru

Leonid A. Pautov
Fersman Mineralogical Museum RAS, Moscow, pla@fmm.ru

Tamara V. Dikaya
Fersman Mineralogical Museum RAS, Moscow, pla@fmm.ru

G.K. Bekenova
Satpaev Institute of Geological Sciences, Kazakh AS

The finds of rare nickelalumite was made on occurrences of vanadium-bearing schists of Kara-Chagyr and Kara-Tangi (Batkensk Region, Kirgizia). The mineral forms radiate-fibrous segregations, spherulites up to 1−2 mm in size in assemblage with ankinovichite, volborthite, tyuyamunite, allophane. The mineral colour is from light blue, almost colourless, to dark green. The intensive green colour is due to increased content of vanadium, which enters in the mineral as isomorphous admixture (up to 6.54% V_2O_5). Refractive index of vanadium-free nickelalumite are n_g = 1.533(2), n_p = 1.524(2), high-vanadium nickelalumite n~1.575−1.580 (average index). In the article there are a table of chemical compositions of nickelalumite and the diagrams of correlation dependence for pairs Ni — (sum of divalent cations), S−V, Si−V, Al−Si, Al−S. High-zinc nickelalumite is characteristic for Kara-Tangi, some analyses corresponds to zinc analogue of this mineral. The following scheme of heterovalent isomorphism is proposed: $Al^{3+} + (SO_4)^{2-} \Longleftrightarrow Si^{4+} + (VO_4)^{3-}$, that is also confirmed by IR-spectroscopy data. Taking into account this scheme, the formula of nickelalumite is $(Ni,Zn,Cu^{+2})(Al,Si)_4[(SO_4),(VO_4)](OH)_{12}{\cdot}3H_2O$.
The origin of this mineral is connected to low-temperature alteration of carboniferous-siliceous schists, having increased contents of nickel and zinc. The find of nickelalumite is, obviously, the second in the world.
2 tables, 11 figures, and 6 references.

Looking through the V.I. Kryzhanovskii collections of minerals from vanadium-bearing schists of Kara-Chagyr (Batkensk Region, Sought Kirgizia), which are dated by 1926 year and kept in funds of Fersman Mineralogical Museum, the authors discovered among samples, registered as kolovratite*, the light blue, sometimes whitish crusts, composing by thin needle-shaped radiate-fibrous aggregates. The instrumental diagnostic has shown the mineral, composing the crusts, is nickelalumite, $(Ni,Cu^{+2})Al_4[(SO_4),(NO_3)_2](OH)_{12}{\cdot}3H_2O$, monoclinic system, i. e. extremely rare mineral.

Along with other representatives of this group, mbobomkulite, $(Ni,Cu^{+2})Al_4[(NO_3)_2,SO_4]_2(OH)_{12}{\cdot}3H_2O$, monoclinic system, and hydrombobomkulite, $(Ni,Cu^{+2})Al_4(NO_3,SO_4)_2(OH)_{12}{\cdot}13-14H_2O$, monoclinic system, it occurs only in South Africa in Mbobo Mkulu cave (Martini, 1980). In autumn 2002 we have visited the areas of carboniferous-siliceous schists outcrops in South Fergana, which are most rich in vanadium mineralization (Kara-Chagyr, Kara-Tangi), with the purpose of material collecting for data refinement on a whole number of minerals. Among minerals collected by us the nickelalumite also was found. The find of this rare mineral allows making its detail study.

In spite of extremely rich vanadium and nickel mineralization, vanadium-bearing schists of Mt. Kara-Chagyr (Photo 1) (right slope of middle current of River Isfairamsai, Batkensk Region, Kirgizia) remain a very little studied mineralogical object till now. First mineralogical researches on this area are concerned to work period of Radium expedition, when kolovratite (Vernadsky, 1922; Popov, 1925), volborthite (named «uzbekite») (Fersman, 1928), and also nickel-enriched asbolan-like mineral (Saukov, 1926) were described. Studying Tyuya-Mun mine, A.E. Fersman (1928) broached a geochemistry of processes, occurring of Kara-Chagyr. Unfortunately, these works limit mineralogical and geochemical investigation of Kara-Chagyr till now. The outcrops of secondary minerals on Kara-Chagyr are confined to belt of spreading of uranium-bearing carboniferous-siliceous schists, extending on several hundred kilometers along foothills of Alai range. They belong to Early Carboniferous South Fergana melange complex, which serpentinite matrix contains large blocks of Early

* Today's the status of kolovratite calls in question because the absence of accurate chemical formula and crystal structural data till now, nevertheless, there was not the discredit of the mineral. Jambor and Lachance (1962) make the X-ray data for phase, which by set of chemical elements does not contradict that be consider to kolovratite. Although, the mineral undoubtedly requires completing of study, the authors incline to opinion the kolovratite has the right on existence as independent species.

Paleozoic carboniferous-siliceous rocks, carrying vanadium mineralization. Kara-Tangi is located at the same belt, 25 km westward from village Kadamdzhai. This is uranium deposit, exploited during 1960-th years. Unfortunately, in open press there are no publications on mineralogy of this deposit.

Occurrence

Nickelalumite on Kara-Chagyr was found in dumps and also in primary occurrence at mouth of old mine working among multicoloured mass of nickel and vanadium minerals, developing in the cracks of quartz breccias in carboniferous-siliceous schists. In the samples this mineral looks like recently discovered nickel analogue of alvanite, ankinovichite, $(Ni,Zn)Al_4(VO_3)_2(OH)_{12}\cdot 2H_2O$, monoclinic system. But if ankinovichite forms crystals of good facet, then apexes of nickelalumite crystals often will block, split (Fig. 1a, 1b). The colour of nickelalumite is from light blue, almost colourless, to pistachio-coloured green. The following study has shown that deeper green colour is characteristic for vanadium-bearing minerals, and bluish, almost colourless, segregations do not practically contain vanadium. The mineral forms radiate-fibrous aggregates with length of separate fibres from 0.05 up to 0.1 – 0.5 mm (Fig. 1a, 1b), which is in close assemblage with ankinovichite, volborthite, allophane, tyuyamunite, rarely tangeite. As a rule, nickelalumite forms the crusts of solid spherulite aggregates of light green (Photo 2a, 2b), rich-green (Photo 3) colours. The concentric-zonal structure is observed on cross split of these aggregates. Rarely in the rock cavities it forms practically ideal spheres, growing on lamellar skeletal crystals of volborthite (Photo 4a, 4b). Spherulites sizes reach 1.5 mm. It is interesting to note the different on colour and vanadium content individuals occur together within the bounds of one small cavity.

Often crystal crust of ankinovichite of green colour with different tints and thickness up to 1.5 – 2 mm (Photo 5) grows on spherulite crusts of nickelalumite. Between these crusts, as a rule, there is the allophane intercalation, at the expense of that the upper crust is sufficiently easy separated. Sometimes spherulites of nickelalumite are coved by downy coating of the smallest ankinovichite crystals, which are oriented perpendicular to spherulite surface (Photo 6). In single samples the lamellar crystals of tyuyamunite grows on nickelalumite-ankinovichite spherulites (Photo 7).

At Kara-Tangi deposit nickelalumite was found in the sample from dumps of adit in the right side of the same name sai. Here the mineral forms crystal crust of light blue colour on the surface of carboniferous-siliceous schist. This crust is composed by radiate-fibrous, lamellar aggregates with individual sizes up to 1 – 1.5 mm. Some of nickelalumite spherulites are replaced by allophane (Photo 8). The peculiarity of nickelalumite from Kara-Tangi is increased zinc content, in single crystals zinc prevails on nickel, which corresponds to new phase, zing analogue of nickelalumite (Table 1, analyses №№ 15 – 16).

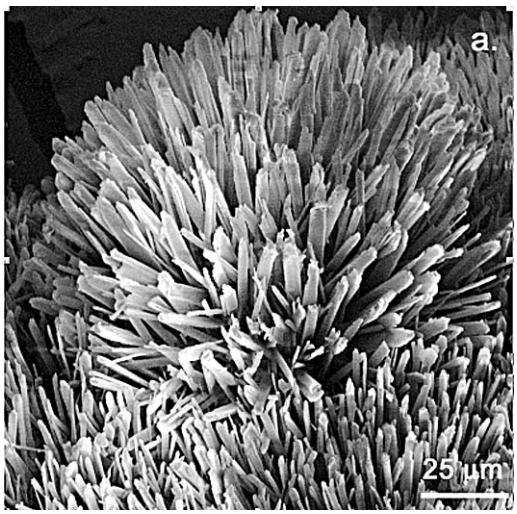

a

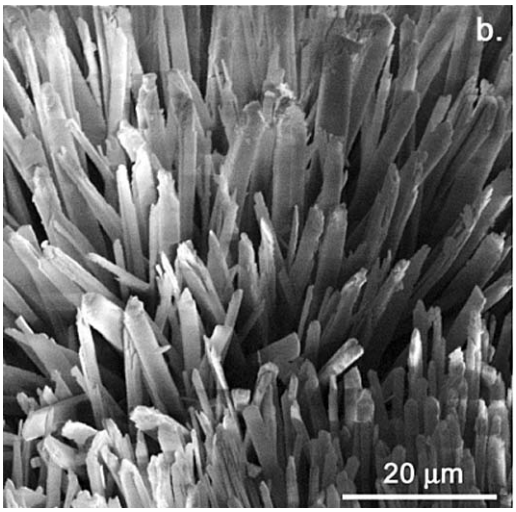

b

FIG. 1. Morphology of non — vanadium nickelalumite spherolites (FMM № 6794). a) A general view of spherolite; b) fragment. SEM- photo

Table 1. Chemical compositions of nickelalumite and its zinc analogue

	1	*2*	*3*	*4*	*5*	*6*	*7*	*8*	*9*	*10*	*11*	*12*	*13*	*14*	*15*	*16*
№№	*597/24 (FMM)*	*6794 (FMM)*	*5341*	*5341*	*5434*	*5439*	*5439*	*5334*	*5360*	*5360*	*5360*	*5360*	*Martini* (1980)	*theoreti* cal	*5360*	*5360*
NiO	12.07	11.00	10.03	8.87	9.81	9.63	9.45	7.77	10.03	9.87	8.08	7.05	6.59	14.34	4.34	2.36
ZnO	0.66	2.04	1.15	0.34	1.92	2.40	2.05	2.25	4.83	4.88	6.24	6.64	0.00		9.45	13.02
CuO	0.00	0.12	1.10	0.31	1.63	1.90	2.44	0.95	0.22	0.1	0.52	0.72	2.35		0.95	0.06
FeO	0.02	0.00	0.00	0.00	0.24	0.08	0.00	1.80	0.03	0.29	0.33	0.02	0.00		0.41	0.20
Al_2O_3	38.05	37.78	36.35	38.99	40.35	37.19	36.23	38.77	38.83	37.67	37.73	37.76	39.30	39.15	37.85	39.42
SiO_2	0.77	0.45	1.08	0.61	0.00	3.76	2.12	1.10	0.69	0.41	0.64	0.38	8.95**		0.42	0.52
SO_3	14.45	14.19	11.99	13.10	11.63	9.44	10.36	11.96	14.80	14.11	14.54	14.38	10.28	15.38	14.54	14.63
V_2O_5	0.00	0.06	5.40	5.60	5.24	6.54	5.62	5.07	0.00	0.21	0.11	0.04	0.00		0.00	0.06
H_2O	31.10	31.10	31.10	31.10	31.10	31.10	31.10	31.10	31.10	31.10	31.10	31.10	28.53	31.10	31.10	31.10
Total	**97.12**	**96.74**	**98.20**	**98.92**	**101.92**	**102.04**	**99.37**	**100.77**	**100.53**	**98.64**	**99.29**	**98.09**	**100.70**	**99.97**	**99.06**	**101.37**
Formula calculated on 4 (Al + Si)																
Ni^{+2}	0.85	0.79	0.73	0.61	0.66	0.65	0.68	0.53	0.69	0.71	0.58	0.51	0.75	1.00	0.31	0.16
Zn^{+2}	0.04	0.13	0.08	0.02	0.12	0.15	0.14	0.14	0.31	0.32	0.41	0.44			0.62	0.82
Cu^{+2}	0.00	0.01	0.08	0.02	0.10	0.12	0.16	0.06	0.01	0.01	0.03	0.05	0.25		0.06	0.00
Fe^{+2}	0.00	0.00	0.00	0.00	0.02	0.01	0.00	0.13	0.00	0.02	0.02	0.00			0.03	0.01
$\Sigma(Me^{+2})$	**0.89**	**0.93**	**0.89**	**0.65**	**0.90**	**0.93**	**0.98**	**0.86**	**1.01**	**1.06**	**1.04**	**1.00**	**1.00**	**1.00**	**1.02**	**0.99**
Al^{+3}	3.93	3.96	3.90	3.95	4.00	3.68	3.81	3.91	3.94	3.96	3.94	3.97	4.00	4.00	3.96	3.96
Si^{+4}	0.07	0.04	0.10	0.05	0.00	0.32	0.19	0.09	0.06	0.04	0.06	0.03			0.04	0.04
(Al+Si)	**4.00**	**4.00**	**4.00**	**4.00**	**4.00**	**4.00**	**4.00**	**4.00**	**4.00**	**4.00**	**4.00**	**4.00**	**4.00**	**4.00**	**4.00**	**4.00**
S^{+6}	0.95	0.95	0.82	0.84	0.73	0.60	0.69	0.77	0.69	0.95	0.97	0.96	0.75	1.00	0.97	0.93
V^{+5}	0.00	0.00	0.32	0.32	0.29	0.36	0.33	0.29	0.33	0.01	0.01	0.00			0.00	0.00
(S+V)	**0.95**	**0.95**	**1.14**	**1.16**	**1.02**	**0.96**	**1.02**	**1.06**	**1.02**	**0.96**	**0.98**	**0.96**	**0.75**	**1.00**	**0.97**	**0.93**
$(OH)^-$	11.95	12.00	11.28	10.71	11.47	11.91	11.78	11.40	11.71	12.23	12.17	12.11	12.00	12.00	12.14	12.16
H_2O	3.12	3.23	3.81	3.56	2.99	2.20	3.37	3.17	3.08	3.15	3.12	3.19	3.00	3.00	3.15	2.75

Note:
All analyses are performed by microprobe (except № 13 — wet chemistry (Martini, 1980)). The contents of H_2O (except analysis 13) are theoretical. The content of N_2O_5 is 4.70% (0,50 apfu) for № 13 and undetermined for other samples.
1–8 — Nickelalumite, Kara-Chagyr: 1–2 — light blue needle-shaped, 3–4 — light green spherulites, 5–7 — central zone of dark-green spherulite, 8 — green spherulite. 9–12 — Nickelalumite, Kara-Tangi: light blue radiate-fibrous segregations. 13 — Nickelalumite, Mbobo Mkulu (S. Africa) (** — admixtures of opal and allophane). 14 — Nickelalumite, theoretical values. 15–16 — Zinc analogue of nickelalumite, Kara-Tangi: light blue radiate-lamellar segregations.

Chemical composition

The chemical composition of nickelalumite was studied in polished preparations on electron microprobe JXA-50A with energy-dispersive spectrometer Link (Tabl. 1). The experimental conditions were as follows: accelerating voltage 20 kV, absorbed electron current 3×10^{-9} A. The standards: microcline USNM 143966 (Si, Al), ilmenite USNM 96189 (Fe), gahnite USNM 145883 (Zn), metallic V and Cu (V, Cu), NiO (Ni), barite (S). The concentrations were calculated using ZAF-correction. Formula was recalculated on 4 atoms (Al+Si).

The samples from Kara-Chagyr and Kara-Tangi with different colour and morphology were analyzed. The wide variation of components contents in nickelalumite attracts attention. Because of paucity of analytical data on chalcoalumite group minerals, there are no sufficient data for estimation of possible izomorphous variations within the group limits till now. The results of our analyses allow partly filling this gap. The correlation diagrams of dependence between contents of main components of the mineral demonstrate availability of isomorphism between divalent cations and also between silica, sulfur, and vanadium (Fig. 2a-2e). The isomorphism between divalent metals (mainly between nickel and zinc) brings to continuous series from zing-free nickelalumite up to its zinc analogue. Taking into account the constant presence of small amounts of copper, there is, probably, an isomorphism in threefold system nickelalumite — chalcoalumite — zinc analogue of nickelalu-

mite.

More complicated scheme of isomorphism is visible between Al, Si, S, and V. The negative dependences between pairs Al-Si and V-S, the positive trends between contents of silica and vanadium, and also aluminum and sulfur are observed. In all probability, vanadium is present as anion $(VO_4)^{3-}$, that is indirectly confirmed by IR-spectroscopy data. Thus, the following scheme of isomorphism is seems to be probable: $Al^{3+} + (SO_4)^{2-} \Longleftrightarrow Si^{4+} + (VO_4)^{3-}$.

It is obvious from this equation, that excess positive charge, arising from partial replacement of aluminum by silica, can be compensated by excess negative charge, which is introduced, in our case, by anion $(VO_4)^{3-}$. Thus, taking in account this scheme of isomorphism, the ideal formula of nickelalumite from Kara-Chagyr can be record as following: $(Ni,Zn,Cu^{+2})(Al,Si)_4[(SO_4),(VO_4)](OH)_{12}{\cdot}3H_2O$.

Nickelalumite from Kara-Tangi is practically vanadium-free, whereas on Kara-Chagyr the content of vanadium fluctuates in wide range, up to significant vanadium variety. The characteristic distinction of nickelalumite with different chemical composition is the colour of the sample. As a rule, vanadium-free nickelalumite forms light blue, almost colourless crystals, while vanadium one has green colour of different tints, from light green to grass deep green. The central parts of some spherulites from Kara-Chagyr are enough high-vanadium (see analyses №№ 5—7, Tabl. 1), whereas the peripheral part is depleted by vanadium. Because of that there is a probability of existence of phase with predominance of $(VO_4)^{3-}$ over $(SO_4)^{2-}$, i. e. the mineral, which is vanadium analogue of nickelalumite.

Optical properties. X-ray data

Under microscope vanadium-free nickelalumite is transparent, almost colourless. Its crystals are flattened prismatic and rich in length up to 0.1 mm. Nickelalumite is optically biaxial, negative. The mineral extinction is oblique, extinction angle relatively to crystal elongation is 40°, $n_g = 1.533(2)$, $n_p = 1.524(2)$. The aggregates of vanadium-bearing nickelalumite under microscope have fine-fibrous structure; here it was possible to measure the middle index n ~ 1.575—1.580 (for sample № 5439, analyses №№ 5—6 in Tabl. 1). Nevertheless, it is evident, that the presence of vanadium leads to increasing of refractive indexes of this mineral.

X-ray data are in the Tabl. 2. It is necessary to note that most satisfactory data was per-

Table 2. X-ray powder data for nickelalumite

1		*2*		*3*		
I	*d/n*, Å	*I*	*d/n*, Å	*I*	*d/n*, Å	*hkl*
10wb	8.35	10wb	8.54	100	8.543	0 0 2
				20	7.877	0 1 1
3	6.61			5	6.667	1 1 0
		1wb	6.35	5	6.364	1 1 -1
				5	6.073	1 1 1
					5.431	1 1 -2
		3wb	5.00	5	5.095	1 1 2
				10	4.778	0 1 3
3wb	4.62			10	4.577	2 0 -2
9	4.27	9	4.26	60	4.267	0 0 4
				10	4.179	2 0 2
2wb	3.71					1 1 -4
5	3.30	3	3.36	2	3.332	2 2 0
4	3.16	2	3.16	5	3.177	2 2 -2
6	3.02	3	3.01	10	3.044	3 1 1
6	2.683	1wb	2.700	5	2.718	1 3 -2
				2	2.623	0 3 3
2	2.592					2 1 5
8	2.508	7	2.516	15	2.507	1 3 3
		3	2.412			2 3 2
7	2.276	8	2.282	15	2.289	1 2 6
3	2.222	1	2.210	5	2.208	-4 1 4
		<1	2.140			2 3 4, 1 4 1
2	2.067			1	2.098	2 2 6
				1	2.027	2 4 0, 3 3 3
9	1.981	9	1.993	20	1.997	2 3 5
				1	1.899	2 0 8, 0 0 9
				1	1.855	-4 0 7, 3 4 -1
3	1.824					1 3 7
3	1.811	1	1.811	5	1.81	1 4 5
4	1.740					1 4 -6, 1 5 -1
4	1.710	2	1.714	10	1.72	209
1	1.647					5 3 1 , 4 4 1
3	1.556	2	1.558	1	1.56	319
6	1.480	7wb	1.479			
6	1.455	7wb	1.457			
4	1.400	1	1.397			
4	1.361					
		2	1.350			
1	1.302					
1	1.272					
1	1.241					
1	1.217	1	1.221			
4	1.189	4	1.188			
		3	1.122			

Experimental conditions (1-2): CuKa radiation, Ni filtre, RKD-57.3, the preparation is rubber post.
1 — Nickelalumite (vanadium-free), Kara-Chagyr (specimen 6794, FMM).
2 — Vanadium-bearing nickelalumite, Kara-Chagyr (specimen 5332).
3 — Nickelalumite, Mbobo Mkulu (Martini, 1980);
wb — wind band

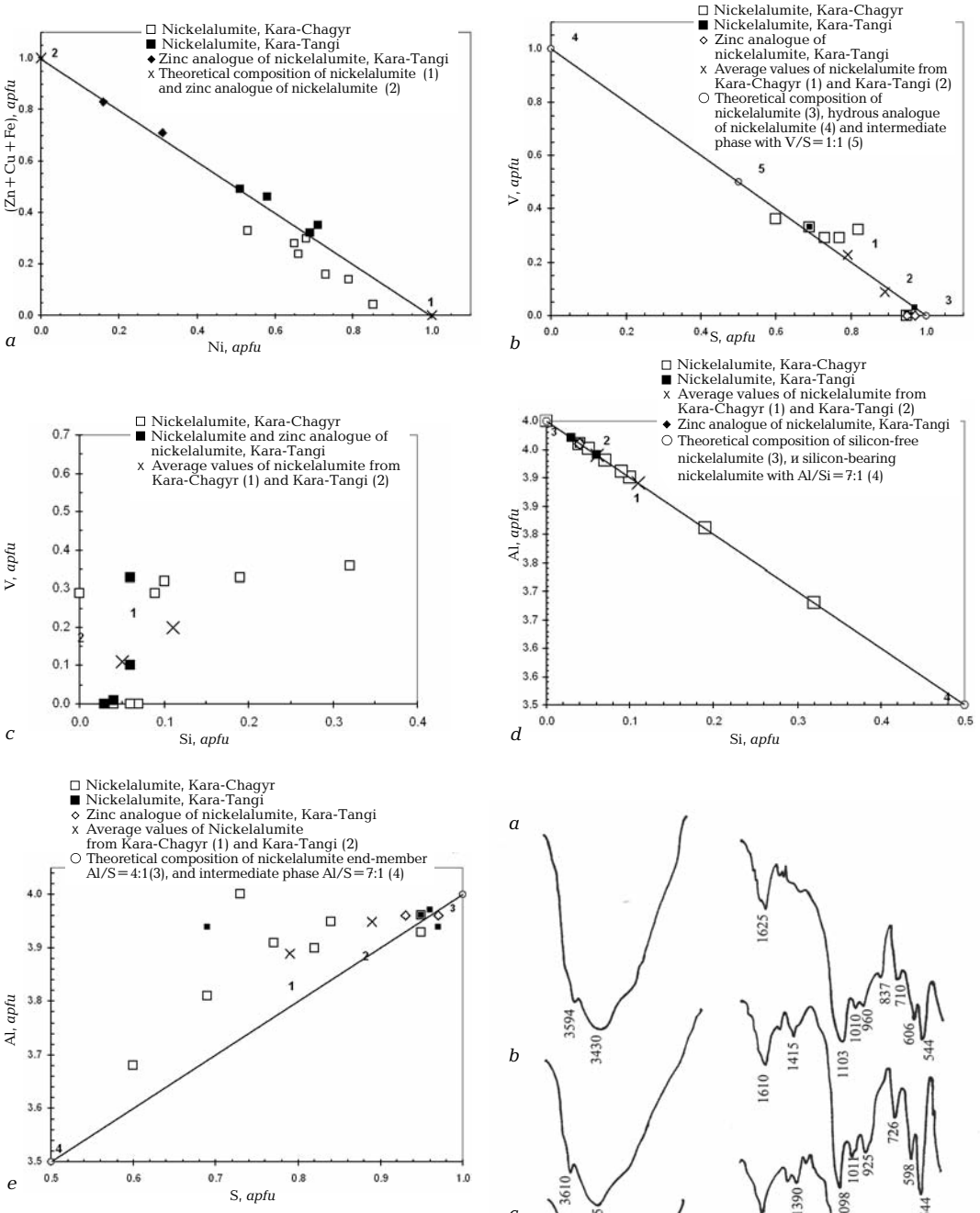

FIG. 2. Crystallochemical dependence for nickelalumite and it's Zn-analogue: a) S (2-valence metals) versus Ni; b) V versus S; c) V versus Si, d) Al versus Si; e) Al versus S

FIG. 3. IR-spectra of nickelalumite and chalcoalumite:
a) chalcoalumite, Grand Canyon, Az., USA, FMM № 79266;
b) nickelalumite non-vanadious (light acicular xls), Kara-Chagyr, Kirgizia, FMM № 597/24;
c) nickelalumite vanadious (apple-green spherolites), Kara-Chagyr, Kirgizia, № 5434

formed by photomethod (URS-50, CuKα radiation, Ni filter, camera RKD-57.3). The quality of diagram was extremely low, that is, apparently, connected to texturization of the sample during preparation.

IR–spectroscopy

IR-spectra of studied nickelalumite, and also, for comparison, chalcoalumite, are on Fig. 11a-11c. The spectrum of pure nickelalumite is very close to that of chalcoalumite, which is confirmed the structural closeness of two minerals. The bands 598 – 606, 1010 – 1011, and 1098 – 1103 cm^{-1}, connected to oscillations of SO_4-tetrahedra, are characteristic. The band 1098 – 1103 cm^{-1} of both the pure nickelalumite, and chalcoalumite differs by enough intensity with respect to the band 1010 – 1015 cm^{-1}, that is peculiar to sulphates, which compositions the significant isomorphous admixtures is not observed in. At the same time for vanadium-bearing nickelalumite the intensity of the band 1092 cm^{-1} is significant decreased. This fact is known to be connecting with activization of full-symmetrical valent oscillations of SO_4-tetrahedra that, in its turn, is caused by violation of local symmetry at the isomorphous replacement of sulphate anion by other one. Moreover, in the spectra of vanadium-bearing nickelalumite (the data for several samples was made) the appearance of small additional band in the range 750 – 800 cm^{-1} is observed. Very probable this band is connected to oscillations of V^{+5} in tetrahedron coordination (the same bands are characteristic for vanadates, for example, descloizite, tyuyamunite *et cetera*). Thus, IR-spectroscopy data do not contradict to our assumption about isomorphous replacement of $(VO_4)^{3-}$ and $(SO_4)^{2-}$ groups. At last, the absence of pronounced band 3590 – 3610 cm^{-1} in «water» area of spectre of vanadium-bearing nickelalumite indicates the structural changes, taking place in it. It is necessary to note, that on IR-spectra of nickelalumite in the range 1390 – 1415 cm^{-1} there is a small band, which is evidence of the present of small amount of nitrate component in the mineral. Unfortunately, we cannot yet confirm the presence of nitrogen by other methods. Microprobe analysis is unacceptable in this case, the mineral is almost on one third consists of water, that assumes its extremely unstable behaviour under the electron beam.

The verification of nitrate presence by qualitative reactions did not succeed. Vanadium is presence in our samples everywhere and prevents the reaction on nitrate-ion with diphenyl-amin. Reaction with alkali and Deward alloy turns out insufficiently sensible. We shall note in nickelalumite from type locality there are enough large amount of $(NO_3)^-$ anion up to formation of its nitrate analogue, mbobokulite.

Genesis

Apparently, the low-temperature hydrothermal processes play a considerable part in genesis of nickelalumite from Kara-Chagyr, which was noted by A.E. Fersman (1928). The presence of such rare mineral on Kara-Tangi is evident, in all probability, of community of the processes of late mineral formation, which take place in black schist rocks of South Fergana. The origin of nickelalumite along with such minerals as ankinovichite, kolovratite, and also some unnamed nickel-zinc silicates is undoubtedly connected to increased contents of nickel and zinc in these schists. The find of nickelalumite in South Kirgizia is, evidently, the second in the world.

Acknowledgments

The authors are grateful to geologists of South Kirgizian GRE V.N. Bobylev and V.C. Gurskii, chief geologist AO «Alaurum» (Osh, Kirgizia), V. Smirnov for assistance in field works, chief curator of Fersman Mineralogical Museum RAS (Moscow, Russia) M.E. Generalov for Kara-Chagyr samples, given to study, and also N.V. Chukanov (Institute of Problems of Chemical Physics RAS, Chernogolovka, Moscow Region) for help in interpretation of IR-spectra. The authors express their special gratitude to N.A. Pekova, making the photos of samples.

References

Fersman A.E. To morphology and geochemistry of Tyuya-Muyun // Trudy po izucheniyu radiya i radioaktivnykh rud. **1928**. P. 3. P. 1 – 90. (Rus.)

Jambor J.L., Lachance G.R. On kolovratite// *Can.Mineral.* **1962.** 7. P. 311 – 314.

Martini J.E.J. Mbobokulite, hydrombobokulite, and nickelalumite, new minerals from Mbobo Mkulu cave, eastern Transvaal//Annals.Geol. Survey S. Africa 14. **1980**. № 2. P. 1 – 110.

Popov P.I. Preliminary announcement about prospecting of Kara-Chagyr // Trudy Turk. Nauch. O-va. **1925.** V. 2. P. 185 – 188. (Rus.)

Saukov A.A. Investigation of manganese mineral from Kara-Chagyr of Fergana Region. GRI 23 II 1926 // Dokl. AN SSSR. **1926.** Ser. A. April. P. 77 – 79. (Rus.)

UDC 549.621.4

KALSILITE IN THE ROCKS OF KHIBINY MASSIF: MORPHOLOGY, PARAGENESIS, GENETIC CONDITIONS

Olga A. Ageeva,
Institute of Ore Deposit Geology, Petrography, Mineralogy and Geochemistry RAS, Moscow, ageeva@igem.ru

Boris Ye. Borutzky
Institute of Ore Deposit Geology, Petrography, Mineralogy and Geochemistry RAS, Moscow, ageeva@igem.ru

Kalsilite in Khibiny massif is typical for poikilitic nepheline syenites (ristschorrites) where it occurs in close intergrowth with nepheline and orthoclase. This mineral is observed in the nepheline grains as veinlets, segregations of irregular shape or rims at the boundaries of nepheline and orthoclase grains. Also it occurs in the composition of radiate-fibrous kalsilite-orthoclase intergrowths, as a rule, framing nepheline grains.
Formation of kalsilite is determined to concern to most early stage of K-Si-metasomatosis, influencing on massive coarse-grained urtites. It is caused by strong increasing activity of potassium relatively to sodium. Nepheline of initial rocks was the matrix for kalsilite formation, which was accompanied and changed by formation of other potassium minerals, including the main rock-forming mineral of ristschorrites — potassium feldspar.
Different chemical activity of potassium and silica, which has determined kalsilite presence, degree of its development, and other peculiarities of ristschorrites mineralogy, is caused by both the character of replaced rocks, and the chemical composition of influencing solutions (the potassium concentration in them).
4 tables, 3 figures, and 24 references.

The problem of kalsilite formation in ristschorrites of Khibiny massif (Kola peninsula) as a problem of genesis of ristschorrites themselves is a discussion subject till now. We shall note that ristschorrites (poikilitic nepheline syenites) in Khibiny massif are spatially connected to massive coarse-grained urtites and form together with them the gradual transitions across the rocks of intermediate composition (juvites, feldspar urtites *etc.*). Together with rocks of ijolite-urtite complex they compose the Central Arc of Khibiny massif, which is located between nepheline syenites: khibinites (outside) and foyaites (inside). On quantitative-mineral composition ristschorrites corresponds to «common» nepheline syenites of this massif (khibinites, foyaites *etc.*), having, as it is known, primary magmatic genesis, but on a number of mineralogical and petrological features are distinguished from them. First of all they are characterized by strongly pronounced poikilitic structure, very inconsistent mineral composition and irregular granularity (the size of feldspar poikilocrystals fluctuates from 1 up to 15 cm, and its content — from 50% to 80%). Their high-potassium chemical composition is their second peculiarity: ristschorrites are strongly stood out against all rocks of Khibiny massif by its increased content of potassium (Table 1). That is caused, first of all, by feldspars in them do not have potassium-sodium chemical composition as in common nepheline syenites, but significantly potassium one (in ristschorrites the adularia-like orthoclase is most widespread).

From the beginning of research of geological structure of Khibiny massif till now the alternative hypotheses of magmatic (N.A. Eliseev, S.I. Zak, A.V. Galakhov, T.N. Ivanova, A.A. Arzamastsev *et al.*) and metasomatic (L.L. Solodovnikova, I.P. Tikhonenkov, B.Ye. Borutzky *et al.*) genesis of ristschorrites are developed. The discovery of potassium analogue of nepheline, kalsilite, in ristschorrites (Borutzky etc., 1973, 1976) was unexpected, raised a number of new problems before mineralogists, and resulted in appearance of new views on the ristschorrites genesis, and, in particular, on source of potassium, which is necessary to formation of such high-potassium rocks within the bounds of significantly sodium agpaitic nepheline syenites massif.

In ristschorrites kalsilite plays, as a rule, the role of accessory mineral and yields to nepheline on its content in the rock, but in some areas its amount is strongly increased. The optical properties of these two feldspathoids are very close to each other, which make some difficulties in diagnostics and study of kalsilite segregation forms. But just the occurrence form of kalsilite and the character of its relations with nepheline and feldspar are the most important indicator features, allowing to detect the mechanism of its formation in the rocks, and, consequently, to reconstruct the history of formation of these rocks. In this article there are the new results of detail study of chemical composition, segregation forms of kalsilite and its relations with other minerals in the rocks of Khibiny massif, which was performed by high-permission scanning microscope JSM-5300 with X-ray energy-dispersive spectrometer Link ISIS.

Kalsilite occurrences in the rocks of different genesis

Kalsilite is widespread only in the alkaline rocks of ultrapotassium series. As a rock-forming mineral it is noted in the rocks of different genesis: volcanites, intrusive and metasomatic rocks. In ultrapotassium ultrabasic volcanites from Uganda (Holmes, 1942), Nyragongo (Zaire), Saint Venanzo (Italy) kalsilite is associated with diopside, olivine, pyroxene, biotite, perovskite, glass etc. From leucocratic minerals, besides kalsilite, the leucite, melilite, and nepheline can be present in these rocks. Kalsilite is mainly observed in small-grained matrix in assemblage with other feldspathoids and feldspar or without them, rarely it occurs in the compound macro- and micropertite intergrowths in nepheline phenocrysts, which is considered as the structures of disintegration of solid kalsilite-nepheline solution (Sahama, 1960; Aurissicchio, Federico, 1985).

In alkaline rocks of ultrapotassium intrusive complexes the morphology of kalsilite segregations and the character of its intergrowths with other minerals are very diverse that in a number of cases complicates their interpretation. Often it is observed the thin dactyloscopic and subgraphic intergrowths of kalsilite with potassium feldspar, which have the distinct eight-angle and ovoid contours and are interpreted as pseudoleucite, the product of postcrystalization disintegration of leucite. The most important criteria for such explanation are the preservation of crystallographic contours of tetragonthreeoctahedron and equal molecular ratio of kalsilite and potassium feldspar (1:1) in the bounds of «intergrowth». That sort of intergrowths is observed in kalsilite-orthoclase syenites (synnyrites) of Synnyr, Yakshin (Pribaikalia), Murun, Sakun (East Transbaikalia) and other massifs. The content of kalsilite in synnyrites of Synnyr massif reaches 20—35% at 60—75% of orthoclase. The phenocrysts of pseudoleucite up to 20 cm in size compose from 10 to 60% of the rock volume and occur in small-grained matrix, consisting of potassium feldspar, nepheline, and pyroxene (Kurepin, 1973).

However, in the rocks of these massifs there are the other types of intergrowths: micrographic kalsilite-(nepheline)-feldspar intergrowths without distinct shape and fixed mineral ratios, irregular poikilitic ingrowths of

Table 1 Chemical composition (wt %) of poikilitic nepheline syenites and contacting with them rocks of Khibiny massif

	urtite	*nepheline syenite*		*ristschorrite-I*	*ristschorrite-II*			*ristschorrite-III*	
№ of sample / *Constituents*	*1*	*2*	*3*	*4*	*5*	*6*	*7*	*8*	*9*
SiO_2	43,19	54,45	58,95	57,93	54,56	55,98	52,86	56,06	54,02
TiO_2	0,79	1,43	0,44	0,19	0,98	0,57	1,57	0,07	0,16
ZrO_2	0,04	0,051	0,018	0,033	0,016	0,03	0,03	0,002	0,002
Nb_2O_5	0,01	0,032	0,013	0,002	0,018	0,01	0,08	0,001	0,001
P_2O_5	3,81	0,224	0,123	0,038	0,051	0,58	0,41	0,059	0,015
Al_2O_3	23,32	24,13	20,65	23,90	21,38	18,26	18,96	22,66	20,82
Fe_2O_3	3,53	4,50*	3,62*	1,43*	3,78*	2,20	2,96	1,14*	2,51*
FeO	1,47	—	—	—	—	0,56	2,71	—	—
MgO	0,10	0,53	0,61	0,17	0,30	0,19	0,15	0,09	0,14
MnO	0,07	0,146	0,151	0,044	0,078	0,07	0,72	0,017	0,033
CaO	5,94	1,35	0,61	0,18	1,23	0,95	1,41	0,628	0,21
SrO	0,42	0,158	0,024	0,017	0,131	0,13	0,10	0,066	0,025
BaO	0,12	0,311	0,044	0,065	0,316	0,24	0,10	0,060	0,092
Na_2O	10,46	6,47	7,07	8,41	5,58	3,22	4,85	5,22	1,45
K_2O	5,33	6,68	6,21	6,97	10,33	12,38	12,44	13,11	19,66
Rb_2O	0,009	0,014	0,023	0,026	0,029	0,035	0,085	0,096	0,132
Cl	0,03	0,047	0,021	0,018	0,034	0,17	0,39	0,018	0,056
S	0,25	0,02	0,01	0,02	0,03	0,17	0,16	0,12	0,07
Loss	1,4	—	—	—	—	0,41	0,43	—	—
Total	100,47	100,54	98,59	99,44	98,84	96,26	100,38	99,41	99,96

Note.
Analyst A.I. Yakushev, Philips Analytical (PW2400) IGEM RAS. The distribution of Fe^{+2}/Fe^{+3} was performed by method of wet chemistry, analyst O.G. Unanova.
Analyses: 1 — massive coarse-grained urtite (hole 1456, Mt. Rasvumchorr); 2-3 — nepheline syenites: 2 — khibinite (from indigenous outcrop, Mt. Takhtarvumchorr), 3 — foyaite (Northern Ristschorr ravine); 4 — micaceous ristschorrite of I group, analyses 3—4 was made from one sample, representing the zone of sharp contact of ristschorrite and foyaite; 5 — micaceous ristschorrite of II group (Mt. Kukisvumchorr); 6—7 — pyroxene ristschorrite of II group (Mt. Rasvumchorr); 8—9 — ultrapotassium ristschorrites of III group (hole 1292, Mt. Poachvumchorr). The dash is the absence of data. * — The sum of iron, detected as Fe_2O_3.

Table 2. Chemical composition (wt %) of nepheline and alkaline feldspar from the rocks of Khibiny massif

№ of sample	Nepheline					Alkaline feldspar				
Constit.	1	2	3	4	5	6	7	8	9	10
SiO_2	44,30	44,79	42,50	40,77	43,33	64,98	61,64	63,36	64,13	64,95
$Al2O_3$	31,94	32,11	31,43	32,67	31,05	19,44	18,05	17,64	18,24	17,48
Fe_2O_3	0,91	0,65	0,83	1,30	1,68	0,31	0,19	0,95	0,46	1,23
CaO	0,00	0,02	0,00	0	0,14	0,36	0,21	0	0,01	0,26
BaO	0	0	0	0	0	0	3,36	0,48	0,04	
Na_2O	16,67	17,15	17,29	16,33	14,37	5,02	2,81	0,74	0,45	0,62
K_2O	5,81	6,15	8,08	8,79	8,82	9,20	12,36	15,72	15,54	16,17
Rb_2O	0	0	0	0	0	0	0	0,030	0,110	no data
Total	99,63	100,87	100,13	99,86	99,39	99,31	98,62	98,92	98,98	100,70
	Numbers of ions on the basis of									
	cations sum = 12					cations sum = 5				
Si	1,09	1,09	1,03	1,00	1,09	2,95	2,91	2,97	3,00	2,99
Al	0,93	0,92	0,90	0,95	0,92	1,04	1,00	0,98	1,01	0,95
Fe	0	0	0	0	0	0,01	0,01	0,03	0,02	0,04
Ca	0	0	0	0	0	0,02	0,01	0	0	0,01
Ba	0	0	0	0	0	0	0,06	0,01	0	0
Na	0,80	0,81	0,82	0,78	0,70	0,44	0,26	0,07	0,04	0,06
K	0,18	0,19	0,25	0,28	0,28	0,53	0,74	0,94	0,93	0,95
Rb	0	0	0	0	0	0	0	0	0,002	0
O	16,27	16,19	15,80	15,79	16,24	7,99	7,92	7,97	8,03	7,98

Note.
Analyses: 1–5 — nepheline: 1–2 — from the zone of contact of ristschorrite and nepheline syenite (foyaite), Northern Ristschorr ravine, an. 1 — from foyaite; an. 2 — from ristschorrite of I group; an. 3 — from massive coarse-grained urtite (Mt. Rasvumchorr); an. 4 — from pyroxene ristschorrite of II group (Mt. Rasvumchorr); an. 5 — from ultrapotassium ristschorrite of III group (Mt. Poachvumchorr); 6–10 — feldspars: an. 6 — from nepheline syenite — foyaite (Mt. Partamchorr), an. 7 — from pyroxene ristschorrite of I group; an. 8 — from massive coarse-grained urtite (Mt. Yukspor); an. 9 — from pyroxene ristschorrite of II group (Mt. Rasvumchorr); an. 10 — from ultrapotassium ristschorrite of III group (Mt. Poachvumchorr). Analyses 1–5, 7 — analyst V.V. Khangulov (Camebax SX-50, IGEM RAS), analyses 6, 8-9 (Borutzky, 1988); an. 10 — analyst N.V. Trubkin (JSM-5300 + Link ISIS, IGEM RAS).

kalsilite and nepheline in feldspar, kalsilite poikilocrystals with inclusions of dark-coloured minerals etc. An appearance of these forms can be caused by different reasons. Formation of the ones is explained by direct eutectic or cotectic magmatic crystallization from the melt (Smyslov, 1986, and others), for others — by «feldspathization» of nepheline (Arkhangel'skaya, 1965) or reactionary replacement of earlier feldspar by kalsilite (Bagdasarov, Luk'yanova, 1969; Samsonova *et al.*, 1968). In Murun massif the new type of kalsilite-bearing rocks is detected. It is the analogue of feldspar-free rocks of urtite-jacupirangite series, which kalsilite instead nepheline is developed in (Konev, 1985; Konev *et al.*, 1996). According to (Konev, 1985), these rocks have the primary magmatic origin, but in a number of alkaline complexes, Ozerskii, Tazheran (Priolkhonye), Murun, the typical metasomatic kalsilite-bearing rocks, kalsilitized skarns, are noted (Konev, Samoilov, 1974).

It is necessary to record that in above-mentioned intergrowths with orthoclase in most of enumerated massifs the nepheline can be present instead kalsilite and together with it, forming the same segregation shapes as kalsilite. In Lugijn Gol massif (Mongolian People's Republic) «pseudoleucitic syenites» are widespread, which do not absolutely contain kalsilite (Kovalenko *et al.*, 1974). The leucocratic part of these rocks has nepheline-feldspar composition. Nepheline and potassium feldspar form globular «pseudoleucite» intergrowths, which are considered as the product of disintegration of K,Na-analcime or reaction of primary potassium leucite with sodium melt (Kononova *et al.*, 1981).

Kalsilite in the rocks of Khibiny massif

In Khibiny massif kalsilite is widespread in the rocks of ristschorrites complex. For the first time it was detected in juvites at apatite deposit Yukspor (Borutzky *et al.*, 1973). Later the kalsilite-bearing rocks (ristschorrites and juvites) were noted in region of mountains Eveslogchorr, Poachvumchorr, Kukisvumchorr, Rasvumchorr, and others. Although within the bounds of studied massif in the most of cases kalsilite associates with nepheline, the ris-

tschorrites strongly enriched by kalsilite (up to 15—20%) and practically without nepheline (Kozyreva *et al.*, 1990). The zones of ultrapotassium rocks are more characteristic for inner side of ijolite-urtite arc, i.e. for its upper (in geological section) parts. Also enrichment by kalsilite is noted for ristschorrites, joined to hanging wall of ore rock mass of apatite-nepheline deposits (Kozyreva *et al.*, 1990).

All ristschorrites of Khibiny massif can be divided into three groups by kalsilite presence and degree of its development:

I group — ristschorrites, non-containing kalsilite

These ristschorrites are noted near the contacts of considered rocks with nepheline syenites (khibinites, foyaites *et al.*), and sometimes at significant distance from those contacts. In near-contact zones they contain the areas, composed by relics of nepheline syenites. By content of main petrogenic elements these ristschorrites (Table 1, an. 4) are close to «common» nepheline syenites (Table 1, an. 2—3). On the diagram SiO_2-Na_2O-K_2O the points, corresponding to compositions of both rocks, fall into the same field and approach to the point, conforming the chemical composition of potassium-sodium feldspar (Fig. 1). In comparison with other groups of ristschorrites these rocks are less potassium and more silicic.

The peculiarity of this rocks group, contrary to tendency established for ristschorrites, is the slightly increased content of sodium in feldspar (Table 2, an. 7) and presence in this feldspar the corroded and redistributed albite pertite intergrowths, i.e. relic potassium-sodium feldspars (Tikhonenkov, 1963; Borutzky, 1988; Borutzky *et al.*, 1975, 1986). Among accessories the potassium-free and low-potassium alkaline minerals prevail: lamprophyllite $Na_2Sr_2(Ti,Fe,Mn)_3(SiO_4)_4(OH,F)_2$, sodium eudialyte $Na_{15}Ca_6Fe_3Zr_3Si_{26}O_{73}(OH,Cl)_5$, aenigmatite $NaFe_5TiSi_6O_{20}$.

II group — ristschorrites and juvites with low content of kalsilite (from 0.1 to 5%)

In Khibiny massif this group is most widespread. On the diagram SiO_2-Na_2O-K_2O the position of points, corresponding to most potassium compositions of rocks of this group, is close to orthoclase (Fig. 1).

Kalsilite (Table 3, an. 1—7) by its content in rock significantly yields to nepheline, which in its turn is characterized by increased content of potassium (Table 2, an. 4). Feldspar has considerably potassium composition (Table 2, an. 9). The increased content of rubidium (Table 2, an. 8—9) is noted in it that can be connected to high-alkali conditions of these rocks formation (Borutzky, 1988). Among accessories there are potassium and potassium-containing minerals: astrophyllite, magnesioastrophyllite, wadeite, delhayelite, fenaksite, scherbakovite (Table 4, an. 1, 3—5) *etc.*, and potassium-enriched varieties of sodium minerals: potassium eudialyte, potassium barytolamprophyllite (Table 4, an. 6—7) *et al.* From dark-coloured rock-forming minerals there are aegirine, alkali amphibole, and biotite. The minerals, determined in this group of ristschorrites, as a rule replace the primary minerals of initial urtites (nepheline, aegirine-diopside, titanite, Sr-lamprophyllite, Na-eudialyte *etc.*), which relics are constantly discovered in these rocks.

Kalsilite occurs both independently (Fig. 2a) and in intergrowth with nepheline, forming poikilitic ingrowths in feldspar. It is observed as veinlets, cutting the nepheline crystals (Fig. 2b, 2c), which in longitudinal (rectangular) sections of nepheline crystals are parallel, and in cross (hexagonal) ones are subparallel and situated fan-shaped to each other. In longitudinal sections the kalsilite veinlets parallel each other cuts the nepheline crystal parallel axis [001] or diagonally. Often the intergrowths of kalsilite and nepheline in orthoclase poikilocrystals of ristschorrites have irregular intricate shape (Fig. 2d). In a number of cases the intersection of several close to each other nepheline grains by the same veinlet of kalsilite was documented. The veinlets as a rule have very insignificant thickness (n × 0,01 mm) and are broken in the contacts of nepheline with feldspar (Fig. 2e).

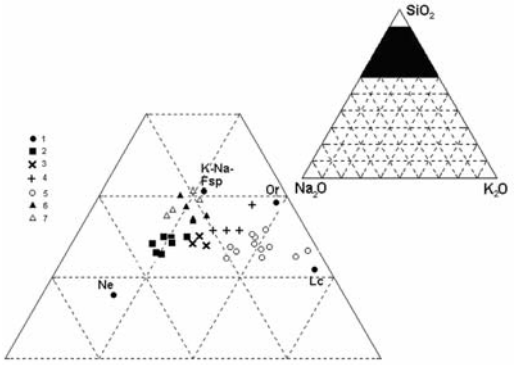

FIG. 1. The ration of silica and alkali metals ($SiO_2 + Na_2O + K_2O = 100\%$) in minerals (1): nepheline (Ne), leucite (Lc), orthoclase (Or), K-Na-feldspar (K-Na-Fsp) and in the main types of the rocks of Khibiny massif: 2 — massive coarse-grained urtites; 3 — juvites; 4 — ristschorrites of II group; 5 — ristschorrites of III group; 6 — ristschorrites of I group; 7 — nepheline syenites

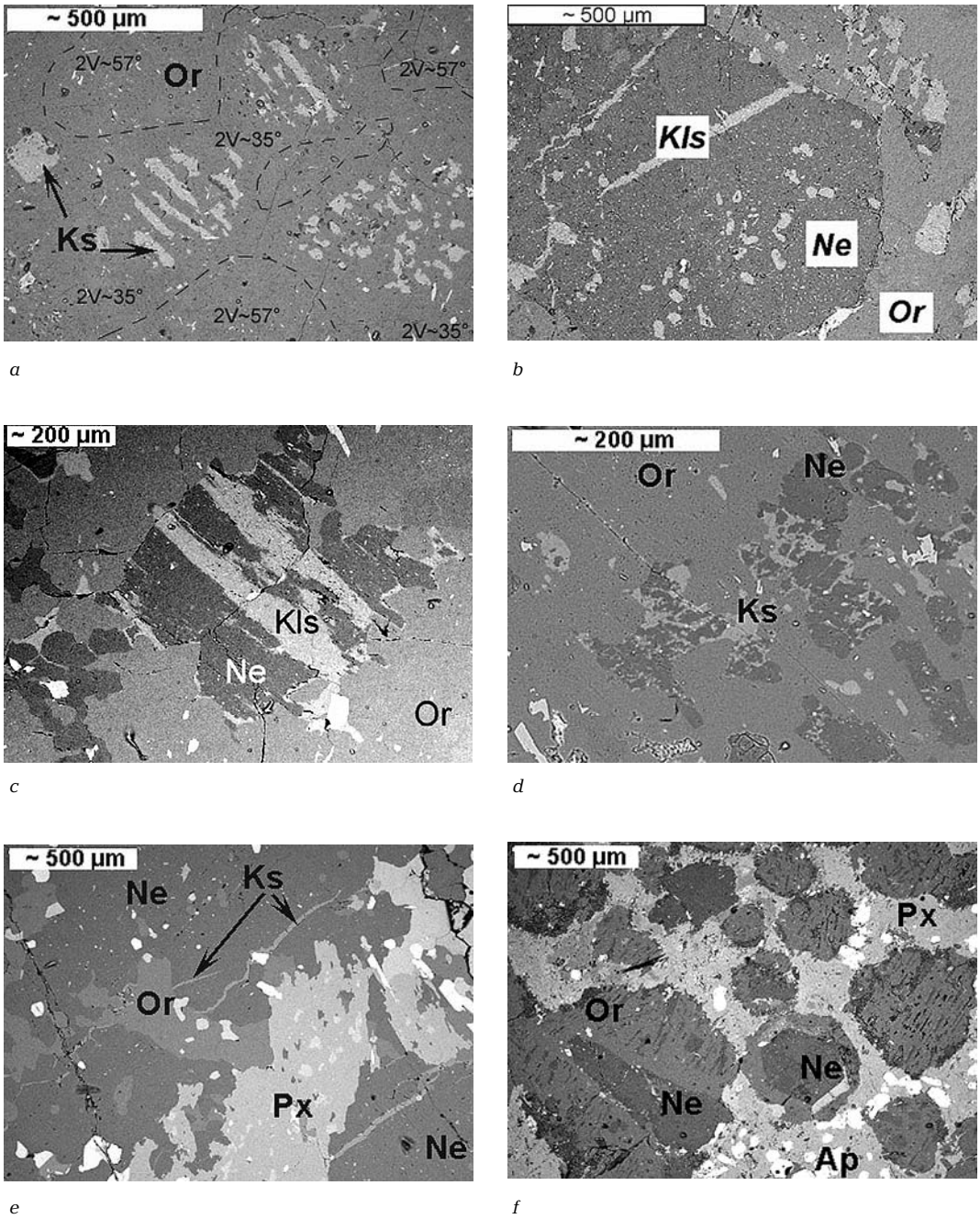

FIG. 2. The segregation forms of kalsilite (Ks) in ristschorrites of II group (Ne — nepheline, Or — orthoclase, Px — pyroxene, Ap — apatite), in reflected electrons (JSM-5300, Link ISIS):
a) the dislocation of kalsilite segregations groups (with similar orientation) in orthoclase poikilocrystal (dash line divides the parts with different 2V values, the explanation is in text);
b-c) the dislocation of kalsilite veinlets in cross (b) and longitudinal sections of nepheline crystal (c);
d) irregular intergrowths of kalsilite and nepheline in orthoclase poikilocrystals;
e) intersection of several close to each other nepheline grains by the same kalsilite veinlet;
f) nepheline-orthoclase inclusions in pyroxene poikilocrystal

Table 3. Chemical composition (wt %) of kalsilite from the rocks of Khibiny massif

№ of sample / *Constituents*	*1*	*2*	*3*	*4*	*5*	*6*	*7*	*8*	*9*	*10*
SiO_2	39,83	40,17	37,14	37,16	37,98	37,42	37,51	38,78	39,32	39,32
Al_2O_3	27,32	27,88	28,51	30,34	29,27	30,34	30,92	28,82	30,06	30,05
Fe_2O_3	5,12	1,51	3,56	0,79	1,03	0,79	0,62	3,10	1,41	1,41
CaO	0,34	0,36	0,55	0,38	0,29	0,00	0,17	0,40	0,44	0,44
Na_2O	0,09	0	0,20	0,35	0,77	0,70	0,20	0	0	0
K_2O	27,40	29,69	29,77	30,52	29,71	30,34	30,57	29,70	29,13	29,13
Total	100,1	99,61	99,73	99,54	99,05	99,59	99,99	100,80	100,36	100,40
Number of ions on the basis of cations sum = 3										
Si	1,07	1,07	0,99	0,98	1,01	0,99	0,99	1,03	1,04	1,04
Al	0,87	0,88	0,90	0,94	0,92	0,94	0,96	0,90	0,94	0,94
Fe	0,10	0,03	0,07	0,02	0,02	0,02	0,01	0,06	0,03	0,03
Ca	0,01	0,01	0,02	0,01	0,01	0,00	0,00	0,01	0,01	0,01
Na	0,00	0,00	0,01	0,02	0,04	0,04	0,01	0,00	0,00	0,00
K	0,94	1,01	1,01	1,03	1,01	1,02	1,03	1,00	0,98	0,98
O	4,09	4,02	3,94	3,95	3,95	3,94	3,95	4,01	4,03	4,03

Note.
Analyses 1, 2 — from micaceous ristschorrite of II group (Mt. Yukspor); 3–7 — from pyroxene ristschorrites of II group, 4–7 — from one sample (Mt. Rasvumchorr); an. 8–10 — from ultrapotassium ristschorrites of III group (Mt. Poachvumchorr); an. 9–10 — from one sample. Analyst — N.V. Trubkin (JSM-5300 + Link ISIS, IGEM RAS)

We consider the described segregation forms of kalsilite are caused by its metasomatic genesis: kalsilite replace nepheline (and is observed in the grains of latter), and in the case of following replacement of nepheline by potassium feldspar it will remain as relic.

III group — ristschorrites with high content of kalsilite (from 5–10 to 20%)

By appearance they are most resembled to «pseudoleucite» syenites, but in Khibiny massif have not wide spreading. By mineral composition these rocks are close to ristschorrites of II group. In the chemical composition of rock-forming and accessory minerals (Table 2, an. 5, 10; Table 3, an. 8–10; Table 4, an. 2) the potassium content most possible for these minerals are detected. On the diagram SiO_2-Na_2O-K_2O the position of points, corresponding to most potassium rocks of considered group, is approached to leucite (Fig. 1). The rubidium concentration is strongly increased and even in comparison with ristschorrites of II group (Table 1, an. 8–9).

In these rocks, as in ristschorrites of II group, the corroded or (rarely) idiomorphic nepheline grains, cut by above-mentioned kalsilite veinlets, occur (Fig. 3a), but more often they are located in the centre of kalsilite-(nepheline)-orthoclase intergrowths, forming isolated inclusions in orthoclase poikilocrystal. Three types of these intergrowths are distinguished:

First type. The optical orientation of orthoclase in the plane of section is not changed and coincides with optical orientation of all poikilocrystal, and elongated kalsilite segregations, increasing on width and length from centre to periphery of «intergrowth», are oriented in the system close to radial.

The largest development is characteristic for one of the directions (Fig. 3b), which the optical orientation of single kalsilite segregations remains in constant for ingrowths elongated in reciprocally perpendicular directions. Usually kalsilite, forming the peripheral rims of central (relic) nepheline grains has the same optical orientation (Fig. 3b). In the same orthoclase poikilocrystal, preserving the single optical orientation at the significant area (up to 10×10 cm), the several kalsilite-orthoclase intergrowths are found. As a rule, these parts are isometric, but do not have the distinct shape.

The second type is distinguished from the first one that the groups of equally oriented kalsilite segregations, located in poikilocrystal, do not show the radiate-fibrous structure and are characterized by development of irregular (Fig. 3a, 3c, 3d) or idiomorphic thin- and thick-tabular, and sometimes dactyloscopic segregations. It is essential the nepheline forms the similar intergrowths with orthoclase. This type of intergrowths occurs in ristschorrites of II group. The measurements on Fedorov universal table show that in areas of feldspar poikilocrystals, which the accumulation of equally or regular oriented feldspathoid inclusions (presumably replaced by kalsilite or unaltered relics of primary nepheline, (Fig. 2a)) is observed in, the angle of optical axes is ~35°, that corresponds to low sanidine (low-ordered modification of feldspar), and is distinguished from

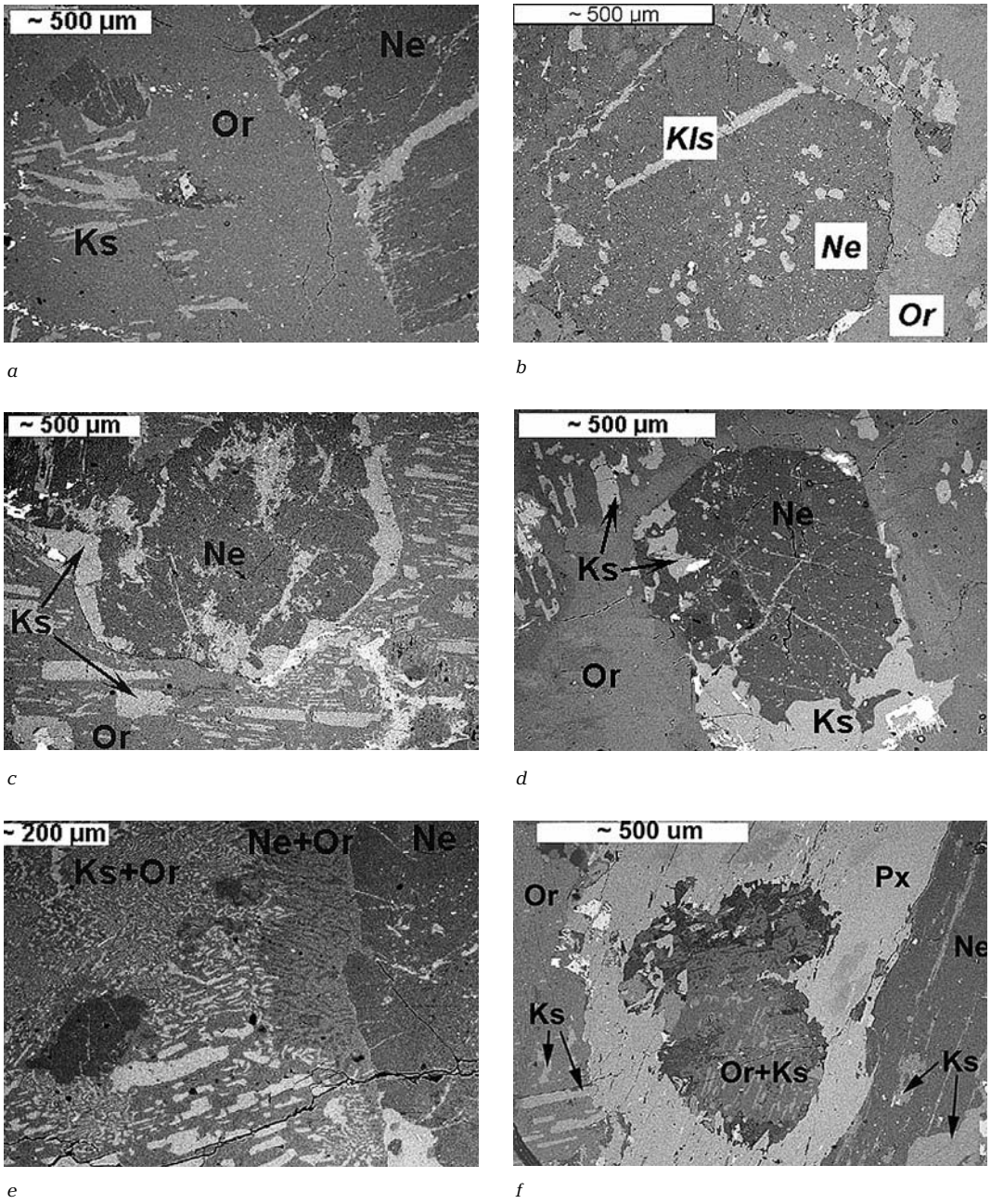

FIG. 3. Kalsilite (Ks) segregation forms in ristschorrites of III group (Ne — nepheline, Or — orthoclase, Vd — wadeite) in reflected electrons (JSM-5300, Link ISIS):
a) idiomorphic nepheline grain (to the right), crossed by kalsilite veinlet and isolated kalsilite segregations in orthoclase poikilocrystal (to the left);
b) nepheline grain, rounded by radiate-fibrous kalsilite-orthoclase intergrowth (of the first type);
c-d) kalsilite segregations in rims, framing the relic nepheline grains, and in kalsilite-orthoclase intergrowths (of the second type);
e) radiate-fibrous fine needle-shaped and symplektitic nepheline- and kalsilite-feldspar intergrowths (of the third type) in peripheral parts of nepheline grain;
f) kalsilite-feldspar intergrowth, forming poikilitic inclusion in pyroxene

this value for other part of the poikilocrystal, non-containing such inclusions, in which the angle of optical axes is increased up to ~56—58° and corresponds to high orthoclase (more ordered modification). It is essential that between these modifications there is gradual transition (with gradual increasing of optical axes angle), besides that the spatial (and optical) orientation of poikilocrystal remains single at all its area. The central zones of nepheline grains were replaced by feldspar later than peripheral ones that can be the reason of observed heterogeneity. As a result of that in these parts the relics of replaced feldspathoid remained, and the process of Si/Al-ordering of feldspar was developed in smaller degree than in edge zones, where the solution action was longer.

The third type is represented by radiate-fibrous fine needle-shaped and symplektitic intergrowths, which are characterized by synchronous wavy extinction both kalsilite and feldspar. That sort of intergrowths is observed in peripheral parts of nepheline grains and sometimes is separated from these grains by zones of nepheline-orthoclase intergrowths, analogous to them both on morphology and segregation sizes (Fig. 3e). The above-mentioned kalsilite veinlets are often characterized by the wavy extinction, and the kalsilite rims on the nepheline grains surface have the same extinction, and, by our opinion, can be the base for formation of considered type of kalsilite-feldspar intergrowths during the process of rock orthoclasization.

Kalsilite often composes the kalsilite-(nepheline)-feldspar intergrowths, forming poikilitic inclusions in pyroxene (rarely in other minerals: lamprophyllite, lomonosovite, titanite), composing the characteristic for ristschorrites (of II and III groups) melanocratic parts. These inclusions (0.2—2 mm in size) often have roundish contours (Fig. 2f, 3f), but along with them the monomineral idiomorphic inclusions of hexagonal nepheline grains are observed. The ingrowths of feldspathoid within the poikilitic inclusion are as a rule elongated, but sometimes they have isometric shape. Quite often the peripheral part of nepheline and kalsilite-(nepheline)-orthoclase poikilitic inclusions is formed by orthoclase (Fig. 2a). The optical orientation of feldspathoid in all (or in group) poikilitic inclusions, corresponding to single pyroxene poikilocrystal often proves to be similar. The optical orientation of orthoclase, growing together with it, is distinguished from the orientation of feldspathoid, but is single for all ingrowths and coincides with orientation of orthoclase poikilocrystal joining to this pyroxene crystal. In the areas of contact of aegirine-diopside with kalsilite-(nepheline)-orthoclase intergrowths its replacement by aegirine, biotite, and potassium-bearing amphibole is noted.

According to (Plechov, Serebryakov, 2003) these parts are the relics of fergusites (the plutonic rocks, containing nearly 70% of pseudoleucite and 30% of pyroxene), grasped by ristschorrites. However, our researches have shown that the distribution of feldspathoid ingrowths in feldspar of ristschorrites is very irregular and along with kalsilite-feldspar intergrowths, which analyses are exactly recalculated on leucite formula (at ratio of kalsilite and feldspar 1:1), the areas with strong predominance of some or different phase are noted. Moreover, in these rocks we did not detect the intergrowths with distinct crystallographic contours, which could reflect the cubic habit of primary leucite. By our opinion, these mineral

Table 4. Chemical composition (wt %) of accessory minerals from ristschorrites

№ of sample Constituents	*1*	*2*	*3*	*4*	*5*	*6*	*7*
SiO_2	45,98	47,46	44,54	61,80	42,44	51,87	30,17
TiO_2	1,80	8,27	0	0	23,27	0,55	26,93
ZrO2	28,97	20,99	0	0	0	11,54	0
Nb_2O_5	0	0	0	0	5,34	0	1,80
Al_2O_3	0	0,08	5,88	0	0,19	0	0
Fe_2O_3	0	0	0	0	0,99	0	3,43
FeO	0,04	0	0,34	12,07	0	2,24	0
MnO	0,02	0	0,09	5,09	0,06	1,26	1,02
MgO	0,07	0	0,03	0,46	0	0	0,19
CaO	0,20	0,20	13,17	0,35	0,21	10,70	0,67
SrO	0	0	0	0	0	1,90	1,05
BaO	0	0	0	0	9,44	0	20,67
Na_2O	0	0,06	6,52	8,44	6,87	12,95	9,32
K_2O	24,01	23,91	18,39	12,40	11,52	5,92	4,05
Cl	0	0	3,57	0	0	1,78	0
$-O=C_{l2}$	-	-	0,81	-	-	0,41	-
Total	100,96	100,97	91,72	100,61	100,33	100,95	99,30

Formulae:

1. $(K_{2,00}Ca_{0,01})_{2,01}(Zr_{0,92}Ti_{0,09})_{1,01}Si_3O_{9,03}$ - $\sum_{Si,Al}=3$
2. $(K_{1,92}Na_{0,01}Ca_{0,01})_{1,94}(Zr_{0,65}Ti_{0,39})_{1,04}(Si_{2,99}A_{l0,01})_3O_{9,05}$ - $\sum_{Si,Al}=3$
3. $K_{3.65}\ Ca_{2.19}Na_{1.96}\ Fe_{0.04}Mn_{0.01}Mg_{0.01}Si_{6.92}\ Al_{1.08}Cl_{0,96}O_{19,58}$ - $\sum_{Si,Al}=7$
4. $Na_{1,06}K_{1,02}Ca_{0,02}Fe_{0,65}Mn_{0,28}Mg_{0,04}Si_4O_{10,04}$ - $\sum_{Si,Al}=4$
5. $Na_{1,25}(K_{1,38}Ba_{0,35}Ca_{0,02})_{2,99}(Ti_{1,64}Nb_{0,23}Fe_{0,08})_{1,95}(Si_{3,98}Al_{0,02})_4$ $O_{13,60}$ - $\sum_{Si,Al}=4$
6. $(Na_{12,57}K_{3,78}Sr_{0,55})_{16,90}(Ca_{5,74}TR_{0,12}Mn_{0,14})_6(Fe_{0,84}Mn_{0,39})_{1,24}$ $(Zr_{2,79}Ti_{0,21})3\times(Si_{25,98}Zr_{0,02})_{26}O_{73,27}Cl_{1,51}$ - $\sum_{Si,Al,Zr,Ti,Nb}=29$
7. $(Ba_{1,08}K_{0,68}Sr_{0,08})_{1,84}Na_1(Na_{1,40}Fe_{0,34}Mn_{0,12}Ca_{0,10}Mg_{0,04})_{1,99}$ $(Ti_{0,69}Nb_{0,11})_{0,80}Si_4O_{16,92}$ - $\sum_{Si,Al}=4$

Note.

An. 1 — wadeite, an. 2 — titanium wadeite; an. 3 — delhayelite; an. 4 — fenaksite; an. an. 5 — scherbakovite; an. 6 — potassium eudialyte; an. 7 — potassium barytolamprophyllite. An. 2 — from ristschorrite of III group, other analyses — from ristschorrites of II group. An. 1, 5, 7 — analyst O.A. Ageeva (Cameca MS-46), an. 2—4 — analyst V.V. Khangulov (Camebax SX-50, IGEM RAS), an. 6 — analyst N.V. Trubkin (JSM-5300 + Link ISIS, IGEM RAS). The sum of an. 6 contains $Ce_2O_3=0,65$.

relations can be explained by metasomatic hypothesis of ristschorrites genesis. They are caused by particular inheritance the structure of massive coarse-grained urtites by ristschorrites, which replaces them. For these urtites the melanocratic parts, consisting of enlarged (up to 10–20 mm) pyroxene poikilocrystals and accessory minerals (lamprophyllite, lomonosovite, titanite) with small ingrowths of nepheline (2–3 mm in size) are characteristic. Orthoclase and kalsilite mainly replaced the nepheline of initial rocks. Therefore, at replacement of nepheline in leucocratic parts of rock the feldspathoid-feldspar poikilitic intergrowths as if «sink» in large feldspar poikilocrystals, than at replacement of nepheline ingrowths in melanocratic parts they form roundish polymineral aggregates, distinctly rising above the background of dark-coloured mineral.

Genesis of kalsilite–bearing rocks in Khibiny massif

Kalsilite morphology in the rocks of Khibiny massif is very diverse and does not allow giving simple explanation of its genesis way. The succession of formation (or transformation) of leucocratic minerals of kalsilite-bearing ristschorrites of the massif is clear determined: relic nepheline → kalsilite (or kalsilite + orthoclase) → orthoclase, and the evident features of metasomatic alteration of nepheline are discovered.

According to authors' hypothesis, ristschorrites in Khibiny alkaline complex was formed during K-Si-metasomatosis, influencing mainly on ijolite-urtites of Central Arc of the massif. The magma, which the metasomatic solutions separated from, apparently, had nepheline-syenite composition, that predetermined the migration first of all potassium and silica in ijolite-urtites, unsaturated by these elements, and the formation of metasotatites of nepheline-syenite composition.

Kalsilite formation is related to most early stage of considered process and caused by strong increasing of potassium activity relatively sodium one. Nepheline of initial rocks was the «matrix» for kalsilite genesis: $2Na_3KAl_4Si_4O_{16} + 3K_2O \rightarrow 8KAlSiO_4 + 3Na_2O$. Kalsilite formation was accompanied by genesis of the other significant potassium accessory and rock-forming minerals, replaced the minerals of initial rocks or crystallized independently. The strong increasing of potassium activity at this stage, which causes the anomalous enrichment of forming metasomatites by potassium and the appearance of specific potassium mineralization among significant sodium rocks, can be explained by development of acid-basic interaction during influence of alkaline solutions (separated from nepheline-syenite magma) on more basic matrix, ijolite-urtites (Zotov, 1989). The increasing of ratios of more basic components to less basic ones (K/Na, Mn/Fe, Ba/Sr, Sr/Ca, Ca/Mn, Zr/Ti), noted in accessory minerals (Ageeva *et al.*, 2002), and the increased content of rubidium in feldspar of these rocks indicate the development of acid-basic interaction. The absence of kalsilite and distinctly revealed potassium mineralization in ristschorrites of I group, which are formed during replacement of nepheline syenites, is exlplained by less basicity in comparison with ijolite-urtites composition of these rocks, and its similarity to composition of influencing solutions. The differences in mineralogy and geochemistry of ristschorrites of II and III groups are probably caused by different potassium concentration in solutions.

In ristschorrites of II and III groups the crystallization of potassium feldspar took place simultaneously with kalsilite formation, and in the most part after that. Also the significant introduction not only potassium (exceeding its content in nepheline syenites), but silica (up to values in nepheline syenites), the carrying-out of other components (up to values in nepheline syenites), and the fall of rocks basicity index occur (Borutzky, 1988). Feldspar of ristschorrites, as it was mentioned, is distinguished by significantly potassium chemical composition. In ristschorrites rock-forming adularia with $t_1 0$ 0,36–0,38 and 2V 33–43° (650–550°C, according to G. Hovis) coexists with more Si/Al-ordered orthoclase with $t_1 0$ 0,39–0,43 and 2V 45–65° (490–370°C, according to G. Hovis) and maximum-ordered nonlatticed microcline with 0,92–0,99, 2V 80–83°, which are forming the main volume of poikiloblast and were crystallized definitely below 500°№ (Borutzky, 1988). At the same time, determined feldspars in the bounds of single poikiloblast are subordinated to single optical orientation and there are no phase borders between them. The presence of feldspars of different structural modifications in ristschorrites is the evidence of unbalanced conditions of their formation and their cristallization in wide temperature range, that indicates the long history of ristschorrites formation.

The different development of the chemical activity of potassium and silica, which determined the peculiarities of mineralogy and geochemistry of distinguished ristschorrites groups, are caused by two major factors: the character of replaced rocks (in comparison of ristschorrites of I group with ristschorrites of II

and III groups) and the composition of metasomatic solutions, the concentration of potassium in them (in comparison ristschorrites of II and III groups among each other). One of the main indicative signs of manifestation of either factor in given geological conditions are kalsilite presence and degree of its development.

The work was supported by the grant of Russian Foundation for Basic Research (project № 03−05−64139).

References

Ageeva O.A. Evolution of mineral formation in the rocks of ristschorrites complex (Khibiny massif) // Geologiya i Geoekologiya: Issledovaniya Molodykh. 2002 g. Materialy XIII Konferentsii, Posvyashchennoi Pamyati K.O. Krattsa. V. 2. Apatity, **2002.** P. 7-11 (Rus.)

Ageeva O.A., Borutzky B.Ye., Khangulov V.V. Eudialyte as a mineral-geochemical indicator of metasomatic processes at formation of the rocks of poikilitic nepheline syenite complex of Khibiny massif // Geokhimiya, **2002,** № 10. P. 1098-1105 (Rus.)

Arkhangel'skaya V.V. Genesis of pseudoleucites of Synnyr massif of alkaline rocks // Dokl. AN SSSR. **1965.** V. 164, № 3. P. 662-665 (Rus.)

Aurissicchio C., Federico M. Nepheline-kalsilite microperthites in ejecta from the Alban Hills (Italy)//. Bull. Geol. Soc. Finl. **1985.** Vol.57, pt. 1/2. P. 129-137

Bagdasarov E.A., Luk'yanova T.A. Nepheline, potassium feldspar and kalsilite from the rocks of ditroite series of Synnyr massif // Problemy Metasomatisma. L.: VSEGEI i n.-t. gorn. ob-vo, **1969.** P. 367-374 (Rus.)

Borutzky B.Ye. Rock-forming Minerals of High-alkali Complexes (Porodoobrazuyushchie Mineraly Vysokoshchelochnykh Kompleksov). M., Nauka. **1988.** 205 p (Rus.)

Borutzky B.Ye., Borutzkaya V.L., Nekrasova L.P. Alkaline feldspars of poikilitic nepheline syenites of Khibiny massif // In: Izomorfizm v Mineralakh. M., Nauka. **1975.** P. 246-273 (Rus.)

Borutzky B.Ye., Organova N.I., Marskii I.M. Crystal structure Si/Al-ordered adular-like orthoclase from poikilitic nepheline syenites of Khibiny massif // Izv. AN SSSR, ser. Geol. 1986, № 6. P. 69-74 (Rus.)

Borutzky B.Ye., Tsepin A.I., Kuznetsov Zh.M. Kalsilite from Khibiny massif of nepheline syenites // Izv. AN SSSR, ser. Geol. **1973,** № 5. C. 132-136 (Rus.)

Borutzky B.Ye., Tsepin A.I., Vlasova E.V. New data on kalsilite from Khibiny // In: Novye Dannye o Mineralakh SSSR. M. **1976.** P. 25. P. 130-133 (Rus.)

Holmes A. A suite of volcanic rocks from south-west Uganda containing kalsilite (a polymorph of KAlSiO4)//. Miner. Mag. **1942.** Vol. 26, №177. P. 197-217

Konev A.A. New rock and new type of ultrapotassium aluminous raw materials // In: Geologiya i Poleznye Iskopaemye Vostochnoi Sibiri. Novosibirsk, Nauka. **1985.** P. 191-195 (Rus.)

Konev A.A., Samoilov V.S. Contact Metamophism and Metasomatosis in Aureole of Tajeran Alkaline Intrusion (Kontaktovyi Metamorfizm i Metasomatoz v Oreole Tazheranskoi Shchelochnoi Intruzii). Novosibirsk, Nauka. **1974.** 123 p (Rus.)

Konev A.A., Vorob'ev E.I., Lazebnik K.A. Mineralogy of Murun Alkaline Massif (Mineralogiya Murunskogo Shchelochnogo Massiva). Novosibirsk. SO RAN, **1996.** 222 p (Rus.)

Kononova V.A., Pervov V.A., Kovalenko V.I., Laputina I.P. Pseudoleucite syenites, the questions of their genesis and formation belonging (at example of Lugijn Gol massif, Mongolian People's Republic) // Izv. AN SSSR, ser. Geol. **1981.** № 5. P. 20-37 (Rus.)

Kovalenko V.I., Vladykin N.V., Goreglyad A.V., Smirnov V.N. Lugijn Gol massif of pseudoleucite syenites in Mongolian People's Republic (first find) // Izv. AN SSSR, ser. Geol. **1974.** № 8. P. 38-49 (Rus.)

Kozyreva L.V., Korobeinikov A.N., Men'shikov Yu.P. New variety of ultrapotassium rocks in Khibiny massif // In: Novoe v Mineralogii Karelo-Kol'skogo Regiona. Petrozavodsk, **1990.** P. 116-129 (Rus.)

Kurepin V.A. Mineral parageneses and forming conditions of pseudoleucite syenites of Synnyr massif // In: Mineraly i Paragenezisy Mineralov Gornykh Porod. Leningrad, Nauka. **1973.** P. 53-60 (Rus.)

Plechov P.Yu., Serebryakov N.S. Relics of fergusites in the rocks of ristschorrite complex of Khibiny massif // Geokhimiya Magmaticheskikh Porod: Trudy XXI Vserossiiskogo Seminara po Geokhimii Magmaticheskikh Porod. 3-5 September, **2003** g. Apatity, GI KNTs RAN (Rus.)

Sahama Th.G. Kalsilite in lavas of Nyiragongo // J. Petrology. **1960.** Vol. 1, № 2. P. 146-172

Samsonova N.S., Donakov V.I. Kalsilite from Murun alkaline massif (East Siberia) // ZVMO. **1968.** P. 97. V 3. P. 291-300 (Rus.)

Smyslov S.A. Kalsilite-bearing rocks of Malomurun massif // Geologiya i Geofizika. **1986.** № 8. P. 33-38 (Rus.)

Tikhonenkov I.P. Nepheline Syenites and Pegmatites of Khibiny Massif and the Role of Postmagmatic Phenomena in Their For-

UDC 549.742

GENETIC MINERALOGY OF THE BURBANKITE GROUP

Yulia V. Belovitskaya
Geological Faculty, Lomonosov Moscow State University, Moscow, Russia, mineral@geol.msu.ru

Igor V. Pekov
Geological Faculty, Lomonosov Moscow State University, Moscow, Russia, yuky@newmail.ru

The burbankite group consists of six mineral species with general formula $A_3B_3(CO_3)_5$ where A = Na > Ca, REE^{3+}, □; B = Sr, Ca, Ba, REE^{3+}, Na: burbankite, khanneshite, calcioburbankite, remondite-(Ce), remondite-(La), and petersenite-(Ce). The burbankite structural type (space group $P6_3mc$) is exclusively stable for chemical composition variations: khanneshite, calcioburbankite, remondite hexagonal analogue, and burbankite are isostructural and form the system of continous solid solutions. All chemical compositions (94 analyses) of the burbankite group minerals can be described within the isomorphous system with end members: $(Na_2Ca)M^{2+}{}_3(CO_3)_5$ and $Na_3(REE_2Na)(CO_3)_5$, where M^{2+} = Sr, Ba, Ca. There are three genetic types of the burbankite mineralization: 1) in carbonatites where the minerals with the "most averaged" chemical composition and increased contents of Ba and Ca are formed; 2) in alkaline hydrothermalites where the range of chemical compositions of the burbankite-like phases is extremely wide; 3) in pectolite metasomatites where burbankite is strongly REE-depleted. In carbonatites the burbankite group minerals are early phases formed under high-temperature conditions, whereas in nepheline syenite massifs they are formed during hydrothermal stages under low temperatures, which is due to different regime of CO_2. Under alkalinity decrease the burbankite group minerals are replaced by a whole series of secondary minerals, among which the alkali-free carbonates of REE, Sr, Ba, and Ca prevail.
5 tables, 3 figures, 50 references.

The burbankite group consists of six mineral species with general formula $A_3B_3(CO_3)_5$ where A = Na > Ca, REE^{3+},□; B = Sr, Ca, Ba, REE^{3+}, Na: burbankite $(Na,Ca,□)_3(Sr,REE,Ba,Ca)_3(CO_3)_5$, khanneshite $(Na,Ca)_3(Ba,Sr,REE,Ca)_3(CO_3)_5$, calcioburbankite $(Na,Ca,REE)_3(Ca,REE,Sr)_3(CO_3)_5$, remondite-(Ce) $Na_3(Ce,Ca,Na,Sr)_3(CO_3)_5$, remondite-(La) $Na_3(La,Ce,Ca)_3(CO_3)_5$, and petersenite-(Ce) $(Na,Ca)_4(Ce,La,Sr)_2(CO_3)_5$. The first three minerals are hexagonal (space group $P6_3mc$), and others are pseudohexagonal monoclinic (sp. gr. $P2_1$, $\gamma = 119.8-120.5°$).

In the crystal structures of hexagonal members of this group there are two independent cationic sites — *A* (Na и Ca) and *B* (REE, Sr, Ba и Ca), and three types of carbonate groups with different orientations. Ten-vertex *B*-polyhedra connected to CO_3-groups by vertices form the layers of six-member rings parallel (001). Eight-vertex *A*-polyhedra form infinite zigzag columns where neighboring polyhedra are contacted by planes (Voronkov, Shumyatskaya, 1968; Effenberger *et al.*, 1985; Belovitskaya *et al.*, 2000, 2001, 2002). The crystal structure of remondite is quite similar to that of burbankite (Ginderow, 1989). In the crystal structure of petersenite atoms of Na occupy with order two *B*-polyhedra out of six, which results to doubling of *a*-parameter (Grice *et al.*, 1994).

Burbankite group carbonates form hexagonal prismatic crystals but occur more often as irregular grains and their aggregates. These minerals are transparent, without cleavage, have vitreous up to greasy luster and light colours: yellow, green, pale-brown, pink. Frequently colorless and white, less often red, orange and gray varieties occur.

Burbankite is a widespread mineral, whereas other members of the group are rare. In one of types of «rare-earth carbonatites» (Khibiny, Vuoriyarvi, Gornoe Ozero *etc.*) burbankite and its alteration products will form huge accumulations, being the main potentially industrial component and easily enriched complex ore of REE, Sr, and Ba.

In spite of a semi-centennial history of research, significant number of the publications, and extensive geography of finds, generalizing papers on the burbankite group minerals are absent. We have attempted to systematize earlier published materials and having supplemented them with comparable volume of new data to show the connection of chemical composition and structural features of these minerals with conditions of their formiation. We have studied 32 samples from eight alkaline complexes — Khibiny, Lovozero (Kola Peninsula), Vuoriyarvi (Northen Kareliya), Vishnevye Gory (Southern Urals), Gornoe Ozero, Murun (East Siberia), Mont Saint-Hilaire (Quebec, Canada), and Khanneshin (Afghanistan).

The cation composition of the minerals (Tables 1−3) was studied by electronmicroprobe method. All analyses including reference data were calculated on charge sum equal 10.00, i.e. equivalent $(CO_3)_5$. *B*-site was filled up to 3.00 *atoms per formula unit* (*apfu*) by atoms of Sr, Ba, REE, Th, K, in case of their deficiency

by atoms of Ca, and then atoms of Na was added. After that the rest of Na and Ca atoms was placed in *A*-site. If the *A*-cations sum appeared less 3.00, the missing value was attributed to vacancy according to the crystallochemical data (Effenberger *et al.*, 1985; Belovitskaya *et al.*, 2000). At calculation the atomic mass of Ce is conditionally taken for old analyses where the rare-earth elements were determined as a sum. The cation composition of the burbankite group minerals widely varies (Fig. 1, 2). In *A*-sites, sodium always prevails (1.3—3 *apfu*), but sometimes amounts of calcium is also essential (up to 1.25 *apfu*). The cation composition is more diverse in *B*-sites where atoms of Sr, Ba, Ce, La, and Ca can dominate.

We make the X-ray powder studies for 11 samples (Table 4) including five species with different chemical composition, which crystal structures was refined by Rietveld method: 1) REE-depleted burbankite (an. 92), its X-ray diffraction pattern contains distinct doublets; 2) burbankite with «typical» composition (an. 64) and nonsplit peaks on X-ray spectrum; 3) khanneshite (an. 21); 4) calcioburbankite (an. 12); 5) the mineral with chemical composition of remondite-(Ce) (an. 79), but according to its X-ray powder diagram identical to representatives of the burbankite structural type.

Burbankite group minerals form complex isomorphous system with end members: REE-free phases $(Na_2Ca)M^{2+}{}_3(CO_3)_5$ where M^{2+} = Sr, Ba, Ca and petersenite $Na_3(REE_2Na)(CO_3)_5$, without divalent cations. All chemical compositions of the minerals are situated in interval between these two points forming extended field — Fig 1, and 2a, b. In spite of two structural transitions: from hexagonal members to monoclinic remondite and then to petersenite, essential mixable intermissions in this system aren't determined. These structural transitions are concerned to the second type, i.e. they are realized gradually, without break of chemical bonds.

Occurrences and formation conditions

Generalizing an available material, it was possible to distinguish three main genetic types of burbankite mineralization. Each of them is connected to alkaline rocks. The largest burbankite concentrations occur in carbonatites. This genetic type is studied better then others. In alkaline hydrothermalites the widest variations of chemical compositions and, accordingly, the greatest species variety are observed at relatively small amounts. We have distinguished the third genetic type, accumulations of REE-depleted burbankite, connected to specific pectolite metasomatites of Khibiny and Murun massifs. In each case the minerals are characterized by individual features of cation ratios (Fig. 1). Burbankite from soda-bearing sedimentary Green River Formation (USA) is in association with the majority of the same minerals as in carbonatites and alkaline hydrothermalites (Fitzpatrick, Pabst, 1977) and, probably, has low-temperature hydrothermal origin.

Occurrences of the burbankite group minerals with known chemical composition are briefly described in Table 5. They are grouped for genetic types. Localities connected to rocks enclosing carbonatites and also with products of hydrothermal activity in carbonatites are conditionally referred to carbonatite type. The finds made in late parageneses of pegmatite from nepheline syenite complex are referred to alkaline hydrothermalites.

Thus, burbankite group minerals are formed in alkali-carbonate systems connected to geological objects of different types. The temperature range these minerals crystallize in is extremely wide.

A number of massifs contain carbonatites where the burbankite group minerals are the main concentrators of strontium, barium, and rare-earth elements. Here burbankite and its analogs crystallize on early carbonatite formation stages under high temperatures (not below 500°C). That confirmed by the signs of joint growth with essential minerals of carbonatite rocks, the presence of the burbankite group minerals in primary inclusions, and the replacement of these minerals by products of later hydrotermal stages.

In alkaline hydrothermalites the burbankite group minerals are the late formations forming at essentially lower temperatures. Their crystals in cavities are frequently observed together with zeolites and hydrous soda minerals. Formation temperatures for these associations can be estimated as 100—250°C.

The difference in time of crystallization are first of all connected to different regime of carbon dioxide. The excess of CO_2 is present in carbonatite formation systems, and already at early stages burbankite and its analogs appear under sufficient activity of sodium. In nepheline syenite massifs, with which the burbankite-bearing hydrothermalites are in general connected, increase of potential of CO_2 and, accordingly, the development of carbonate mineralization take place mainly on a final stage of evolution

Typochemism and structural typomorphism

The wide variations of cation composition make the burbankite group minerals very in-

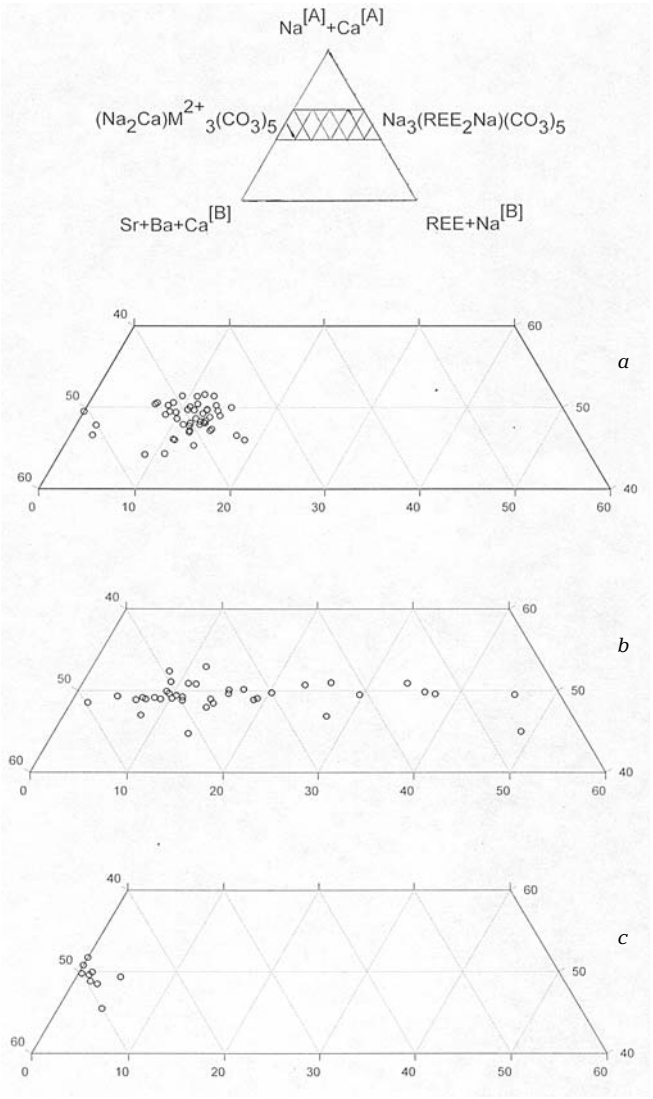

FIG. 1. Cation ratios in the burbankite group minerals: a — from carbonatites, b — from alkaline hydrothermalites, c — from pectolite metasomatites

formative in genetic relation.

In the system with end members $(Na_2Ca)M^{2+}{}_3(CO_3)_5$ and $Na_3(REE_2Na)(CO_3)_5$ (Fig. 1) samples from carbonatites occupy intermediate position making compact field. As a rule in the *B*-sites of these minerals atoms of Sr, rarely Ca and Ba prevail (Fig. 2a). Only in one sample from Vuoriayrvi domination of rare-earth elements is noted. The phases with «maximum averaged» chemical composition, often with comparable amounts of Sr (usually 0.7−1.5 *apfu*), Ba (on average 0.4−1.0 *apfu*), Ca (as a rule in *B*-site 0.3−1.0 *apfu*), and REE (usually 0.5−0.8 *apfu*), are typical for carbonatite complexes. Exactly in carbonatites the highest contents of barium for minerals of this group are fixed, and only here khanneshite is known (Khanneshin, Khibiny, Afrikanda, Kovdor). Usually 0.3−0.7 *apfu* of calcium are present in *A*-sites (Table 1). «Averaged» chemical composition of these minerals from early carbonatite associations (Fig. 1) and high content of barium, the largest cation (Fig. 2a), is explained by high-temperature conditions of crystallization. High concentration of a certain cation as well as considerable depletion of it is not typical for the samples from carbonatites. The ratios of rare-earth elements in burbankite-like phases from carbonatites are sufficiently stable and in general typical for most other minerals from alkaline rocks: Ce>La>>Nd. The increase of content of strontium from early generations to late ones is characteristic for the burbankite

Table 1. Chemical composition of burbankite group minerals from carbonatites

Constituents	Burbankite									Remon-di te-(Ce)
	Vuoriyarvi									
	an. 1	an. 2	an. 3	an. 4**	an. 5	an. 6	an. 7	an. 8	an. 9	an. 10
	wt. %									
Na_2O	10.51	10.10	11.44	12.19	10.70	10.41	10.43	11.92	10.25	10.18
K_2O	-	-	0.99	0.74	0.06	0.06	-	-	-	0.10
CaO	11.31	8.97	10.86	9.81	10.16	11.00	11.31	12.47	6.81	9.82
SrO	14.82	14.30	12.86	9.96	18.36	16.86	17.83	21.10	23.21	10.35
BaO	13.24	15.84	11.62	14.60	9.24	10.18	12.02	7.44	2.81	14.88
$\sum REE_2O_3$	n.d.	n.d.	15.12	16.22	n.d.	n.d.	n.d.	n.d.	n.d.	n.d.
Y_2O_3	0.30	0.19	n.d.	n.d.	-	-	-	-	-	-
La_2O_3	6.26	5.69	-"-	-"-	7.67	8.13	6.10	1.73	3.31	5.90
Ce_2O_3	8.24	8.75	-"-	-"-	10.22	9.94	8.33	5.14	13.98	12.96
Pr_2O_3	0.56	0.81	-"-	-"-	0.83	0.85	0.90	0.42	1.34	1.36
Nd_2O_3	1.42	1.96	-"-	-"-	1.87	1.73	1.66	3.16	6.92	3.65
Sm_2O_3	-	-	-"-	-"-	0.45	0.36	0.33	0.34	0.52	0.50
CO_2	n.d.	n.d.	34.30	32.14	n.d.	n.d.	n.d.	n.d.	n.d.	n.d.
Sum	66.68	66.60	100.23*	98.42*	69.55	69.50	68.89	63.72	69.15	69.70
	Formula									
$Na^{[A]}$	2.24	2.25	2.54	2.74	2.20	2.14	2.16	2.52	2.15	2.16
$Ca^{[A]}$	0.54	0.51	0.48	0.34	0.49	0.53	0.58	0.53	0.41	0.44
$\sum[A]$	2.78	2.76	3.02	3.08	2.70	2.67	2.74	3.05	2.56	2.60
$K^{[B]}$	-	-	0.14	0.11	0.01	0.01	-	-	-	0.01
$Ca^{[B]}$	0.80	0.60	0.85	0.87	0.66	0.72	0.71	0.93	0.39	0.71
$Sr^{[B]}$	0.95	0.95	0.85	0.67	1.13	1.04	1.11	1.33	1.46	0.66
$Ba^{[B]}$	0.57	0.71	0.52	0.66	0.38	0.42	0.50	0.32	0.12	0.64
$\sum M^{2+[B]}$	2.32	2.26	2.22	2.20	2.18	2.18	2.32	2.58	1.97	2.01
$Y^{[B]}$	0.02	0.01	n.d.	n.d.	-	-	-	-	-	-
$La^{[B]}$	0.25	0.24	-"-	-"-	0.30	0.32	0.24	0.07	0.13	0.24
$Ce^{[B]}$	0.33	0.37	-"-	-"-	0.40	0.39	0.33	0.20	0.56	0.52
$Pr^{[B]}$	0.02	0.03	-"-	-"-	0.03	0.03	0.03	0.02	0.05	0.05
$Nd^{[B]}$	0.06	0.08	-"-	-"-	0.07	0.07	0.06	0.12	0.27	0.14
$Sm^{[B]}$	-	-	-"-	-"-	0.02	0.01	0.01	0.01	0.02	0.02
$\sum REE^{[B]}$	0.68	0.74	0.64	0.69	0.82	0.81	0.68	0.42	1.03	0.97
$\sum[B]$	3.00	3.00	3.00	3.00	3.00	3.00	3.00	3.00	3.00	3.00
(CO_3)	5.00	5.00	5.00	5.00	5.00	5.00	5.00	5.00	5.00	5.00

Table 1. Chemical composition of burbankite group minerals from carbonatites (continuation)

Constituents	Calcioburbankite			Burbankite				Khanneshin		
	Vuoriyarvi			Gornoe Ozero		Khanneshin				
	an. 11	an. 12	an. 13	an. 14	an. 15	an. 16	an. 17	an. 18	an. 19	an. 20
	wt %									
Na_2O	13.67	13.27	12.98	11.13	11.62	9.39	11.67	10.15	8.63	8.39
K_2O	0.22	-	-	-	0.03	0.89	0.49	0.43	0.95	0.77
CaO	12.85	10.80	11.54	8.55	12.38	6.34	5.21	4.09	6.40	9.25
SrO	6.17	8.44	12.68	23.15	16.60	18.77	17.82	12.74	7.16	8.32
BaO	7.14	11.36	10.42	6.05	5.49	18.72	19.57	30.24	36.38	31.92
$\sum REE_2O_3$	23.00	n.d.	n.d.	n.d.	20.00	n.d.	n.d.	n.d.	10.41	11.18
Y_2O_3	n.d.	-	-	0.49	n.d.	-	0.05	0.06	n.d.	n.d.
La_2O_3	-"-	6.17	7.26	7.83	-"-	4.42	7.61	5.94	-"-	-"-
Ce_2O_3	-"-	10.86	9.74	8.79	-"-	7.20	4.49	4.43	-"-	-"-
Pr_2O_3	-"-	0.58	0.57	0.64	-"-	0.92	-	0.36	-"-	-"-
Nd_2O_3	-"-	2.56	1.53	1.47	-"-	1.57	0.61	0.54	-"-	-"-
Sm_2O_3	-"-	-	0.23	-	-"-	-	-	-	-"-	-"-
CO_2	35.97	n.d.	n.d.	n.d.	32.40	n.d.	n.d.	n.d.	28.48	28.85
Sum	99.62*	64.04	66.95	68.09	99.52*	68.22	67.52	68.98	(100.00)*	(100.00)*
	Formula									
$Na^{[A]}$	2.88	2.87	2.68	2.32	2.39	2.15	2.68	2.46	2.09	1.93
$Ca^{[A]}$	0.12	0.16	0.28	0.45	0.42	0.69	0.42	0.54	0.79	0.85
$\sum^{[A]}$	3.00	3.03	2.96	2.78	2.81	2.84	3.10	3.00	2.88	2.78
$K^{[B]}$	0.03	-	-	-	-	0.13	0.07	0.07	0.15	0.12
$Ca^{[B]}$	1.37	1.14	1.03	0.53	0.98	0.11	0.24	-	0.07	0.33
$Sr^{[B]}$	0.39	0.55	0.78	1.45	1.02	1.28	1.22	0.92	0.52	0.57
$Ba^{[B]}$	0.30	0.50	0.43	0.26	0.23	0.86	0.91	1.48	1.78	1.49
$\sum M^{2+[B]}$	2.09	2.19	2.24	2.23	2.23	2.26	2.37	2.41	2.37	2.39
$Y^{[B]}$	n.d.	-	-	0.03	n.d.	-	-	-	n.d.	n.d.
$La^{[B]}$	-"-	0.25	0.28	0.31	-"-	0.19	0.33	0.27	-"-	-"-
$Ce^{[B]}$	-"-	0.44	0.39	0.35	-"-	0.31	0.19	0.20	-"-	-"-
$Pr^{[B]}$	-"-	0.02	0.02	0.02	-"-	0.04	-	0.02	-"-	-"-
$Nd^{[B]}$	-"-	0.10	0.06	0.06	-"-	0.07	0.03	0.02	-"-	-"-
$Sm^{[B]}$	-"-	-	0.01	-	-"-	-	-	-	-"-	-"-
$\sum REE^{[B]}$	0.91	0.81	0.76	0.77	0.77	0.61	0.56	0.52	0.48	0.49
$\sum[B]$	3.00	3.00	3.00	3.00	3.00	3.00	3.00	3.00	3.00	3.00
(CO_3)	5.00	5.00	5.00	5.00	5.00	5.00	5.00	5.00	5.00	5.00

Table 1. Chemical composition of burbankite group minerals from carbonatites (continuation)

Constituents	Khanneshite	Burbankite								
	Khibiny									
	an. 21	an. 22	an. 23	an. 24	an. 25••	an. 26••	an. 27	an. 28	an. 29	an. 30
	wt %									
Na_2O	11.86	11.47	7.61	11.50	11.40	12.80	11.5	12.45	11.93	11.80
K_2O	-	-	-	-	1.73	0.03	-	0.02	-	-
CaO	5.37	3.26	11.82	12.00	13.60	11.31	12.6	12.60	11.94	12.57
SrO	9.04	34.80	19.08	20.54	14.10	14.60	19.2	19.60	24.74	24.57
BaO	22.99	1.61	5.61	2.38	4.76	6.31	3.6	0.78	1.76	1.86
$\sum REE_2O_3$	n.d.	n.d.	n.d.	19.84	18.60	19.24	19.2	17.33	n.d.	n.d.
Y_2O_3	-	0.72	-	n.d.	n.d.	n.d.	n.d.	n.d.	-	-
La_2O_3	4.07	7.12	6.35	-"-	-"-	-"-	-"-	-"-	5.65	5.11
Ce_2O_3	10.46	7.39	8.84	-"-	-"-	-"-	-"-	-"-	7.15	6.97
Pr_2O_3	1.01	0.63	-	-"-	-"-	-"-	-"-	-"-	0.47	0.47
Nd_2O_3	3.60	1.20	2.11	-"-	-"-	-"-	-"-	-"-	1.24	1.33
Sm_2O_3	-	-	-	-"-	-"-	-"-	-"-	-"-	0.07	0.10
CO_2	n.d.	n.d.	n.d.	34.20	34.40	33.50	36.1	35.40	(34.77)	(34.89)
Sum	68.40	68.20	61.42	100.46	99.52•	99.78•	102.2	99.78•	99.72	99.67
	Formula									
$Na^{[A]}$	2.74	2.47	1.72	2.34	2.35	2.70	2.34	2.58	2.43	2.41
$Ca^{[A]}$	0.21	0.39	0.77	0.45	0.58	0.27	0.46	0.38	0.50	0.53
$\sum[A]$	2.95	2.86	2.49	2.79	2.93	2.97	2.80	2.96	2.93	2.94
$K^{[B]}$	-	-	-	-	0.23	-	-	0.02	-	-
$Ca^{[B]}$	0.47	-	0.71	0.89	0.98	1.05	0.94	1.05	0.85	0.89
$Sr^{[B]}$	0.62	2.24	1.29	1.25	0.87	0.92	1.17	1.22	1.51	1.50
$Ba^{[B]}$	1.07	0.07	0.26	0.10	0.20	0.27	0.15	0.03	0.07	0.08
$\sum M^{2+[B]}$	2.17	2.31	2.26	2.24	2.05	2.24	2.26	2.32	2.43	2.47
$Y^{[B]}$	-	0.04	-	n.d.	n.d.	n.d.	n.d.	n.d.	-	-
$La^{[B]}$	0.18	0.29	0.27	-"-	-"-	-"-	-"-	-"-	0.22	0.20
$Ce^{[B]}$	0.46	0.30	0.38	-"-	-"-	-"-	-"-	-"-	0.28	0.26
$Pr^{[B]}$	0.04	0.03	-	-"-	-"-	-"-	-"-	-"-	0.02	0.02
$Nd^{[B]}$	0.15	0.05	0.09	-"-	-"-	-"-	-"-	-"-	0.05	0.05
$Sm^{[B]}$	-	-	-	-"-	-"-	-"-	-"-	-"-	-	-
$\sum REE^{[B]}$	0.83	0.71	0.74	0.76	0.72	0.76	0.74	0.68	0.57	0.53
$\sum^{[B]}$	3.00	3.02	3.00	3.00	3.00	3.00	3.00	3.00	3.00	3.00
(CO_3)	5.00	5.00	5.00	5.00	5.00	5.00	5.00	5.00	5.00	5.00

Table 1. Chemical composition of burbankite group minerals from carbonatites (continuation)

Constituents	Burbankite			Calciobur-bankite	Burban-kite	Khanneshite			Burbankite	
	Khibiny		Arbara-stakh	Srednyaya Zima	Kovdor		Afrikanda			
	an. 31	an. 32	an. 33••	an. 34	an. 35	an. 36	an. 37	an. 38	an. 39	an. 40
	wt %									
Na_2O	12.60	12.03	11.56	10.50	9.07	11.34	7.31	9.26	9.02	9.00
K_2O	-	-	0.60	-	-	-	-	-	-	-
CaO	10.20	10.08	13.91	15.12	9.35	7.16	8.43	7.23	8.81	7.96
SrO	18.38	17.71	16.65	12.43	45.06	10.45	13.49	12.61	15.65	16.29
BaO	2.52	6.65	4.10	8.39	4.07	31.73	23.96	24.47	18.74	18.42
$\sum REE_2O_3$	n.d.	n.d.	16.15	14.50	n.d.	n.d.	n.d.	n.d.	n.d.	n.d.
Y_2O_3	-	-	n.d.	n.d.	-	-	-	-	-	-
La_2O_3	7.05	4.77	-"-	-"-	-	2.63	5.75	6.00	7.53	8.46
Ce_2O_3	11.06	9.26	-"-	-"-	-	5.89	6.63	7.13	6.46	6.38
Pr_2O_3	0.80	0.88	-"-	-"-	-	0.40	0.00	0.00	1.45	0.45
Nd_2O_3	2.53	3.11	-"-	-"-	-	1.15	1.40	1.47	1.04	0.72
Sm_2O_3	0.31	0.39	-"-	-"-	-	-	-	-	-	-
(CO_2)	(34.21)	(33.38)	34.66	35.71	n.d.	n.d.	n.d.	n.d.	n.d.	n.d.
Sum	99.66	98.62•	99.93•	99.62•	67.55	70.87•	66.97	68.17	68.7	67.68
	Formula									
$Na^{[A]}$	2.61	2.56	2.41	2.27	1.89	2.58	1.73	2.16	2.00	2.04
$Ca^{[A]}$	0.27	0.35	0.52	0.57	1.06	0.50	0.83	0.60	0.65	0.64
$\sum[A]$	2.88	2.91	2.93	2.84	2.94	3.07	2.56	2.76	2.66	2.68
$K^{[B]}$	-	-	0.08	-	-	-	-	-	-	-
$Ca^{[B]}$	0.90	0.84	1.08	1.24	0.02	0.40	0.28	0.33	0.43	0.36
$Sr^{[B]}$	1.14	1.13	1.04	0.80	2.81	0.71	0.96	0.88	1.04	1.11
$Ba^{[B]}$	0.11	0.29	0.17	0.37	0.17	1.46	1.15	1.15	0.84	0.84
$\sum M^{2+[B]}$	2.15	2.26	2.29	2.41	3.00	2.57	2.38	2.36	2.31	2.31
$Y^{[B]}$	-	-	n.d.	n.d.	-	-	-	-	-	-
$La^{[B]}$	0.28	0.19	-"-	-"-	-	0.11	0.26	0.27	0.32	0.37
$Ce^{[B]}$	0.43	0.37	-"-	-"-	-	0.25	0.30	0.31	0.27	0.27
$Pr^{[B]}$	0.03	0.04	-"-	-"-	-	0.02	-	-	0.06	0.02
$Nd^{[B]}$	0.10	0.12	-"-	-"-	-	0.05	0.06	0.06	0.04	0.03
$Sm^{[B]}$	0.01	0.01	-"-	-"-	-	-	-	-	-	-
$\sum REE^{[B]}$	0.85	0.74	0.63	0.59	0.00	0.43	0.62	0.64	0.69	0.69
$\sum[B]$	3.00	3.00	3.00	3.00	3.00	3.00	3.00	3.00	3.00	3.00
(CO_3)	5.00	5.00	5.00	5.00	5.00	5.00	5.00	5.00	5.00	5.00

Table 1. Chemical composition of burbankite group minerals from carbonatites (end)

Constituents	Burbankite						
	Afri-kanda	Kalkfeld		Shaxingdong	Chipman Lake		
	An. 41	an. 42	an. 43	an. 44	an. 45	an. 46	an. 47
	wt %						
Na_2O	7.47	10.6	13.1	6.03	7.38	7.20	6.70
K_2O	-	-	-	-	-	-	-
CaO	8.24	3.6	5.5	14.52	21.09	15.01	13.53
SrO	16.82	25.6	26.7	29.49	29.12	30.44	28.63
BaO	20.17	5.5	5.2	4.88	4.06	1.85	3.37
$\sum REE_2O_3$	n.d.	n.d.	n.d.	12.53	n.d.	n.d.	n.d.
Y_2O_3	-	-	-	n.d.	0.47	0.71	0.45
La_2O_3	6.10	7.0	6.2	-"-	0.76	0.54	4.34
Ce_2O_3	5.92	9.0	8.8	-"-	1.20	0.77	5.80
Pr_2O_3	0.93	-	-	-"-	0.18	0.15	0.60
Nd_2O_3	0.70	1.5	2.1	-"-	0.21	0.26	1.64
Sm_2O_3	-	-	-	-"-	0.15	0.07	0.00
(CO_2)	n.d.	(29.8)	(33.3)	32.58	n.d.	n.d.	n.d.
Sum	66.35	92.6	100.9	100.03	65.06*	60.54*	65.19*
	Formula						
$Na^{[A]}$	1.76	2.51	2.79	1.24	1.43	1.62	1.37
$Ca^{[A]}$	0.82	0.35	0.26	1.14	1.22	1.13	1.02
$\sum[A]$	2.57	2.86	3.05	2.38	2.62	2.75	2.39
$K^{[B]}$	-	-	-	-	-	-	-
$Ca^{[B]}$	0.25	0.13	0.39	0.51	1.03	0.75	0.52
$Sr^{[B]}$	1.18	1.82	1.70	1.81	1.68	2.05	1.75
$Ba^{[B]}$	0.96	0.26	0.22	0.20	0.16	0.08	0.14
$\sum M^{2+[B]}$	2.39	2.21	2.31	2.52	2.87	2.88	2.41
$Y^{[B]}$	-	-	-	n.d.	0.03	0.04	0.02
$La^{[B]}$	0.27	0.32	0.25	-"-	0.03	0.02	0.17
$Ce^{[B]}$	0.26	0.40	0.36	-"-	0.04	0.04	0.22
$Pr^{[B]}$	0.04	-	-	-"-	0.01	0.01	0.02
$Nd^{[B]}$	0.03	0.07	0.08	-"-	0.01	0.01	0.16
$Sm^{[B]}$	-	-		-"-	0.01	-	-
$\sum REE^{[B]}$	0.61	0.79	0.69	0.48	0.13	0.12	0.59
$\sum[B]$	3.00	3.00	3.00	3.00	3.00	3.00	3.00
(CO_3)	5.00	5.00	5.00	5.00	5.00	5.00	5.00

Note.
1, 2 — samples №№ 65111 and 65105 accordingly from collection of Fersman Mineralogical Museum RAS; 3, 4 (Borodin, Kapustin, 1962); 5–7, 10 — samples from V.V. Subbotin collection; 8, 9 (Subbotin *et al.,* 1999); 11 (Kukharenko *et al.,* 1965); 12, 13 (Subbotin *et al.,* 1999); 14 — sample № 65503 from collection of Fersman Mineralogical Museum RAS; 15 (Zdorik, 1966); 16 — sample from A.P. Khomyakov collection (Pekov *et al.,* 1998); 17, 18 — sample № 81605 from collection of Fersman Mineralogical Museum RAS (Pekov *et al.,* 1998); 19, 20 (Eremenko, Vel'ko, 1982); 21, 22 (Pekov *et al.,* 1998); 24 (Tikhonenkova, 1974); 25 (Tikhonenkova *et al.,* 1977); 26 (Mineralogy.., 1978); 27 (Dudkin *et al.,* 1981); 28 (Zaitsev *et al.,* 1990); 29, 30 (Zaitsev *et al.,* 1997); 31, 32 (Zaitsev *et al.,* 1998); 33 (Zhabin *et al.,* 1971); 34 (Pozharitskaya, Samoilov, 1972); 35, 36 (Ivanyuk *et al.,* 2002); 37–40 (Zaitsev, Chakhmouradian, 2002); 41 (Zaitsev, Chakhmouradian, 2002); 42, 43 (Buhn *et al.,* 1999); 44 (Shi Li, Tong Wang, 1993); 45–47 (Platt, Woolley, 1990); №№ 1, 2, 5–7, 10, 14, 23 — data of present research.
* — The sum of analysis also contains (wt %): 3 — 0.35 MgO, 1.05 Al_2O_3, 0.48 Fe_2O_3, 0.19 SiO_2, 0.97 H_2O; 4 — 0.10 Fe_2O_3, 0.06 SiO_2, 2.60 H_2O; 11 — 0.03 Al_2O_3, 0.22 Fe_2O_3, 0.10 SiO_2, 0.25 H_2O; 15 — 0.14 MgO, 0.41 Al_2O_3, 0.24 Fe_2O_3, 0.16 SiO_2, 0.023 H_2O, 0.03 F; 19 — 1.59 H_2O; 20 — 1.32 H_2O; 25 — 0.93 Fe_2O_3; 26 — 0.10 MgO, 0.20 Al_2O_3, 0.10 Fe_2O_3, 0.22 SiO_2, 1.37 H_2O; 28 — 0.02 MgO, 0.07 MnO, 0.44 FeO, 0.20 SiO_2, 0.85 H_2O, 0.04 F, 0.02 -O=F_2; 32 — 0.16 ThO_2, 0.20 Gd_2O_3 (0.01 apfu); 33 — 0.05 MnO, 0.37 Fe_2O_3, 1.76 H_2O, 0.20 F, 0.08 -O=F_2; 34 — 0.93 Al_2O_3, 0.23 Fe_2O_3, 1.81 H2O; 36 — 0.12 TiO2; 45 — 0.25 FeO, 0.15 MnO, 0.04 MgO; 46 — 0.53 FeO, 0.13 MnO, 2.88 MgO; 47 — 0.13 FeO. n.d. — constituent was not determined, dash — the amount of constituent is below detection limit.
** — The mineral was described as «burbankite», but according to chemical composition, corresponds to calcioburbankite.

group minerals from carbonatites: burbankite replaces khanneshite in Khibiny (Pekov *et al.*, 1998) and calcioburbankite in Vuoriayrvi (Subbotin *et al.*, 1999), the high-strontian burbankite was found in the late association in Kovdor (Ivanyuk *et al.*, 2002).

In alkaline hydrothermalites all this group members are known except khanneshite. Here the range of their chemical composition is extremely wide (Fig. 1): from strongly REE-depleted burbankite (an. 73) to petersenite. Essential predominance of strontium (usually 1.6–2.3 *apfu*) over other *B*-cations (Fig. 2b) is observed in burbankite from alkaline hydrothermalites almost of all geological objects. High content of barium in burbankite-like phases is not typical for this genetic type (reraly more than 0.6 *apfu*), which is explained by that with temperature decrease the tendency of very large Ba^{2+} to isolation intensifies, and it will form own phases practically without strontium: zeolites, BaTi-silicates, BaREE-fluorcarbonates, and others. Almost all finds of high-sodium members of the burbankite group are made in alkaline hydrothermalites. The maximum contents of sodium are reached here, which is a necessary condition for origin of remondite and petersenite. The specimens of the burbankite group in alkaline hydrothermalites are characterized by increased part of strontium and a little one of neodymium in spectrum of REE.

Burbankite from pectolite metasomatites approaches in its chemical composition to REE-free end member $(Na_2Ca)M^{2+}{}_3(CO_3)_5$ (Fig. 1). It is strongly Sr-enriched (usually 2.1–2.5 *apfu*, Table 3). All samples from both Khibiny and Murun are characterized by predominance of lanthanum over cerium together with insignificant contents of praseodymium and neodymium.

The widest prevalence of burbankite forming very large accumulations among other members of the group is evidence of maximum stability of this structural type exactly under predominance of strontium in *B*-site. Also that can be confirmed by sharply Sr-enriched chemical compositions of burbankite from alkaline hydrothermalites. Here crystallization proceeds from water solutions under sufficiently low-temperature conditions, consequently, the fractionating of similar in properties chemical elements is accomplished by the best way, and affinity of different structural types to certain components is realized as much as possible. In high-alkaline hydrothermal systems the separation of strontium from more widespread calcium, which caused by the crystallochemical reasons, is clear demonstrated by stable paragenesis of high-strontian burbankite with shortite $Na_2Ca_2(CO_3)_3$ almost non-containing strontium.

Table 2. Chemical composition of burbankite group minerals from alkaline hydrothermalites

Constituents	Burbankite									
	Vishnevye Gory	Lovozero							Khibiny	
	an. 48	an. 49	an. 50	an. 51	an. 52	an. 53	an. 54	an. 55	an. 56	an. 57
	wt %									
Na_2O	9.83	14.52	12.3	11.73	9.56	10.54	9.47	10.61	12.03	10.95
K_2O	-	-	-	-	-	-	-	-	0.60	-
CaO	9.07	7.09	4.1	2.89	4.85	3.60	3.48	1.88	10.89	8.05
SrO	36.38	26.35	27.4	22.28	28.30	28.28	23.51	23.95	22.57	32.68
BaO	3.46	2.33	8.2	10.12	12.03	8.70	5.82	7.84	3.86	2.47
$\sum REE_2O_3$	n.d.	18.95	n.d.	n.d.	n.d.	n.d.	n.d.	n.d.	13.50	13.50
Y_2O_3	0.54	n.d.	0.6	-	0.53	0.47	0.47	0.39	n.d.	n.d.
La_2O_3	2.04	-"-	1.9	3.26	3.00	3.28	4.69	5.37	-"-	-"-
Ce_2O_3	2.91	-"-	5.1	8.38	4.06	5.97	7.84	7.91	-"-	-"-
Pr_2O_3	0.22	-"-	0.3	0.58	0.36	0.76	0.80	0.80	-"-	-"-
Nd_2O_3	0.59	-"-	3.1	1.90	1.09	2.07	2.81	3.03	-"-	-"-
Sm_2O_3	-	-"-	1.1	0.22	-	-	0.53	0.35	-"-	-"-
ThO_2	-	-	1.6	-	-	-	1.60	-	-	-
CO_2	n.d.	30.77	(32.2)	(29.25)	n.d.	n.d.	n.d.	n.d.	34.50	32.20
Sum	65.04	100.01	100.1*	90.61	63.80	63.68	60.99	62.12	99.04*	99.85
	Formula									
$Na^{[A]}$	2.10	2.92	2.63	2.89	2.28	2.50	2.35	2.63	2.56	2.29
$Ca^{[A]}$	0.82	0.18	0.22	0.22	0.64	0.46	0.37	0.26	0.53	0.59
$\sum[A]$	2.92	3.10	2.85	3.11	2.92	2.96	2.72	2.89	3.05	2.88
$Na^{[B]}$	-	-	-	-	-	-	-	-	-	-
$K^{[B]}$	-	-	-	-	-	-	-	-	0.08	-
$Ca^{[B]}$	0.26	0.61	0.27	0.17	-	0.01	0.10	-	0.78	0.34
$Sr^{[B]}$	2.33	1.58	1.75	1.65	2.02	2.01	1.75	1.77	1.43	2.03
$Ba^{[B]}$	0.15	0.09	0.35	0.51	0.58	0.42	0.29	0.39	0.17	0.10
$\sum M^{2+[B]}$	2.74	2.28	2.37	2.33	2.60	2.43	2.14	2.17	2.38	2.47
$Y^{[B]}$	0.03	n.d.	0.04	-	0.03	0.03	0.03	0.03	n.d.	n.d.
$La^{[B]}$	0.08	-"-	0.08	0.15	0.14	0.15	0.22	0.25	-"-	-"-
$Ce^{[B]}$	0.12	-"-	0.20	0.39	0.18	0.27	0.37	0.37	-"-	-"-
$Pr^{[B]}$	0.01	-"-	0.01	0.03	0.02	0.03	0.04	0.04	-"-	-"-
$Nd^{[B]}$	0.02	-"-	0.13	0.09	0.05	0.09	0.13	0.14	-"-	-"-
$Sm^{[B]}$	-	-"-	0.04	0.01	-	-	0.02	0.02	-"-	-"-
$\sum REE^{[B]}$	0.26	0.72	0.59	0.67	0.42	0.57	0.81	0.84	0.54	0.53
$Th^{[B]}$	-	-	0.04	-	-	-	0.05	-	-	-
$\sum^{[B]}$	3.00	3.00	3.00	3.00	3.01	3.00	3.00	3.01	3.00	3.00
(CO_3)	5.00	5.00	5.00	5.00	5.00	5.00	5.00	5.00	5.00	5.00

Table 2. Chemical composition of burbankite group minerals from alkaline hydrothermalites (continuation)

Constituents	Burbankite									
	Khibiny									
	an. 58	an. 59	an. 60	an. 61	an. 62	an. 63	an. 64	an. 65	an. 66	an. 67
	wt %									
Na_2O	12.00	14.30	12.38	12.67	12.56	11.12	10.61	11.35	11.72	11.40
K_2O	-	-	0.21	0.39	0.09	-	-	-	0.38	-
CaO	6.99	5.40	1.68	1.53	3.94	6.28	6.96	3.56	0.59	3.40
SrO	31.45	25.99	19.18	18.65	19.57	35.57	33.73	33.40	18.83	35.27
BaO	2.40	7.06	13.23	12.37	3.37	4.85	7.92	3.74	10.71	1.39
$\sum REE_2O_3$	16.00	n.d.	n.d.	n.d.	n.d.	n.d.	n.d.	n.d.	n.d.	n.d.
Y_2O_3	n.d.	-	-	-	-	-	0.57	0.48	0.35	0.64
La_2O_3	-"-	5.01	11.17	12.89	14.17	5.20	2.94	4.74	13.58	6.62
Ce_2O_3	-"-	7.07	9.23	10.05	10.82	6.65	5.74	7.83	9.78	7.03
Pr_2O_3	-"-	-	-	-	-	0.29	0.44	0.78	-	0.50
Nd_2O_3	-"-	0.58	0.89	0.73	0.85	0.63	1.36	2.07	0.82	1.37
Sm_2O_3	-"-	-	-	-	-	0.06	-	-	-	-
ThO_2	-	-	-	-	-	-	-	-	-	-
CO_2	31.90	(34.58)	n.d.	n.d.	n.d.	n.d.	n.d.	n.d.	n.d.	n.d.
Sum	100.74	99.99	67.97	69.28	65.37	70.65	70.26	67.95	66.76	67.62
	Formula									
$Na^{[A]}$	2.48	3.12	2.86	2.87	2.81	2.29	2.21	2.47	2.77	2.47
$Ca^{[A]}$	0.45	0.18	0.12	0.09	0.05	0.61	0.67	0.43	0.08	0.41
$\sum[A]$	2.93	3.30	2.98	2.96	2.86	2.90	2.88	2.91	2.85	2.88
$Na^{[B]}$	-	-	-	-	-	-	-	-	-	-
$K^{[B]}$	-	-	0.03	0.06	0.01	-	-	-	0.06	-
$Ca^{[B]}$	0.34	0.48	0.09	0.10	0.43	0.12	0.12	-	-	-
$Sr^{[B]}$	1.94	1.69	1.33	1.26	1.31	2.19	2.10	2.18	1.33	2.29
$Ba^{[B]}$	0.10	0.31	0.62	0.57	0.15	0.20	0.33	0.16	0.51	0.06
$\sum M^{2+[B]}$	2.38	2.48	2.04	1.93	1.89	2.51	2.56	2.34	1.85	2.35
$Y^{[B]}$	n.d.	-	-	-	-	-	0.03	0.03	0.02	0.04
$La^{[B]}$	-"-	0.21	0.49	0.55	0.60	0.20	0.12	0.20	0.61	0.27
$Ce^{[B]}$	-"-	0.29	0.40	0.43	0.46	0.26	0.23	0.32	0.44	0.29
$Pr^{[B]}$	-"-	-	-	-	-	0.01	0.02	0.03	-	0.02
$Nd^{[B]}$	-"-	0.02	0.04	0.03	0.04	0.02	0.05	0.08	0.04	0.05
$Sm^{[B]}$	-"-	-	-	-	-	-	-	-	-	-
$\sum REE^{[B]}$	0.62	0.52	0.93	1.01	1.10	0.49	0.44	0.66	1.11	0.67
$Th^{[B]}$	-	-	-	-	-	-	-	-	-	-
$\sum^{[B]}$	3.00	3.00	3.00	3.00	3.00	3.00	3.00	3.00	3.01	3.02
(CO_3)	5.00	5.00	5.00	5.00	5.00	5.00	5.00	5.00	5.00	5.00

Table 2. Chemical composition of burbankite group minerals from alkaline hydrothermalites (continuation)

Constituents	Burbankite	Remon-dite-(Ce)	Remondite-(La)		Petersen-ite-(Ce)	Burban-kite	Calcioburbankite		Petersenite-(Ce)	
	Khibiny					Mont Saint-Hilaire				
	an. 68	an. 69	an. 70	an. 71	an. 72	an. 73	an. 74	an. 75	an. 76	an. 77
	wt %									
Na_2O	10.80	15.3	12.84	15.48	17.51	8.30	15.17	13.81	17.38	16.77
K_2O	-	-	1.54	0.58	-	-	-	-	-	-
CaO	4.74	4.9	2.33	5.13	5.52	12.03	11.81	12.48	1.32	5.07
SrO	22.98	7.8	14.66	2.93	4.10	32.35	7.65	7.90	1.70	2.37
BaO	14.45	3.1	6.34	0.18	0.42	11.02	0.46	6.00	0.32	0.54
$\sum REE_2O_3$	n.d.	n.d.	n.d.	n.d.	n.d.	n.d.	n.d.	n.d.	n.d.	n.d.
Y_2O_3	0.36	-	-	-	0.04	-	-	-	-	-
La_2O_3	5.61	11.3	18.01	19.75	11.97	-	9.30	12.51	14.49	12.14
Ce_2O_3	5.31	17.8	12.22	16.67	17.80	2.12	14.38	10.89	23.66	21.29
Pr_2O_3	0.24	1.4	-	0.99	1.54	-	1.26	-	2.00	2.10
Nd_2O_3	0.71	3.7	0.86	2.27	5.20	0.13	3.76	0.74	5.82	5.04
Sm_2O_3	-	0.22	-	0.37	0.39	-	0.48	-	0.60	0.66
ThO_2	-	-	-	1.34	0.78	-	-	-	-	-
CO_2	n.d.	(32.7)	n.d.	n.d.	n.d.	(33.17)	(35.13)	(34.98)	(32.92)	(34.07)
Total	65.20	98.22	68.80	65.69	65.27	99.30*	99.40	99.31	100.21	100.05
	Formula									
$Na^{[A]}$	2.53	2.94	2.78	2.87	3.09	1.76	2.97	2.86	2.94	2.95
$Ca^{[A]}$	0.46	-	0.07	-	-	1.07	-	0.10	-	-
$\sum[A]$	2.99	2.94	2.85	2.87	3.09	2.83	2.97	2.96	2.94	2.95
$Na^{[B]}$	-	0.35	-	0.47	0.60	-	0.09	-	0.83	0.59
$K^{[B]}$	-	-	0.23	0.08	-	-	-	-	-	-
$Ca^{[B]}$	0.15	0.59	0.21	0.60	0.64	0.35	1.31	1.32	0.16	0.60
$Sr^{[B]}$	1.61	0.51	0.97	0.19	0.26	2.07	0.46	0.49	0.11	0.15
$Ba^{[B]}$	0.68	0.14	0.28	0.01	0.02	0.48	0.02	0.25	0.01	0.02
$\sum M^{2+[B]}$	2.45	1.24	1.46	0.80	0.92	2.90	1.79	2.06	0.28	0.77
$Y^{[B]}$	0.02	-	-	-	-	-	-	-	-	-
$La^{[B]}$	0.25	0.47	0.76	0.80	0.48	-	0.36	0.49	0.59	0.49
$Ce^{[B]}$	0.24	0.72	0.51	0.68	0.71	0.09	0.55	0.42	0.97	0.85
$Pr^{[B]}$	0.01	0.06	-	0.04	0.06	-	0.05	-	0.08	0.08
$Nd^{[B]}$	0.03	0.15	0.04	0.09	0.20	0.01	0.14	0.03	0.23	0.20
$Sm^{[B]}$	-	0.01	-	0.01	0.01	-	0.02	-	0.02	0.02
$\sum REE^{[B]}$	0.55	1.41	1.31	1.62	1.46	0.10	1.12	0.94	1.89	1.64
$Th^{[B]}$	-	-	-	0.03	0.02	-	-	-	-	-
$\sum^{[B]}$	3.00	3.00	3.00	3.00	3.00	3.00	3.00	3.00	3.00	3.00
(CO_3)	5.00	5.00	5.00	5.00	5.00	5.00	5.00	5.00	5.00	5.00

Table 2. Chemical composition of burbankite group minerals from alkaline hydrothermalites (continuation)

Constituents	Remondite-(Ce)		Burbankite				Remondite-(Ce)
	Mont Saint-Hilaire		Rocky Boy	Ridge Moskal	Pokrovo-Kireevskoe		Ebounja
	an. 78	an. 79**	an. 80	an. 81	an. 82	an. 83	an. 84
	wt %						
Na_2O	13.09	12.60	9.69	8.34	9.81	7.33	17.16
K_2O	0.22	0.24	0.15	-	2.35	-	-
CaO	1.68	3.89	13.46	11.47	6.76	6.62	10.54
SrO	1.67	14.63	19.42	25.08	18.45	30.87	3.98
BaO	0.50	0.85	13.56	11.47	9.97	4.51	-
$\sum REE_2O_3$	n.d.	n.d.	9.48	n.d.	14.81	n.d.	n.d.
Y_2O_3	-	-	n.d.	-	n.d.	-	0.24
La_2O_3	11.69	16.13	-"-	3.37	-"-	10.00	11.60
Ce_2O_3	25.50	17.27	-"-	5.39	-"-	7.74	14.99
Pr_2O_3	2.72	0.96	-"-	0.46	-"-	0.36	1.49
Nd_2O_3	9.00	2.57	-"-	1.26	-"-	0.24	3.34
Sm_2O_3	1.13	0.33	-"-	0.14	-"-	0.08	0.50
ThO_2	-	-	-	-	0.50	-	-
CO_2	n.d.	n.d.	32.55	33.24	32.55	(32.26)	(35.24)
Sum	67.20	69.47	99.31*	100.68*	100.02*	100.09*	99.554*
	Formula						
$Na^{[A]}$	2.42	2.61	2.06	1.77	2.23	1.62	3.11
$Ca^{[A]}$	-	-	0.79	0.89	0.64	0.81	-
$\sum^{[A]}$	2.42	2.61	2.85	2.66	2.87	2.43	3.11
$Na^{[B]}$	0.50	0.05	-	-	-	-	0.35
$K^{[B]}$	0.04	0.04	0.02	-	0.35	-	-
$Ca^{[B]}$	0.21	0.46	0.79	0.46	0.20	0.01	1.17
$Sr^{[B]}$	0.11	0.93	1.23	1.60	1.25	2.03	0.24
$Ba^{[B]}$	0.02	0.04	0.58	0.49	0.46	0.20	-
$\sum M^{2+[B]}$	0.34	1.43	2.60	2.55	1.91	2.24	1.41
$Y^{[B]}$	-	-	n.d.	-	n.d.	-	0.01
$La^{[B]}$	0.50	0.64	-"-	0.13	-"-	0.42	0.45
$Ce^{[B]}$	1.08	0.69	-"-	0.22	-"-	0.32	0.57
$Pr^{[B]}$	0.12	0.04	-"-	0.02	-"-	0.01	0.06
$Nd^{[B]}$	0.37	0.10	-"-	0.05	-"-	0.01	0.12
$Sm^{[B]}$	0.05	0.01	-"-	0.01	-"-	-	0.02
$\sum REE^{[B]}$	2.12	1.48	0.38	0.45	0.64	0.76	1.23
$Th^{[B]}$	-	-	-	-	0.10	-	-
$\sum^{[B]}$	3.00	3.00	3.00	3.00	3.00	3.00	3.00
(CO_3)	5.00	5.00	5.00	5.00	5.00	5.00	5.00

Note.
48 — sample from S.N. Nikandrov collection (Pekov *et al.,* 1996); 49 (Tikhonenkova, Kazakova, 1964); 50, 51 (Khomyakov, 1990); 52–55 — samples from A.P. Khomyakov collection (Pekov, 2001); 56 (Shlyukova *et al.,* 1972); 57 (Tikhonenkova *et al.,* 1977); 58 (Tikhonenkova *et al.,* 1977); 59 (Khomyakov, 1990); 60–63 (Yakovenchuk, 1995); 64 (Belovitskaya *et al.,* 2000); 68 — sample from A.P. Khomyakov collection; 69 (Khomyakov, 1990); 70 (Yakovenchuk *et al.,* 1999); 71 (Pekov *et al.,* 2000); 72 (Pekov *et al.,* 1998); 73 (Chen, Chao, 1974); 74, 75 (Van Velthuizen *et al.,* 1995); 76 (Grice *et al.,* 1994); 77 (Van Velthuizen *et al.,* 1995); 80 (Pecora, Kerr, 1953); 81 (Effenberger *et al.,* 1985); 82 (Efimov *et al.,* 1969); 83 (Litvin *et al.,* 1998); 84 (Cesbron *et al.,* 1988); 65–68, 78, 79 — data of present research. * — The sum of analysis also contains (wt %): 50 — 1.2 Gd_2O_3 (0.05 apfu), 0.5 Dy_2O_3 (0.02 apfu), 0.5 Er2O3 (0.02 apfu); 56 — 0.19 Fe_2O_3, 0.9 SiO_2; 73 — 0.08 Dy_2O_3, 0.10 Yb_2O_3; 79 — 0.14 MgO, 0.25 Al_2O_3, 0.03 Fe_2O_3, 0.16 SiO_2, 0.18 H_2O, 0.12 P_2O_5, 0.24 S, 0.12 -O=S; 81 — 0.41 Gd_2O_3 (0.02 apfu), 0.05 Tb2O3; 82 — 0.32 MgO, 0.37 Al_2O_3, 0.19 Fe_2O_3, 3.94 H_2O; 83 — 0.08 Gd_2O_3; 84 — 0.09 Eu_2O_3, 0.24 Gd_2O_3 (0.01 apfu), 0.07 Dy_2O_3, 0.01 Ho_2O_3, 0.03 Er_2O_3, 0.03 Yb_2O_3, 0.004 Lu_2O_3. n.d. — constituent was not determined, dash — the amount of constituent is below detection limit. ** — According to structural refinement by Rietveld method, this mineral is a hexagonal (sp. gr. P63mc) analogue of remondite (Gobetchiya *et al.,* 2001).

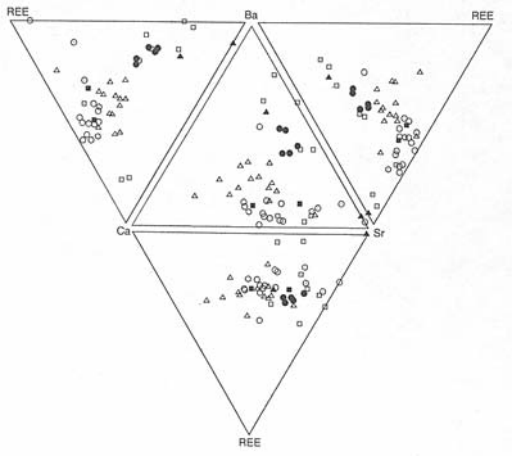

FIG. 2a. Ratios of Sr, Ca, Ba, and REE in B-site of the burbankite group minerals from carbonatites:
● — Afrikanda, ⬭ — Arbarastakh, Δ— Vuoriyarvi, ■ — Gornoe Ozero, ⊙— Kalkfeld, ▲— Kovdor,◬— Srednyaya Zima, □— Khanneshin, ○— Khibiny, ⊡— Chipman Lake, ⦶ — Shaxiongdong

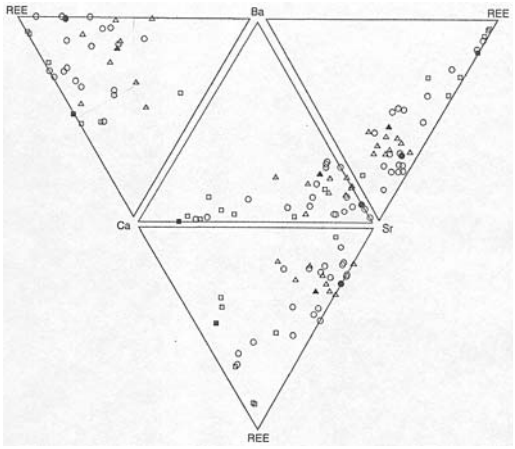

FIG. 2b. Ratios of Sr, Ca, Ba, and REE in B-site of the burbankite group minerals from alkaline hydrothermalites:
⬭ — Vishnevye Gory, ● — Pokrovo-Kireevskoe, Δ — Lovozero, ▲ — Ridge Moskal, — Rocky Boy, □ — Mont Saint-Hilaire, ○ — Khibiny, ■ — Ebounja

Location of calcium in *A*-site, than in *B*-site is more typical for burbankite-like phases from low-temperature formations, i.e. isomorphism of calcium with sodium is preferable than with strontium. Probably, relative rarity of Ca-, Ba-, and REE-dominant members of the burbankite group is connected to their ability to crystallize only in strontium deficiency conditions, which is untypical for alkaline complexes as a whole.

The rare-earth elements in burbankite occupy ten-vertex *B*-polyhedra where the large ion Sr^{2+} with radius 1.32 Å (Shannon, Prewitt, 1969) predominates. As a rule the more widespread in nature ion Ce^{3+} (radius 1.26 Å) prevails in spectrum of REE of burbankite-like phases. However, La^{3+} (1.28 Å), largest ion of REE^{3+}, is closer in size to Sr^{2+} that is the reason of its presence in significant amount. The degree of fractionating of rare-earth elements increases with temperature lowering, which results in increase of lanthanum role that is turned out especially significant than more strontium is contained by the mineral. The ratios of lanthanides in burbankite of different genetic types from Khibiny massif are the evident example of that. High-strontian burbankite from relatively low-temperature differentiates (hydrothermalites of Mt. Kukisvumchorr and metasomatites of Mt. Ni'orkpahk) is also sharply enriched by La (up to 85% from sum of REE), whereas the high-temperature burbankite from carbonatites of Khibiny has «averaged» chemical composition which is typical for these minerals from other carbonatite objects: Ce — 45−50, La — 35−45, Nd — 5−10% from the sum of REE.

X-ray powder diffraction diagrams of hexagonal burbankite-like minerals are divided into two groups. The first group contains spectra of the samples from carbonatites and hydrothermalites. The spectra of REE-depleted burbankite from pectolite metasomatites make the second group. The most of peaks on the latter are split (Fig. 3). This splitting is most strongly displayed on reflections in areas 2.74−2.77 Å (*hkl* 112, 301) and 2.62−2.65 Å (*hkl* 202, 220): burbankites from carbonatites and alkaline hydrothermalites give single peaks, while burbankite from pectolite metasomatites gives clear distinguished doublets (Fig. 3). All that together with stability of value of ratio Na:Ca ≈ 2:1 in *A*-site of REE-depleted burbankite has caused the assumption about order of *A*-cations in this mineral. However, it isn't confirmed: all studied samples proved to be isostructural with sp. gr. $P6_3mc$ and disordered distribution of sodium and calcium in *A*-sites (Belovitskaya *et al.*, 2000, 2001, 2002; Gobetchiya *et al.*, 2001). The cause of reflection splitting is only ratio of unit cell parameters: $c/a = 0.621$ for REE-depleted burbankite and $c/a \approx 0.615$ for burbankite with «typical» composition (Table 4). The closing in values of interplaner distances in many pairs of reflections takes place with decrease of c/a. Thus, full coincidence for pairs (112)-(301) and (202)-(220) will occur at $c/a = 0.61237$.

We shall especially note the detection of earlier unknown hexagonal modification of remondite-(Ce) established in the sample from Mont Saint-Hilaire (Gobetchiya *et al.*, 2001).

Thus, the burbankite structural type is very stable. It is maintained in wide interval of cationic ratios: from REE-free end member $(Na_2Ca)(Sr,Ca,Ba)_3(CO_3)_5$ at least to chemical composition $Na_{2.6}(REE_{1.5}Sr_{0.9}Ca_{0.5}Na_{0.1})_{\Sigma 3.0}(CO_3)_5$ which hexagonal analog of remondite corresponds to. The representatives of this

Table 3. Chemical composition of burbankite from pectolite metasomatites and Green River Formation

Constituents	Pectolite metasomatites									Green River Formation
	Murun				Khibiny					
	an. 85	an. 86	an. 87	an. 88	an. 89	an. 90	an. 91	an. 92	an. 93	an. 94
	wt %									
Na_2O	9.83	5.64	8.44	8.04	9.92	8.84	8.51	8.29	9.72	10.47
K_2O	-	-	1.06	0.82	-	-	-	-	-	-
CaO	12.30	10.27	12.04	13.59	11.22	7.85	10.04	10.32	8.59	8.00
SrO	42.18	32.00	34.60	33.10	37.88	26.10	36.28	36.94	34.00	15.61
BaO	2.72	13.38	1.79	1.83	10.21	21.05	9.91	6.61	6.83	5.73
Y_2O_3	0.33	-	-	-	-	-	0.48	0.49	-	0.19
La_2O_3	-	3.04	-	-	1.58	1.16	1.32	2.06	3.58	3.73
Ce_2O_3	-	2.90	-	-	0.33	0.40	0.44	0.90	2.65	8.65
Pr_2O_3	-	-	-	-	-	-	-	-	-	1.57
Nd_2O_3	-	0.02	-	-	-	0.34	-	-	0.17	4.60
Sm_2O_3	-	-	-	-	-	-	-	-	-	0.55
CO_2	n.d.	31.08	30.86	29.19	n.d.	n.d.	n.d.	n.d.	n.d.	(29.73)
Sum	67.36	98.31	90.94*	93.71*	71.14	65.73	66.98	65.59	65.54	88.83
	Formula									
$Na^{[A]}$	1.96	1.26	1.92	1.82	1.98	2.07	1.82	1.78	2.11	2.50
$Ca^{[A]}$	1.01	1.25	1.12	1.15	0.98	0.92	1.04	1.04	0.81	0.32
∑[A]	2.97	2.50	3.04	2.97	2.95	2.99	2.86	2.82	2.92	2.82
$K^{[B]}$	-	-	0.16	0.12	-	-	-	-	-	-
$Ca^{[B]}$	0.35	0.02	0.40	0.55	0.26	0.09	0.15	0.19	0.22	0.75
$Sr^{[B]}$	2.52	2.13	2.36	2.24	2.26	1.83	2.32	2.37	2.21	1.11
$Ba^{[B]}$	0.11	0.60	0.08	0.08	0.41	1.00	0.43	0.29	0.30	0.28
$\sum M^{2+[B]}$	2.98	2.75	2.84	2.88	2.93	2.92	2.90	2.85	2.73	2.14
$Y^{[B]}$	0.02	-	-	-	-	-	0.03	0.03	-	0.01
$La^{[B]}$	-	0.13	-	-	0.06	0.05	0.05	0.08	0.15	0.17
$Ce^{[B]}$	-	0.12	-	-	0.01	0.02	0.02	0.04	0.11	0.39
$Pr^{[B]}$	-	-	-	-	-	-	-	-	-	0.07
$Nd^{[B]}$	-	-	-	-	-	0.01	-	-	0.01	0.20
$Sm^{[B]}$	-	-	-	-	-	-	-	-	-	0.02
$\sum REE^{[B]}$	0.02	0.25	-	-	0.07	0.08	0.10	0.15	0.27	0.86
∑[B]	3.00	3.00	3.00	3.00	3.00	3.00	3.00	3.00	3.00	3.00
(CO_3)	5.00	5.00	5.00	5.00	5.00	5.00	5.00	5.00	5.00	5.00

Note.
85 — sample № 82976 from collection of Fersman Mineralogical Museum RAS; 86-88 (Konev *et al.,* 1996); 92 (Belovitskaya *et al.,* 2000); 93 (Yakovenchuk *et al.,* 1999); 94 (Fitzpatrick, Pabst, 1977); 85, 89−91 — data of present research.
* — The sum of analysis also contains (wt %): 87 — 0.01 MgO, 0.01 MnO, 0.05 TiO2, 0.08 H_2O, 0.10 F; 88 — 0.04 MgO, 0.02 MnO, 0.08 TiO_2, 0.01 H_2O, 0.05 F.

Table 4. Symmetry and unit cell parameters of burbankite group minerals

	Sp. gr.	a, Å	b, Å	c, Å	γ, gradus	V, Å^3	*c/a*	Reference
REE-depleted burbankite								
an. 85	*P6$_3$mc*	10.525(1)	10.525(1)	6.492(1)	120	619.64(1)	0.6168	The authors' data
an. 92	*P6$_3$mc*	10.5263(1)	10.5263(1)	6.5392(1)	120	627.49(1)	0.6212	Belovitskaya et al., 2000
Burbankite								
an. 2	*P6$_3$mc*	10.494(1)	10.494(1)	6.498(1)	120	622.82(1)	0.6192	The authors' data
an. 23	*P6$_3$mc*	10.458(1)	10.458(1)	6.381(3)	120	604(1)	0.6102	The authors' data
an. 64	*P6$_3$mc*	10.5313(1)	10.5313(1)	6.4829(1)	120	622.68(1)	0.6156	Belovitskaya et al., 2000
an. 65	*P6$_3$mc*	10.516(2)	10.516(2)	6.482(4)	120	620(1)	0.6164	The authors' data
an. 66	*P6$_3$mc*	10.54(1)	10.54(1)	6.48(1)	120	623(1)	0.615	The authors' data
without chemical data	*P6$_3$mc*	10.52(4)	10.52(4)	6.51(2)	120	624(2)	0.619	Voronkov, Shumyats-kaya, 1968
an. 81	*P6$_3$mc*	10.512(2)	10.512(2)	6.492(2)	120	621.3	0.6176	Effenberger *et al.*, 1985
Calcioburbankite								
an. 12	*P6$_3$mc*	10.4974(1)	10.4974(1)	6.4309(1)	120	613.72(1)	0.6126	Belovitskaya et al., 2001
Khanneshite								
an. 21	*P6$_3$mc*	10.5790(1)	10.5790(1)	6.5446(1)	120	634.31(1)	0.6186	Belovitskaya et al., 2002
Hexagonal analogue of remondite								
an. 79	*P6$_3$mc*	10.4889(1)	10.4889(1)	6.3869(1)	120	608.53(6)	0.6089	Gobetchiya *et al.,* 2001
Remondite-(Ce)								
an. 84	*P2$_1$*	10.412(4)	10.414(4)	6.291(3)	119.80(5)	591.9	0.6042	Ginderow, 1989
Remondite-(La)								
an. 71	*P2$_1$*	10.49(1)	10.50(1)	6.417(4)	119.80(1)	613(1)	0.6117	Pekov *et al.,* 2000
Petersenite-(Ce)								
an. 76	*P2$_1$*	20.872(4)	10.601(2)	6.367(1)	120.50(1)*	1213.9(4)	0.6006**	Grice *et al.*, 1994

Note.
The numbers of analyses correspond to tables 1−3. * — In original publication b and c are changed. ** — *c/b.*

Table. 5. Localities and occurrence conditions of burbankite group minerals

Localities	Minerals	Occurrence conditions and typical satellites	Sources
		Localities connected with carbonatites	
Vuoriyarvi, Northern Kareliya	Burbankite Calcioburbankite Remondite-(Ce)	Calcite carbonatites: pyrrhotite, phlogopite, barytocalcite, norsethite, ewaldite, donnayite, vaterite, strontianite, olekminskite, ancylite, pyrochlore, franconite; dolomite carbonatites: calcite, siderite, ancylite, barite, amphibole, chlorite, serpentine, sulphides	Borodin, Kapustin, 1962; Kukharenko et al., 1965; Subbotin *et al,* 1999; the authors' data
Gornoe Ozero, East Siberia	Burbankite	Amphibole- and aegirine-dolomite, amphibole-calcite and ankerite carbonatites	Zdorik, 1966
Khanneshin, Afghanistan	Khanneshite Burbankite	Hydrothermally altered volcanic dolomite and dolomite-ankerite carbonatites: barite, calkinsite, carbocernaite, mckelveyite, chlorite	Eemenko, Vel'ko, 1982; Pekov *et al.*, 1998
Khibiny, Kola Peninsula	Burbankite Khanneshite Calcioburbankite	Calcite carbonatites: biotite, apatite, carbocernaite, fluorite, sulphides, dawsonite	Kirnarskii, Kozyreva, 1974; ; Zaitsev *et al.*, 1997 Pekov *et al.*, 1998; the authors' data
Arbarastakh, Yakutiya	Calcioburbankite	Dolomite-ankerite carbonatites: witherite, strontianite, bastnasite, huanghoite, magnetite, sphalerite, galena; calcite carbonatites: fluorite	Zhabin *et al.,* 1971
Srednyaya Zima, Siberia	Calcioburbankite	Calcite carbonatites: ankerite	Pozharitskaya, Samoilov, 1972
Kovdor, Kola Peninsula	Burbankite Khanneshite	Cavities in dolomite carbonatites: bakhchisaraitsevite (for burbankite)Calcite-shortite carbonatites: phlogopite, bonshtedtite (for khanneshite)	Ivanyuk *et al.*, 2002
Afrikanda, Kola Peninsula	Burbankite Khanneshite	Calcite-amphibole-clinopyroxene rock: inclusions in apatite	Zaitsev, Chakhmouradian, 2002
Kalkfeld, Namibia	Burbankite	Inclusions in quarts from quartzites containing carbonatites: nahcolite, halite, sylvite, fluorite, calcite, cryolite, sulphides, phosphates	Buhn *et al.*, 1999
Chipman Lake, Ontario, Canada	Burbankite	Dolomite carbonatites: apatite, magnetite, sulphides, pyrochlore, barite, monazite, calcite, magnesite, siderite, norsethite, strontianite, REE-fluorcarbonates, albite, orthoclase	Platt, Wooley, 1990
		Localities connected with alkaline hydrothermalites	
Vishnevye Gory, South Urals	Burbankite	Cracks in miaskites: microcline, albite, chlorite, muscovite, ilmenorutile, calcite, siderite, strontianite, ancylite, donnayite, nenadkevichite, korobitsynite, franconite	Pekov *et al.,* 1996
Lovozero, Kola Peninsula	Burbankite	Hyperalkaline pegmatites: common potassic feldspar, aegirine, sidorenkite, nahcolite, shortite, catapleiite, kogarkoite, neighborite, belovite; microcline veins of contact zone	Tikhonenkova, Kazakova, 1964; Khomyakov, 1990; Pekov, 2001
Khibiny, Kola Peninsula	Burbankite Remondite-(Ce) Remondite-(La) Petersenite-(Ce)	Hyperalkaline pegmatites: microcline, aegirine, sodalite, biotite, natrolite, pectolite, cancrisilite, villiaumite, shortite, pirssonite, trona, bonshtedtite, vinogradovite, lamprophyllite, rasvumite, mackinawite, vitusite-(Ce), nacaphite, lomonosovite, sazykinaite-(Y); aegirine and feldspar-fluorite veinlets	Shlyukova *et al.,* 1972; Tikhonenkova *et al.,* 1977; Khomyakov, 1990; Pekov *et al.,* 1998, 2000; Yakovenchuk *et al.,* 1999; Belovitskaya et al., 2000; the authors' data
Mont Saint-Hilaire, Quebec, Canada	Burbankite Calcioburbankite Remondite-(Ce) Petersenite-(Ce)	High-alkaline pegmatites: microcline, albite, aegirine, analcime, natrolite, chlorite, apatite, rhodochrosite, biotite, catapleiite, epididymite, eudialyte, serandite, shomiokite-(Y), rutile, cryolite, siderite, sabinaite. Xenoliths of marbles: calcite, fluorite, leucophanite, narsarsukite, schairerite, shortite, thermonatrite; miaroles in nepheline-syenites	Chen, Chao, 1974; Horvath, Gault, 1990; Grice *et al.*, 1994; Van Velthuizen *et al.*, 1995; Horvath, Pfenninger-Horvath, 2000; the authors' data
Rocky Boy, Montana, USA	Burbankite	Calcite veinlets: aegirine, barite, calkinsite, lanthanite, ancylite, sulphides	Pecora, Kerr, 1953
Ridge Moskal, South Urals	Burbankite	Sodalite-analcime-cancrinite veinlets in alkaline metasomatites: neighborite	Efimov *et al.*, 1969
Pokrovo-Kireevskoe, Ukraine	Burbankite	Hydrothermalites of nepheline-syenites: calcite, fluorite, natrolite	Litvin *et al.,* 1998

Table. 5. *Localities and occurrence conditions of burbankite group minerals* *(continuation)*

Localities	Minerals	Occurrence conditions and typical satellites	Sources
Ebounja, Cameroon	Remondite-(Ce) Burbankite	Veinlets in nepheline-syenites: calcite, aegirine	Cesbron *et al.*, 1988
Green River Formation, Utah and Wyoming, USA	Burbankite	Hydrothermally altered soda-bearing sediments: nahcolite, trona, mckelveyite	Fitzpatrick, Pabst, 1977
		Localities connected with pectolite metasomatites	
Murun, East Siberia	Burbankite	Veins in microclinites and fenites: pectolite, charoite, magnesio-arfvedsonite	Konev et al., 1996; the authors' data
Khibiny, Kola Peninsula	Burbankite	Lenses and veins in ijolite-urtites: pectolite, fluorite, biotite, sphalerite, galena	The authors' data

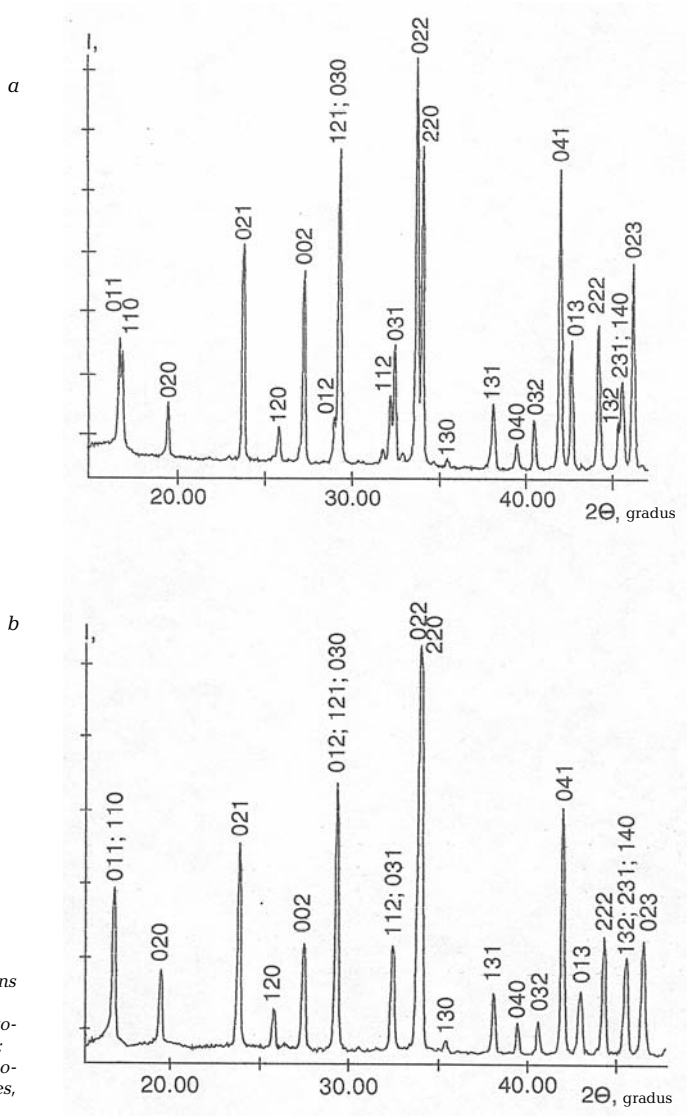

FIG. 3. Fragments of X-ray diffraction patterns (λCuKa) of burbankite:
a) REE-depleted burbankite (an. 92) from pectolite metasomatites, Mt. Ni'orkpakhk, Khibiny;
b) burbankite with «typical» chemical composition (an. 64) from alkaline hydrothermalites, Mt. Kukisvumchorr, Khibiny

high-symmetrical structural type can crystallize in wide range of conditions and in nature greatly prevail over monoclinic members of this group. The latter are typomorphic for low-temperature alkaline hydrothermalites and are extremely rare.

Secondary alterations

Burbankite group minerals become unstable at decrease of alkalinity and easily alter, being replaced by a whole number of secondary products. As components of pseudomorphs after burbankite almost two tens (!) of the minerals of REE, Sr, Ba, and Ca are known. Above all that are the alkali-free carbonates. Burbankite and its analogues from early carbonatite parageneses are exposed to alteration most frequently. Their replacement takes place at hydrothermal stages.

In carbonatites of Vuoriyarvi burbankite is usually replaced by aggregates of barite, strontianite, and ancylite or carbocernaite. Less often here there are the partial pseudomorphs after burbankite, which consist of lanthanite, aragonite, and celestine, but sometimes of calkinsite, barite, strontianite, and pyrite (Kapustin, 1971). At dolomitization of calcite carbonatites of Vuoriyarvi the mixes of calcite, ancylite-(Ce), olekminskite, strontianite, and barite develop after calcioburbankite and burbankite; less often in the alteration products there are carbocernaite, witherite, alstonite, kukharenkoite-(Ce), Ce-ewaldite, Nd-mckelveyite (Subbotin *et al.*, 1999). In aegirine-dolomite carbonatites of Gornoe Ozero massif carbocernaite and ancylite develop after burbankite, and in ankerite carbonatites the burbankite completely replaced by aggregates of strontianite (70–80%), bastnäsite (20–30%), calcite, barite, and allanite (Zdorik, 1966). In carbonatites of Khibiny the burbankite sometimes wholly replaced by ancylite-(Ce), synchysite-(Ce), strontianite, and barite (Zaitsev *et al.*, 1998). In Khanneshin, formation of barite (Eremenko, Vel'ko, 1982) and mckelveyite (Pekov *et al.*, 1998) after khannesite is mentioned. In hydrothermally altered carbonatites of Sebl'yavr (Kola Peninsula) the primary plentiful burbankite is entirely replaced by ancylite-(Ce) (N.V. Sorokhtina data).

In alkaline hydrothermalites the alteration processes of burbankite group minerals are developed much poorly. In Rocky Boy calkinsite grows after burbankite (Pecora, Kerr, 1953). In Mont Saint-Hilaire remondite-(Ce) and petersenite-(Ce) are replaced by alkali-free carbonates of REE: synchysite-(Ce), calico-ancylite-(Ce), bastnäsite-(Ce) (Horvath, Pfenninger-Horvath, 2000; the authors' data), at the latest stages. In Kirovskii mine in Khibiny the development of ancylite-(Ce) after burbankite is observed. Probably, exactly burbankite was the protomineral of cellular ancylite pseudomorphs after hexagonal prisms of undetermined mineral that are widely spread in hydrothermally altered pegmatites of Khibiny.

Conclusions

The crystal structures of all hexagonal members of the burbankite group were studied (Belovitskaya *et al.*, 2000, 2001, 2002; Gobetchiya *et al.*, 2001). The results of this research have allowed ascertaining that the burbankite structural type (sp. gr. $P6_3mc$) is exceptionally steady to variations of cationic composition in *B*-polyhedra: all these minerals are isostructural and form system of continuous solid solutions. Judging by relative prevalence of these minerals in nature and by parageneses, this crystal structure is most steady at predominance of strontium in *B*-site.

All chemical compositions of the burbankite group minerals are described within the limits of system with end members: $(Na_2Ca)M^{2+}{}_3(CO_3)_5$ and $Na_3(REE_2Na)(CO_3)_5$, where M^{2+} = Sr, Ba, Ca. Three groups of chemical compositions are distinguished, they correspond to three genetic types of burbankite mineralization which connected to alkaline rocks. The first of them is confined to carbonatites where the minerals with «maximum averaged» chemical composition containing increased amounts of barium and calcium will be formed. The industrial accumulations of burbankite occur here. The second type is allocated in alkaline hydrothermalites where the range of chemical compositions of burbankite-like phases is extremely wide. The third type is connected to pectolite metasomatites of Khibiny and Murun massifs where strongly REE-depleted burbankite is present in considerable amounts. In carbonatites the burbankite group minerals for rare exception are the early high-temperature formations, and vise versa in agpaitic massifs they are formed at late stages under low temperatures that is connected to various regimes of carbon dioxide.

At alkalinity decrease the burbankite group minerals become unstable and at hydrothermal conditions they are easily replaced by a whole series of secondary minerals, among which alkali-free carbonates of REE, Sr, Ba, and Ca prevail.

Acknowledgments

The authors are grateful to Yu.K. Kabalov, E.R. Gobetchiya, J. Schneider, N.N. Kononkova, N.N. Korotaeva, I.M. Kulikova, and N.V. Chukanov for the help in researches, to

S.N. Nenasheva for discussion of the article, to A.P. Khomyakov, A.S. Podlesnyi, V.V. Subbotin, S.N. Nikandrov and colleagues from Fersman Mineralogical Museum of the Russian Academy of Sciences for provided samples. The work was supported by the grants of Russian Foundation for Basic Research (03-05-64054) and Fundamental Science School (NSh-1087-2003-5).

References

Belovitskaya Yu.V., Pekov I.V., Gobetchiya E.R., Kabalov Yu.K., Schneider J. Determination of crystal structure of khanneshite by Rietveld method // Kristallografiya. **2002**. V. 47. № 1. P. 46–49 (Rus.)

Belovitskaya Yu.V., Pekov I.V., Gobetchiya E.R., Kabalov Yu.K., Subbotin V.V. Crystal structure of calcioburbankite; peculiarities of structural type of burbankite // Kristallografiya. **2001**. V. 46. № 6. P. 1009–1013 (Rus.)

Belovitskaya Yu.V., Pekov I.V., Kabalov Yu.K. Refinement of the crystal structures of low-rare-earth and «typical» burbankites by Rietveld method // Kristallografiya. **2000**. № 1. P. 32–35 (Rus.)

Borodin L.S., Kapustin Yu.L. Burbankite, the first find in USSR // Dokl. Akad. Nauk USSR. **1962**. V. 147. № 2. P. 462–465 (Rus.)

Bühn B., Rankin A.H., Radtke M., Haller M., Knöchel A. Burbankite, a (Sr,REE,Na,Ca)-carbonate in fluid inclusions from carbonatite-derived fluids: Identification and characterization using Laser Raman spectroscopy, SEM-EDX, and sinchrotron micro-XRF analysis // Amer. Miner. **1999**. V. 84. P. 1117–1125.

Cesbron F., Gilles C., Pelisson P., Saugues J.-C. La remondite-(Ce), un nouveau carbonate de terres rares de la famille de la burbankite // C.R. Acad. Sci. Paris. **1988**. V. 307. № 8. P. 915–920.

Chen T.T., Chao G.Y. Burbankite from Mont St. Hilaire, Quebec // Canad. Miner. **1974**. V. 12. Pt. 5. P. 342–345.

Dudkin O.B., Polezhaeva L.I., Minakov F.V. Carbonates of Khibiny carbonatites // In book: Veshchestvennyi sostav shchelochnykh intruzivnykh kompleksov Kol'skogo poluostrova. Apatity. Izd. KFAN USSR. **1981**. P. 78–81 (Rus.)

Effenberger H., Kluger F., Paulus H., Wolfel E.R. Crystal structure refinement of burbankite // N. Jb. Miner. Mh. **1985**. H. 4. S. 161–170.

Efimov A.F., Es'kova E.M., Kataeva E.T. The find of burbankite from alkaline metasomatites of Urals // Trudy Min. muzeya RAS. **1969**. V. 19. P. 165–169 (Rus.)

Eremenko G.K., Vel'ko V.A. Khanneshite, (Na, Ca)$_3$(Ba, Sr, TR, Ca)$_3$(CO$_3$)$_5$, a new mineral of the burbankite group // Zapiski VMO. **1982**. Pt. 1. P. 321–324 (Rus.)

Fitzpatrick J., Pabst A. Burbankite from the Green River Formation, Wyoming // Amer. Miner. **1977**. V. 62. № 1–2. P. 158–163.

Ginderow P.D. Structure de Na$_3$M$_3$(CO$_3$)$_5$ (M= Terre Rare, Ca, Na, Sr), rattache a la burbankite // Acta Crist. **1989**. C. 45. P. 187–191.

Gobetchiya E.R., Kabalov Yu.K., Belovitskaya Yu.V., Pekov I.V. Crystal structure of hexagonal analog of remondite // Godichnaya nauchnaya sessiya VMO. Traditsionnye i novye napravleniya mineralogicheskikh issledovanii v novom tysyacheletii. Moscow. **2001**. 13–14 dekabrya. P. 49–50 (Rus.)

Grice J.D., Van Velthuizen J., Gault R.A. Petersenite-(Ce), a new mineral from Mont Saint-Hilaire, and its structural relationship to other REE carbonates // Canad. Miner. **1994**. V. 32. P. 405–414.

Horvath L., Gault R.A. The Mineralogy of Mont Saint-Hilaire, Quebec // Min. Record. **1990**. V. 21. № 4. 284–368 p.

Horvath L., Pfenninger-Horvath E. I minerali di Mont Saint-Hilaire (Quebec, Canada) // Rivista Mineralogica Italiana. **2000**. № 3. P. 140–202.

Ivanyuk G.Yu., Yakovenchuk V.N., Pakhomovskii Ya.A. Kovdor. Apatity. **2002**. 320 p (Rus.)

Kapustin Yu.L. Mineralogy of carbonatites (Mineralogiya karbonatitov). Moscow. **1971**. 288 p (Rus.)

Khomyakov A.P. Mineralogy of hyperagpaitic alkaline rocks (Mineralogiya ultraagpaitovykh shchelochnykh porod). Moscow. **1990**. 196 p (Rus.)

Kirnarskii Yu.M., Kozyreva L.V. Carbonatite veins in the rocks of Khibiny alkaline massif // In book: Mineraly i paragenezisy mineralov magmaticheskikh gornykh porod. Leningrad. **1974**. P. 64–72 (Rus.)

Konev A.A., Vorob'ev E.I., Lazebnik K.A. Mineralogy of Murun alkaline massif (Mineralogiya Murunskogo shchelochnogo massiva). Novosibirsk. **1996**. 222 p. (Rus.)

Kukharenko A.A., Orlova M.P., Bagdasorov E.A., Bulakh A.G. et al.. Caledonian complex of ultrabasic alkaline rocks and carbonatites of Kola Peninsula and Northern Kareliya (Kaledonskii kompleks ultraosnovnykh shchelochnykh porod i karbonatitov Kol'skogo poluostrova i Severnoi Karelii). Moscow. **1965**. 768 p. (Rus.)

Litvin A.L., Egorova L.N., Kul'chitskaya A.A., Mel'nikov V.S., Sharkin O.P. Sr-enriched burbankite from nepheline syenites of Priazov'e // Mineral. Zhurnal. **1998**. V. 20. № 2.

P. 12—18. (Rus.)
Mineralogy of Khibiny massif (Mineralogiya Khibinskogo massiva). Moscow. **1978**. V. 2. 585 p. (Rus.)
Pecora W.T., Kerr J.H. Burbankite and calkinsite, two new carbonate minerals from Montana // Amer. Miner. **1953**. V. 38. Pt. 11-12. P. 1169—1183
Pekov I.V. Lovozero massif: history of research, pegmatites, minerals (Lovozerskii massiv: istoriya issledovaniya, pegmatity, mineraly). Moscow. **2001**. 464 p. (Rus.)
Pekov I.V., Chukanov N.V., Belovitskaya Yu.V. Khanneshite and petersenite-(Ce) from Khibiny // Zapiski VMO. **1998**. № 2. P. 92—100 (Rus.)
Pekov I.V., Chukanov N.V., Kononkova N.N., Zadov A.E., Belovitskaya Yu.V. Remondite-(La), $Na_3(La,Ce,Ca)_3(CO_3)_5$, new mineral of the burbankite family from Khibiny massif, Kola Peninsula // Zapiski VMO. **2000**. № 1. P. 53—60 (Rus.)
Pekov I.V., Kulikova I.M., Nikandrov S.N. Chemical composition of rare-earth carbonates from hydrothermalites of Vishnevogorskii alkaline massif // Materialy Ural'skoi letnei mineralogicheskoi shkoly-96. Ekaterinburg. **1996**. P. 137—141 (Rus.)
Platt R.G., Woolley A.R. The carbonatites and fenites of Chipman Lake, Ontario // Canad. Miner. **1990**. V. 28. P. 241—250
Pozharitskaya L.K., Samoilov V.S. Petrology, mineralogy and geochemistry of carbonatites of East Siberia (Petrologiya, mineralogiya i geokhimiya karbonatitov Vostochnoi Sibiri). Moscow. **1972**. 268 p. (Rus.)
Shannon R.D., Prewitt C.T. Effective ionic radii in oxides and fluorides // Acta Cryst. **1969**. C. 25. P. 925—945
Shi Li, Tong Wang. Origin of burbankite in biotite-aegirine carbonatite from Hubei, China. Rare Earth Minerals: chemistry, origin and ore deposits // Mineralogical Society Spring Meeting, Natural History Museum, London, UK, Conference Extended Abstracts. **1993**. P. 72.
Shlyukova Z.V., Kazakova M.E., Vlasova E.V. The first find of burbankite in Khibiny massif // In book: Avtoreferaty rabot sotrudnikov IGEM AS USSR za 1971 g. Moscow. **1972**. P. 77. (Rus.)
Subbotin V.V., Voloshin A.V., Pakhomovskii Ya.A., Bakhchisaraitsev A.Yu. Calcioburbankite and burbankite from Vuoriyarvi carbonatite massif (new data) // Zapiski VMO. **1999**. № 1. P. 78—87 (Rus.)
Tikhonenkova R.P. Sr-burbankite from Khibiny massif // In book: Novye dannye po mineralogii i geokhimii redkikh elementov. Moscow. **1974**. P. 89—92 (Rus.)
Tikhonenkova R.P., Kazakiva M.E. The first find of burbankite in nepheline syenite massif // In book: Mineralogiya i geneticheskie osobennosti shchelochnykh massiviv. Moscow. **1964**. P. 40—44 (Rus.)
Tikhonenkova R.P., Shumyatskaya N.G., Kazakova M.E. Strontian burbankite and the burbankite group // In book: Novye dannye po mineralogii i mineralogicheskim metodam issledovaniya. Moscow. **1977**. P. 3—11 (Rus.)
Van Velthuizen J., Gault R.A., Grice J.D. Calcioburbankite, $Na_3(Ca, REE, Sr)_3(CO_3)_5$, a new mineral species from Mont Saint-Hilaire, Quebec, and its relationship to the burbankite group of minerals // Canad. Miner. **1995**. V. 33. P. 1231—1235
Voronkov A.A., Shumyatskaya N.G. X-ray study of crystal structure of burbankite $(Na, Ca)_3(Ca, Sr, Ba, TR)_3(CO_3)_5$ // Kristallografiya. **1968**. V. 13. № 2. P. 246—252 (Rus.)
Voronkov A.A., Shumyatskaya N.G., Pyatenko Yu.A. Crystal structure of burbankite // Kristallografiya. **1967**. V. 12. № 1. P. 135 (Rus.)
Yakovenchuk V.N. Mineralogy and forming conditions of carbonatites in hydrothermal veins of Kukisvumchorr deposit (Khibiny massif). Ph. D. thesis Apatity. **1995**. 189 P. (Rus.)
Yakovenchuk V.N., Ivanyuk G.Yu., Pakhomovskii Ya.M., Men'shikov Yu.P. Minerals of Khibiny massif (Mineraly Khibinskogo massiva). Moscow. **1999**. 326 p. (Rus.)
Zaitsev A.N., Bell K., Wall F. Le Bas M.J. Alkali-rare-earth carbonates from carbonatites of Khibiny massif: mineralogy and genesis // Dokl. Akad. Nauk USSR. **1997**. V. 355. № 2. P. 241—245 (Rus.)
Zaitsev A.N., Chakhmouradian A.R. Calcite-amphibole-clinopyroxene rock from the Afrikanda Complex, Kola Peninsula, Russia: Mineralogy and a possible link to carbonatites. II. Oxysalt minerals // Canad. Miner. **2002**. V. 40. P. 103—120
Zaitsev A.N., Men'shikov Yu.P., Polezhaeva L.I., Latysheva L.G. The minerals of Ba, Sr, and REE from carbonatites of Khibiny alkaline massif // In book: Novoe v mineralogii Karelo-Kol'skogo regiona. Isd. KNTs AU USSR (Rus.)
Zaitsev A.N., Wall F., Le Bas M.J. REE-Sr-Ba minerals from the Khibina carbonatites, Kola Peninsula, Russia: their mineralogy, paragenesis and evolution // Miner. Mag. **1998**. V. 62. № 2. P. 225—250

UDC 549.657

GENESIS AND TYPOCHEMISM OF LAMPROPHYLLITE–BARYTOLAMPROPHYLLITE SERIES MINERALS FROM LUJAVRITE–MALIGNITE COMPLEX OF KHIBINY MASSIF

Yulia V. Azarova
Institute of Ore Deposits, Geology, Petrography, Mineralogy and Geochemistry RAS, Moscow, azarova@igem.ru

The detail analysis of chemical composition and character of postmagmatic alteration of lamprophyllite-barytolamprophyllite series minerals from lujavrite-malignites of Khibiny massif was made by local roentgenospectral and electron-microscopic methods. It is determined that in lujavrites high-barium lamprophyllite is a typomorphic accessory mineral. In malignites two stages of lamprophyllite alteration are ascertained, which correspond to two stages of their formation: 1) at the stage of primary rocks (lujavrite or titanite trachytoid melteigite-urtites) transformation in result of K,Si-metasomatosis the recrystallization of primary Ba-lamprophyllite without change of chemical composition (in case of lujavrites) and enrichment of primary strontium lamprophyllite by barium and potassium (in case of melteigite-urtites) take place; 2) at the stage of low-temperature rocks transformation by action of solutions enriched by strontium and/or calcium the replacement of Ba-lamprophyllite by strontium analogue (in malignites genetically connected to lujavrites) and development of titanite after Ba,K-lamprophyllite (in malignites connected to ijolite-urtites) occur.
It is detected that the character of postmagmatic alteration of primary strontium lamprophyllite in «porphyraceous malignites» is also the evident of primary rocks (trachytoid ijolites) transformation during K,Si-metasomatosis.
4 figures, 1 table and 16 references.

Lamprophyllite, $(Sr,Ba,K)_2Na(Na,Fe,Mn)_2Ti_3(Si_4O_{16})(O,OH,F)_2$, is one of the most characteristic accessory minerals of Khibiny alkaline massif. It occurs in rocks of almost all this massif complexes: nepheline syenites, melteigite-urtites, apatite-nepheline rocks, ristschorrites, lujavrite-malignites. A whole number of works was devoted to lamprophyllite, however, the systematical study of accessory lamprophyllite from rocks of Khibiny massif, in particular, the study of genetic aspect of its mineralogy, was not practically undertaken till now. The minerals of lamprophyllite-barytolamprophyllite series from rocks of lujavrite-malignites complex have become the object of present study.

The crystal structure of lamprophyllite has a layered constitution, which allows free entering of large cations (Sr, Ba, K, Ca, Na) into inter-layer space and significant variations of their ratios (Rastsvetaeva *et al.*, 1995a, Rastsvetaeva, Dorfman, 1995b). This crystal structure peculiarity makes lamprophyllite perspective from the point of view of use it as one of the mineralogogeochemical indicators of changes of minerogenesis environment conditions.

General characteristic of research objects

Lujavrites and malignites in Khibiny massif are spatially connected to trachytoid melteigite-urtites of Central Arc. Their alternating bed bodies are traced in upper part of this complex along contact of Kukisvumchorr-Rasvumchorr apatit-nepheline deposit with overlapping ristschorrites up to the upper course of Kuniiok. The lujavrites from Khibiny are the late melanocratic phase of nepheline syenites; they consist of orthoclase, nepheline, and dark-coloured minerals, are characterized by clear trachytoid texture, being the result of orthoclase laths orientation. The question about malignites genesis remains disputable. According to opinion of one researches group, they are the late phase of melteigite-urtites or ristschorrites (N.A. Eliseev, T.N. Ivanova, S.I. Zak *et al.*). Others, I.A. Zotov, B.Ye. Borutzky, A.I. Serebritskii, consider them as a product of metasomatic alteration (orthoclazization) of melteigite-urtites or ijolites at their contact with lujavrites, khibinites, and lyavochorrites. In present research malignites are considered as rocks of metasomatic genesis, according to analysis of earlier works and features, determined by us. On their mineral composition they are divided into three types: 1) malignites (below denoted by us as «malignites-L») formed as a result of metasomatic alteration of lujavrites and confined to endocontact zone of lujavrites with trachytoid melteigite-urtites; they have mineral composition similar to that of lujavrites, but with poikilitic structure caused by large poikiloblasts of orthoclase and amphibole; 2) malignites (denoted as «malignites-U») confined to exocontact zone of lujavrites with titanite trachytoid melteigite-urtites and formed as a result of metasomatic alteration of the latter; they are also characterized by poikilitic structure, but according to

Table 1. Chemical composition of lamprophyllite-barytolamprophyllite series minerals from lujavrite-malignites complex rocks of Khibiny massif

Rocks	lujavrites				«malignites-L»				«malignites-U»			«porphyric malignites		
Phases	*I*		*I-a*		*I, II-a*			*II-b*	*I*	*II-a*		*I*	*II-a*	
№	*1*	*2*	*3*	*4*	*5*	*6*	*7*	*8*	*9*	*10*	*11*	*12*	*13*	*14*
Na_2O	10.32	9.05	9.24	9.09	9.65	9.53	9.77	11.95	10.50	9.15	8.67	9.53	9.35	9.07
K_2O	1.01	1.70	1.21	1.12	1.71	1.50	1.67	1.89	1.77	1.88	2.69	1.78	1.76	2.56
CaO	1.00	0.97	0.91	0.87	1.02	0.92	1.17	1.57	1.35	1.11	1.34	1.39	1.22	0.94
SrO	10.55	7.53	5.26	3.93	5.30	8.07	9.60	11.62	14.59	8.46	6.39	14.48	9.74	4.81
BaO	10.80	15.28	19.71	21.39	17.05	14.35	10.09	4.08	3.26	14.21	18.03	5.88	10.68	19.71
MgO	0.35	0.44	0.41	0.45	0.00	0.43	0.48	0.52	0.70	0.26	0.62	0.77	0.45	0.53
MnO	1.57	1.22	1.66	1.60	2.09	1.76	1.87	1.36	1.27	2.30	1.70	0.85	1.15	0.00
FeO	2.96	2.64	2.70	2.56	2.71	2.61	2.98	3.87	4.63	2.66	2.85	4.24	3.64	2.34
Al_2O_3	0.27	0.38	0.51	0.68	0.44	0.35	0.27	0.00	0.20	0.27	0.24	0.50	0.24	0.61
SiO_2	29.70	29.08	28.65	27.85	30.90	29.37	30.06	32.60	29.55	30.95	29.59	30.20	29.54	30.35
TiO_2	27.97	26.86	25.62	26.08	30.00	26.27	27.62	30.45	27.77	29.65	28.07	29.35	27.18	28.77
Nb_2O_5	0.77	0.11	0.00	0.20	0.80	0.10	0.69	0.90	0.39	0.00	0.15	1.72	0.25	0.17
Total	**97.27**	**95.26**	**95.88**	**95.82**	**101.67**	**95.26**	**96.27**	**100.81**	**95.98**	**100.90**	**100.34**	**100.69**	**95.20**	**99.86**
Numbers of ions on the basis of (Si + Al) = 4														
Na	2.67	2.38	2.45	2.46	2.38	2.48	2.49	2.84	2.73	2.27	2.25	2.40	2.43	2.66
K	0.17	0.29	0.21	0.20	0.28	0.26	0.28	0.30	0.30	0.31	0.46	0.29	0.30	0.42
Ca	0.14	0.14	0.13	0.13	0.14	0.13	0.17	0.21	0.19	0.15	0.19	0.19	0.18	0.13
Sr	0.82	0.59	0.42	0.32	0.39	0.63	0.73	0.83	1.14	0.63	0.50	1.09	0.76	0.36
Ba	0.56	0.81	1.06	1.17	0.85	0.76	0.52	0.20	0.17	0.71	0.95	0.30	0.56	0.99
Mg	0.07	0.09	0.09	0.09	-	0.09	0.09	0.10	0.14	0.05	0.12	0.15	0.09	0.10
Mn	0.18	0.14	0.19	0.19	0.23	0.20	0.21	0.14	0.14	0.25	0.19	0.09	0.13	-
Fe	0.33	0.30	0.31	0.30	0.29	0.29	0.33	0.40	0.52	0.28	0.32	0.46	0.41	0.25
Al	0.04	0.06	0.08	0.11	0.07	0.06	0.04	-	0.03	0.04	0.04	0.08	0.04	0.09
Si	3.96	3.94	3.92	3.89	3.93	3.94	3.96	4.00	3.97	3.96	3.96	3.92	3.96	3.91
Ti	2.80	2.74	2.63	2.74	2.87	2.65	2.74	2.81	2.80	2.85	2.83	2.87	2.74	2.78
Nb	0.05	0.01	0.01	-	0.05	0.01	0.04	0.05	0.02	-	0.01	0.10	0.02	0.01
Ba:Sr	**0.69**	**1.37**	**2.53**	**3.67**	**2.17**	**1.20**	**0.71**	**0.24**	**0.15**	**1.14**	**1.91**	**0.27**	**0.74**	**2.77**

Note:
Phase I — primary lamprophyllite of the rock; I-a — barytolamprophyllite (in lujavrites); II-a — lamprophyllite, formed during K,Si-metasomatosis; II-b — lamprophyllite, formed by influence of the late more low-temperature solutions. Analysts: an. 1-4, 6, 7, 9, 13 — V.V. Khangulov (Camebax SX-50, IGEM RAS); an. 5, 8, 10-12, 14 — N.V. Trubkin (electron microscope JSM-5300 with X-ray spectrometer Link ISIS, IGEM RAS). An. 9. 14 — average on two analyses; an. 2, 3, 5, 8 — on three; an. 12, 10, 11 — on five; an. 6, 13 — on seven; an. 1, 7 — on ten analyses

their composition, are closer to melteigite-urtites; these rocks contain significantly more nepheline and dark-coloured minerals than «malignites-L», and less potash feldspar; titanium enrichment is also their characteristic feature; 3) «porphyric malignites», according to S.I. Zak terminology (Zak *et al.*, 1972), which are traced in lower part of trachytoid melteigite-urtites series at the contact with underlying khibinites and among ristschorrites, and apparently, represent the small-grained trachytoid ijolites altered by metasomatic processes. They are characterized by porphyritic structure caused by the poikilocrystals of lamprophyllite or feldspar, which stand out among more small-grained matrix, composed by dark-coloured minerals and nepheline, and the trachytoid texture caused by orientation of aegirine-hedenbergite needle-shaped crystals and laths of metasomatic potash feldspar replaced nepheline. Outcrops of these rocks are noted at Mt. Poachvumchorr. Bedrocks of «malignites-L» and «malignites-U» are traced at Mt. Kukisvumchorr.

Morphology, typical assemblages and chemical compositions of lamprophyllite from lujavrite–malignites

In lujavrites lamprophyllite forms prismatic crystals of goldish-brown colour from some millimeters up to 1 cm in size and their growths disposed between high-barium (up to 3.0—3.5 % BaO) orthoclase laths, among magnesio-arfvedsonite and aegirine. Lamprophyllite is associated with eudialyte (proper eudialyte, according to (Johnsen *et al.*, 2003)), titanite, rarely rinkite and apatite. Here lamprophyllite is one of the latest mineral phases: it forms later than dark-coloured and most of accessory min-

erals, i. e. rinkite, apatite, which inclusions are observed in the crystals of lamprophyllite, titanite (sometimes replaced by lamprophyllite), and eudialyte.

Primary lamprophyllite from lujavrites, according to its chemical composition, is high-barium, although there are perceptible variations in content of both BaO, in most of cases from »10—11 to »15 %, and SrO, from »8 to 11 % (Table 1); the ratio (in *atoms per formula unit*) Ba/Sr = 0.7—1.4. Continuous isomorphous series between Sr- and Ba-dominant specimens is traced (Fig. 1). Potassium and calcium are contained in lamprophyllite in subordinate amounts. The content of manganese is also insignificant.

At the late mineral formation stages barium lamprophyllite are replaced by varieties with yet higher content of barium right up to barytolamprophyllite (the content of BaO increases to 20—21%, the content of SrO is near 4—5%; Ba/Sr = 2.5—3.7, an. 3, 4 in Table 1), growing at the grains edges. Apparently, this phenomenon is caused by accumulation of barium in residual mineral forming environment because of its non-cogerency.

The appearance of high-barium lamprophyllite in lujavrites of Khibiny is their distinctive typomorphic peculiarity. The predominantly strontium lamprophyllite with significant content of manganese is spread in the analogous rocks from Lovozero massif (Kola Peninsula): lujavrites from differentiated complex of lujavrites-foyaites-urtites; eudialyte, lamprophyllite, and porphyric lujavrites (Bussen, Sakharov, 1972; Vlasov *et al.*, 1959). Strontium lamprophyllite is observed also in leucocratic nepheline syenites of Kibiny: khibinites, foyaites *etc*. Barium lamprophyllite and barytolamprophyllite till now are noted practically only in pegmatites and late cross-cutting veinlets, which occur among apatite-nepheline rocks and nepheline syenites in Khibiny (Dudkin, 1959; Peng Tze-Chung, Chang Chien-Hung, 1965; Kapustin, 1973; Rastsvetaeva, Dorfman, 1995a) and Lovozero massifs, Kola Peninsula (Semenov, 1972; Kapustin, 1973; Bussen, Sakharov, 1972; Bussen et al, 1978), and also among albitized fenites at Turii cape (Kola Peninsula), metasomatites in Inagli and Murun massifs (South Yakutiya) (Rastsvetaeva *et al.*, 1995b; Lazebnik *et al.*, 1998), syenitized schists in Botogol'skii massif (East Sayan) (Kapustin, 1973). Moreover, high-barium lamprophyllite is described in a number of other massifs in the world (Zaitsev, Kogarko, 2002).

«Malignites-L» are characterized by irregular distribution of lamprophyllite. Here there are its large (up to 2—3 cm and larger) poikilocrystals (with inclusions of aegirine, nepheline, apatite, sometimes fersmanite), growing among poikilocrystals of high-barium orthoclase and Na-Ca-amphiboles of magnesioarfvedsonite — richterite series. Rarely lamprophyllite forms small tabular crystals. In a number of cases lamprophyllite is corroded by high-barium orthoclase. The mineral assemblage, coexisting with lamprophyllite, is close to «lujavrite» one: it contains eudialyte, titanite, rarely rinkite, later Sr-apatite (6—10% SrO), taseqite, growing after proper eudialyte (Johnsen *et al.*, 2003), fersmanite, sometimes pectolite, which accumulations are noted into interstitions between other minerals grains.

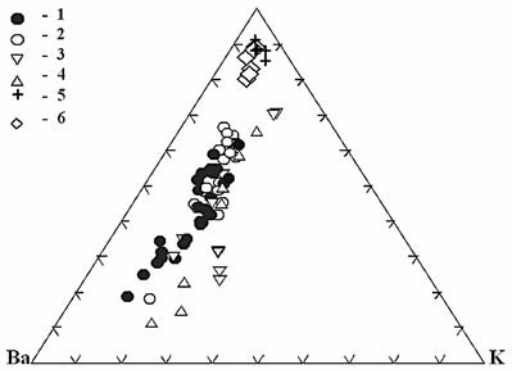

FIG. 1. The ratios of barium, strontium, and potassium (in apfu) in lamprophyllite from lujavrite-malignites complex rocks of Khibiny massif: lujavrites (1); «malignites-L» (2); «malignites-U» (3); «porphyric malignites» (4); and nepheline syenites of Khibiny massif (5); lujavrites of differentiated complex and eudialyte lujavrites of Lovozero massif (6)

The chemical composition of early lamprophyllite from «malignites-L» is in whole identical to barium lamprophyllite and barytolamprophyllite from lujavrites: BaO — from »10 to 17 %, SrO — 5—10 %; Ba/Sr = 0.7—2.2 (Table 1, an. 5—7). However, here barium lamprophyllite is, as a rule, changed. In the most of cases in its poikilocrystals there are, together with Ba-dominant parts, the areas with gradually decreasing barium content (up to 4% BaO) and increasing content of strontium (on average »12 % SrO, Table 1, an. 8). These areas are traced parallel cleavage cracks of lamprophyllite poikilocrystals (Fig. 2). The ratio Ba/Sr in these zones is decreased up to 0.25, on chemical composition they corresponds to proper lamprophyllite, i. e. strontium lamprophyllite.

In the levels of **«malignites-U»** lamprophyllite, in contrast to above-mentioned rocks, is noted enough rarely. Its prismatic crystals are

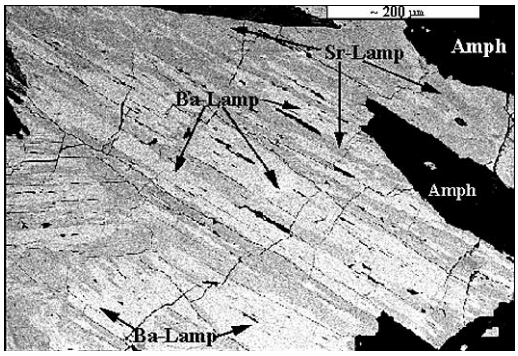

FIG. 2. The development of strontium lamprophyllite after poikilocrystal of high-barium lamprophyllite in «malignites-L» (image in reflected electrons, scanning electron microscope JSM-5300, IGEM RAS). Ba-lamp — high-barium lamprophyllite; Sr-lamp — strontium lamprophyllite; Amph — magnesioarfvedsonite

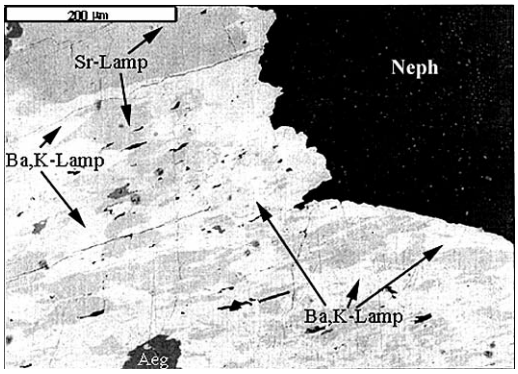

FIG. 3. The replacement of primary strontium lamprophyllite by barium-potassium lamprophyllite during K,Si-metasomatosis in «malignites-U» (image in reflected electrons, scanning electron microscope JSM-5300, IGEM RAS). Ba-lamp — high-barium lamprophyllite; Sr-lamp — strontium lamprophyllite; Neph — nepheline; Aeg —

nearly 0.3—0.5, seldom 1 cm in length. They are located together with dark-coloured minerals (mainly aegirine, rarely magnesioarfvedsonite are noted) between poikilocrystals of potash feldspar (barium-free, in contrast to «malignites-L») and Na-amphiboles of magnesioarfvedsonite — richterite series. Lamprophyllite is corroded by feldspar in different degree. It associates also with eudialyte group minerals (eudialyte with high-sodium and potassium-sodium chemical composition and taseqite, growing after it), djerfisherite, late titanite, Sr-apatite (the content of SrO up to 10%), pectolite, and pyrochlore. The latter is noted, as a rule, in cavities and crack of altered lamprophyllite.

In these rocks early lamprophyllite is significantly strontian, the content of BaO is not exceed on average 3% (Table 1, an. 9). Very often it is, in different degree, sometimes practically wholly, replaced by late barium-potassium lamprophyllite (Fig. 3). The content of SrO is near to 6—8%, BaO » 14—18 %, Ba/Sr » 1.1—1.9, the content of K_2O in most high-barium parts reaches 2.7% (Table 1, an. 11) (in primary lamprophyllite of above-mentioned rocks, this ratio fluctuates from 1.0 to 1.7%, and in late lamprophyllite it achieved 1.9%, Table 1). On the diagram, showing the ratios of barium, strontium, and potassium in *apfu* (contained in Table 1), the points of its chemical compositions are slightly displaced in «potassium» area (Fig. 1). At yet later stages Ba,K-lamprophyllite is, in its turn, replaced by titanite (Fig. 4).

In **«porphyric malignites»** lamprophyllite forms large poikilocrystals (up to 2—4 cm in size) among matrix, consisting of fine-needle-shaped crystals of aegirine-hedenbergite and magnesioarfvedsonite and small grains of nepheline. Here lamprophyllite is corroded by potash feldspar and often replaced by micrograined aggregates of feldspar and aegirine. Except lamprophyllite, the typical accessory minerals here are eudialyte group minerals (high-sodium and potassium-sodium eudialyte is most widespread), forming large accumulations in these rocks, and also rinkite, lorenzenite, titanite, apatite, and others.

On its chemical composition lamprophyllite in «porphyric malignites» is strontian (Table 1, an. 12), however, also as in «malignites-U», it is often replaced in significant degree by lamprophyllite, enriched by barium and potassium. In late lamprophyllite the content of BaO achieves 19%, K_2O — 2.6% (Table 1, an. 14). On Fig. 1 the points, corresponding to chemical compositions of this lamprophyllite, lies in the area close to chemical composition of late Ba,K-lamprophyllite from «malignites-U».

Genesis of lamprophyllite in the rocks of lujavrite–malignites complex

The analysis of the evolution of chemical composition of lamprophyllite-barytolamprophyllite series minerals from the studied complex rocks and the character of their alteration as a result of postmagmatic processes, compared with peculiarities of general evolution of accessory mineralization of lujavrite-malignites, allows in significant degree reconstructing the history of lujavrite-malignites formation. The analysis of alterations, detected for lamprophyllite from malignites of this complex, is high informative in genetic relation.

Barium lamprophyllite from «malignites-L».

«Malignites-L» is seems to be mainly the product of lujavrites transformation as a result of K,Si-metasomatosis, and barium lamprophyllite is here inherited from initial rock. This assumption is confirmed by following: 1) in malignites of these levels there are the mineral relics of primary assemblage, which is analogous to «lujavrite» one; 2) early postcrystallization changes, i. e. recrystallization of mineral grains, formation of poikilitic structure, corrosion of primary minerals by orthoclase; 3) gradual transition between lujavrites and «malignites-L», existing of «transitional» varieties with composition, corresponding to lujavrites, but combining trachytoid («lujavrite») and poikilitic («malignite») parts of rock. On this stage barium lamprophyllite is exposed to recrystallization and forms poikilocrystals.

The later transformation of lamprophyllite in «malignites-L» is a gradual replacement of barium lamprophyllite by significant strontian one, which, apparently, was influenced by late solutions, enriched by strontium and calcium. Formation of late «Ca-Sr-mineral assemblage», containing Sr-apatite, taseqite, pectolite, and fersmanite, in «malignites-L» can be explained by action of these solutions.

Lamprophyllite from «malignites-U». Most probably, early (strontian) lamprophyllite from «malignites-U» is also inherited from protorocks, in that case from trachytoid titanite melteigite-urtites, later undergone a K,Si-metasomatosis transformation. The relics of these rocks in a number of cases are noted in «malignites-U». Moreover, the absence of sharp contacts between these rocks (they are connected to each other by gradually transitions), indirectly indicates the existence of their genetic connection with trachytoid melteigite-urtites. In trachytoid melteigite-urtites accessory lamprophyllite is not enough widespread. According to data of Arzamastsev *et al.* (1987), its amount is not exceeding 0.9% from total rock mass, which, probably, explains the rarity of lamprophyllite in «malignites-U».

The character of postmagmatic alteration of lamprophyllite, the barium and some calcium enrichment and corrosion by potash feldspar (identical to character of lamprophyllite alteration in massive melteigite-urtites, undergone an intensive transforming with formation of ristschorrites complex rocks during K,Si-metasomatosis), indicates the significant role of K,Si-metasomatosis in formation of «malignites-U». The similar scheme of lamprophyllite alteration was, in particular, described (Ageeva, 2001, 2002) for massive urtites, which is a main «matrix» for ristschorrites formation. The rising alkalinity of mineral formation environment, which causes the increase of activity of most basic components (in this case barium) and the decrease of activity of less basic ones (i. e. strontium), is a reason of barium activity increasing during K,Si-metasomatosis, according to O.A. Ageeva data.

In «malignites-U» as well as in «malignites-L» the more low-temperature lamprophyllite alteration takes place because of influence of late solutions. Here the character of lamprophyllite alteration is different: in contrast to «malignites-L», the development to titanite pseudomorphs after Ba,K-lamprophyllite is typical for these rocks. However, later transformation of «malignites-U», probably, was realized as a result of influence of the same solutions, enriched by calcium and strontium that solutions caused transformation of «malignites-L». The composition of late mineral assemblage, close to composition of «Ca,Sr-assemblage» of «malignites-L» indicates that. The former assemblage contains Sr-apatite, pektolite, pyrochlore, taseqite, and is practically distinguished from the later one only by wide prevalence of late titanite, forming pseudomorphs after lamprophyllite here.

Lamprophyllite from «porphyric malignites». As it is evident from above-mentioned data, the early strontium lamprophyllite in «porphyric malignites» is undergone by practically the same alterations that lamprophyllite in «malignites-U», these changes, apparently, caused by processes of K,Si-metasomatosis: lamprophyllite poikilocrystals are intensive corroded by late potash feldspar, the enrichment of strontium lamprophyllite by barium and potassium is observed. Small-grained trachytoid ijolites, spatially connected to «porphyric malignites», are, possibly, the primary rocks, which strontium lamprophyllite of «porphyric malignites» was inherited from.

Conclusion

The data, observed as a result of detail analysis of the chemical composition of lamprophyllite and the peculiarities of its postcrystallization alteration, allow determine following.

1. The enrichment by primary high-barium lamprophyllite is a typomorphic peculiarity of lujavrites from Khibiny. At present moment barium accessory lamprophyllite is noted neither in analogous rocks, lujavrites of Lovozero massif, no in other (leucocratic) nepheline syenites of large high-alkali massifs (Khibiny, Lovozero *etc*).

2. In «malignites-L» (genetically connected to lujavrites) and «malignites-U» (connected to melteigite-urtites) the character of alteration of lamprophyllite-barytolamprophyllite series mi-

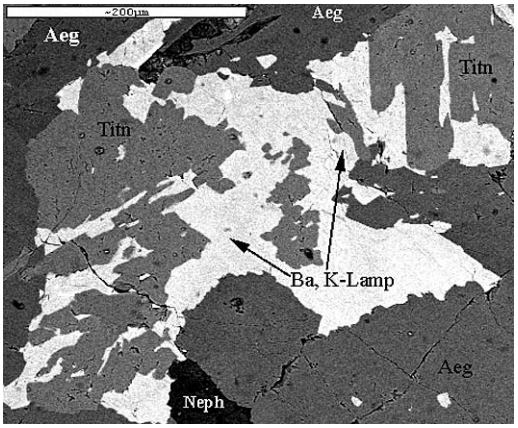

FIG. 4. Titanite pseudomorph after barium-potassium lamprophyllite in «malignites-U» (image in reflected electrons, scanning electron microscope JSM-5300, IGEM RAS). Ba,K-lamp — barium-potassium lamprophyllite; Titn — titanite; Neph — nepheline; Aeg — aegirine-hedenbergite

nerals and minerals, associated with them, indicates two stages of their formation. The first stage is a transformation of initial rocks (lujavrites for «malignites-L» and trachytoid titanite ijolites for «malignites-U») during K,Si-metasomatosis. In the case of «malignites-L» it is accompanied by recrystallization of primary barium lamprophyllite, forming poikilocrystals, without change of chemical composition; in the case of «malignites-U» there is enrichment of primary strontium lamprophyllite by barium and potassium. The second stage is the more low-temperature transformation, connected to influence of late solutions, enriched by strontium and calcium. In «malignites-L» barium lamprophyllite and barytolamprophyllite are replaced by proper lamprophyllite (strontian), in «malignites-U» titanite replaces them at this stage. The influence of these solutions causes calcium-strontium character of late mineralization in «malignites-L» and «malignites-U».

3. In «porphyric malignites» the alteration of early strontium lamprophyllite, inherited from their protorocks (small-grained trachytoid ijolites), caused by transformation of the latter during processes of K,Si-metasomatosis (as well as in «malignites-U»).

The author would like to thank V.V. Khangulov and N.V. Trubkin for help.

The work was supported by the grant of Russian Foundation for Basic Research (03—05—64139).

References

Ageeva O.A. Evolution of the mineral formation in the rocks of ristschorrites complex (Khibiny massif) // In: Researchs of young. Proceedings of the XIII youths Scientific conference, K. O. Krats memorial. V. 2. Apatity, **2002**. P. 7—11 (Rus.)

Ageeva O.A. Minerals association and typomorphism of accessory minerals of pyroxene ristschorrites (Khibiny massif) in connexion with hypothesis of their metasomatic genesis // In: Geology and geoecology of the Fenoscandian shield, East-European platform and their surrounding. Proceedings of the XII youth scientific conference, K. O. Krats memorial. SPb., **2001**. P. 91—92 (Rus.)

Arzamastsev A.A., Ivanova T.N., Korobeinikov A.N. Petrology of Ijolite-Urtites of Khibiny and regularity of Allocation of Apatite Deposit in them. Leningrad, Nauka, **1987**. 110 p. (Rus.)

Bussen I.V., Sakharov A.S. Petrology of Lovozero alkaline massif. M., Nauka, **1972**. 294 p. (Rus.)

Bussen I.V., Es'kova E.M., Men'shikov Yu.P. et al. Mineralogy of ultraalkaline pegmatites // The problems of geology of elements rare. M., Nauka, **1978**. P. 251—271 (Rus.)

Dudkin O.B. Barium lamprophyllite // ZVMO, **1959**. V. 88. №6. P. 713—715 (Rus.)

Johnsen O., Ferraris G., Gault R. A., et al. The nomenclature of eudialyte-group minerals // Canadian Mineralogist, **2003.** V. 41. pt. 3. 785—794.

Kapustin Yu.L. New finds of barium lamprophyllite and chemical formula of lamprophyllite // Dokl. AS USSR, **1973.** V. 210. № 4. P. 921—924 (Rus.)

Lazebnik K.A., Zayakina N.V., Patskevich G.P. Strontium-free lamprophyllite is a new member of the lamprophyllite group // Dokl. RAS, 1998. V. 361. №6. P. 799—802 (Rus.)

Peng Tze-Chung, Chang Chien-Hung. New varieties of lamprophyllite-barytolamprophyllite and orthorhombic lamprophyllite // Scientifica Sinica, **1965.** 14. 12. 1827—1840.

Rastsvetaeva R.K., Dorfman M.D. Crystal structure of Ba-lamprophyllite in the lamprophyllite-barytolamprophyllite isomorphous series // Kristallogr., **1995a.** V. 40. № 6. P. 1026—1029 (Rus.)

Rastsvetaeva R.K., Evsyunin V.G., Konev A.A. Crystal structure of K-barytolamprophyllite //Kristallogr., **1995b.** V. 40. №3. P. 517—519 (Rus.)

Semenov E.I. Mineralogy of Lovozero Alkaline Massif. M., Nauka, **1972**. 305 p.

Vlasov K.A., Kuz'menko M.V., Es'kova E.M. Lovozero alkaline massif. M., Izd. AS USSR,

UDC 549-1.02.09.1:553.8.46.495

MINERAL COMPOSITION OF RARE–METAL–URANIUM, BERYLLIUM WITH EMERALD AND OTHER DEPOSITS IN ENDO– AND EXOCONTACTS OF THE KUU GRANITE MASSIF (CENTRAL KAZAKHSTAN)

Andrei A. Chernikov
Fersman Mineralogical Museum, Moscow

Moisei D. Dorfman
Fersman Mineralogical Museum, Moscow

The Permian granite massif of Kuu, making part of the Akchatau ore-bearing complex of the Central Kazakhstan, is characterized by occurences of quartz-felspathic pegmatites, some of which comprise accumulations of ore minerals — wolframite, molybdenite, cassiterite, monazite, beryl and less often others. Molybdenite is also present in some aplite dikes. Diverse veined formations, greisens, quartz and quartz-ore veins are common in the *Kuu* massif.
The *rare-metal-uranium* deposit Komsomolskoye is confined to *greisenization* zones in western *endo-* and exocontacts of granite massif, and the southern contact of *Kuu* massif *comprises a* beryllium deposit. The exocontact of massif, where quartz mineralization passes from granite into *schistose* ultrabasites, comprises an emerald manifestation and molybdenum deposit *Shalguiya*. This paper considers features of mineral composition of these deposits and ore manifestations and the history of geological evolution of mineralization.
1 table, 8 color photos, 14 references.

The region of *Kuu* granite massif has a long geological history. Late Sinian rocks of Late Proterozoic are the most ancient. Early and Middle Devonian *(D_1-D_2) rocks* discordantly *occur on the washed-out* surface of Sinian sequences. They are covered by a variegated and red sequence of Middle and Late Devonian *(D_2-D_3fr)*, which is discordantly covered by Famenian *(D_3fm)* limestones. The last are in turn covered by calcareous and *limestone-terrigenous* Carboniferous sediments.

Recent deposits are represented by Cenozoic deluvium and eluvium and Mesozoic weathering products. In addition, birbirites, rocks of ancient weathering rocks on ultrabasites, consisting of opal, chalcedony (up to 80 % of volume), limonite and smaller quantities of other minerals, develop within the Shalgiinsky ultrabasite massif. Cenozoic deposits with abundant gypsum are thin, below ten meters. Within the limits of Kuu massif, they accumulate cassiterite, topaz and monazite.

Intrusive rocks, in addition to Kuu granite, include Shalgiinsky ultrabasite massif. This Proterozoic massif is mainly composed of gabbro, amphibolites, serpentinites, schists and dikes of plagioclasites. Proterozoic basic rocks are hardly metamorphosed near the contact with granite.

The Kuu granite massif is confined the northwest part of Betpak-Dala folded structures, in the north of the large Shalguiya-Karaoba fault zone having northwest strike. The outcrops of Kuu granite extend in latitudinal direction. According to A.I. Ezhov (1964), there were three phases of intrusion and a phase of vein rocks. Aplites and quartz-felspathic pegmatites are characteristic. Ore minerals — wolframite, molybdenite, cassiterite, monazite, less often other minerals — are related to light gray quartz. In the southwest part of Kuu intrusion, some pegmatites veins show zonal occurrence of quartz and potassic felspar. Molybdenite appears when such veins pass from granite into hosting rocks. Molybdenite is also present in aplite dikes as thin flakes in mass of rock without appreciable hydrothermal alterations, as notes M.A. Konoplyantsev (1959). Beryl crystals occur in some pegmatites, for example, on the southern slope of the Kuu Mountain, west of quartz vein «Glavnaya», which crosses the Kuu massif approximately in its middle part.

Diverse vein bodies, greisens and quartz veins are widely distributed in the massif, and a number of ore occurrence are registered in the contact zone. They are typical vein bodies of quartz-wolframite-greisen association with molybdenite. Characteristic minerals of these ore veins are wolframite, cassiterite, monazite, molybdenite, topaz, fluorite, etc.

Kuu granites are specialized for beryllium. All accessory minerals are enriched with Be, beryl is present in some pegmatites and topaz veins with beryl, bertrandite and helvite are known among greisens.

The western and southwestern contacts of granite massif comprise the Komsomolskoye rare-metal-uranium deposit, the southern endocontact hosts a small uranium-beryllium

deposit (site 2), and schistose ultrabasites of Shalgiinsky massif hosts an emerald and molybdenum deposit Shalguiya, which mineralogical features are considered below.

Mineralogical features of the Komsomolskoye deposit

The ore mineralization of the deposit relates to a system of feathering faults of a regional corrugation zone in the western endocontact part of Kuu granite massif and in its exocontact. Ore bodies are quartz veins, sometimes with pyrite, molybdenite, wolframite, less often with chalcopyrite, galena, and quartz-micaceous greisenization zones with topaz, fluorite, sometimes with molybdenite and less often with wolframite. Quartz veins and greisenization zones have abrupt dip, they are accompanied by zones of fracturing, caolinization, hematitization, and fluoritization of granite. Granite and greisenization zones in the ore field are pigmented by hematite, acquiring orange-red-brown coloring. Dark-violet fluorite frequently appears near silicification zones in granite, forming topaz-fluorite metasomatites. As noted A.I. Yezhov (1964), these associations are similar to fluorite-feldspathic rocks developed on the Cornwall Peninsula, England. Sericite-fluorite bodies are also distributed on the Karaoba molybdenum-tungsten deposit located southeast of the Komsomolskoye deposit.

Uranium minerals described for the first time in nonoxidized ore of the Komsomolskoye deposit are represented by pitchblende $UO_2 \cdot kUO_3$, uraninite UO_2, brannerite $(U,Ca,Th,TR)(Ti,Fe)_2O_6$ and uranium blacks (friable powder of pitchblende, coffinite $U[(SiO_4)_{1-x}(OH)_{4x}]$, brannerite and small quantities of other minerals). Pitchblende, uraninite and brannerite are little abundant being relics of altered ore in the zone of hypergenesis. Pitchblende occurs as dot colloform segregations, uraninite — as almost square cuts of crystals $n \cdot 10^{-2}$ mm. Brannerite was observed as fine and ultrafine segregations, which, in the data of spectral analysis, contain some percents of titanium, calcium, iron, lead and traces of niobium, wolfram, TR, in addition to uranium.

Hypergene zone is distinctly manifested, as was noted earlier (Chernikov, 1981; Chernikov, 1982; Chernikov, 2001). Uranium minerals in its limits are distributed by zoning. The main mineral in the upper part is schrö ckingerite $NaCa_3[(UO_2)(CO_3)_3(SO_4)F] \cdot 10H_2O$ (Photo 1). Its accumulations form a near-surface subzone considerably enriched with uranium as compared with lower parts of exogenous zone. Its vertical thickness varies from 2 to 10 m. Gypsum is common here and small amounts of uranophane $Ca(H_3O)_2[UO_2SiO_3]_2 \cdot 3H_2O$ was registered. Schrö ckingeritev appears along mineralized tectonic cracks, but more often in wall rocks, far outside of ore-bearing structures. It is also widely distributed in friable deposits.

Schrö ckingeritev in the deposit rather frequently forms large almost monomineral accumulation (Photo 2) in clayey material with abundant gypsum. Two samples from the deposit were subject to chemical analysis, which results are given in Table 1 in comparison with schrö ckingeritev from another ore locality of this region and with theoretical composition. The analyzed samples are similar to each other and differ a little from theoretical composition of schrö ckingeritev. If all aluminum and silicon to consider as admixtures, the analyzed samples have a little lower contents of uranium and carbonic acid and increased amount of fluorine, water, and the in some samples — of SO_3.

The optical properties of schrö ckingeritevs from the Komsomolskoye deposit, as well as from ore localities and radioactive anomalies of the region of Betpak-Dala and Chu-Ili mountains, differ a little from those described in literature. So, Nm values usually do not exceed 1.525 — 1.535, rarely attaining 1.540 — 1.545 cited in literature for schrö ckingeritev (Getseva and Savelyev, 1956; Soboleva and Pudovkina, 1957; Frondal, 1958). Nr of schrö ckingeritevs of the Komsomolskoye deposit is 1.505 — 1.517 and rarely goes down to values of 1.500 — 1.485 known from publications. A little lower intensity of some lines in X-ray powder diffraction pattern in comparison with published data probably reflects the worse crystallization in connection with the composition feature of the mineral noted above.

Below the schrö ckingeritev subzone, to a depth from tens to one hundred meters, only small amounts of calcium minerals of uranyl (uranophane, autenite $Ca[UO_2PO_4]_2 \cdot 8 - 12H_2O$ and, probably, uranospinite $Ca[UO_2AsO_4]_2 \cdot 8H_2O$) were registered.

Uranium-bearing limonite, manganese oxides and clay minerals are common here. Uranium was intensively leached from this part of hypergenesis zone, hence, it can be considered as a leached subzone. Uranyl minerals are established in it in the data of physical, optical and spectral analysis, and uranophane, in addition to these data, in X-ray powder diffraction patterns. Autenite has pale greenish-blue color, perfect cleavage by (001) and less perfect by (100). Nm = 1.580 — 1.590; rarely to 1.600 —

1.605. Its varieties with average index of refraction 1.618 – 1.620 corresponding to uranospinite are also present. However, in the samples analyzed by spectral method, the content of arsenic was 0.*n* %, at *n* % of phosphorus and calcium and n·10 % of uranium; hence, uranospinite in them, if any, is in very limited amounts.

Below the subzone of calcium minerals of uranyl (leaching of uranium), only uranium blacks are distributed (cementation zone from several meters to tens of meters thick). Clay substance containing sorbed uranium is present in smaller quantities.

With depth, the zone of uranium blacks is replaced by a horizon poor in uranium, in which pitchblende, uraninite, and brannerite are present only in dense plots of greisenized granite, whereare crushed rocks represent hematitized and argillized deep-seated zone of hypergenesis. Intensive hypergene redistribution of uranium in the section of Komsomolskoye deposit is distinctly registered by isotope composition of uranium-bearing and uranium minerals and by mineral associations.

The radiogenic additive of lead (0.01 – 0.023 %), as well as its gross content (0.03 – 0.04 %), is almost constant in the vertical section of the hypergenesis zone. At the same time, values of analytically detected uranium oscillate in a wide range of mineral associations. In the leached subzone, modern uranium content is tens of times below the value designed by radiogenic lead in minerals and rock. Sharp increase of uranium content, in times exceeding the values designed by radiogenic lead, is typical for uranium blacks of the cementation zone. These values only coincide in one ore sample from a deep-seated hypergene zone. Other studied minerals and mineral associations of deep-seated hypergene zone show a significant shortage of analytically measured uranium in comparison with that designed by radiogenic lead in them. It gives the base to consider that uranium was leached out and therefore it is possible to suppose insufficient study of the deposit regarding presence of commercial accumulations of uranium minerals at a depth.

Ratios Io(^{230}Th)/^{238}U, ^{234}U/^{238}U and ^{226}Ra/^{238}U in minerals and ore samples from the deep-seated hypergene zone are close to 1. In minerals and samples of rock with increased content of uranium from the zone of cementation and leaching of uranium, they vary within the determination error. Such isotope ratios in minerals and rocks indicate that they were formed earlier than ~ 1.5 m.a. ago. Only for ^{226}Ra and ^{234}U obvious deviations from their balance with ^{238}U are sometimes noted. Surplus of ^{226}Ra in minerals of the middle of leaching zone and some shortage in it to its balance with ^{238}U in minerals and ores of cementation zone is probably related to insignificant modern redistribution of radium in this part of hypergene zone. Preferable migration of ^{234}U from the middle part of leaching zone to the lover part of it and upper part of cementation zone was also registered. This, as well as for radium, could be explained by almost modern redistribution of ^{234}U.

Table 1. Chemical composition of schrockingeritev

Oxides	*1/71, Northern ore manifestation*	*502/71 Komsomolskoye-deposit*	*503/71, Komsomolskoye deposit*	*Theoretical composition*
Na_2O	3,32	3,40	3,42	3,49
K_2O	0,09	0,17	n.d.	-
CaO	18,90	18,56	18,76	18,91
SO_3	9,17	9,20	9,00	9,02
UO_3	30,26	30,31	30,46	32,21
CO_2	14,46	14,13	14,62	14,86
$H_2O\pm$	20,31	20,34	20,31	20,27
F	2,72	2,68	2,81	2,14
Al_2O_3	0,80	0,81	0,85	-
SiO_2	1,30	1,61	0,64	-
Σ	101,33	101,21	100,87	100,90
$O=F_2$	-1,15	-1,13	-1,18	-0,90
Σ	100,18	100,08	99,69	100,00

Note:
Chemical analysis was made in the laboratory of VIMS, Moscow (analyst S.P. Purusova)

Schröckingeritev from granite and greisen lenses is characterized by stable high values for all three determined isotope ratios. Such phenomenon probably indicates that during last hundreds thousands of years uranium with sharply increased ratio ^{234}U/^{238}U was introduced into the near-surface layer. Preferable migration of ^{238}U out of it occurred during the last several thousands of years. It has resulted in increase in ratios in schröckingeritev: Io/^{238}U (on the average, to 1.42), ^{234}U/^{238}U (to 2.85) and ^{226}Ra/^{238}U (on the average, to 1.78).

Oscillations of ^{234}U/^{238}U ratio in schrockingeritev from clay-rubbly weathering products are within 1.78 – 2.38 (mean 1.92) and Io/^{238}U ratios within 0.2 – 0.6 (mean 0.36). Such ratios of radioactive isotopes indicate obviously imposed character of schröckingeritev in clayey-rubbly weathering rocks in last hundreds thousands of years with essentially inc-

reased $^{234}U/^{238}U$ ratio. Uranium migrated in vertical and horizontal directions. Therefore, sites of modern accumulation of schrockingeritev not always fix places of hypogene ore exposition, making little reliable the deposit evaluation at a depth.

$^{234}U/^{238}U$ ratio in schrö ckingeritev and ore oscillates in Quaternary deposits above the clayey-rubbly weathering rocks from 1.32 to 4.59 (the last is the maximum value ever detected in minerals or rocks) giving the highest average we have detected in minerals — 3.37. Io/^{238}U ratio changes from 0.89 to 2.59. The average of 1.63 also essentially exceeds the radioactive equilibrium. Such ratios of radioactive isotopes in minerals and ore indicate an essential addition of uranium into friable deposits during all Late Quaternary epoch with significant displacement of isotopes of uranium towards ^{234}U. In the last some thousands of years, due to some moistening of climate, an appreciable leaching of uranium from schrockingeritev of Quaternary formations occurred, therefore, Io/^{238}U ratio in them is, on the average, above one.

As a whole, the near-surface oxidation zone of the Komsomolskoye deposit is characterized by an intensive and long leaching of uranium up to the Quaternary period and formation of distinctly manifested zone of uranium blacks of this age. Uranium also was leached from hypogene minerals in the deep-seated zone of hypergenesis, but less intensively than from minerals of the near-surface oxidation zone. Schrö ckingeritev intensively deposited in the uppermost levels of near-surface oxidation zone and in modern deposits.

Occurrence of beryl and emerald mineralization at Site 2

In addition to the above finds of beryl and bertrandite in the central sites of the Kuu granite massif, locality of emerald mineralization was met in the exocontact of a small uranium-beryllium deposit. Beryllium minerals and ore bodies are first described. Larger ore bodies of beryllium mineralization are located at Site 2, in the southeast contact of the Kuu massif. The site is composed of large-grain biotite porphyry granite, which contacts in the south with basically Devonian quartz porphyries and in the most western part of the site with amphibolous schists of Shalgiinsky ultrabasite massif. The contact strike is latitudinal, with abrupt dip to the south. Granite and quartz porphyries in the south of the site are intensively kaolinized to a depth of up to 8 m from the surface and schists are altered into birbirites.

The site comprises some greisen bodies in granite. Greisens are fringes accompanying quartz veins or ramified vein-like bodies and lenses, or irregular-shaped bodies. By mineral composition, greisens are classified as quartz-micaceous, quartz-hematite and phenakite-beryle, sometimes, with helvite. Quartz-micaceous and quartz-hematite greisens prevail. Two largest greisen bodies were explored for beryllium mineralization. Ore body # 2 was traced by superficial workings. In plan, this is a lenticular body. The lens is 50 m long and from 0.2 to 7.0 m thick. The lens strikes at 320° NW dipping to SW at 75−80°. The ore body is basically composed of quartz-hematite greisen with plots of micaceous and phenakite-beryle greisen with helvite. The contents of beryllium does not exceed 0.23 %.

Ore greisen # 3 is a vein-like ramified body of irregular thickness — from several mm to 8.5 m, striking almost in latitudinal direction, dipping to south at 70−75°. The length of greisen body is 220 m, beryl is irregularly distributed, enriching the northern part of body on the extent of about 150 m, where the average content of beryllium is 0.245 %. The ore body wedges out at a depth of 30 m. Schrockingeritev mineralization analogous to the Komsomolskoye deposit develops near the surface at a depth of 0.1−2.0 m in the southern part of site # 2 in argillized granite and greisens. Wells have penetrated the increased γ-activity in quartz-micaceous greisens with fluorite, pyrite, galena and limonite at a depth of 99,5 and 110.75 m as films of uranium blacks, also analogous to the Komsomolskoye deposit.

Similar schrö ckingeritev accumulations are detected on Northern and Northwestern sites (northern contact of the Kuu granite massif).

In the western part of Site 2, quartz vein with beryl occur in amphibolitic schist of the Shalgiinsky ultrabasite massif, near its contact with granite. Forms of beryl crystals change from isometric to prismatic (Photo 3). Crystal sizes vary from parts of mm to 5 cm in length at 0.5 cm in diameter. Ultrabasites and amphibolitic schists are enriched with chromium and vanadium in tens of times above the percent abundance, therefore, beryl from schist and its transparent variety emerald (Photo 4) contain chromium and vanadium in increased concentration (0.n % Cr and 0.0n % V). This is why their color changes to pale-green and bright green, whereas beryl from granite is grayish-white and brown-gray and contain 0.00n %

Cr and V. Emeralds frequently have irregular color, which changes in a crystal along the long axis from rich green to pale bluish-green (Photo 5). In green beryl crystals (Photo 6) the transparency also varies from opaque through zones of translucent beryl to zones of transparent emerald of rich green color.

Beryl and emerald of Site 2 have low refractive indexes (No 1.570—1.575; Ne 1.568—1.572) and belong to varieties with small concentration of alkalis (Winchell, 1949; Dorfman, 1952; Winchell and Winchell, 1953). Sodium concentration in minerals makes tenth parts of percent.

Quartz-hematite and quartz-micaceous greisens of the endocontact parts of granite locally have increased concentration of beryl and phenakite, becoming phenakite-beryl greisens, sometimes with helvite. Phenakite in these greisens is subordinated to beryl and forms achromatic or grayish-yellow lenticular or prismatic translucent crystals (Photo 7) from dot segregations to 3—5 cm in length and 0.5 cm in diameter. Its hardness is 7.5—8, Ne-1.672—1.674, No-1.660—1.665. It is sometimes substituted by bertrandite (Photo 8), acquiring lamellar by (001) and prismatic shape of crystals with perfect cleavage by (110) and less perfect by (001) and (010). Its hardness reduces to 6.5. The mineral is biaxial (-), Ng 1.612; Nm 1.602; Np 1.588. Gem value of phenakite, as well as of other beryllium minerals is low, but their collection worth is undoubtedly very high.

Helvite in greisens is registered as individual tetrahedral honey-yellow crystals with vitreous luster and hardness of about 6 and density of 3.2—3.4. Schist on the Kuu granite contact comprises three quartz-hematite lenses with helvite, the dimensions of each of them are 8—6 m by 3.5—3 m, with the helvite content to 30 %. Beryl deposits on the periphery of lenses in a layer of 2—2.5 cm.

Further from the contact, the Shalguiya molybdenum deposit was formed. It is located between the Permian granite massif of Kuu and pre-Late Devonian granite Munglu. Serpentinites, amphibolous and amphibole-plagioclase schist are most widely developed here after rocks of the Shalgiinsky Early Caledonian basic-ultrabasic pluton.

The mineralization is multiphase. The earliest phase represent abundant monomineral streaks of quartz, sometimes containing thin magnetite impregnation. After them, judging by intersections, molybdenite-quartz streaks of several generations were formed. Thin streaks (5 mm and less) of fine crystalline quartz are most distributed. They contain molybdenite, rather regularly disseminated or concentrated as zones parallel to exocontacts of veins. Rather rare streaks of coarse-crystalline quartz with fringes of coarse-scaly molybdenite formed later. Almost monomineral molybdenite streaks in quartz and in hosting rocks formed much later.

Streaks of fine crystalline quartz with poor impregnation of wolframite and thin streaks of coarse-crystalline crested quartz with carbonates (ankerite, calcite, dolomite), sulfides (pyrite, chalcopyrite, sphalerite, galena, molybdenite, less often cobaltite and millerite) and fluorite were formed after early generations of molybdenite-quartz streaks and probably later coarse-crystalline quartz with fringes of coarse-scaly molybdenite. Streaks of potassic feldspar also segregated after coarse-crystalline quartz with fringes of coarse-scaly molybdenite, but they before fine crystalline quartz with wolframite and streaks of crested quartz with carbonates and sulfides. Monomineral molybdenite streaks are the latest, they cross all above listed mineral formations and in age they are at least much younger of femolite from the Djideli deposit (south-southwest) and molybdenite from the Bezymyannoe deposit (northwest of the Kuu massif). Femolite in ores of Djideli deposit and in molybdenite in the Bezymyannoe deposit are in close associations with pitchblende, which age by lead isotopes is 330—360 m.a. (Modnikov *et al.*, 1971). Early generations of molybdenite-quartz streaks could by related to molybdenite of uranium ores by the contents of elements-admixtures in them. Other generations of molybdenite-quartz streaks formed later as they cross and cement streaks of early generations. Mean of isotope age of Permian granite and related tin-tungstem-molybdenum mineralization in Kuu granite and Karaoba deposit (Yermilov, 1964) is ~270 m.a. Hence, streaks of fine crystalline quartz with wolframite and streaks of crested quartz with carbonates and sulfides including molybdenite could be correlated to this time interval. All streaks of monomineral molybdenite were deposited even later. Some monomineral streaks of fine molybdenite were probablly formed in the cementation zone as the oxidation zone of the Shalguiya deposit is practically deprived of molybdenum, which naturally deposited in reducing conditions below the oxidation zone and by age is much younger than 270 m.a. Some of them are probably modern deposits. This shows that formation of molibdenic mineral associations occupied rather a long time.

Ore streaks of early generations of quartz were formed before dikes of the second phase, while carbonate-quartz and felspathic streaks — after these dikes. Under M.M. Povilaitis observations (1990), streaks of early quartz generations have undergone intensive dynamic and thermal metamorphism at introduction of later dikes expressed in lamellar deformation. However, other ore-bearing quartz streaks cross these dikes and re-crystallized molybdenite is redistributed and concentrated in cracks of diverse orientation, which cross veined quartz.

In the oxidation zone to a depth of 40 to 60 m, sulfides are completely oxidized and molybdenum is intensively leached from oxidized ore. In the oxidation zone, only insignificant amount of powellite Ca [MoO_4] and extremely rare wulfenite Pb [MoO_4] were preserved, in addition, molybdenum is sorbed by iron hydroxides and manganese oxides impregnating rocks through numerous joint cracks. However, the average molybdenum content in the oxidation zone is low.

Thus, Permian granite of the Kuu massif is characterized by manifestations of diverse mineralizations. These include quartz-feldspathic pegmatites, some of which bear small amount of ore minerals — wolframite, molybdenite, cassiterite, monazite, beryl and less often others. Molybdenite is also present in aplite dikes. Various veined bodies — quartz veins, diverse greisens, fluorite and quartz-ore — are widely distributed in the Kuu massif. Many of them are most intensively manifested in contacts of massif, and some on a significant distance from the granite massif.

The endocontacts contain quartz veins, sometimes with pyrite, molybdenite, wolframite, less often with chalcopyrite and galena, as well as quartz-micaceous greisen bodies with topaz, fluorite, rare molybdenite and less often with wolframite. Feldspar-fluorite, sericite-fluorite and topaz-fluorite bodies are common; this is the pitchblende-uraninite-brannerite mineral association. Quartz-micaceous, quartz-hematite and first described phenakite-beryl greisens, sometimes with helvite, are less distributed. In exocontacts, quartz-beryl veins with emerald and, less often, poorly investigated quartz-hematite veins with helvite were registered. A large part of ore minerals is first described.

Quartz-ore stockwork of the Shalguiya molybdenum deposit, which occur in Shalgiinsky Early Caledonian basic-ultrabasic pluton, is more removed from Permian granite. Polyhronic mineral associations were first descried for the Shalguiya deposit ore.

As shown earlier (Chernikov, 2001), in Betpak Dala, Chu-Ili Mountains and in Kendytaks, the basic erosion of Paleozoic rocks has taken place before the Late Triassic. Later, tectonic evolution of the region, change of climate and exogenous processes had four basic phases. In the first phases or even earlier, before the Late Triassic and basic erosion of Paleozoic rocks, hematitization developed in granite, intensively manifested in the Komsomolskoye deposit.

Intensive exogenous formation of minerals with redistribution of ore elements occurred during long geological time in deposits and ore occurences in the contacts of the Kuu granite massif. Oxidation of hypogene minerals was accompanied by formation of limonite, manganese oxides, clay minerals, hematite and limited deposition of uranyl minerals. Uranium, molybdenum and other elements were intensively leached from the oxidized zone and newly formed minerals deposited in the near-surface and deep-seated zones of cementation.

Only in modern time gypsum began to deposit in soil, Quaternary deposits and upper levels of the weathering rocks, as well as formation of schröckingeritev in near-surface deposits and in upper levels of earlier leached oxidized zones. As Late Quaternary accumulation of schröckingeritev occurred at various distances from the primary source and leached zones are poorly investigated on the depth, the discovered diverse mineralization is insufficiently evaluated and the possibility is rather high to discover at a depth at least commercial accumulations of uranium minerals and probably of molybdenum and beryllium. Schrockingeritev from the Komsomolskoye deposit chemically differ a little from theoretical chemical composition and is characterized by high ratios of radioactive isotopes. The highest ratios $^{234}U/^{238}U$ ever detected in uranium minerals were observed in them.

References

Chernikov A.A. Glubinnyi gipergenez, mineralo- i rudoobrazovanie (Deep-seated hypergenesis, mineral and ore formation). M.: Fersman Mineralogical Museum of the Russian Academy of Sciences. **2001**, 100 p. (Rus.)

Chernikov A.A. Tipomorfizm mineralov urana i ego prakticheskoe znachenie (Typomorfism of uranium minerals and its practical importance). Sov. Geologiya **1981**, # 4.

P. 209—214 (Rus.)

Chernikov A.A. Typomorphism of uranium minerals and its practical significance. International Geology Review. **1982**. Vol. 24, N 5. P. 567—576 (Rus.)

Dorfman M.D. K voprosu ob opredelenii genezisa berilla (To the problem of definition of beryl genesis. Doklady AS USSR. **1952**. T. 82, # 4. P. 623,624 (Rus.)

Ermilova L.P. Mineraly molibdeno-volframovogo mestorozhdeniya Karaoba v Tsentralnom Kazakhstane (Minerals of the molybdenum-tungsten deposit Karaoba in the Central Kazakhstan). M.: Nauka. **1964**, 176 p. (Rus.)

Ezhov A.I. Granitoidy Shalgiinskogo raiona i svyazannye s nimi poslemagmaticheskie obrazovaniya (Tsentralnyi Kazakhstan) (Granitoids of the Shalgiya region and related postmagmatic formations (Central Kazakhstan). M.: Nauka. **1964**, 192 p. (Rus.)

Frondel C. Systematic Mineralogy of Uranium and Thorium. Washington: United States Government Printing Office. **1958**. 400 p.

Getseva R.V., and Savelyev K.T. Rukovodstvo po opredeleniyu uranovykh mineralov (Reference book for identification of uranium minerals). M.: Gosgeoltekhizdat, **1956**. 260 p. (Rus.)

Konoplyantsev M.A. Molibdenovye mestorozhdeniya Tsentralnogo Kazakhstana (Molybdenum deposits of the Central Kazakhstan). Sov. Geologiya **1959**, # 2. P. 85—104 (Rus.)

Modnikov I.S., Tarkhanova G.A., and Chesnokov L.V. O sootnosheniyakh uran-molibdenovogo i olovo — volfram — molibdenovogo gidrotermalnogo orudeneniya (On relations of uranium-molybdenum and tin-tungstem-molybdenum hydrothermal mineralization). GRM. **1971**, #2. P. 92—97 (Rus.)

Povilaitis M.M. — Ritmichno — rassloennye granitnye intruzii i orudenenie (Stratified granite intrusions and mineralization). M.: Nauka. **1990**, 240 p. (Rus.)

Soboleva M.V., Pudovkina I.A. Mineraly urana. Spravochnik (Uranium minerals. Reference book). M.: Gosgeoltekhizdat, **1957**. 408 p. (Rus.)

Crystal Chemistry, Minerals as Prototypes of New Materials, Physical and Chemical Properties of Minerals

UDC 549.283 : 548.51

NANOCRYSTALS OF NATIVE GOLD AND THEIR INTERGROWTHS

Margarita I. Novgorodova
Fersman Mineralogical Museum of the Russian Academy of Sciences, Moscow, min@fmm.ru

Nanocrystals of native gold showing morphological similarity to their synthesized analogs were discovered as inclusions in quartz and sulfides. Nanocrystals tens of nanometers in size are of cubic, cubooctahedral crystalline and dodecahedral quasi-crystalline form. Numerous twins, absent in gold macrocrystals, including polysynthetic twins by (100), and penetration twins by cube were found, reducing the symmetry of the face-centered cubic structure of gold. 1 table, 11 figures, 23 references.

Nanocrystals, which are a special dimensional group (<0.1 micrometer across) in the class of finely dispersed gold, are rarely preserved in the mineralogenic processes. Being the initial form of growth of larger gold crystals, they can be detected among elements of a non-uniform, usually mosaic blocks or zonal, *gold particles*. Nanocrystals and their aggregates are preserved as inclusions in the mineral matrix. These are so-called *matrix*-stabilized nanocrystals preserved in unaltered ores during geological time in tens, hundreds, millions and billions of years, i.e. eternally from the experimenter's point of view.

The history of nanoparticle study — their morphology, properties, synthesis methods, including diverse composite materials used in modern industrial, technical and medical *nanotechnologies* — totals hundreds of publications. Natural nanoparticles of minerals are investigated insufficiently; published in one of the last issues of the Mineralogical Society of America review «Nanoparticles and the environment» (Nanoparticles ..., 2001) contains the data on structure of nanoparticles and their aggregates, phase transformations in nanoparticles, computer modeling of their properties and behaviour, magnetic characteristics of *nanomaterials* received at studies of synthesized *nanocomposites*. Few works on studies of nanoparticles of natural Fe, Ti, and Al oxides, Zn sulfides, and natural and technogenous nanoparticles in atmosphere are exclusions.

Special properties and in some cases unusual structures of nanoparticles are defined by thin equilibrium between surface energy and energy of crystal lattice in volume. At this, the dimensional effect is especially notable as with increase of particle size the share of surface atoms drops and the number of lattice cells of atoms in volume increases (Fig. 1). The dimensional effect is manifested in

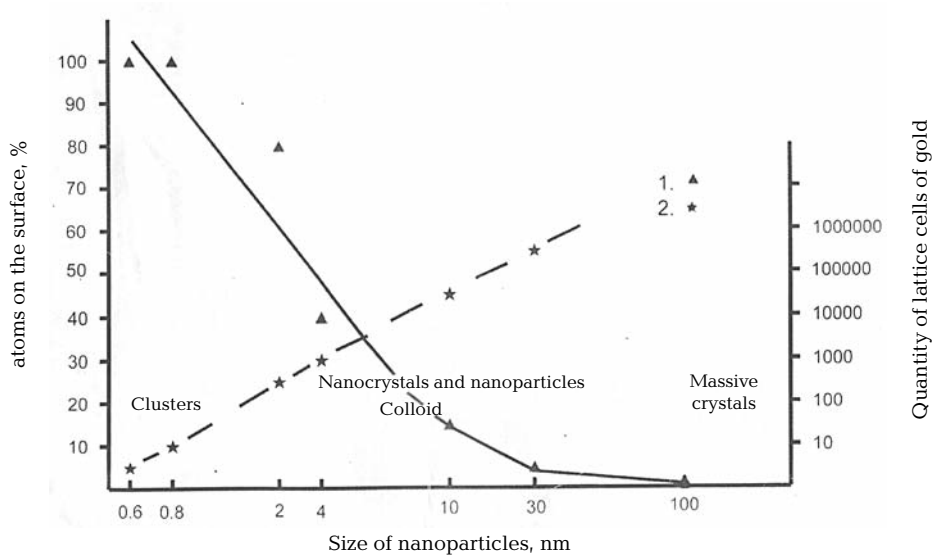

FIG. 1. Share (in %) of atoms on the surface and number of lattice cells in volume of gold nanocrystals depending on their size: 1 — atoms on the surface, %, 2 — quantity of lattice cells

Table 1. Concentration, sizes and form of particles of thin gold in sulfides

Deposit	*Sulfides*	*Au content, ppm*	*Size and form of sulfides grains*	*Size and form of gold particles*
Muruntau, Uzbekistan	Arsenopyrite	120-250	0,05-0,1 mm, rodlike crystals	0.07-0.1 micrometer, rounded inclusions
Bakyrchik, Kalba, Kazakhstan	Arsenopyrite	30-75	0,5-1 mm, prismatic crystals	2-25 micrometer, irregular particles
	Arsenopyrite	51-550	0,05-0,1 mm, rodlike crystals	0,1-1,5 micrometer , dendrites 0,01-0,1 micrometer , orounded particles
	Pyrite	2-32	0,3-1,2 mm cubic crystals	1-40 micrometer micrometer, wrong and flatted particles
	Pyrite	20-105	0,1-0,2 mm pentagon-dodecahedral crystals	0,5-1,5 micrometer rounded inclusions, microcrystals
Lebedinskoye, Central Aldan, Russia	Pyrite	2-125	0,4-1,0 mm cubic crystals	10-75 micrometer irregular and flatted particles
	Pyrite	5-220	0,1-0,2 mm octahedral holohedral and flatted crystals	1-10 micrometer, dendrites
	Pyrite	100-350	0,01-0,1 mm spheroids	0,1-1,0 micrometer, rounded particles

the morphology of nanoparticles and deviation of their structure from the structure of larger crystals. For metals with cubic face-centered cells, transition from the equilibrium cubooctahedral form of crystals to *quasicrystalline — icosahedral* and *dodecahedral — was established*. The *quasicrystalline* form of nanocrystals for the first time has been detected in gold, and later in other face-centered cubic metals.

Diffraction pattern of *icosahedral* and *dodecahedral* crystals of gold, in which structure translation of atoms are theoretically absent, are characterized by the presence of irrational and regular reflections from coherently connected domains, each of which has *face-centered cubic structure*. The domain structure is conditioned by the presence of twins — single or multiple, parallel or radial. The model of *icosahedron* and dodecahedron as multiple twins with *tetrahedral nucleus*, on face (111) of which five or twelve tetrahedrons consecutively growing for the first time was proposed by S. Ino in 1966 and later supplemented by a model of dodecahedron composed of multitwins by (100) (Ino, Ogawa, 1967). Ino (1969) has distinguished three types of twinned nanocrystals — with hexagonal cross-section (icosahedron composed of 12 tetrahedrons aggregated by (111); with pentagonal cross-section (dodecahedron composed of 5 tetrahedrons aggregated by (111); with rhomboid cross-section (dodecahedron of 5 tetrahedrons aggregated by (100)). The critical size of twinned nanocrystals is calculated as a function of such parameters as specific surface energy for planes (111) and (100), energy of twin borders, adhesive energy and density of elastic tension energy. Under calculations, limiting diameter of particles is 10.68 nanometers for Au and 7.56 nanometers for Ag; however, icosahedrons of gold with a diameter of 40 nanometers and dodecahedrons of silver with a diameter of about 300 nanometers were practically observed. The large multitwins grow due to introduction of dislocations reducing energy of elastic tension (Ino, 1969). In icosahedral particles, Schocli partial dislocations locate near surface, in dodecahedrons defects locate on twin borders (Marks, Smith, 1983). Theoretically, the stability of nanocrystals decreases in the series cubooctahedron > dodecahedron > icosahedron (Marks, 1984). The elementary tetrahedron (with four planes (111), considered as a nucleus in S. Ino's standard base model, is still less stable.

Decrease of energy saturation of synthesized nanoparticles and their ability to quick clustering is provided with formation of protective shells, most often as organic ligands (Martin *et al.*, 2000; Lee Penn, Banfield, 1998) or synthesis in stabilizing environments — sol-gel synthesis, settling on polymeric matrixes, etc. (Petrov, 1986; Pomogailo *et al.*, 2000).

It has been established in experiment that clusters (nanocrystals) of metals (Ag, etc.), precipitated on a flat basal surface of graphite are mobile and diffuse with formation of films, which growth stops when mobile clusters achieve the size of 14 nanometers; the diffusion is hindered at steps of matrix plane growth (Caroll *et al.*, 1997). Collective movement of many thousands of atoms incorporated in nanoparticles of crystal structure is stated in many works (Gao *et al.*, 1987; Thurn-Albrecht *et al.*, 1999).

In the nature, matrix-stabilized nanoparticles of native gold precipitate from hydrothermal solutions of inorganic salts on a mineral matrix, on which surface they stabilize in active points or in micropores. Natural sol-gel synthesis occurs at formation of ore in some epithermal deposits.

Despite of numerous publications regarding finely dispersed gold (Bürg, 1930;

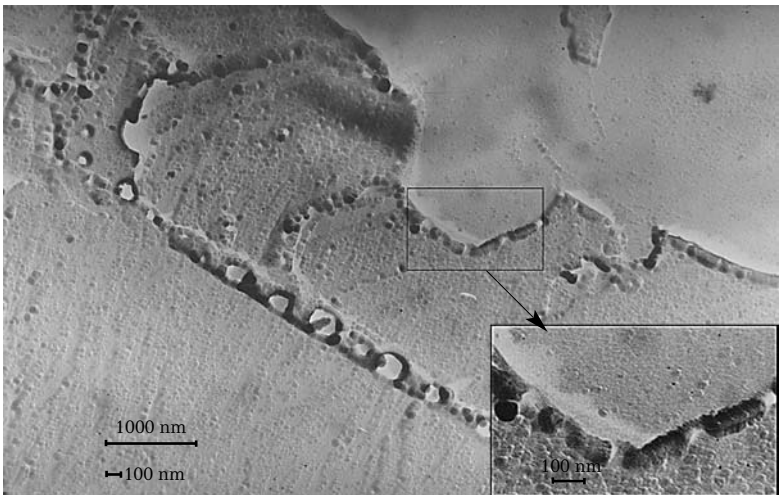

FIG. 2. Gold nanocrystals extracted on a replica (black) in a zonal arsenopyrite crystal in intergrowth with pyrite (light gray). Polished section etched by agua regia. Length of scales is 1000 and 100 nanometers. Bakyrchik deposit, Kalba

Haycock, 1937; Coleman, 1957; Schweigart, 1965; Hausen, Kerr, 1965; Peter, 1973, etc.), its most thin part — nanocrystals — is insufficiently investigated. The objective of this paper is to fill this gap to some extent on the example of nanoinclusions of gold in sulfides and quartz from gold-ore deposits of Siberia, Transbaikalian region, Far East and Central Asia.

Investigation Methods

The miniaturization of investment objects requires application of precision methods, the main of which for direct-viewing is the complex of analytical methods of electronic microscopy — scanning (SEM) and transmission (TEM) microscopy. We used transmission electronic microscopy with application of target cellulose-coal replicas from the chip surface of samples and polished sections. At such approach, a preliminary separation of thin class gold is not required; the sample preparation consists in examination of selected objects using light microscope and labeling of the necessary site for plating. For manufacturing of replicas, coal film was applied on samples in vacuum ionization-thermocouple gage VIT-3 at high vacuum. The received coal film (one-stage coal replica) was separated using gelatin solution, which solidification resulted in formation of two-step cellulose-coal replica. Particles of substance extracted on the film were investigated for determination of composition with the help of the energy-dispersion analysis and structure with the help of electron diffraction method.

Both fresh chips of samples and previously chemically or ionically etched surfaces were studied. As etching agents, acids HNO_3 for sulfides and aqua-regia — HNO_3 + HCl (1:3) — for native gold were used. The etching revealed the internal structure, borders of grains and disorder of studied crystal surfaces.

Experimental works on settling of gold nanoparticles from aqueous solution of gold chloride [$AuCl_4$] on sulfide substrate have been also carried out.

Gold Nanocrystals in Sulfides

Earlier, at study of finely dispersed gold in sulfides, direct dependence of gold concentration in

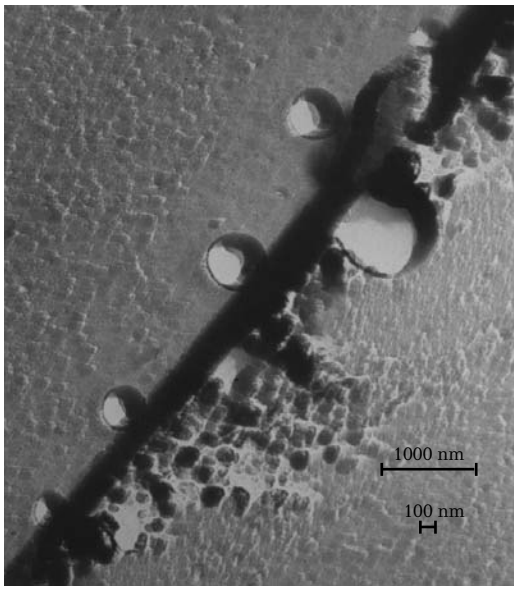

FIG. 3. Imprints of rounded gold dodecahedrons at a step of crystal growth in arsenopyrite. Polished section etched by agua regia. Length of scales is 1000 and 100 nanometers. Bakyrchik deposit, Kalba

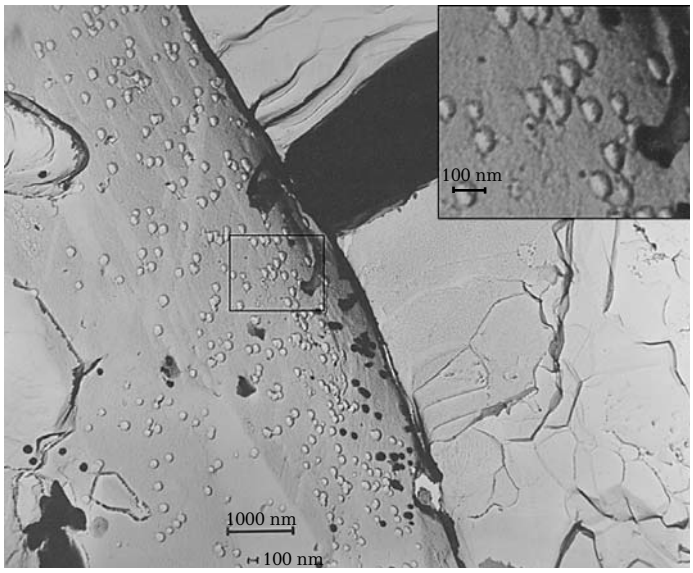

FIG. 4. Gold nanocrystals precipitated on a prism face of arsenopyrite crystal. Length of scale is 1000 nanometers; in box — 100 nanometers

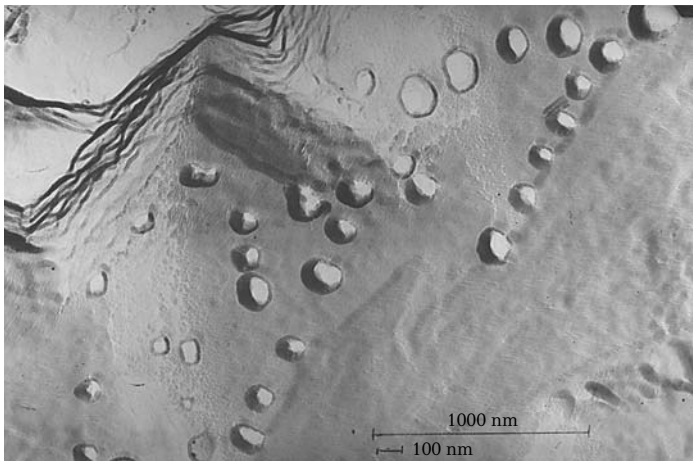

a

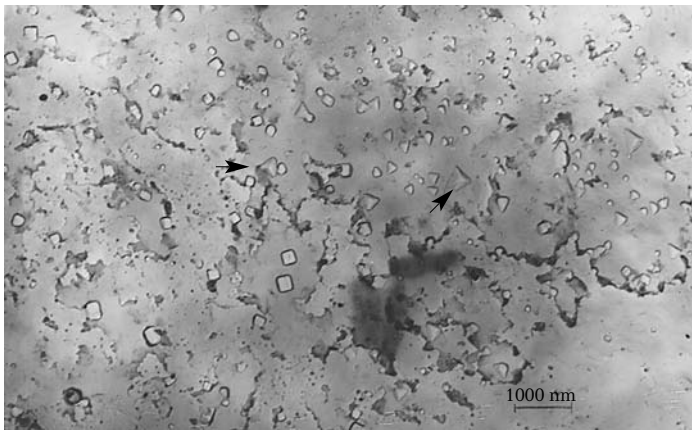

b

FIG. 5. Gold nanocrystals in silicates: a — on sericite-quartz matrix; arrows show twin aggregates of tetrahedrons; length of scales is 1000 and 100 nanometers; b — on sericite-chlorite-quartz matrix, length of scales is 1000 and 100 nanometers. A chip of sample, without etching. Sovietskoye deposit, Yenisei Ridge

pyrite and arsenopyrite on sizes of sulfide grains, which also correlate with sizes of fine segregations gold particles (Table 1), has been shown. For arsenopyrite from the Bakyrchik deposit (Kalba), the highest concentration of fine gold particles along corrosion borders of relicts of early arsenopyrite (for which As/S ratio is <1) in late arsenopyrite with As/S ratio > 1 has been established (Novgorodova, 1994). Fine gold particles also settle on contacts of pyrite and arsenopyrite aggregates and along rectilinear steps of growth in sulfides.

Thin gold in zonal arsenopyrite for about 70 % consist of nanocrystals with sizes 50 to 100 nanometers, rarely up to 150 nanometers. Prevailing forms are cubes and cubooctahedrons; on pyrite/arsenopyrite contact chains of closely aggregated by (100) deformed cubooctahedrons occur, which form wire segregations with hexagonal end faces and ribbed extended surface (Fig. 2). Rounded segregations of gold 70—150 nanometers across, oriented in parallel to ternary articulation of pentagonal planes, occur on steps of growth in arsenopyrite. Morphology of such particles allows to attribute them to the ideal dodecahedron, i.e. to a quasicrystalline construction. Larger nanocrystals (> 250 nanometers) are represented by octahedrons with rounded edges (Fig. 3). The revealed inclusions of gold on zones of growth in pyrite are represented by cubooctahedrons, larger (> 200 nanometers) than nanoinclusions in arsenopyrite.

Artificially settled monodeispersed gold nanocrystals on the prism surfaces of a prismatic crystal of arsenopyrite are of similar sizes (~80 nanometers across). They are characterized by a little deformed, short by (111) form of cubooctahedron and the same orientation of ternary axis of nanocrystals. All gold nanocubooctahedrons grow together with arsenopyrite with face (111), forming interrupted chains

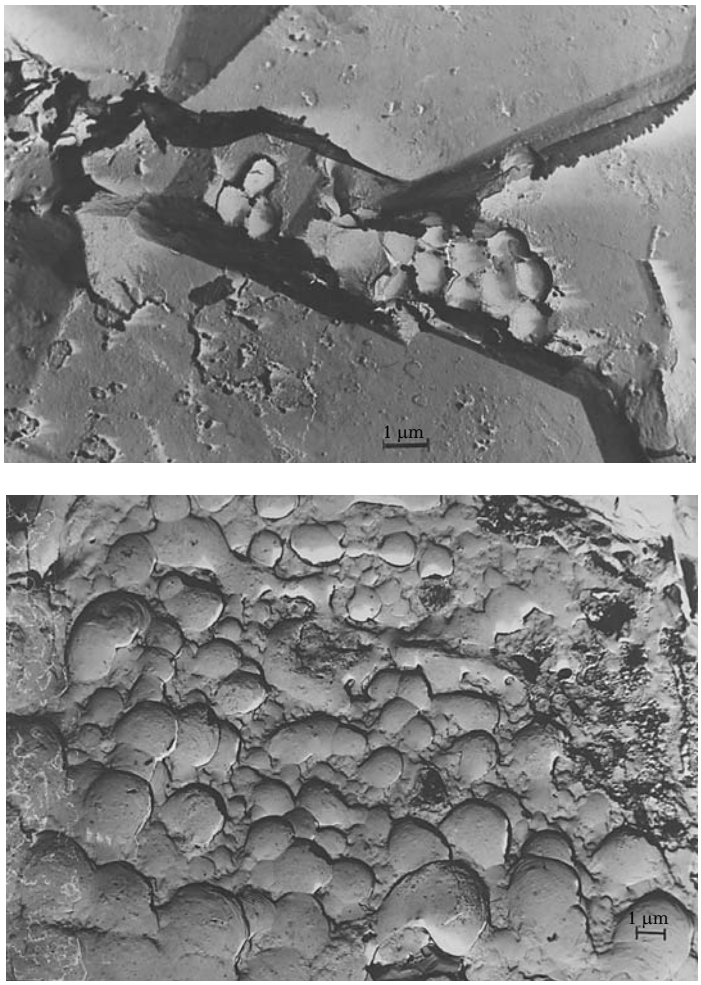

FIG. 6. Colloidal gold in quartz: a — in interstitial spaces of quartz microcrystals as closely packed aggregates of poorly poligonized globules; Taceevskoye deposit, Transbaikalian region; b — in aggregates of inequigranular globules. Sample chips without etching. The size of scale is 1 micrometer. Kualdy deposit, Uzbekistan

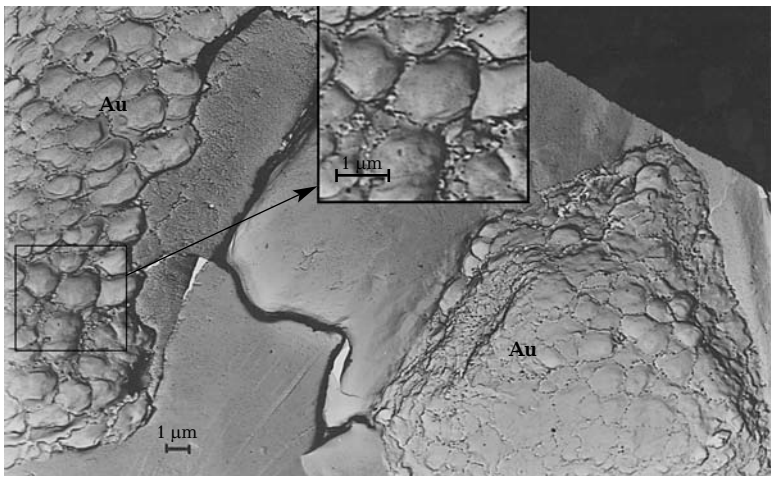

a

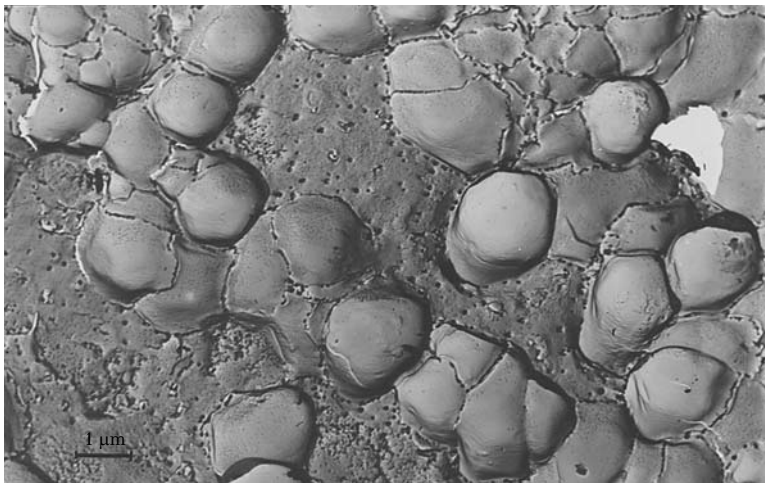

b

FIG. 7. Clots (a) and linear accumulations (b) of metacolloidal gold with syneresis cracks and detached polyhedral blocks in quartz. In box — blocks of dodecahedral shape. Sample chips etched with agua regia. Agatovskoye deposit, Kolyma. Length of scales is 1 micrometer

of close nanocrystals (Fig. 4). The greatest concentration of precipitated gold nanocrystals was established for the peripheral part of arsenopyrite grains.

Gold nanocrystals precipitated on the surface of cubic pyrite crystal are heterodispersed (60—90 nanometers across), have octahedral or cubooctahedral forms and have no orientation. Gold nanocrystals concentrate in the near-apical zone of cubic face of pyrite.

Gold Nanocrystals in Quartz and Silicates

Gold nanocrystals detected in relics of sericite-chlorite-quartz metasomatite in a gold-bearing quartz vein (Sovietskoye deposit, the Yenisei Ridge, Siberia) have sizes, close to those established for gold nanoinclusions in sulfides (10 to 100 nanometers). The nanocrystals are mainly cubic; however, extremely rare in gold nanotetrahedrons and their twins were also detected. Simple twins by (111) with penetrating angle (Fig. 5a), and more complex twins with rhomboid, pentagonal and hexagonal cross-sections supposing the multitwin nature of nanoparticles (Fig. 5b) are also present.

Much more complex crystal constructions of gold nanoparticles are characteristic of gold accumulations in fine festoons and thin-banded quartz streaks and veins from epithermal gold-silver deposits. Attributes of metacolloidal fabrics of such ores, established for many deposits of similar type (Petrovskaya, 1973), specify an original accumulation of colloidal substance in separate plots of ore deposition zones. It is shown that chalcedony-like quartz from thin-banded quartz veins, colored in yellowish tone, is saturated with

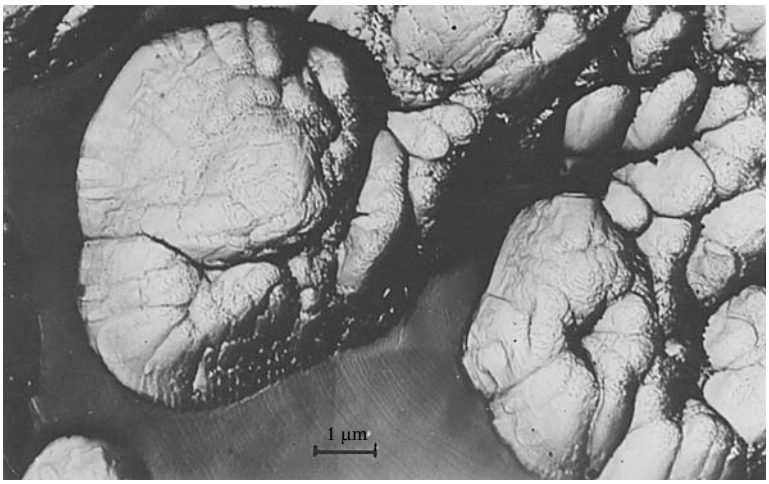

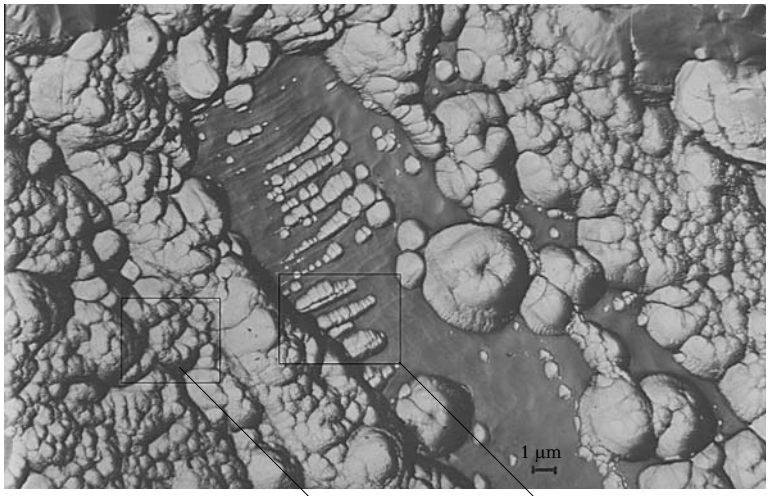

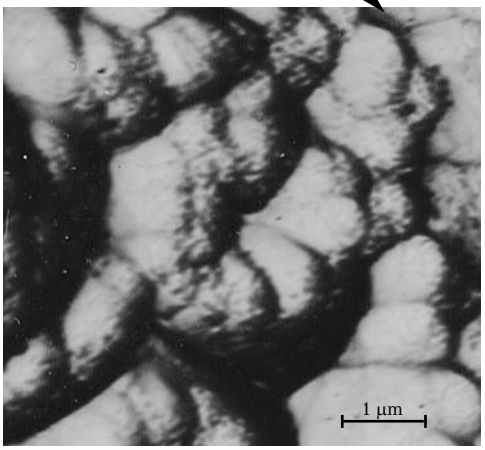

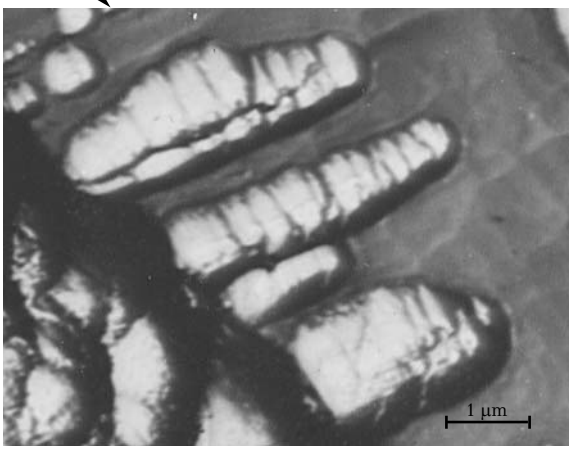

FIG. 8. Structures of metacolloidal gold as complex crystalline zonal constructions; below at the left — with elements of rotational twirl, below at the right — polysynthetic twins. A chip of samples; ionic etching. Agatovskoye deposit, Kolyma. Length of scales is 1 micrometer

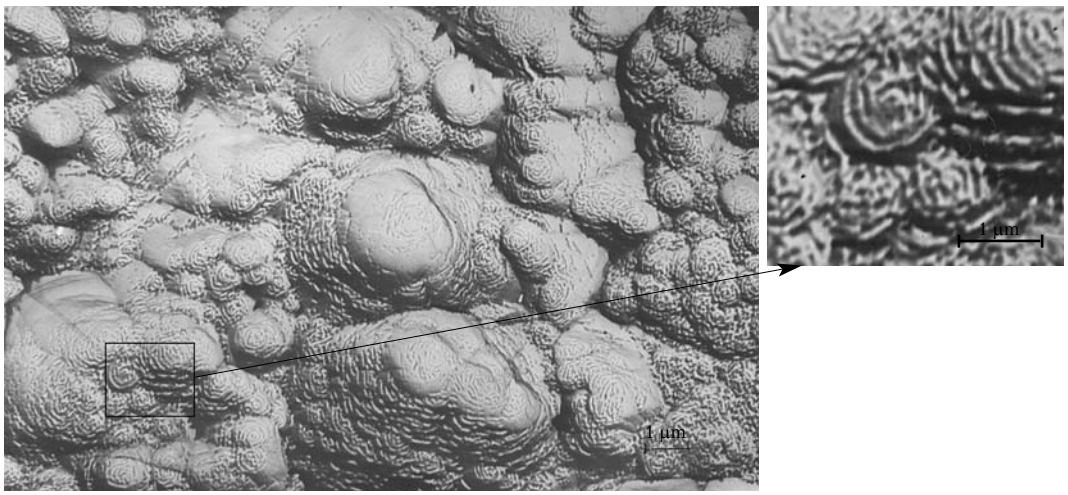

FIG. 9. Reniform aggregates of metacolloidal gold; right — a detail showing skeletal structure of fine blocks with an exit of screw dislocation at the centre. Sample chips; ionic etching. Agatovskoye deposit, Kolyma. Length of scales is 1 micrometer (left) and 100 nanometers (right)

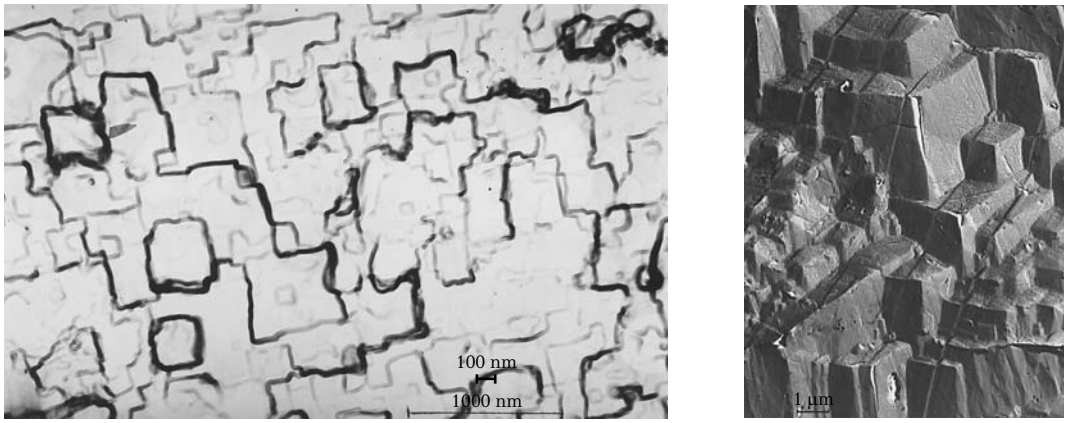

FIG. 10. Domain structure of plane (001) of flatted gold particle (a) and a step microrelief of a lateral border. Sample chips; ionic etching. Taseyevskoye deposit (Transbaikalian region). Length of scales is 1000 and 100 nanometers (left), and 1 micrometer (right)

so-called colloidal gold (Zhirnov, 1972). Colloidal gold includes linear and irregular accumulations of globular particles of 1—3 micrometers in size with smoothed or badly expressed polygonal outlines (Fig. 6). In some cases, a network of syneresis cracks with very thin pores on block contours detached as a result of coalescence can be seen on the surface of gold clots in chalcedony-like quartz after etching. Attributes of plastic flow (Fig. 7a) indicate that separation of blocks began before the complete solidification of colloidal substance. Chemical etching of gold globules reveals their polyhedral structure (Fig. 7b) and ionic etching — their complex internal structure (Fig. 8). Cross-sections of polyhedrons have hexagonal, rhomboidal or pentagonal form; the last is formed by intergrowths of fine blocks with formation of a general dodecahedral form (Fig. 7a). Blocks of a rounded form and zonal structure with an internal nucleus and an external shell (Fig. 8) also occur. The external shell and interblock substance consist of extended columnar individuals with reniform heads showing after etching a skeletal structure and attributes of spiral growth with the exit of screw dislocation at the centre (Fig. 9). The internal nucleus is non-uniform, it consists of closely aggregated subblocks with split apexes; subblocks grow together with rotational twirl along the vertical axis (Fig. 8).

The initial form of such complex skeletal crystals is a flatted cube complicated with faces {hk0} with high symbols, 15—20 nanometers thick, oriented by two most developed faces per-

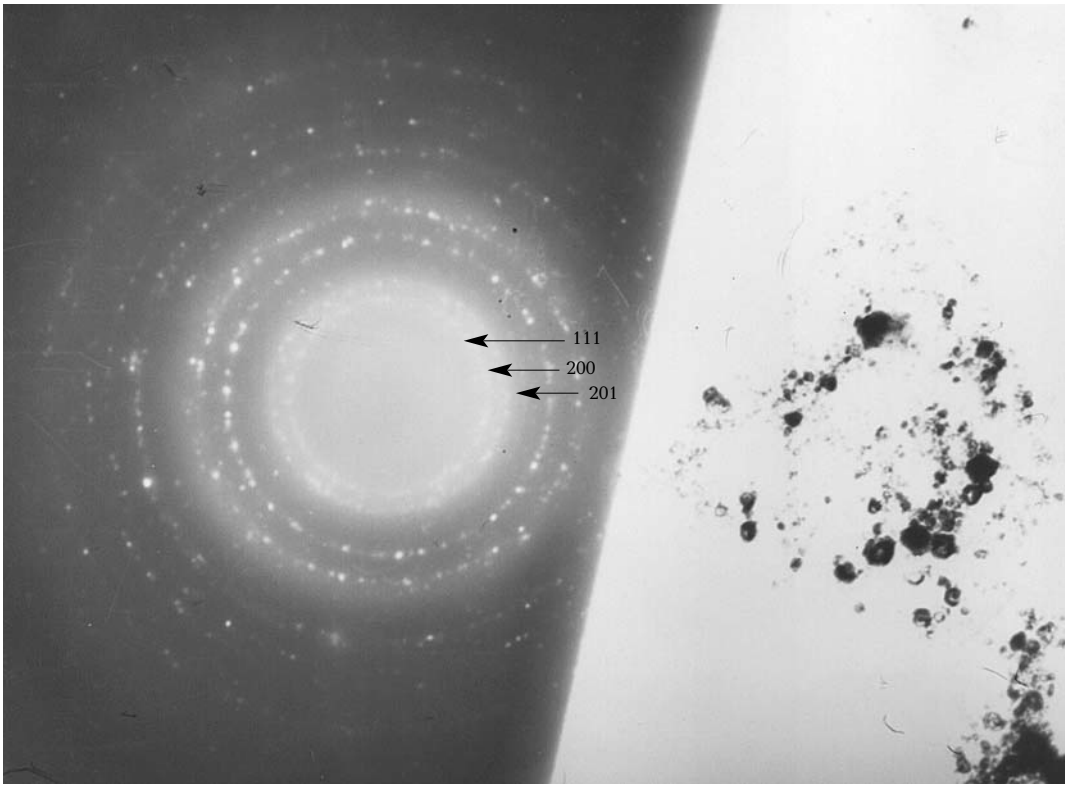

a

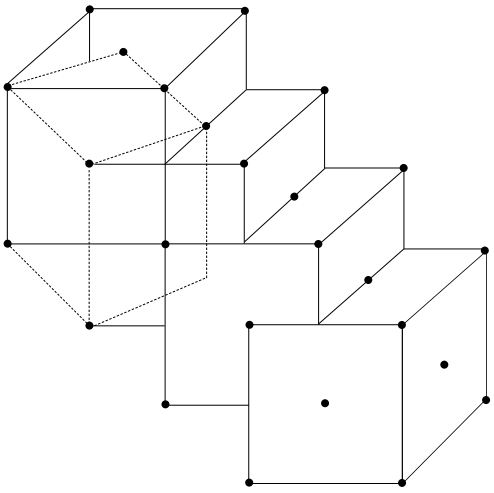

b

FIG. 11. Discrete-ring image of electron diffraction (a) and the scheme of tetragonal cell in interpenetration twins by cube in gold nanocrystals

pendicularly to the quartz matrix surface. In case of parallel intergrowth of flatted cubes, polysynthetic twins are formed, extended normally to composition plane and unknown in gold macrocrystals (Fig. 8). At a shift of intergrowth planes by S plane (010), twins of interpenetration by cube are formed. If such regular intergrowths aggregate with formation of flat gold particle, their traces are seen in the domain structure of plane (001) of gold particles or in unusual microrelief in steps of lateral chips (Fig. 10).

Electron Diffraction Images of Gold Nanoparticles

Similar subparallel orientation of polyhedral blocks in metacolloidal aggregates of gold calls attention. It is possible that orienting effect is rendered by the superstructure of the initial precipitated on quartz layer of colloidal gold. Experimental works (Connoly *et al.*, 1998; Martin *et al.*, 2000) show a tendency of metal nanoparticles, including gold, to collective self-organizing in closely packed cubic or hexagonal monolayers with the distal order. The parameter of such superstructure built not of separate atoms, but of their ensembles —

nanoparticles — is determined, for example, for Ag as 81 Å (interplane distance d_{111}) (Connoly *et al.*, 1998), and for Au ~60 Å (distance between centers of nanoparticles with the size of 2 nanometers) (Martin *et al.*, 2000). These authors state that the superstructure is also preserved and volumetric 3D nanocrystals with the maximum size in some micrometers.

Crystallographically formed matrix-stabilized gold nanocrystals give both dot and discrete-ring images of microdiffraction with irrational reflections (111), inherent to multitwinned nanoparticles. The detailed consideration of such microdiffraction images is the theme for a separate paper, which is being prepared for publishing. The discrete-ring image of electron diffraction taken from cubic and cubooctahedral gold nanoparticles shows an additional reflection (201) (1.72 Å) indicating tetragonalization of face-centered cubic structures of gold. The decrease of symmetry is probably conditioned by ineterpenetration twins by cube, as shown in Fig. 11.

Conclusion

First discovered in nature matrix-stabilized nanocrystals of native gold in sulfides and quartz show morphological similarity to their synthesized analogs, differing by one order bigger sizes (tens of nanometers). They are cubic and cubooctahedral nanocrystals and dodecahedral quasicrystals, which are multitwin aggregates.

Unknown in gold macrocrystals polysynthetic twins by (100) and interpenetration twins by cube were detected, which reduce the symmetry of face-centered cubic structure of gold,

The author is sincerely grateful to K.E. Frolova, in teamwork with which the electron-microscopic images of gold have been received. This work was executed due to the assistance of the Basic Researches Program of the Russian Academy of Sciences, the State Contract # 10002-251/ONZ-04/182-188/160703-1081

References

Zhirnov A.M. Gipogennoe kolloidnoe zoloto v zolotorudnom mestorozhdenii Kauldy (Srednyaya Aziya) (Hypogene colloidal gold in the Kauldy gold-ore deposit (Central Asia) // Uzb. geol. zhurn. **1972**. # 1 (Rus.)

Petrov Yu.I. Klastery i malye chastitsy (Clusters and small particles) // M. Nauka. **1986** (Rus.)

Petrovskaya N.V. Samorodnoe zoloto (Native gold)// M.Nauka. **1973**. 347 p. (Rus.)

Pomogailo A.D., Rosenberg A.S., and Uflyand I.E. Nanochastitsy metallov v polimerakh (nanoparticles of metals in polymers). M.: Khimiya. **2000** (Rus.)

Burg G. Natur des Piriten nicht sichtbar enthalten goldes // Z. prakt. Geol. **1935**. Bd 43. H2.

Carrol S.J., Sceger K., Palmer R.E. Trapping of size-selected Ag clusters at surface step // Appl. Phys. Lett. **1998**. V. 72. N 3

Coleman I.C. Mineralogy of the Giant Yellow Knife gold mine // Econ. Geol. **1957**. V.52. N 4

Connoly S., Fullam S., Korgel B., Fitzmaurice D. Time-resolved small-angle X-ray scattering studies of nanocrystal superlattice self-aggregate // J.Am. Chem. Soc. **1998**.120. P. 2969–2970

Gao P., Gletter H. High resolution electron microscope observation of small gold crystals // Acta metal. **1987**. V. 35, N 7, P. 1571–1575

Hansen D.M., Kerr P.F. Fine gold occurrence at Carlin, Nevada // Ore deposits of the United States, **1933–1967**. N.Y. 1968

Haycock M.H. The role of the microscope in the study of gold ores // Canad. Min. a Metall. Bull. **1937**, V. 40, N 504

Ino Sh., Ogawa Sh. Multiply twinned particles at earlier stages of gold film formation on alkalihalide crystals // Journ. Phys. Soc. Japan. **1967**. V. 22. N 6. P 1365–1374

Ino Sh. Stability of multiply — twinned particles // Journ. Phys. Soc. Japan. **1969**

Lee Penn R., Banfield J.F. Imperfect oriented attachment: dislocation generation in defect-free nanocrystals // Science. 1998. V. 281. P. 969–971

Marks L.D., Smith D.J. HREM and STEM of defects in multiply-twinned particles // Journ. Microscopy. **1983**. V. 130, p. 2, P. 249–261

Marks L.D. Surface structure and energetics of multiplay twinned particles // Phil. Mag. **1984.** V. 49, N 1, p. 81–93

Martin J.E., Wilcoxon J.P., Odinek J., Provencio P. Control of the interparticles spacing in gold nanoparticles superlattices // J.Phys. Chem. B. **2000**, V. 104, N 40, p. 9475–9486

Nanoparticles and the Environment // Ed. J.F.Banfield, A.Navrotsky // Rev. Miner. A geochem. **2001**. V. 44

Novgorodova M.I. Finely dispersed gold from gold deposits of various genetic types // Process mineralogy XII. **1994**. TMS. P. 119–130

Schweigart H. Solid solutions of gold in sulfides // Econ. Geol. **1965**. V. 60. N 7

Turn-Albrecht T., Meier G., Müller-Buschbaum P., Patkowski A., Steffen W., Grübel G., Abernathy D.L., Diat O., Winter M., Koch M.G.,

UDC 548.4

STACKING DISORDER OF ZINC SULFIDE CRYSTALS FROM BLACK SMOKER CHIMNEYS (MANUS BACK–ARC BASIN, PAPUA–NEW GUINEA REGION)

Nadezhda N. Mozgova, Natalija I. Organova,
IGEM of the Russian Academy of Sciences, Moscow

Yuriy S. Borodaev
Lomonosov Moscow State University, Moscow

Nikolay V. Trubkin
IGEM of the Russian Academy of Sciences, Moscow

Margareta Sundberg
Arrenius Laboratory, Stockholm University

Hexagonal ZnS platelets and prisms (up to 1 mm in size) from black smoker chimneys of hydrothermal field of Manus back-arc basin (Papua-New Guinea) were studied using a set of methods (ore microscopy, SEM, electron microprobe analysis, X-ray and electron diffraction, and HRTEM). The most prominent isomorphic admixture is Fe (6.6 — 9.6 mol.% in the ZnS structure). Both X-ray and electron diffraction patterns and HRTEM images have shown that ZnS-crystals despite of their hexagonal habitus contain three different modifications in nanoscale: polytypes 3C and 2H and defect phase with alternating layer- stacking. This fact is a result of nonequilibrium growth conditions.
2 tables, 6 figures, 34 references.

Zinc sulfide in nature mainly occurs as cubic sphalerite (3C) and hexagonal wurtzite (2H)[1] though among synthetic products more than 190 ZnS polytypes are known, the most of which is formed from the gas phase (Mardix, 1986).

Synthetic ZnS crystals are of large interest being important semi-conductors. Structural stacking disorder, twinning, intergrowths, dislocations in synthetic ZnS crystals were in detail discussed in many papers and some studies are conducted with use of high-resolution electronic microscopy (HRTEM) (Qin *et al.*, 1986; Mizera, Sundberg, 1986; Strock, Brophy, 1996, etc.). The disordered distribution of different polytypes (3C, 2H, 4H, 9R, etc.) was also described in natural ZnS crystals from different continental deposits (Fleet, 1975, 1977; Akizuki, 1981; Pósfai *et al.*, 1988; Vergilov *et al.*, 1992, etc.). However, there are problems in understanding the reasons of such defective microscopic structures in ZnS till now. Studies of zinc sulfides from modern oceanic hydrothermal formations can help to get additional data regarding this problem.

A characteristic feature of ocean hydrothermal mounds formed at a depths of more than one kilometer is the presence of sulfide chimneys, from a «pencil» size of some centimeters to thick columns raising to the height of 2—3 storey building (to 10 m and more). Chimneys grow in hot fluids (300 — 400° C) discharge places at the front of their mixing with cold (about 2° C) sea water. An outflow velocity of fluids is usually very high (up to 15 m/s in the Mid-Atlantic Ridge). In outflow places, lifting fluids in the active phase form extensive plumes of smoke in sea water (from here their name — «smokers»), presented by very fine mineral suspension, in quantities dispersing in ocean water.

Sulfides of the system Cu-Fe-Zn-S form the mineral base of ocean ores. Among zinc sulfides, sphalerite is the main mineral of underwater mounds, but wurtzite, which is not common in continental deposits, is frequently registered also. This is one of features of ocean ores (Mozgova, 1999, 2001, 2002; Mozgova, 2002). It is necessary to emphasize that in most cases wurtzite, because of very fine segregations, is diagnosed in underwater ore by the hexagonal form of crystals.

The purpose of this work is to give a detailed characteristic of hexagonal ZnS crystals from modern ocean sulfide ores from the Manus basin.

Geological position

Back-arc spreading centre of the Manus basin is within the axial volcanic arch «Red Star» of the internal rift about 2 km in width, characterized by extremely high spreading speed (up to 12 cm/year). Hydrothermal deposits form on pillow basalts at a depth of about 2500 m being represented by numerous chimneys from 1 m to 4 m in height (the main tower attains 14 m). Socle parts of chimneys are composed of ore crusts mainly consisting of barite

[1] Matraite, the third ZnS polymorph (R3m), named after the unique place of find, is indicated as an independent species — hexagonal (Anthony *et al.*, 1990), trigonal (Blackburn *et al.*, 1997), rhombic (Vaughan, Craig, 1978) or as trigonal wurtzite (Minerals, 1960)

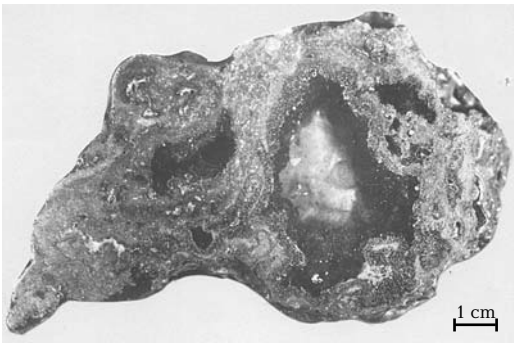

FIG. 1. Polished section of specimen № 2255-15A from an inactive chimney. Sulfides (mainly ZnS) have a zonal arrangement around the channels. The channels were cemented with epoxy resin before polishing. White irregular inclusions and fine zones are anhydrite and partly opal

and opal with disseminated impregnation of sulfides (Bogdanov, Sagalevich, 2002). Samples for studies were received from the Shirshov Oceanological Institute of the Russian Academy of Sciences. They have been collected in 21st cruise of the scientific vessel «Academician Mstislav Keldysh» in 1990 (Lisitsyn *et al.*, 1992).

Methods of studies

The morphology of revealed ZnS crystals was studied using two scanning electronic microscopes — JEOL JSM-T20 and Hitachi S-800. Structural relations between zinc sulfides and other minerals (sample №2255-15A) were observed under microscope in reflected light. Polished sections were made without heating.

The chemical composition was studied by X-ray microanalyser MS-46 «CAMECA» under the following conditions: accelerating voltage 20 kV, probe current 20 – 40 nA, standards (analytical lines) — ZnS (ZnKα and SKα), FeAsS (FeKα), $CuFeS_2$ (CuKα), CdSe (CdLα) and pure metals Mn and Ag (MnKα and AgLα).

X-ray diffraction characteristics were received in Guinier camera (Cu-radiation, internal standard — Si) and Laue and Weissenberg singlecrystal cameras. Electronic diffraction was studied in microscopes JEOL JEM 100CX (IGEM) and JEOL JEM 200CX (Arrenius Laboratory). The same material was used to receive a diffraction pattern (GIN of the Russian Academy of Sciences).

For studies under electronic microscope, selected ZnS grains were pulverized in an agate mortar in presence of *n*-butanol and then a drop of suspension was put on a copper grid. HRTEM images were received in electronic microscope JEOL JEM 200CX, equipped with the goniometric device (inclination ±10°), at operating voltage of 200 kV.

Sample description

We have studied a polished cross section of an inactive chimney 8 cm long and about 6 cm wide, with abundant pores and irregular-shaped channels, from 1 – 3 mm up to 3 cm in size (Fig. 1). Most of channels are empty, some are filled in with anhydrite. Fine-grained aggregates of sulfides, mainly zinc sulfides, surround large channels, repeating their outlines. Zonality is notable in distribution of sulfides around of channels, basically due to alternation of thin zones of non-metal minerals (anhydrite and subordinated quantities of opal).

Walls of channels are covered with crusts of microdruses consisting of well crystallized fine ZnS crystals with mirror faces — hexagonal prisms up to 30 microns in height and to 20 microns wide (Fig. 2a) and hexagonal platelets up to 60 microns in diameter (Fig. 2b). It is necessary to emphasize that prisms also show a subparallel transverse structure. Fine chalcopyrite tetrahedrons are notable on faces of lamellar crystals. The base of microdruses consists of cone-shaped and columnar aggregates of transverse subparallel platelets (Fig. 2c, d). They make walls of channels. In transverse sections it is visible that size of platelets in cone-shaped aggregates increases towards the channel and thus the aggregate in this direction extends. Similar morphology of hexagonal wurtzite crystals was described in earlier publications (Oudin, 1983; Rö sch, Marchig, 1991). The conic form of aggregates and their lamellar structure are well manifested in polished sections in reflected light, and there are numerous chalcopyrite grains basically located near edges of ZnS aggregates (Fig. 3). Columnar aggregates voutward from the channel are usually changed by assemblaes of irregular grains of the same sulfides cemented by anhydrite and opal.

Prismatic and lamellar ZnS crystals in microdruses have light brown color, columnar aggregates are dark brown with a greenish tone. Both varieties of ZnS in polished sections have in reflected light usual gray color and strong reddish-brown internal reflexes. Despite of hexagonal shape of crystals, the anisotropy is not noted in them.

X–ray microanalysis

Chemical composition was determined in polished sections of five ZnS crystals. Pre-

Table 1. Electrron microprobe data of zinc sulfides from Manus (Sample № 2255-5A)

		Contents, mass. %								
Grain	*Anal*	*Zn*	*Fe*	*Cu*	*Mn*	*Ag*	*Cd*	*S*	*Total*	*Formula*
I*	1	62,68	3,83	0,05	0,08	0,02	0,00	32,63	99,29	$(Zn_{0,94}Fe_{0,07})_{1,01}S_{0,99}$
	2	61,42	3,96	0,04	0,07	0,04	0,00	32,90	98,43	$(Zn_{0,92}Fe_{0,07})_{0,99}S_{1,01}$
	3	62,00	3,75	0,05	0,06	0,04	0,00	32,37	98,27	$(Zn_{0,94}Fe_{0,07})_{1,01}S_{1,00}$
II*	4	61,07	5,28	0,12	0,09	0,04	0,00	32,54	99,14	$(Zn_{0,91}Fe0,09)_{1,00}S_{0,99}$
	5	61,98	4,46	0,12	0,08	0,04	0,00	32,56	99,24	$(Zn_{0,93}Fe_{0,08})_{1,01}S_{0,99}$
	6	60,80	5,42	0,11	0,11	0,05	0,00	32,53	99,02	$(Zn_{0,91}Fe_{0,10})_{1,01}S_{0,99}$
	7	61,67	4,77	0,09	0,08	0,04	0,00	32,77	99,42	$(Zn_{0,92}Fe_{0,08})_{1,00}S_{1,00}$
III**	8	61,01	5,22	0,13	0,12	0,00	0,11	30,67	97,31	$(Zn_{0,94}Fe_{0,10})_{1,04}S_{0,.96}$
	9	61,76	5,28	0,13	0,12	0,00	0,11	31,13	98,53	$(Zn_{0,94}Fe_{0,09})_{1,03}S_{0,96}$
IV**	10	62,04	3,83	0,06	0,08	0,00	0,00	33,30	99,31	$(Zn_{0,92}Fe_{0,07})_{0,99}S_{1,01}$
V**	11	62,04	4,03	0,33	0,09	0,00	0,11	34,11	100,72	$(Zn_{0,91}Fe_{0,07})_{0,98}S_{1,02}$
	12	62,09	4,74	0,23	0,09	0,00	0,00	34,47	101,62	$(Zn_{0,90}Fe_{0,08})_{0,98}S_{1,02}$

*I and *II — two crystals previously investigated by X-ray monocrystal method. Analysis 1 — core of the crystal; analyses 2 and 3 — its peripheral part; analyses 4 — 7 from different points of the second crystal (Fig. 2a);
** III — V — ZnS crystals previously investigated under scanning electronic microscope. Analyses 8 — 9 — columnar aggregate of dark brown crystals with greenish tint, containing abundant fine inclusions of chalcopyrite (Fig. 2c); 10 — hexagonal platelet from microdruses; 11 — 12 — aggregate of dark brown irregular grains with chalcopyrite inclusions from the base of microdruses (Fig. 2d)

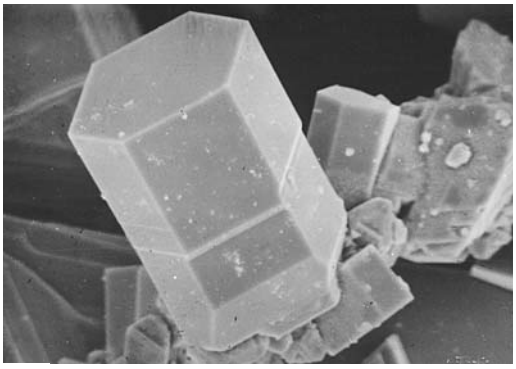
a

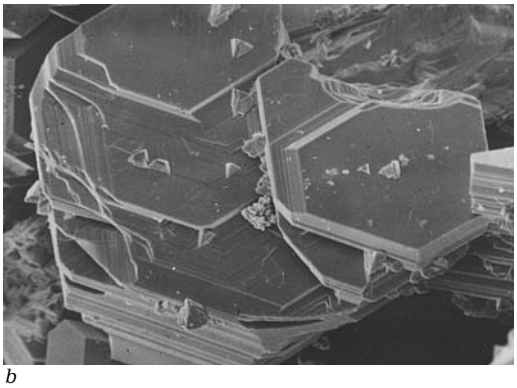
b

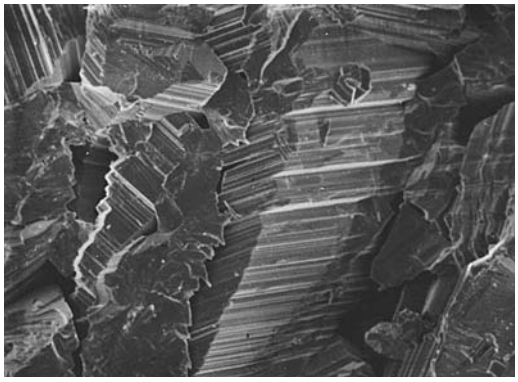
c

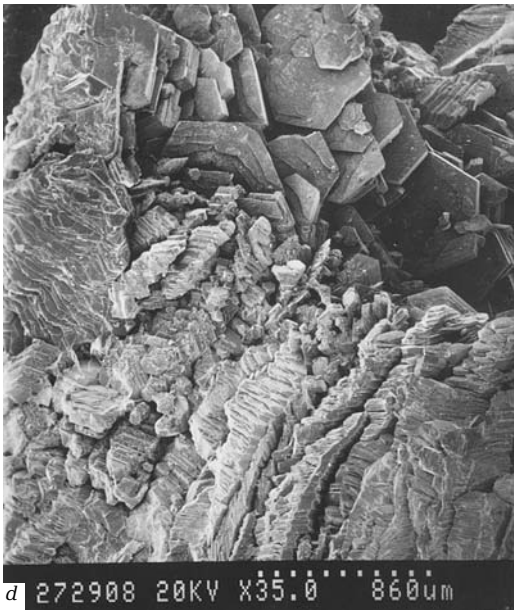

d

FIG . 2. The morphology of ZnS crystals and their aggregates (scanning electron micrographs): a — regular hexagonal prism; b — aggregate of hexagonal platelet ZnS with small chalcopyrite tetrahedrons on their faces; c — columnar cone-shaped aggregates of platelet crystals; d — microdruses of hexagonal platelet ZnS on its columnar aggregates

Table 2. X-ray data of zinc sulfides from Manus in comparison with standard data of wurtzite (JCPDS 36-1450) and sphalerite (JCPDS 5-566)

		wurtzite JCPDS 36-1450			*sphalerite JCPDS 5-566*		
I	*d*	*I*	*d*	*(hkl)*	*I*	*d*	*(hkl)*
5	3,311	100	3,310	100			
10	3,131	84	3,129	002	100	3,123	111
4	2,934	87	2,926	101			
2	2,707				10	2,705	200
1	2,276	28	2,2734	102			
10	1,914	81	1,9103	110	51	1,912	220
1	1,766	54	1,7642	103			
2	1,657	11	1,6543	200			
10	1,633	47	1,6303	112	30	1,633	311
1	1,603	12	1,5994	201			
1	1,566	2	1,5641	004	2	1,561	222
1	1,251	6	1,2506	210			
1	1,240				9	1,240	331
1	1,229	9	1,2264	211			
1	1,213	2	1,2103	114	2	1,209	420

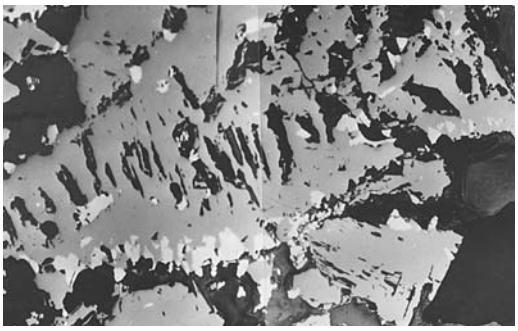

FIG . 3. Cone-shaped columnar ZnS aggregates in polished sections under the microscope in reflected light; the lamellar structure of the aggregate is emphasized by cross dark strips of polish defects (white grains — chalcopyrite, black, at the left — the channel)

viously, two of them were investigated by a single crystal method of, other three, representing different zones — by a method of electron microscopy (Table 1). The results show that the basic isomorphic admixture in all investigated samples is iron, which contents vary between 3.75 and 5.42 mass.% corresponding to 6.6 – 9.6 mol.% FeS. This is much below values of similar ZnS grains from black smokers in East Pacific Rise — 20.1 mol.% FeS (Rö sch, Marching, 1991) and 21.4 – 32.8 mol.% FeS (Oudin, 1983). Variations of iron content within separate crystals and grains do not exceed 1 mass.%.

As seen from Table 1, ten from twelve calculated formulas show insignificant deviations from the stoichiometry — from 0.5 to 2 at. % for S, which agrees with known data on insignificant non-stoichiometry of ZnS (its total volume is about 1 at. %) (Scott, 1968; Scott, Barnes, 1972). In most cases (8 of 10) these deviations in our analyses are directed towards decrease of sulfur. Only two analyses of the darkest granular aggregates from the base of microdruses are characterized by some surplus of this element.

Total amount of other admixtures (Mn, Cu, Ag, Cd) is below 0.5 mass. %. The copper content in part is probably defined by pollution with chalcopyrite, especially in samples III and V, where especially abundant fine inclusions of this mineral are observed under ore microscope.

X-ray powder diffraction

X-ray diffraction pattern received in Guinier camera has shown clear reflections, which can be attributed to two ZnS isomorphs — 3C

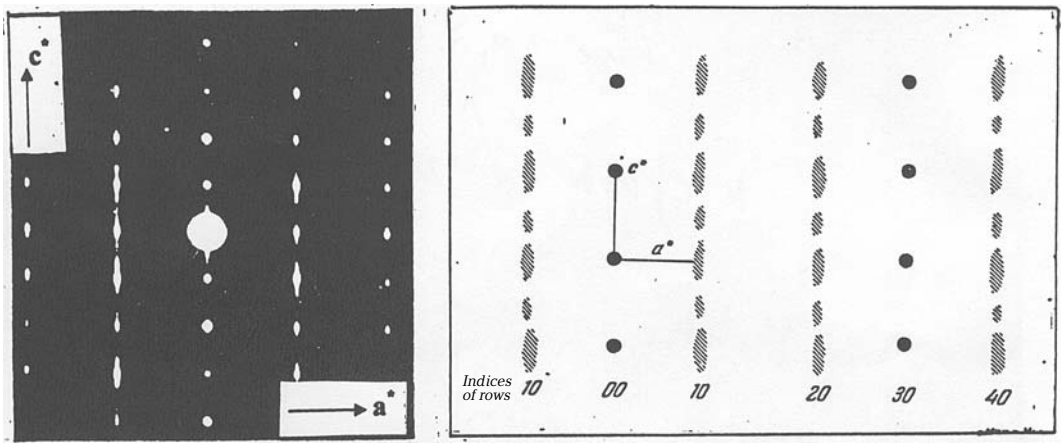

a *b*

FIG. 4. Microdiffraction pattern (or SAED-selected area electro diffraction) from ZnS microcrystal along [010] and its interpretation: a — representative SAED ZnS pattern containing reflections from wurtzite and sphalerite; b — reciprocal lattice diagram of disorder ZnS-microcrystal according to A.Guinier (Guinier, 1961, page 463)

and 2H. Calculations of powder diffraction patterns of investigated samples are given in comparison to standards for wurtzite and sphalerite (Table 2). Most of lines overlap and cannot be used for diagnostic of polytype. At the same time, as seen from the table, the experimental roentgenogram shows two reflections (d = 3.311 and d = 2.934) close to intensive reflexes of wurtzite (d = 3.310 and d = 2.926) and a pair of lines (d = 2.707 and d = 1.240) characteristic of sphalerite (d = 2.705 and d = 1.240). This data indicate the presence of both polymorphs in investigated grains. Distribution of intensities in experimental data cannot be explained by a mechanical mixture of two phases as the intensities of corresponding lines do not correspond to the sum of intensities of two polymorphs.

Diffraction from single crystals

Fig. 4a shows microdiffraction results being a typical image of single crystal along [010]. Its comparison with the scheme (Fig. 4b) shows that both wurtzite and sphalerite are present in the volume of microcrystal. Diffused character of reflections on «layer» lines with index h = 1, 2 is an attribute of layer stacking mistakes of closely packed layers of sulfur atoms, and their elongation along axis c^*, including zero unit — an attribute of small thickness of alternating layers.

The x-ray data received in the Weissenberg camera (Fig. 5) shows zero scan *(h0l)* of one of chips representing the same plane of reciprocal lattice containing diffusion rods at the same h values as in the microdiffraction image (see Fig. 4).

High–resolution electronic microscopy

In images received by methods of high-resolution electronic microscopy (Fig. 6a-c) numerous mistakes of overlapping of closely packed ZnS layers are distinctly visible. At preparing specimens, the material is broken up in a water suspension by ultrasound along planes (100) and this gives a possibility to observe features of stacking disorder and their alternation along axis [001] in wurtzite. It relieves of necessity to prepare a specimen of certain orientation and thickness. In all images, the alternation of sphalerite and wurtzite fields as well as their mixed overlapping are shown. So, in Fig. 6a, plots of cubic stacking with thickness of about 50Å prevail, in Fig. 6b, hexagonal stacking prevails. The image 6c contains a plot of a crystal with the greatest concentration

FIG. 5. Single crystal XRD ZnS pattern (h0l) obtained in Weissenberg camera. Curved lines with 10l and 20l indexes contain diffusion rods in reciprocal space. It is a result of the staking faults

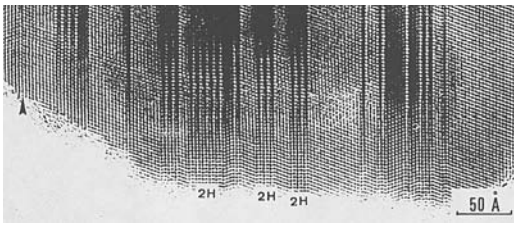

a

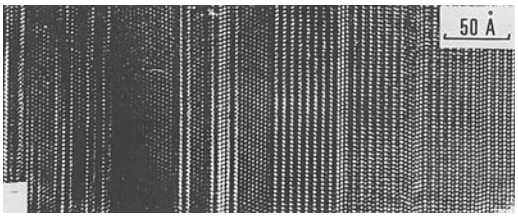

b

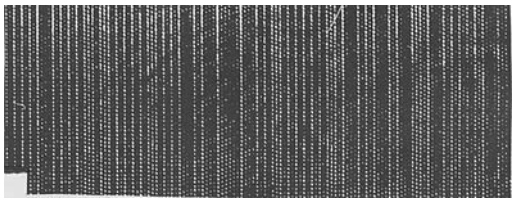

c

FIG . 6. HRTEM-image of some investigated microcrystals. Vertical white point rows are planes of closely packed atoms. Crystal sections with the slope rows are cubic stacking; crystal sections with two layers are hexagonal stacking: a — a part of crystal with dominant cubic stacking (wurtzite 2H stacking is indicated); b — a part of crystal with dominant hexagonal stacking; c — a part of crystal with mixture stacking (it is in this range of defect concentration that the calculation has been conducted)

of stacking disorder.

Interpretation of diffraction features and HRTEM–images

V.A. Drits with co-authors (1994, 1995, 2003) showed that the consecutive alternation of closely packed layers of zinc sulfides is subject to Markovian statistics, which supposes dependence of overlapping style of each subsequent layer on the arrangement of the previous layers, which results in some ordering. It means a possibility of diffraction from a substance, which can be considered, in condition of disorder presence, as intermediate between crystalline and amorphous. The method of calculation of similar layered materials was repeatedly described (Drits, Tshoubar, 1991, etc.).

For this object, the calculation was conducted under earlier described programs (Sakharov at al., 1982). As the use of HRTEM-images made it possible to calculate how many previous layers influence the position of the subsequent one, the value of short-range order factor equal to 2 was used in calculation (its value is usually determined by searching till reception of the best agreement with the experiment).

From a high volume of investigated material representing assemblage of described above crystals, a diffraction pattern has been received. Theoretical calculation of intensities pattern lines in the field of angles 2θ with maximum intensities of reflections for each of three phases — wurtzite, sphalerite and mixed phase — was conducted. Comparison of experiment with theoretical mixtures with various quantitative ratios of components has allowed to establish that the ratio of 14:17:69 best corresponds to the experiment. The sequence of figures corresponds to sphalerite, wurtzite and defective ZnS indicating a prevalence of the most unorganized material in the sample.

Discussion

Wurtzite is traditionally considered a high-temperature polymorphic modification of ZnS. According to D.Vaughan and J. Craig (1980), the stability field of wurtzite is above 1020° C. At the same time, on an example of wurtzite and other minerals, it has been convincingly shown, that «there are forcing factors due to which high-temperature forms are not only formed outside of stability fields, but also are preserved in a metastable state or a state of compelled equilibrium for a long time» (Urusov *et al.,* 1997, p. 57). One of essential factors of the compelled equilibrium is the phase dimensional effect representing «change of physical and chemical transformation parameters under effect of sizes of phases or other parameter related to the size, which is considered independent» (ibid., page 58). The action mechanism of this factor also was repeatedly illustrated on an example of zinc sulfides (Tauson, Chernyshev, 1981; Tauson, Abramovich, 1982, Urusov *et al.*, 1997, etc.). In addition, intergrain and interblock borders, structure defects, stabilizing action of admixtures, effect of sulfur activity, high hydrostatic pressure detaining increase of the surface of mineral phases, and other were registered as forcing factors. This concept helps to understand appearance of hexagonal and rhombohedral polytypes of ZnS in rather low-temperature deposits on continents (Vergilov *et al.*, 1992; Минеva-Stefanova, 1993, etc.) and a wide distribution of wurtzite in ocean hydrothermal ores, which temperature of formation does not exceed 400° C (Krasnov at al., 1992).

The study has shown that crystals of zinc sulfides from the Manus basin, despite of hexagonal shape, are represented by coexisting at nanolevel three polymorphs of zinc sulfides: finely intergrowing polytypes 3C and 2H and partly ordered defective phase. Considering mentioned above conditions of black smoker formation, the mechanism of formation of «mixed» structural states of zinc sulfides could be interpreted from the concept of compelled equilibrum (Urusov *et al.*, 1997). Crystals 2H occur first, as most themodynamically stable in microparticles (the forcing factor is a «developed surface of phases», Tauson, Abramovich, 1982). With growth of crystals, when they get out of dimensional interval of the phase dimensional effect influence, structural transformations into more stable in new conditions phase 3C begins. However, impact of other forcing factors (internal factors — structural admixtures and disorder — and external — high hydrostatic pressure and decrease of sulfur concentration with evolution of process) creates a new condition of compelled equilibrium, at which the formed mixed structures are preserved and true equilibrium with complete transformation of crystal structure into sphalerite is not reached.

According to V.L. Tauson and L.V. Chernyshev (1981), finely dispersed heterogeneous systems are favorable for microblock growth of crystals, when a crystal grows due to accretion of not separate atoms, but their blocks. As plumes-smokes of smokers belong to such systems, it is possible to assume that the lamellar

structure of hexagonal prisms described above can be explained by such a mechanism of growth.

Detected in the investigated samples of zinc sulfides insignificant deviations of Me/S ratio from ideal value agrees with the idea of non-stoichiometry of this compound (Scott, 1968; Scott, Barnes, 1972). The data indicated in quoted works characterize wurtzite by some deficit of sulfur and respectively surplus of zinc, and sphalerite has opposite ratio of these elements. This allows to assume that variations of this ratio in Manus samples reflect variability of quantitative ratio of three various polymorphs of zinc sulfides, established within different investigated hexagonal ZnS crystals. It is necessary to note that, as all three polymorphs meet within one «monocrystal», the form of crystals in this case cannot be a sufficient diagnostic attribute for wurtzite and sphalerite. As noted above, at optical studies in polished sections under ore microscope this nanoheterogeneity is also not manifested. E. Oudin (1983) is probably right, describing morphologically similar crystals in ocean ores 21° N under the generic name «zinc sulfide».

Authors are grateful to A.P. Lisitsyn and Yu.A. Bogdanov for assistance in getting samples for studies, T.I. Golovanova for realization of X-ray microanalysis and A.V. Efimov for the help in preparation of polished sections. N.N. Mozgova and N.I. Organova are grateful to the Royal Swedish Academy of Sciences for financing of short-term visit to the Arrenius Laboratory for realization of scientific studies.

This work was carried out at financial support of the Russian Basic Researches Fund (Grant 01-05-64679) and the Ministry of Industry, Science and Technology of the Russian Federation (Project 3.2.2. of Federal Program «World Ocean»).

References

Akizuki V. Investigation of phase transition of natural ZnS minerals by high resolution electron microscopy // Amer. Miner. **1981.** V. 66. P. 1006–1012

Anthony J.W., Bideaux R.A., Bladh K.W., Nichols M.C. Handbook of mineralogy. I. Elements, sulfides, sulfosalts. Mineral Data Publishing. Tuscon, Arisona. **1990**. 588 c.

Blackburn W.H., Dennen W.H, Russell P.I. Encyclopedia of Mineral Names. The Canadian Mineralogist. Special Publication. 1997. 360 p.

Bogdanov Yu.A. and Sagalevich A.M. Geologicheskie issledovaniya s glubokovodnykh obitaemykh apparatov «Mir» (Geological studies from deep-water habitable apparatuses «Mir». M.: Nauchny Mir. 2002. 270 p. (Rus.)

Drits V.A., Sakharov B.A., Organova N.I., Salyn A.L. Stacking faults distribution in ZnS crystals HRTEM images analysis and simulation of diffraction effects // Coll. Abstracts Powder Diffraction Int. Conf. St. Peterbourg. **1994.**

Drits V.A., Sakharov B.A., and Organova N.I. Raspredelenie defektov upakovki v kristallakh sul'fida tsinka: analiz izobrazhenii, poluchennykh s pomoshch'yu vysoko-razreshayushchei elektronnoi mikroskopii, v svete statistiki Markova (Distribution of stacking disorder in crystals of zinc sulfides: analysis of images received using high-resolution electronic microscopy, in light of Markovian statistics // Krystallographia. **1995**. V. 40. № 4. P. 721–728. (Rus.)

Drits V.A., Tshoubar C. X-ray diffraction by disorder lamellar structures: theory and application**.** Springer. Berlin Heidelberg New York. **1991.**

Fleet M.T. Structural transformations in natural ZnS // Amer. Miner. **1977.** V. 62. P. 540–546

Fleet M.T. Wurzite: long-period polytypes in disordered 2H crystals // Science. **1975.** V. 190. P. 885–886

Guinier A. Rentgenografija kristallov (X-ray study of crystals). **1961.** M.: GIZ Fiz. mat. lit. 604 p. (Rus.)

Krasnov S.G., Cherkashev G.A., Ainemer A.I. et al. Gidrotermal'nye sul'fidnye rudy i metallonosnye osadki okeana (Hydrothermal sulfide ores and metal-bearing oceanic sediments). SPb: Nedra. **1992**. 277 p. (Rus.)

Lisitsyn A.P., Kruk K., Bogdanov Yu.A., Zonnenshajn L.P., Muraviev K.G., Tufar V., Gurvich E.G., Gordeev V.V., and Ivanov G.V. Gidrotermal'noe pole riftovoi zony basseina Manus (Hydrothermal field of the rift zone of the Manus basin) // Izv. RAS. Geol. Series **1992.** №10. P. 34–55 (Rus.)

Mardix S. Crystallographic aspects of polytypism in ZnS // Bulletin de Mineralogie. **1986**. V. 109. P. 131–142

Minceva-Stefanova J. A morphological SEM study of wurtzite-sphalerite relationships in specimens from Zvezdel, Bulgaria // Mineralogy and Petrology. **1993.** V. 49. P. 119–126

Minerals. Handbook. V. I. M.: Academy of Sciences of the USSR. **1960**. 616 p. (Rus.)

Mizera E., Sundberg M. Stacking faults in ZnS crystals — X-ray and HREM investigations // International Conference on Polytypes and Modulated Structures. Wroclaw, Pol-

and, 11—14 August **1986**

Mozgova N.N. — Mineralogy of hydrothermal sulfides ores on the modern seafloor and in the areas of active volcanism on land — features of similarity and distinction // 18th IMA General meeting «Mineralogy for the New Millennium». 1-6 September **2002.** Edinburg, Scotland. Programm with Abstracts. P. 278

Mozgova N.N. Mineralogicheskie osobennosti sovremennykh gidrotermal'nykh rud na dne Okeana (Mineralogical features of modern hydrothermal ores at the Ocean floor)// Abstracts of the XIV International Scientific School on Marine Geology. M. GEOS. **2001.** P. 251—252 (Rus.)

Mozgova N.N. Tipomorfizm mineralov v okeanskikh sul'fidnykh rudakh (Typomorfism of minerals in ocean sulfides ores) // Abstracts of the IX Congress of Mineralogical Society at the Russian Academy of Sciences, devoted to 275 anniversary of the Russian Academy of Sciences. Saint Petersburg, May 17-21 **1999.** p. 93—94 (Rus.)

Mozgova N.N. Znachenie issledovanii sovremennogo gidrotermal'nogo rudoobrazovaniya na dne okeana dlya mineralogii (Importance of studies of modern hydrothermal ore formation at the ocean floor for mineralogy) // Proceedings of the All-Russia Scientific Conference «Geology, Geochemistry, Geophysics on the Boundary of XX and XXI Centuries», to the 10th anniversary of the Russian Basic Researches Fund. Volume 2. «Petrology, Geochemistry, Mineralogy, and Geology of Mineral Deposits; Environmental Geology».-Moscow. OJSC «COMMUNICATION PRINT». **2002.** P. 298—299 (Rus.)

Oudin E. Hydrothermal sulfides deposits of the East Pacific Rise (21°N.) Part I: Descriptive mineralogy // Marine Mining. **1983.** V. 4. P. 39—72

Pósfai M., Dódony I., Soós M. Stacking disorder in the ZnS from Gyöngyösoroszi, Hungary // Neues Jahrbuch für Mineralogy. Monatshefte. **1988.** H. 10. S. 438—445

Qin L.C., Li D.X., Kuo K.H. An HREM study of the defects in ZnS // Philosophical Magazine. **1986.** A 53. P. 543—555

Rösch H., Marchig V. An unusual occurence of wurtzite in massive sulfides vents from the East Pacific Rise // Geologische Jahrbuch. **1991.** A 127. S. 589—592

Sakharov B.A., Naumov A.S., and Drits V.A. Rentgenovskie intensivnosti, rasseyannye sloevymi strukturami s parametrami blizhnego poryadka S≥1, Q≥1 (X-ray intensities dissipated by layer structures with proximal order parameters S≥1, Q≥1) // Dokl. AS USSR. **1982**. V 265. p. 871—874 (Rus.)

Scott S.D. Stoichiometry and phase changes in zinc sulfides. Ph. D. Thesis, Pennsylvania State University, State College, Pennsylvania. **1968**

Scott S.D., Barnes H.L. Sphalerite-wurtzite equilibria and stoichiometry // Geochemica et Cosmochimica Acta. **1972.** V. 36. P. 1275—1295

Strock L.W., Brophy V.A. Synthetic zinc sulfides polytype crystals // Amer. Miner. **1995.** V. 40. P. 94—106

Tauson V.L. and Abramovich M.G O polimorfizme sul'fidov tsinka i kadmiya i fazovom razmernom effekte (About polymorphism of zinc and cadmium sulfides and phase dimensional effect // Miner. zhurn., **1982.** V 4. №3. P. 35—43 (Rus.)

Tauson V.L. and Chernyshev L. V. Eksperimentalnye issledovaniya po kristallokhimii i geokhimii sul'fida tsinka (Experimental studies of crystal chemistry and geochemistry of zinc sulfides). Novosibirsk: «Nauka», Siberian branch. 1981. 190 p. (Rus.)

Urusov V.S., Tauson V.L., and Akimov V.V. Geokhimiya tverdogo tela (Geochemistry of solid). M.: GEOS. 1997. 500 p. (Rus.)

Vergilov Z.V., Dodon' I., Petrov S.L., and Breskovska V.V. Strukturni izsledovaniya na radialno-lchest ZnS ot Madzharovo (Structural studies of radial ZnS from Madjarovo) // Godishnik na Sofiiskiya universitet «Sv. Kliment Okhridski». Geologo-geografski fakultet. **1992.** Book 1 — Geology. T. 82.

UDC 549.332:553.2 (261.03)

TETRAGONAL Cu_2S IN RECENT HYDROTHERMAL ORES OF RAINBOW (MID ATLANTIC RIDGE, 36˚ 14'N)

Irina F. Gablina
Institute of Lithosphere of Marginal and Internal Seas of the, RAS, Moscow, gablina@mdmgroup.ru

Yury S. Borodaev
Lomonosov Moscow State University, Moscow

Nadezhda N. Mozgova
Institute of Geology of Ore Deposits, Petrography, Mineralogy and Geochemistry, RAS, Moscow

Yu. A. Bogdanov
Shirshov Institute of Oceanology of the Russian Academy of Science, Moscow

Oksana Yu. Kuznetzova
Institute of Geology of Ore Deposits, Petrography, Mineralogy and Geochemistry, RAS, Moscow

Viktor I. Starostin,
Lomonosov Moscow State University, Moscow

Farajalla F. Fardust
Lomonosov Moscow State University, Moscow

The ores samples were investigated taken from active chimneys of the Rainbow hydrothermal field (MAR, 36° 14′ N) at a depth of 2,276 m in Cruise R/V 47 of research vessel «Academician Mstislav Keldysh» (2002). Optical, microprobe and X-ray analytical methods were used. The basic method of mineral identification was X-ray analysis (Debye powder photomethod). Samples were fragments of small hydrothermal chimneys having a zonal structure: in direction from the channel to the external wall, isocubanite zone («phase Y») is replaced by chalcopyrite zone, then follows bornite zone, which to the periphery gradually passes into a copper sulfide zone. For the first time the tetragonal form of Cu_2S — metastable isomorph of chalcocite, which stability is limited by the field of high pressure (above 0.8 kilobar) and temperature (above 102° C) − was discovered in modern ocean ore. Tetragonal Cu_2S was identified in one sample in a mixture with chalcocite and djurleite, in the other — in a mixture with bornite. The parameters of its lattice cell designed from an X-ray powder pattern are: a = 4.0042Å, c = 11.3475 Å, V = 181.938 Å^3, average composition of 4 measurements is $Cu_{2.02}S$. The find of high-temperature tetragonal isomprph of chalcocite in modern deep-water active smokers seems natural. Formation of Rainbow sulfide ore occurs under the pressure of water column more than 2000 m and at temperature of 250−362°C. Tetragonal chalcocite is not met in earlier investigated by us inactive (relict) constructions of more ancient Logachev field. After the extinction of hydrothermal activity Cu_2S soon passes into non-stoichiometric sulfide minerals more stable in sea-water ambient.

Until recently, only three minerals were known in the system Cu-S: chalcocite, digenite and covellite. The studies of fiftieth-eightieth years of the last century (Djurle, 1958; Roseboom, 1962,1966; Morimoto *et al.*, 1969; Skinner, 1970; Goble, 1980; Goble, Robinson, 1980; Mumme *et al.*, 1988, etc.) have shown that quite often under these names other minerals are interpreted, close to them by composition, structure and ranges of stability. Now, ten natural compounds of the system Cu-S and two synthetic phases, unstable at usual temperature (hexagonal chalcocite and cubic digenite) are known. Non-stoichiometric minerals — ratio Cu/S in them varies from 1 to 2 — predominate among copper sulfides (Table 1). The big variety of non-stoichiometric minerals in the system Cu-S is conditioned by the fact that even insignificant deviation of copper sulfide structure from stoichiometry is accompanied by structural reorganization of their crystal lattice, i.e. formation of a new mineral individual. The deviation from stoichiometry is conditioned by partial entry of bivalent (oxidized) copper into the crystal lattice of minerals (Belov, 1953; Eliseev *et al.*, 1964; Goble, 1985), which is usually related to oxygen presence in the mineral-forming system. N.V. Belov considered the digenite formula as $Cu^+_{1.6}Cu^{2+}_{0.2}S$. By analogy to this, E.N. Eliseev et al, (1964) have proposed for non-stoichiometric copper sulfide the general formula: $Cu^+_{2-y}Cu^{2+}_{0.5y}S$, in which the content of bivalent copper grows proportionally to the number of defects in the sulfide structure. As a result, in the presence of oxygen, Cu/S ratio changes, though the sum of valencies of cations and anions is preserved in the structure. Later this assumption has been confirmed by studies of lattice cell sizes and character of electron bonds by the method of monocrystal survey (Goble, 1985). R.Goble in quoted work has shown that the content of bivalent copper in sulfide increases with decrease of Cu/S ratio. Stability of the majority of non-stoichiometric sulfides is rather limited and phase transformations are frequently irreversible. These features, as well as ability of non-stoichiometric copper sulfides to fast phase transformations at insignificant oscillations of physical or chemical parameters of environment, allow to use them as indicators of mineralogenesis conditions and subsequent transformations under the

Table 1. Structure, composition, limits of stability temperature of minerals of the system Cu-S (Djurle, 1958; Roseboom, 1966; Morimoto, Koto, 1969; Skinner, 1970; Potter, Evans, 1976; Potter, 1977; Grace, Cohen, 1979; Goble, 1980; Goble, Robinson, 1980; Mumme et al., 1988, etc.)

Mineral	*Composition*	*System*	*Symmetry of sulfur sublattice*	*Stability limits ˚C*	*Phase transformation product*
Chalcocite (high)	$Cu_{2.00}S$	Hexagonal	HSCP	102±2 — 452±3	Digenite (high)
Chalcocite (low)	$Cu_{1.993\text{-}2.001}S$	Monoclinic	HSCP	< 0 — 102±2	Chalcocite (high
Tetragonal $Cu_{2-x}S$	$Cu_{1.96\text{-}2.00}S$	Tetragonal	CFC	102 — 340*	Chalcocite (high
(x = 0-0.04)				340 — 500(?)**	Digenite (high)
Djurleite	$Cu_{1.93\text{-}1.96}S$	Monoclinic	HSCP	< 0 — 93±2	Chalcocite + Digenite
Roxsbyite	$Cu_{1.72\text{-}1.82}S$	Monoclinic	HSCP	< 0 — 65-70	Digenite (low)
Digenite (high)	Cu_2S	Cubic	CFC	>1000	Melt
Digenite (low)	$Cu_{1.75\text{-}1.78}S$	Rhombic	CFC	18 — 76-83	Digenite (high)
Anilite	$Cu_{1.75}S$	Rhombic	CFC	< 0 — 30	Digenite (low)
Geerite	$Cu_{1.5\text{-}1.6}S$	Rhombic (pseudocubic)	CVC	n.d.	n.d.
Spionkopite	$Cu_{1.4}S$	Hexagonal	HSCP	< 0 — 157	Covellite
Yarrowite	$Cu_{1.1}S$	Hexagonal	HSCP	< 0 — 157	Covellite
Covellite	CuS	Hexagonal	HSCP	< 0 — 507	Digenite (high)

Notes:
CFC — cubic face-centered, CVC — cubic volume-centered, HSCP — hexagonal supercompact packing.
* — at pressure > 1 kilobar., ** — at pressure > 9 kilobar. (Grace, Cohen, 1979), the rest — at 1 bar, n.d. — not determed.

impact of endogenous and exogenous factors (Gablina, 1993, 1997). The nanoscale particles, frequently characteristic of copper sulfide segregations, similarity of structure and optical characteristics, low stability (possibility of phase transformations at storage and preparation of samples) hardly hinder the study of these minerals, require the specific approach and application of a complex of methods. The most informative among them is X-ray analysis.

Tetragonal form of Cu_2S-$Cu_{2-x}S$ — a metastable compound met in natural ores, but not having the status of a mineral — occupies a special place among copper sulfides. In literature it is referred to as «tetragonal phase», «tetragonal form of Cu_2S» or «tetragonal chalcocite». For the first time this compound was received in experiments on a high-temperature synthesis of copper sulfide (Djurle, 1958; Roseboom, 1962; Janosi, 1964). As these studies have shown, the synthetic tetragonal form of chalcocite is a metastable phase originating at polymorphic transition of high-temperature hexagonal chalcocite into cubic modification (at 430−450° C after different authors) or into monoclinic (at 102° C). It was established (Roseboom, 1966) that the tetragonal phase forms a solid solution from Cu_2S to $Cu_{1.96}S$. Synthesized at increased temperatures (above ~100° C), it can be tempered at room temperature, but with time it passes into low-temperature polymorphs — monoclinic chalcocite or djurleite — depending on initial structure. As the experiments have shown, the samples synthesized at most high temperatures (above 350° C) are the most stable at usual conditions. Tetragonal form $Cu_{1.96}S$ in experiments (Roseboom, 1966) was safe even after four years of stay at room temperature. E.Roseboom in the quoted work states the assumption that tetragonal form of $Cu_{1.96}S$ is more stable at usual conditions than tetragonal Cu_2S, which stability is limited to the field of high pressures (more than 0.8 kilobar). In an experimental work (Grace, Cohen, 1979), the field of stability of tetragonal Cu_2S is determined in limits 102−500° C and 1−13.5 kilobar. Researchers consider the limit of the field to a certain measure conditional because of lack of data (Grace, Cohen, 1979). The restriction of tetragonal Cu_2S stability by the field of high pressure is reflected in its density: specific weight of tetragonal Cu_2S, determined by B. Skinner (1970), is 5.932, that is much higher than specific weight of usual (monoclinic) chalcocite (5.783) and djurleite (5.747±0.005). Under optical characteristics, the tetragonal form does not differ from usual chalcocite and is only diagnosed on the basis of X-raying. The roentgenogram of the tetragonal form essentially differs from roentgenograms of monoclinic chalcocite and djurleite (Table 2). The most typical for it are reflections 2.740 and 2.302.

Studies of features of natural distribution of Cu-S system sulfides have shown that non-stoichiometric copper sulfides are typomorphic minerals of exogenous ore — copper sandstones and shales, zones of secondary sulfide enriching and oxidation. The stoichiometric chalcocite is more typical for ores of endogenous origin (Gablina, 1997). Metastable tetragonal form of Cu_2S-$Cu_{2-x}S$ in the nature is registered extremely rarely and usually in high-temperature formations: in sulfide crusts, which have precipitated on well casings from thermal salt brines of Solton Sea (Skinner *et al.*, 1967) and in the exocontact of the magmatogenic deposit of Talnakh (Gablina, 1992).

Table 2. Interplanar distances in tetragonal Cu_2S in polymineral mixtures: with monoclinic chalcocite and djurleite (Test 2); with bornite and admixture of djurleite (Test 5)

Sample 4393-2 (Test 2)		*Djurleite (Roseboom, 1962)*		*Monicline chalcocite (Potter, Evans, 1976)*[2]		*Tetragonal Cu_2S (Janosi, 1964)*			*Sample 4412-6 (Test 5)*		*Bornite (Berry, Thompson,1962)*	
I	*d,Å*	*I*[1]	*d,Å*	*I*	*d,Å*	*I*	*d,Å*	*hkl*	*I*	*d,Å*	*I*	*d,Å*
		1	4.28						15	4.18*		
10	3.81*	1	3.89	25	3.735							
		2	3.752									
		2	3.586	13	3.599							
20	3.41*	5	3.386									
		1	3.35	6	3.336							
				18	3.315							
20	3.29	3	3.282	35	3.276	16	3.27	1 0 2	30	3.27	40	3.31
		3	3.192	18	3.188				40	3.17	60	3.18
		2	3.100	25	3.158							
30	3.03*	3	3.04	13	3.057				30	3.02*	5	3.01
		3	3.01	18	2.952							
				13	2.933							
		2	2.89	6	2.886							
30	2.816*	1	2.82			20	2.827	1 1 0	30	2.819	20	2.80
100	2.751	6	2.785	13	2.765	100	2.740	1 0 3	90	2.753	50	2.74
				9	2.732							
		1/2	2.73	35	2.726							
		1	2.69	18	2.668							
		1	2.654	18	2.620							
		1/2	2.595									
50	2.540*	1	2.557	6	2.562							
				13	2.533							
		1/2	2.514	18	2.527				40	2.510	40	2.50
		1	2.477	18	2.477							
40	2.408**	1/2	2.41	50	2.407							
				70	2.403							
		9	2.387	35	2.399							
90	2.317			25	2.330	80	2.302	1 0 4	70	2.309		
30	2.273	1/2	2.289	13	2.242	30	2.259	1 1 3				
				35	2.210							
		1/2	2.142	6	2.182				20	2.134	20	2.13
		1/2	2.107	9	2.120							
		1	2.069									
		1/2	2.047	6	2.028							
80	2.003**			9	2.012	30	1.998	2 0 0	50	2.004		
				9	1.981							
80	1.972**	9	1.964	70	1.975	30	1.967	2 0 1				
		9	1.957	13	1.952							
				6	1.911				100	1.937	100	1.937
				70	1.881	35	1.883	2 0 2	30	1.886		
				100	1.880							
				9	1.877							
70	1.874*	10	1.871	9	1.875							
				6	1.799							
20	1.773			6	1.788	12	1.764	1 1 5	20	1.764		
60	1.714**	1	1.693	9	1.709	30	1.704	2 1 2	40	1.706		
				13	1.704							
				13	1.687				10	1.664	30	1.652
50	1.616					12	1.614	2 1 3	20	1.613		
50	1.488*	1	1.514			6	1.495	1 0 7	30	1.488*		
40	1.407					30	1.401	2 1 5	20	1.405		
									10	1.368	20	1.370
40	1.331					8	1.330	1 0 8	10	1.327	5b	1.335
10	1.283*	12	1.283									
20	1.264	6	1.26			18	1.260	1 1 8	20	1.262	50b	1.258
20	1.239					12	1.234	3 1 2	20	1.238		
30	1.200					16	1.196	1 0 9	10	1.197	10b	1.198
									20	1.116	50	1.119
30	1.093					18	1.087	3 0 6				

* — djurleite lines or strengthened by it; ** — the same for chalcocite
[1] — in 10-score scale
[2] — the strongest lines (above 5) are shown out of 93 in the quoted work

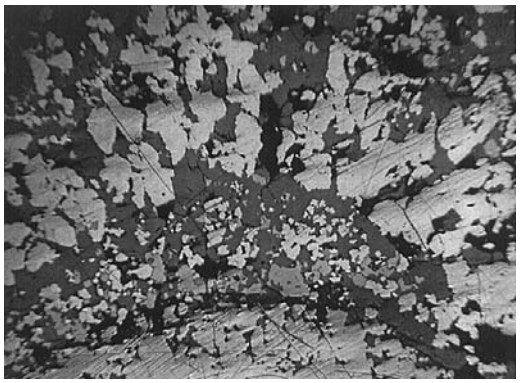

FIG. 1. Copper sulfide (light) in the peripheral zone of active channel wall. Gray — bornite, dark gray — sulfates. Polished section. x90

In a single case, the find of tetragonal $Cu_{1.96}S$ was mentioned in hypergene formations on a wall of adit of the Mina Maria in Chile (Clark, Sillitoe, 1971). Authors of this work do not exclude that their find can appear to be an artifact. However, in experiments on leaching of synthetic chalcocite at usual temperature and pressure, a tetragonal form occurred as a transition to digenite, and then to anilite (Whiteside, Goble, 1986).

Materials and methods of studies

Samples from active chimneys of the Rainbow hydrothermal field (MAR, 36° 14′ N) discovered in 1997, were investigated. Samples were collected in the zone of «smokes» at a depth of 2,276 m with the help of deep-water device «Mir-1» in Cruise VR/V 47 of research vessel «Academician Mstislav Keldysh» in the summer of 2002. The authors have investigated two samples: #4393-2 and #4412-6. Samples were small tubes in diameter to 7 cm, broken off from larger active chimneys or their aggregates. The dimensions of the last change at length from several tens of centimeters to one and a half meters at diameter to 25 cm. Chimneys are covered with a red crust of iron hydroxides and have hollow channels with smooth surfaces.

Optical, microprobe and X-ray methods of analyses were used. Optical studies were conducted on an ore microscope in polished sections, which were produced from cross cuts of chimneys without heating. Chemical compositions of minerals were investigated on the microanalyser «Camebax SX-50» in the Moscow State University (analysis conditions: accelerating potential 20 kV, sound current 10 milliamperes, standards for Fe and S — natural pyrite, for Zn — synthetic ZnSe, for other elements — pure metals), and also in the Moscow State Building University on the microanalyser «Camebax microbeam». Quantitative analysis was conducted with the help of program ZAF-4. Conditions of the analysis: accelerating potential 20 kV, analyzed field 1.5−2 microns, standards for Fe and S — natural pyrite, for other elements — pure metals. Ti, Ni, Ag, Au, Zn, Pb, Sb, As, Bi, Mg, Co, Se, Ce, La were determined in addition to basic elements (Cu, Fe, S). Errors of the analysis (mass %): Cu $\pm$ 0.2-0.6, Fe $\pm$ 0.1-0.2, S +0.15-0.26. Contents of other elements are within the limits of error ($<2\sigma$) and are not cited in the work.

The basic method of mineral identification was X-ray analysis (Debye powder photomethod) for which microsamples were selected under the microscope mainly from the sites investigated by the microprobe. Conditions of the analysis: chamber RKD-57.3 in the unfiltered Fe-radiation, time of exposition — 6 h. Intensity was determined visually by a 100-score scale. Analyses were made in X-ray laboratory of IGEM of the Russian Academy of Sciences.

Received Results

Two samples were investigated. One of them — a fragment of a tube, elliptic in cross-section, 65 x 35mm with wall thickness of 10 mm; another one — a part of a three-channel tube with the cross-section of 35 x 35 mm and height of 80 mm, diameter of channels from 0.5 mm to 18 mm. Tubes have a zonal structure: in the direction from the channel to the external wall isocubanite zone («phase Y») is replaced by chalcopyrite, followed by bornite zone, which to the periphery gradually passes into the zone of copper sulfides (Borodaev *et al.*, in print). In the reflected light, the zone of copper sulfides includes two non-continuous subzones of irregular width (in bulges to 1.5-2 mm): bluish-gray, adjoining to the bornite zone, and more light, gray peripheral subzone.

The first subzone is composed of mixtures of copper sulfides with bornite, which probably represents the chilled high-temperature solid solutions of chalcocite−bornite series and/or products of their disintegration. In the direction to the bornite zone, blue color of mixture very gradually passes in pink. Sometimes fine sliced structures of solid solution disintegration appear in the transition area to the bornite zone, visible in reflected light at magnification x210. However, in the direction from periphery to the centre, the blue matrix with pink lamellaes is very gradually replaced with pink matrix with blue lamellaes.

In the second subzone, sulfides of chalcocite−digenite series predominate, on periphery usually submerged in anhydrite «cement» (Fig. 1). They are mainly presented by monoclinic chalcocite or its fine mixture with tetragonal phase of Cu_2S. Sometimes non-stoichiometric minerals — djurleite and digenite (diagnosed conditionally) — occur on the periphery of chalcocite zone, forming polymineral mixtures with monoclinic

Table 3. Composition of minerals in the mixture of tetragonal phase, monoclinic chalcocite and djurleite from Rainbow active chimneys

Sample (X-ray analysis test)	*Analysis*	*Cu*	*Fe*	*S*	*Total*	*Formula*	*Minerals (according to X-ray analysis, data, see Table 2))*
4393-2(Test 2)	*15*	*79.642*	*0.158*	*19.393*	*99.193*	*$Cu_{2.07}S$*	*Monoclinic chalcocite andetragonal phase*
4393-2(Test 2)	17	79.464	0.437	19.739	99.640	$Cu_{2.03}S$	*Monoclinic chalcocite and tetragonal phase*
4393-2(Test 2)	18	79.556	0.083	20.018	99.657	Cu_2S	*Monoclinic chalcocite and tetragonal phase*
4393-2(Test 2)	19	78.411	0.201	19.818	98.430	Cu_2S	*Monoclinic chalcocite and tetragonal phase*
Average of 4		79.268	0.220	19.742	99.230	$Cu_{2.02}S$	*Monoclinic chalcocite and tetragonal phase*
4393-2	33*	77.749	0.054	21.114	98.917	$Cu_{1.86}S$	Digenite (?)
44393-2(Test 2)	20	78.154	0.413	20.101	98.668	$Cu_{1.96}$ S	Djurleite
4393-2(Test 2)	34*	79.547	0.083	20.621	100.251	$Cu_{1.96}S$	Djurleite
4393-2(Test 2)	35*	78.599	0.106	20.552	99.257	$Cu_{1.93}$ S	Djurleite
Average of 3		78.512	0.164	20.597	99.273	$Cu_{1.95}$ S	Djurleite
Theoretical composition of chalcocite			79.86	-	20.14		Cu_2S
Composition of djurleite (Roseboom 1966)			79.53	-	20.47		$Cu_{1.96}S$

* — analyses made by the Moscow State University, the others — by the Moscow State Building University

chalcocite and/or tetragonal Cu_2S. In rare cases, spionkopite and yarrowite replacing listed above copper sulfides are registered.

Tetragonal Cu_2S is interpreted in roentgenograms in both investigated samples: in one of them (sample 4393-2, test 2) — in a mixture with chalcocite and djurleite, in the other (sample 4412-6, test 5) — in a mixture with bornite (Table 2).

Test 2 for X-raying was selected from the most homogeneous massive part of the copper sulfide zone. Optical characteristics of the analyzed copper sulfide in reflected light (gray color, weak anisotropy) are identical to usual chalcocite, it has xenomorphic-granular structure with the size of separate grains 0.01 to 0.2 mm, rarely larger. Its average composition (from 4 measurements) is $Cu_{2.02}S$ (Table 3). In some sites, in the light microscope at magnification x210, the irregular sliced structure is observed (bluish-gray lamellaes in gray matrix). In the electronic microscope, the difference between these phases is not fixed because of structural similarity. The data of X-raying of test 2 indicated in Table 2 allow to interpret them as a mixture of three minerals: usual (monoclinic) chalcocite, its tetragonal form and djurleite. Judging by maximum intensity of the basic peaks of tetragonal form of Cu_2S in the roentgenogram, it predominates in the mixture. Parameters of lattice cell of this phase, designed from the X-ray powder pattern of test 2 are: a = 4.0042 Å, c = 11.3475 Å, V = 181.938 $Å^3$, they are close to those published for tetragonal $Cu_{1.96}S$: a = 4.008 Å, c = 11.268 Å (Djurle, 1958). Bluish-gray plates in inhomogenous sites are probably represented by djurleite, which presence is confirmed by the data of X-ray and microprobe studies. The average composition of djurleite (3 measurements) corresponds to formula $Cu_{1.95}S$ (Table 3).

Test 5 was taken from the peripheral zone of sample 4412-6, being a thin mixture of copper sulfides and bornite. At usual magnifications in reflected light it has grayish-blue color and looks homogeneous, only local indistinct plots of more intensive bluish-gray color can be noted. In the immersion at magnification x950, a very fine structure of breakup of the mixture is observed: brownish laths to 20 microns thick (bornite) are submerged in a bluish matrix (copper sulfide). The matrix has emulsion-sliced structure of the second order disintegration: it consist of very thin emulsion and bluish-gray laths with higher reflection. Laths are basically thin and short, but separate laths are to 40 microns long. To the periphery, the number and size of bornite laths gradually decreases to complete disappearance. The brownish phase is present at separate sites as thin emulsion.

Under the electronic microscope, the disintegration structure is not fixed. Etching with HNO_3 reveals xenomorphic-granular structure of the mixture with grains 0.05 to 0.25 mm. Grains increase and acquire subradial orientation in the direction from periphery, rich in copper sulfides, to the contact with the chalcopyrite zone. Each grain is usually characterized by fine mosaic fissuring and consists of allotriomorphic aggregate of more fine (0.01-0.03 mm) polygonal isometric grains. Grain borders cross plates of disintegration. The described structures can result from crystallization of solid solution originally segregated as a colloid. The breakup of solid solution probably preceded the crystallization of colloid.

The X-raying identified bornite and tetragonal form of chalcocite approximately in equal ratio in the mixture by intensity of the basic lines (Table 2).

Table 4. Chemical compositions of mixture of copper sulfides and bornite from active chimneys of the Rainbow (sample #4412-6, test #5)

№ analysis	Cu	Fe	S	Sum	Formula	Minerals	Chalcocite/ bornite (n_oS)
1	72.682	4.346	21.491	98.519	$Cu_5FeS_4 + Cu_{2.10}$	Mixture bornite with tetragonal phase of Cu_2S	0.867
2	73.242	3.882	20.617	97.741	$Cu_5FeS_4 + Cu_{2.21}S$	Mixture bornite with tetragonal phase of Cu_2S	0.768
4	72.012	4.564	21.254	97.830	$Cu_5FeS_4 + Cu_{2.20}S$	Mixture bornite with tetragonal phase of Cu_2S	0.973
5	73.012	3.430	21.232	97.674	$Cu_5FeS_4 + Cu_{2.02}S$	Mixture bornite with tetragonal phase of Cu_2S	0.592
6	70.032	6.275	22.078	98.385	$Cu_5FeS_4 + Cu_{2.26}S$	Mixture bornite with tetragonal phase of Cu_2S	1.879
7	68.811	7.737	22.998	99.546	$Cu_5FeS_4 + Cu_{2.39}S$	Mixture bornite with tetragonal phase of Cu_2S	3.397
11	71.025	5.440	21.776	98.242	$Cu_5FeS_4 + Cu_{2.18}S$	Mixture bornite with tetragonal phase of Cu_2S	1.345
12	70.346	5.455	22.413	98.214	$Cu_5FeS_4 + Cu_{2.01}S$	Mixture bornite with tetragonal phase of Cu_2S	1.267
13	69.168	6.722	22.853	98.743	$Cu_5FeS_4 + Cu_{2.10}S$	Mixture bornite with tetragonal phase of Cu_2S	2.080
14	69.333	6.309	23.218	98.860	$Cu_5FeS_4 + Cu_{1.93}S$	Mixture bornite with djurleite (?)	1.659

Analyses made by the Moscow State Building University

Several additional reflections allow to assume the presence of djurleite admixture. The composition of two major phases of the mixture (9 measurements) was designed on the basis of stoichiometric formula of bornite, though usually the composition of bornite in association with chalcocite differs from the stoichiometry towards enrichment in copper and impoverishment in sulfur. This probably explains the overestimation in some cases of the copper content in the structure of tetragonal chalcocite (Table 4).

Quantitative relations of copper sulfides and bornite in the mixtures, designed by sulfur, oscillate in a wide range: from 0.592 to 3.397 (Table 4). It is known that copper sulfides of chalcocite—digenite series easily form solid solutions with bornite. Already at temperature above 65° C, synthetic bornite and digenite form limited solid solutions and above 330° C — unlimited solid solutions, which at fast cooling can be chilled and exist in a metastable state (Kullerud, 1959). No doubt that the investigated mixtures represent the initial products of breakup of chalcocite—bornite solid solutions and wide oscillations of quantitative ratios of coexisting phases can indicate high temperatures of their formation.

Discussion

Thus, the metastable tetragonal form of chalcocite, which is stabile in a limited field of high pressure (above 0.8 kilobar) and temperature (above ~100° C) was detected for the first time in modern hydrothermal ocean ores. At low temperature and atmospheric pressure, this unstable compound with time passes into low-temperature polymorphs of the corresponding composition. As follows from generalization of published experimental data (Gablina, 1993), stability of tetragonal modification of Cu_2S directly depends on synthesis temperature and the most stable are tetragonal structures of composition $Cu_{1.96}S$-Cu_2S synthesized at temperature above 350-400° C. The find of high-temperature dense polymorph of chalcocite in modern deep-water active smoker is natural, as well as its association with solid solutions of chalcocite—bornite series. Formation of Rainbow sulfide ore occurs under pressure of water column more than 2000 m and at increased temperatures: the measured temperatures of fluids in the Rainbow hydrothermal field are 250—362° C (Bogdanov at al., 2002). In similar conditions, the tetragonal form has been earlier established in sulfide crusts of thermal salt brines of Solton Sea, where it was present as lamellae of solid solution breakup in bornite. The temperature of salt brines is 300—350° C. In 30 months at room temperature, the tetragonal phase in samples of sulfide crusts has completely passed into chalcocite (Skinner *et al.*, 1967).

In experiments on leaching and dissolution of chalcocite by iron sulfate at usual temperature and pressure, the tetragonal phase formed as a short-time transition product (Whiteside, Goble, 1986). It was observed at low concentration of iron sulfate (10^{-2}—$5{\cdot}10^{-2}$ M) in the solution. The further leaching resulted in transformation of tetragonal phase into digenite, then anilite and other non-stoichiometric sulfides with increasing shortage in copper. At higher concentration of iron sulfate in the solution (> 10^{-1}), the initial product of chalcocite leaching was djurleite. The fact that tetragonal Cu_2S was met in Rainbow sulfide constructions not only in mixtures with monoclinic chalcocite and djurleite, but also in products of breakup of the high-temperature chalcocite—bornite solid solutions, indicates that in this case it is not a result of oxidation and leaching of chalcocite, but an initial hydrothermal mineral preserved in specific thermodynamic conditions of functioning of deep-water thermal sources. This conclusion is also confirmed by the fact that the tetragonal chalcocite is not met in investigated in detail inactive (relict) constructions of more ancient Logachev field. There, products of chalcocite oxidation — djurleite, anilite, geerite, spionkopite, yarrowite and covellite — develop together with rare relics of chalcocite (Gablina *et al.*, 2000). Currently, roxsbyite as a product of djurleite oxidation is established by the X-ray analysis. Apparently, tetragonal polymorph of chalcocite could be considered a typomorphic mineral of active «smokers», but nevertheless it remains an exotic find, since after the extinction of hydrothermal

activity it is soon converted in non-stoichiometric sulfide minerals more stable against the impact of sea-water ambient. Already now admixture of djurleite and presumably digenite — initial products of chalcocite oxidation — are present in the mixture of monoclinic chalcocite and its tetragonal form in the investigated samples; on the external wall of chimneys these minerals are substituted by low-copper sulfides — spionkopite and yarrowite.

The work was executed at the financial support of the Russian Basic Researches Fund (Grant 01-05-64679) and the Ministry for Science and Technology (Project # 3.2.2. Federal Program «World Ocean»)

References

Belov N.V. Nekotorye osobennosti kristallokhimii sulfidov (Some features of crystal chemistry of sulfides. // In: Issues of petrology and mineralogy. **1953.** V. 2. P. 7-13 (Rus.)

Berry L.G., Thompson R.M. X-ray powder data for ore minerals. // Geol. Soc. American. Mem. **1962**

Bogdanov Yu.A., Bortnikov N.S., Vikentiev I.V., Lein A.Yu., Gurvich E.G, Sagalevich A.M., Simonov V.A., Ikorsky S.V., Stavrova O.O., and Appolonov V.N. Mineralogo-geokhimicheskie osobennosti gidrotermalnykh sulfidnykh rud i flyuida polya Reinbou, assotsiirovannogo s serpentinitami, SAKh (36°14′s.sh.) (Mineral and geochemical features of hydrothermal sulfide ore and fluid of the Rainbow field associated with serpentinites, MAR (36° 14′ N) // Geologiya rudn. mestor. **2002**. V. 44. # 6. P. 510-542 (Rus.)

Borodaev Yu.S., Mozgova N.N., Gablina I.F., Bogdanov J.A., Starostin V.I., and Fardust F. Zonalnye trubki chernykh kurilshchikov iz gidrotermalnogo polya Reinbou (Sredinno-Atlanticheskii khrebet, 36° 14′ s.sh.) (Zonal chimney of black smokers from the Rainbow hydrothermal field (Mid-Atlantic Ridge, 36° 14′ N) // Bulletin of the Moscow State University (**in print**) (Rus.)

Clark A.H., Sillitoe R.H. First occurense in ores of tetragonal chalcocite. // News Garb. Mineral. Mon. **1971.** # 2. P. 418-424

Djurle C. An X-ray study of the system Cu-S // Acta Chem. Scan. **1958.** V. 12. # 7. P. 1415-1426

Eliseev E.N., Rudenko L.E., Sisnev L.A., Koshurnikov B.L., and Solovov N.I. Polymorphism of copper sulfides in the system Cu_2S-$Cu_{1.8}S$. // Mineralogical collectin. Lvov State Univ. **1964.** # 18. P. 385-400 (Rus.)

Gablina I.F. Mineraly sistemy med'-sera (Minerals of the system copper-sulfur). M.: Geoinformmark, 1993. 45 p. (Rus.)

Gablina I.F. Sulfidy medi kak indikatory sredy rudoobrazovaniya (Copper sulfides as indicators of ore formation environment) // Dokl. RAS. **1997**. V. 356. # 5. C. 657-661 (Rus.)

Gablina I.F. Tetragonalnyi sulfid medi (1) v prirodnykh rudakh (Tetragonal copper sulfide (1) in natural ores) // Dokl. RAS. **1992.** V. 323. # 6. P. 1170 — 1173 (Rus.)

Gablina I.F., Mozgova N.N., Borodaev J.S., Stepanova T.V., Cherkashev G.A., and Il'in M.I. Assotsiatsii sulfidov medi v sovremennykh okeanskikh rudakh gidrotermalnogo polya Logachev (Sredinno-Atlanticheskii khrebet, 14°45′ s.sh.) (Association of copper sulfides in modern ocean ores of the Logachyov hydrothermal field (Mid-Atlantic Ridge, 14° 45′ N) // Geologiya rudn. mestor. **2000**. V. 42. # 4. P. 329-349 (Rus.)

Goble R.Y. Copper sulfides from Alberta: yarrowite Cu9S8 and spionkopite $Cu_{39}S_{28}$ // Canad. Mineral. **1980.** V. 18. P. 511-518

Goble R.Y. The relationship between crystal structure, bonding and cell dimension in the copper sulfides // Canad. Miner. **1985.** V. 23. P. 61-76

Goble R.Y., Robinson G. Geerite, Cu 1.60S, a new copper sulfide from Dekalb Township, New. York // Canad. Miner. **1980.** V. 18. P. 519-523

Grace J.D., Cohen L.H. Effect of pressure on Chalcocite phase transition // Econ. Geol. **1979.** V.74. # 3. P. 689-692

Janosi A. La structure du sulfure cuivreux quadratique. // Acta Crist. **1964.** V. 17. P. 311-312

Kullerud G. The join Cu9S5-$Cu_{5F}eS_4$ // Year Book. **1959**/Carnegie Inst. Wahs., 1959/1960. P. 114-116

Morimoto N., Koto K., Shimazaki Y. Anilite, Cu7S4, a new mineral // Amer. Mineral. **1969.** V. 54. P. 1256-1268

Mumme W.G., Sparrow G.J., Walker G.S. Roxbyit, a new copper sulfide mineral from the Olympic Dam deposit, Roxby Downs, South Australia. // Miner. Magaz. **1988.** V. 52. Pt. 3. P. 323-330

Potter R.W. An electrochemical investigation on the system copper — sulfur. // Econ. Geol. **1977.** V. 72. P. 1524-1542

Potter R.W., Evans H.T. Definitive X-ray powder data for covelite, anilite, djurleite and chalcocite. // Jour. Research U.S. Geol. Survey. **1976.** Vol. 4. # 2. P.205-212

Roseboom E.H., jr. Djurleite, Cu1.96S // Amer. Mineral. **1962.** V. 47. P. 1181-1184

Roseboom E.M. An investigation of the system Cu-S and same natural copper sulfides between 25^0C and 700^0C. // Econ. Geol. **1966.** V. 61. # 4 P. 641-671

Skinner B.Y. Stability of the tetragonal polymorph of Cu_2S // Economic Geology. **1970.** V. 65. P. 724-730

Skinner B.Y., White D.E., Rose H.J., Mays R.E. Sul-

UDC 549.328

ON FORMS OF SILVER IN GALENA FROM SOME LEAD–ZINC DEPOSITS OF THE DALNEGORSK DISTRICT, PRIMOR'YE

Oksana L. Sveshnikova
Fersman Mineralogical Museum of the Russian Academy of Sciences, Moscow, min@fmm.ru

Galenas with silver and antimony admixtures from 7 lead-zinc mainly hydrothermal deposits of Dalnegorsk district of Primorsky Territory were investigated. A special technique of chemical phase analysis has been used for determination of silver forms in galena. It was established that the amount of isomorphic silver in galena changes from 0.003 % to 0.01 %. The ratio of isomorphic silver in total silver in galena is insignificant and rarely accedes 10 % of its total in the mineral. The basic part of silver in galena, about 90 rel %, is related to inclusions of various silver minerals (visible or invisible). Sulfide mineral form dominates among inclusions (sulphosalts + Ag_2S), which share is 62 % to 87 % from total silver in the mineral. Much less silver is related to inclusions of native silver and intermetallic compounds, and very little with inclusions of silver-containing cogwhell. The epitaxial intergrowth with galena was established for invisible inclusions of argnetite and native silver using methods of electronic microsclpy.
3 tables, 4 figures and 18 references.

Galena from base-metal and lead-zinc deposits almost always contains an admixture of silver, which amount changes from 0 to some percents. Silver in galena is considered in numerous publications, but many unresolved questions in this problem continue till now.

Currently, existence of two forms of silver in galena is generally accepted: isomorphic and mineral as inclusions of silver minerals. Publications quite often mention invisible (dispersed) silver in galena (Patalakha, Gavrilov, 1971), which should include total amount of silver, isomorphic and related to invisible inclusions of silver minerals.

The conception of isomorphic replacements in natural galena is based on experimental researches. Van Hook (1960) and Hutta and Wright (1964) have shown that Ag_2S dissolves in PbS with formation of solid solutions. The limit of isomorphic replacement in natural galena is 0.6 mol % at 800° C and 0.2 mol % at room temperature. P. Ramdor (1960) has supposed that in conditions close to hydrothermal mineralogenesis solubility of Ag_2S does not exceed 0.1 mol % for high-temperature ore and 0.01 mol % for low-temperature ore.

Studies of the system $PbS - AgSbS_2$ have shown that the heterovalent isomorphism in galena under the scheme $2Pb^{2+}$ by $Ag^{1+} + Sb^{3+}$ is possible. Works Wernick (1960) and Nenasheva (1975) established the existence of solid solutions in the high-temperature part of the system $AgSbS_2$ — PbS. At temperature below 400° C, in data of Nenasheva S.N., continuos series of solid solutions disintegrate into some phases and limited solid solutions. The revealed phases are $Ag_3PbSb_3S_7$ and $AgPbSbS_3$. The last corresponds to a rare mineral — freieslebenite.

Researchers, as a rule, use a complex of methods at the study of silver admixtures in natural galenas. Currently, various kinds of spectral micromethods and electronic microscopy methods are determining among them. In addition, at solution of separate problems, recalculations of chemical analysis data with application of mathematical processing methods are used (Nesterova, 1958; Godovikov, 1966), as well as measurement of lattice cell parameters and some physical characteristics of galena to study correlations between them and silver content in a mineral (Ryabev *et al.*, 1969; Dobrovolskaya *et al.*, 1973).

For the solution of ore-dressing related problems, we used the technique of chemical phase analysis of silver in galena, developed in the Satpaev Institute of Geological Sciences of the Academy of Sciences of the Kazakh SSR (Timerbulatova, Antipin, 1973). This technique enables to determine simultaneously total silver in galena, amount of isomorphic silver and silver in inclusions, separately for diverse mineral forms of inclusions. Ag_2S and silver sulphosalts are determined jointly; native silver and intermetallic compounds of silver (dyscrasite) and separately — silver-containing cogwhell remaining in insoluble residue. The essence of analysis is selective extraction of silver minerals from galena basing on their unequal stability in relation to some dissolvents.

Seven deposits were subject to study: four hydrothermal and three skarn deposits. Galena from hydrothermal deposits was regularly studied and galena from skarn was presented by individual samples.

The list of deposits and brief data on their mineral composition are shown in Table 1.

Table 1. Mineral composition of deposits

Deposit - type	*Deposit*	*Ore minerals*		*Non-ore minerals (main and minor)*	*Visible inclusions of silver minerals in galena*	*Notes*
		Main	*Minor and rare (are italic)*			
Hydro-thermal	Yuzhnoye	Pyrrhotite, sphalerite, galena, magnetite, jamesonite (on upper levels)	Arsenopyrite, *cassiterite,* chalcopyrite, *boulangerite, menegenit, stannite,* Ag-containing tetrahedrite, *dyscrasite, native antimony, pyrargyrite, miargyrite, owyheeite, argentite, native silver, diaphorite (?)*	Mangan-siderite, quartz, calcite, rhodochrosite, actinolite	**Frequent in galena on upper levels:** pyrargyrite (predominates), owyheeite, miar-gyrite, Ag-containing tetrahedrite, native Ag, dyscrasite, argentite. **Rare in galenas on lover horizons:** pyrar-gyrite, dyscrasite, native Ag, argentite.	
	Maiminovskoye	Sphalerite, galena, chalcopyrite	Arsenopyrite, pyrite, chalcopyrite, Ag-containing tetrahedrite, *pyrrhotite, polybasite*	Quartz, carbonate, chlorite	**Rare:** pyrargyrite, polybasite, steph-anite, native Ag. **More frequent***:* Ag-containing tetrahedrite	
	Augustovskoye	Pyrite, marcasite, sphalerite, galena, pyrrhotite	Arsenopyrite, chalcopyrite, magnetite, stannite, *boulangerite, bournonite*	Quartz, dolomite, rhodochrosite, calcite	**Rare:** pyrargyrite, native Ag, Ag-containing tetrahedrite	
	Zayavochnoye	Pyrite, pyrrhotite, marcasite, sphalerite, galena	Chalcopyrite, arsenopyrite, *stannite*	Quartz, carbonate	**Rather rare:** Ag-containing tetrahedrite	For separate samples only composition of ore bodies is characterized
Skarn	Vostochny Partizan — Borisovskoye ore body (hydrothermal)	Sphalerite, galena, chalcopyrite	Arsenopyrite Ag-containing tetrahedrite, bournonite	Calcite, laumontite	**Rare:** Ag-containing tetrahedrite, native Ag	Borisovskoye ore body represents sandstone zone , broken by thick network of frac-tures filled with hydrothermal sulfide
	Verkhneye	Galena, sphalerite	Chalcopyrite	Calcite, hedenbergite	Not observed in the investigated sample	Sample B-465 is presented by crys-tals of late galena from pocket-like segregations of calcite in massive galena-sphalerite ore
	Nikolaevskoye	Sphalerite, galena	Chalcopyrite, pyrrhotite, arsenopyrite	Hedenbergite, calcite, quartz	Were not observed	

Results of chemical phase analysis of galena are indicated in Table 2. The Table shows that the investigated galenas consider-ably differ in total contents of silver in them. The values oscillate in the range of 0.054 to 0.900 mass %. Minimum values are character-istic for galenas from skarn (an. 21-23), maxi-mum — for galena from jamesonite-sphalerite-galena ore developed on upper levels of the Yuzhnoye Deposit (an. 1). According to the data of spectral analysis (quantitative and semi-quantitative) not result-ed in this article, all galenas are also character-ized by increased contents of antimony.

The analysis of the data resulted in Table 2 gives the main conclusion: the part of isomor-phic silver is insignificant and usually makes some percents, rarely above 10 % (an. 19, 21. and 23), from total silver in all investigated galenas. Respectively, the basic amount of sil-ver, about 90 rel %, is related to inclusions of various silver minerals.

As to absolute values of isomorphic silver contents in galena, they are different not only

Table 2 Results of chevical phase analysis of galena (mass %)

Deposit type ##	Deposit	Sample	Location	Total Ag	Isomorphic Ag		Sulfide Ag: Ag2S+sulphosalt		Native Ag and intermetallic compounds		Ag-containing cogwhill	
					abs. %	rel. %	abs. %	rel. %	abs. %	rel. %	abs. %	rel. %
1 Hydro-thermal	Yuzhnoye	52	Level +870m Adit 203	0,900	0,006	0,67	0,740	82,22	0,061	6,78	0,006	0,67
2		83	Level +830m adit 204	0,430	0,005	1,16	0,351	81,63	0,034	7,91	0,007	1,63
3		510	Level +690m adit 205	0,240	0,010	4,17	0,160	66,67	0,056	23,33	0,004	1,67
4		540	Below level +620 Well 505	0,200	0,010	5,00	0,154	77,00	0,024	12,00	0,022	1,00
5		28	Well 488	0,195	0,009	4,62	0,134	68,72	0,023	11,80	0,007	3,59
6		715	Well 511-bis	0,190	0,011	5,79	0,141	73,68	0,033	17,37	0,004	2,11
7		538	Well 508	0,189	0,012	6,35	0,129	68,25	0,033	17,46	0,051	2,70
8		548	Well 501	0,185	0,014	7,63	0,115	62,16	0,030	16,22	0,005	2,76
9		21	Well 84	0,140	0,005	3,57	0,090	64,30	0,040	28,57	Not detected	
10	Maimini-vskoye	614	Well 63	0,165	0,003	1,82	0,120	72,73	0,014	8,49	0,011	6,67
11		570	Well 65	0,160	0,003	1,90	0,100	62,50	0,032	20,00	0,014	8,75
12		872	Well 136	0,110	0,010	9,09	0,074	67,27	0,021	19,09	Traces	Traces
13		803	Well 161	0,096	0,005	5,26	0,069	71,88	0,016	16,57	0,005	5,26
14		854	Well 131	0,059	0,006	10,17	0,045	76,27	0,008	13,56	Traces	Traces
15	Augusto-vskoye	28-a	Well 37	0,460	0,022	4,78	0,400	86,96	0,024	5,22	Traces	Traces
16		288	Site 32	0,400	0,007	1,75	0,320	80,00	0,045	11,25	0,010	2,50
17		993	Adit 2	0,250	Traces	Traces	0,200	80,00	0,024	9,60	Traces	Traces
18		13	Well 35	0,177	0,007	3,95	0,140	79,10	0,010	5,63	0,007	3,95
19	Zayavo-chnoye	829	Well 87a	0,089	0,010	11,23	0,060	69,76	0,011	12,36	0,005	5,62
20 Skarn	Verkhneye	465	Level -162m	0,300	0,010	3,33	0,250	83,33	0,013	4,33	0,005	1,67
21	Vostochny Partizan	75	Level +215m Capital adit	0,054	0,007	12,96	0,040	74,07	0,010	18,52	Traces	Traces
22	Nikola-yevskoye	936	Well 924	0,070	0,005	7,17	0,048	68,57	0,012	17,14	Traces	Traces
23		907	Well 923	0,060	0,007	11,67	0,038	63,33	0,011	18,33	Traces	Traces

Analyses were made by A.I. Antipina in the chemical laboratory of Satpaev Institute of Geological Sciences of Academy of Sciences of the Kazakh SSR in 1990.
Average relative error of the method is 10 %..

for galenas from different deposits, but also within the limits of one deposit. The most vivid example in this respect is the Augustovskoye deposit, where one of galenas shows traces of isomorphic admixture of silver (an. 17), while in another one (an. 15) the silver content riches 0.022 mass %, which is abnormally high value in the studied galenas.

If to exclude extreme values, the amount of isomorphic admixture of silver in 90 % of investigated samples changes in the range of 0.003 to 0.01 mass %. It is difficult to interpret any dependence of the total contents of silver on the amount of isomorphic admixture basing on available data. We shall only notice that galenas with the highest silver contents of 0.900 mass % (an. 1); 0.430 mass % (an. 2) and 0.400 mass % (an. 16) are characterized by very low values of isomorphic admixture: 0.006, 0.005 and 0.007 mass % respectively.

The silver isomorphism in investigated galenas is related to formation of solid solutions in the system $AgSbS_2 - PbS$. Their existence is manifested by regular relation of silver with antimony, established by various analytical methods, and presence of freieslebenite $AgPbSbS_3$ in galena from the Yuzhnoye deposit as submicroscopic inclusions reminding products of solid solution decomposition (Fig. 1), which will be discussed below in more detail, and finally by the data of X-ray studies of galena samples with known amount of isomorphic

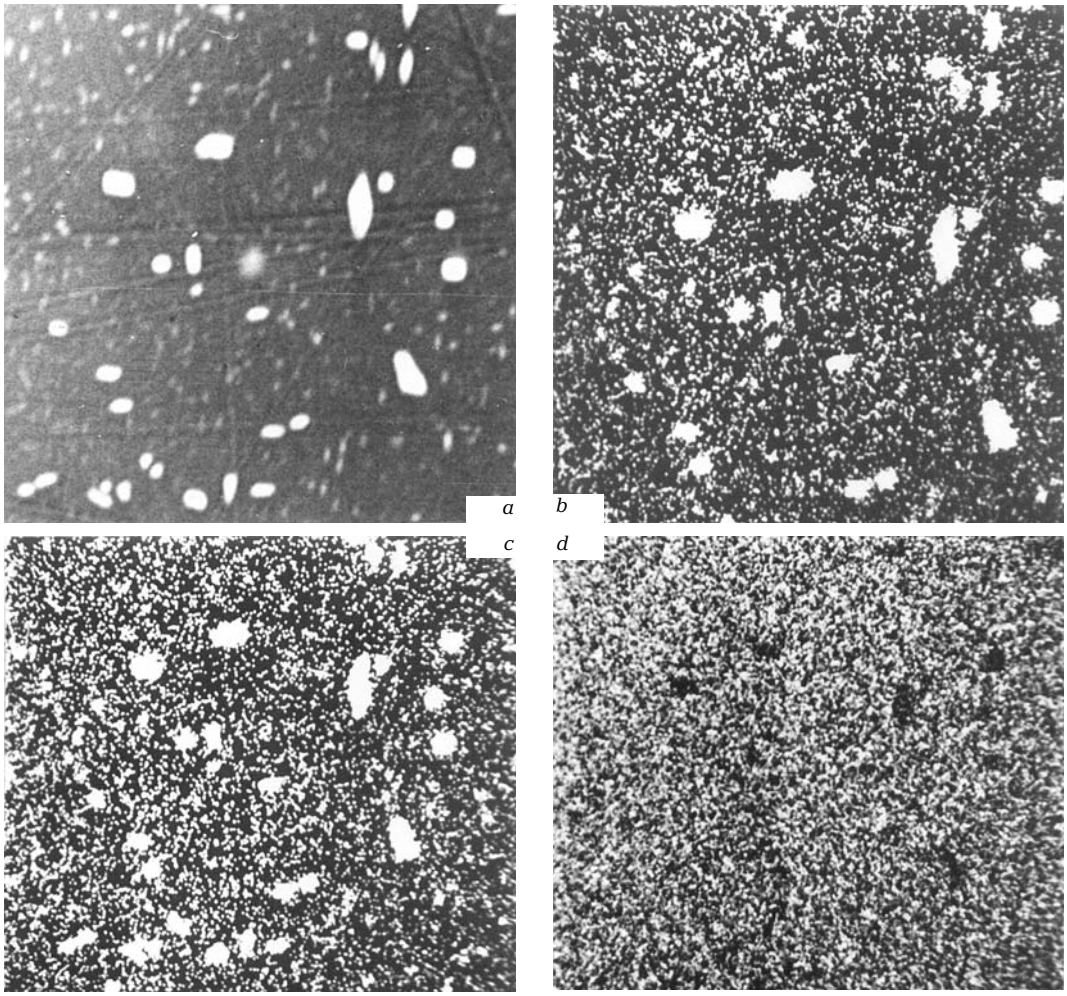

FIG. 1. Freieslebenite inclusions in galena. Yuzhnoye deposit. Surface of galena in the microanalyser: in absorbed electrons (a), in characteristic X-ray radiation: AgLa1 (b), SbLa1 (c), PbLa (d). Scanning site 100 x 100 microns

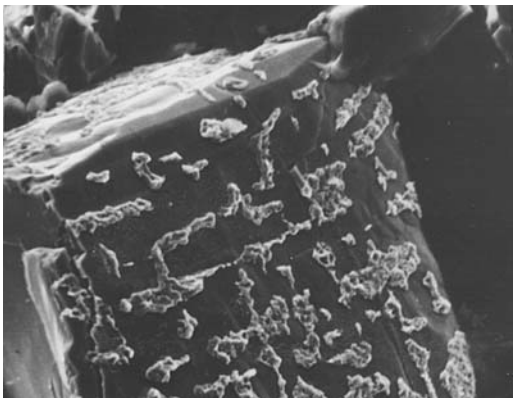

FIG. 2. Dendrites of native silver, epitactically growing up on a plane of galena. Vostochny Partizan deposit. SEM image. x 5000. Photo by R.V. Boyarskaya

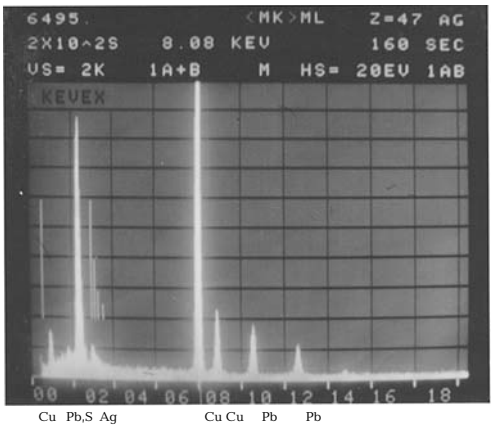

FIG. 3. Energy dispersion spectrum of native silver composition growing up on galena. (Cu peaks in the spectrum result from preparation).

Table 3. Parameter of lattice cell of cell of galena with different contents of total and isomorphic silver

##	Sample	Total Ag mass %	Isomorphic Ag, mass %	a_o, Å
1	993	0,250	-	5,933
2	570	0,160	0,003	5,932
3	614	0,165	0,003	5,932
4	854	0,059	0,006	5,932
5	288	0,400	0,007	5,931
6	829	0,089	0,010	5,931
7	28-a	0,460	0,022	5,929

Conditions:
DRON-3; regime: 40kv-15ma. Internal standard — metal silicon. Accuracy of determination — ±0.001Å.

silver. The work was executed by O.V. Kuzmina in the X-ray laboratory of IGEM of the Russian Academy of Sciences.

Table 3 shows the designed values of a_0 in lattice cell of galenas with diverse contents of total and isomorphic silver. As follows from the Table, the a_0 parameter in galena decreases from 5.933Å to 5.929Å (accuracy ±0.001) in accordance with the increase of isomorphic admixture of silver in it from 0 mass % to 0.022 mass %.

As mentioned above, the mineral form of silver in galena is dominant in the investigated deposits. About 90 % of silver from its total amount in galena are related to inclusions of various silver minerals. Among inclusions, sulfide minerals (Ag_2S + silver sulphosalts) sharply predominate. Their share is from 62 (an. 8) to 87 (an. 15) rel % of silver in galena. Much less silver is related to inclusions of native silver and intermetallic compounds (dyscrasite) and very little with the admixture of silver-containing cogwhell presented in all investigated samples by silver-containing tetrahedrite.

The share of this or that mineral form of inclusions in total silver in galena oscillates even within one deposit; this is related to features of mineral composition of deposits. So, in the Yuzhnoye deposit, the observed decrease with depth of the sulfide silver share (from 82.2 rel % to 62.16 rel %) with simultaneous increase of native silver (fom 6.7 rel % to 28.57 rel %) is related to general change of ore composition, in particular, with disappearance of silver — sulphosalt association of minerals on deep levels. Cogwhell, forming visible accumulations on some plots of ore bodies, is more abundant in the Maiminovskoye deposit than in other deposits. Cogwhell occurs in galena not only as fine inclusions, but also as streaks and replacement rims, which is probably the reason for a significant increase of the share of related to it silver in some samples of galena (an. 10 — 6.67 rel %; an. 11 — 8.75 rel %).

Rare inclusions of silver minerals interpreted in investigated galenas by optical methods cannot explain, in our opinion, all amount of silver related to inclusions, which follows from the data of chemical analysis. A part of this silver, we assume, is unconditionally related to submicroscopic (invisible) inclusions, which sizes lay outside of resolving power of optical microscope. A.P. Pronin with co-authors (1971), who studied silver in galena from the Zyryanovskoye base-metal deposit, earlier came to a similar conclusion. Their data allow to make some assumptions on the silver amount related to invisible inclusions, having received it as a difference of contents of invisible and isomorphic silver. So, the contents of invisible silver determined using the quantitative spectral microanalysis in galenas from late carbonate−quartz−sulfides veins of the Zyryanovskoye deposit oscillate between 0.013 and 0.290 mass % (average of 144 determinations is 0.117 mass %), while the contents of isomorphic silver determined by the selective solution does not exceed 0.079 mass %.

For the purpose to reveal invisible inclusions in investigated galenas, the IGEM laboratory has conducted studies of their surface in backscattered electrons on microprobe MS «Cameca» and also with application of transmission and scanning electron microscopes. Invisible inclusions were only detected in three samples of galena.

So, in «curvistriated» (broken down) galena from jamesonite-sphalerite-galena ore of the Yuzhnoye deposit, submicroscopic inclusions of freieslebenite from parts of micron to 3-5 microns were observed by the microprobe. The most fine grains are dot impregnations, larger have oval, sometimes lanceolate form. The composition of mineral was determined in one of coarse grains and its recalculation well fitted to the formula of freieslebenite: Ag — 21.97 mass %; Pb — 40.29 mass %; Sb — 23.21 mass %; S — 18.23 mass % (analyst Malov V.S.). The microanalyser image of freieslebenite grain surface is given on Fig. 1. The described segregations of freieslebenite can be a product of solid solution decay in the system $AgSbS_2$-PbS and increase of their grains (as well as decay itself) is the consequence of dynamometamorphism. L.N. Indolev (1974) paid attention to a similar fact at studying of

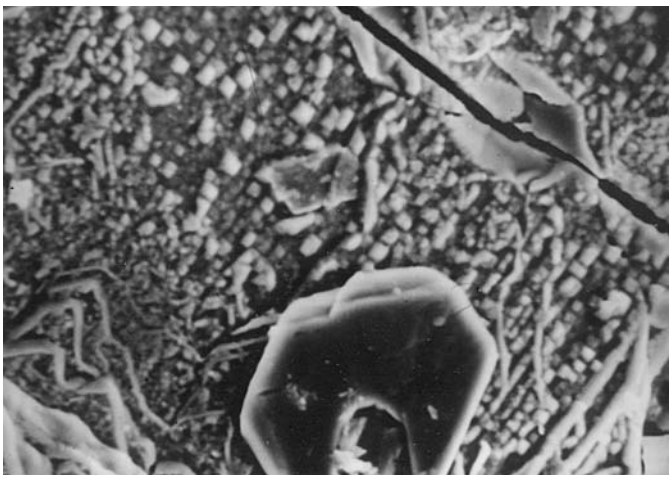

FIG. 4. Cubic crystals of argentite epitactically growing up on a plane of galena. Verkhneye deposit. SEM image. x5000. Photo by R.V. Boyarskaya

lead-zinc deposits of Yakutia. The association of decay products as miargyrite to plots of strained galena was also registered by M.G.Dobrovolskaya *et al.* (1973).

Presence of freieslebenite as a solid solution decay product is a rare phenomenon. In publications (Indolev, 1974; Czamanske and Hall, 1976; Sharp and Buseck, 1993) similar inclusions in galena are usually presented by diaphorite ($Ag_3Pb_2Sb_3S_8$), though some researches (Nenasheva, 1975; Hoda and Chang, 1975) have established existence of solid solution between galena and freieslebenite.

Dendrites of native silver, epitactically growing up on the plane of galena in two perpendicular directions were detected with the help of electronic microscopy in galena from the Vostochny Partizan deposit (Fig. 2, Fig. 3).

Epitactic intergrowths with Ag_2S are characteristic for galena from the Verkhneye deposit. In Fig. 4, cubic crystals representing a pseudomorph of acanthite after argentite are well visible. Diagnostic of acanthite was made on the basis of calculation of microdiffraction data of R.V. Boyarskaya.

Epitactic form of inclusions, in the opinion of some researchers (Frank-Kamenetsky, 1964; Badalov and Povarenykh, 1967), is rather widely distributed in minerals. In galena a significant part of silver mineral inclusions could have the epitactic nature owing to geometrical similarity of their structures to the structure of galena. Epitactic inclusions, as specifies V.A. Frank-Kamenetsky, can originate at different conditions, including, at disintegration of solid solutions.

The nature of silver inclusions in galena can be rather diverse and it is not restricted to the discussed examples. So, P. Costagliola *et al.* (2003) in recent studies using EPR-spectroscopy have revealed the presence of initial native silver (Ag^0) in silver-containing galena from the Tuscan ore region (Italy). This silver forms pairs and clusters, which can associate with pairs of metal gold or silver-gold hetero-nuclear pairs.

References

Badalov S.T. and Povarenykh A.S. O formakh vkhozhdenia elementov-primesei v sulfidy (On forms of entry of elements-admixtures into sulfides). — Mineral. sb. of Lvov Univ., **1967**, #2, issue 1 (Rus.)

Costagliola P., Benedetto F.D., Benvenuti M., Bernardini G.P., Cipriani C., Lattanzi P.F. and Romanelli M. Chemical speciation of Ag in galena by EPR spectroscopy. Am. Min., **2003**, v. 88, pp. 1345-1380

Czamanska G.K. and Hall W.E. The Ag-Bi-Pb-Sb-S-Se-Te mineralogy of the Darvin lead-silver-zink deposit, southern California. Econ. Geol., **1976,** 70, 1092-1110

Dobrovolskaya M.G., Shadlun T.N., Dudykina A.S., Esikova G.S., and Vyalsov L.N. Osobennosti sostava i nekonorykh svoistv galenita otdelnykh mestorozhdenii Vostochnogo Zabaikaliya. (Features of structure and some physical properties of galena from separate deposits of East Transbaikalian region). — Proceedings of Miner. Museum Ac. Sci. of the SSR, **1973**, issue 22 (Rus.)

Frank-Kamenetsky V.A. Priroda strukturnykh primesei v mineralakh (Nature of structural admixtures in minerals). L., LGU, **1964** (Rus.)

Godovikov A.A. O primesyakh serebra, vismuta i surmy k galenitu. (On admixtures of silver, bismuth and antimony in galena.) Geol.

rudn. mestor., **1966**, #2 (Rus.)

Hoda S.N. and Chang L.L.Y. Phase relations in the system PbS-Ag_2S-Sb_2S3 and PbS-Ag_2S-Bi_2S_3. Am. Min., **1975**, 60, 621-633

Hutta J. J., H. D. Wright. The incorporation of uranium and silver by hydrotermally synthesize galena. — Econ. Geol., **1964**., v. 59, #6

Indolev L.N. Serebryano-svintsovye mestorozhdeniay Yakutii (Silver-lead deposits of Yakutia). Novosibirsk. «Nauka», **1974** (Rus.)

Nenasheva S.N. Eksperimentalnoye issledovanie prirody primesi serebra, surmy i vismuta v galenite (Experimental research of the nature of silver, antimony and bismuth admixtures in galena). Novosibirsk. «Nauka», **1975** (Rus.)

Nesterov Yu.S. K voprosu o khimicheskom sostave galenitov (To the problem of chemical composition of galenas). — Geokhimiya, **1958**, #7 (Rus.)

Patalakha G.B. and Parilov Yu.S. Formy vkhozhdeniya serebra v sulfidy svintsovo-tsinkov mestorozhdenii Tsentralnogo Kazakhstana (Forms of entry of silver into sulfides of lead-zinc deposits of the Central Kazakhstan.) — Proceedings of Satpaev Inst. of Geol. Sciences of the Academy of Sciences of the Kazakh. SSR, **1971**, #2 (Rus.)

Pronin A.P., Bespaev Kh.A., and Mukanov K.M. Serebro v galenite Zyryanovskogo polimetallicheskogo mestorozhdeniya (Silver in galena of Zyryanovskoye base-metal deposit). — Proceedings of Satpaev Inst. of Geol. Sciences of the Academy of Sciences of the Kazakh. SSR, **1971**, #2 (Rus.)

Ryabev V.L., Ryabeva E.G., and Malaeva I.P. Nekotorye osobennosti otrazhatelnoi sposobnosti i mikrotverdosti galenitov v zavisimosti ot formy soderzhashchegosya v ikh sostave serebra. (Some features of reflective ability and microhardness of galenites depending on the form of silver contained in their composition). — Proceedings of TsNIGRI, 1969, issue 80 (Rus.)

Sharp T.G. and Buseck P.R. The distribution of Ag and Sb in galena: Inclusions versus solid solution. Am. Min., **1993**, v. 78, pp. 85-95

Timerbulatova M.I. and Antipin A.I. Razrabotka metodiki khimicheskogo fazovogo analiza serebra v galenite. (Development of a technique of chemical phase analysis of silver in galena). — Proceedings of the Academy of Sciences of the Kazakh. SSR, Geological Series, #4 (Rus.)

Van Hook H. J. The ternary system Ag_2S-Bi_2S_3-PbS. — Econom. Geol., **1960**, v. 55, #4

Vernick J. H. Strukturnaya priroda sistem Ag-Sbs_2-PbS, $AgBiS_2$-PbS i $AgBiS_2$-$AgBiSe_2$ (Structural nature of systems $AgSbs_2$-PbS, Ag

UDC 549.324.3 + 548.574

TO THE ONTOGENY OF SPIRAL–SPLIT CUBOOCTAHEADRAL BLOCK–CRYSTALS OF PYRITE FROM THE KURSK MAGNETIC ANOMALY

Juriy M. Dymkov
All-Russia Research Institute of Chemical Engineering, Moscow, geolog@vniiht.ru

Victor A. Slyotov
Moscow, vikslyotov@mail.ru

Vasiliy N. Filippov
Institute of Geology of the Komi Scientific Center of the RAS, Syktyvkar, institute@geo.komi.ru

The morphology and structure of cubooctahedral split crystals of pyrite with spiral rosettes of subindividuals on octahedral faces are described. It is supposed that such block-crystals were formed around axially twisted cubic germs and are in itself germinal centers of spherocrystals.
9 figures, 16 references.

Blocks of different levels (orders) of mosaic crystals of pyrite are covered with own faces resulting in specific sculptural details of the surface, reflecting the internal structure of crystals, especially of their external zones. The paper briefly discusses the genetic information received at interpretation of morphological observations and their graphic presentation on the base of fundamental ontogenetic works by D.P. Grigoriev (1909-2003) and its disciples and followers (N.P. Yushkin, A.G. Zhabin, V.A. Popov, V.I. Pavlishin and others). Pyrite crystals were investigated under stereoscopic microscope and scanning electronic microscope; polished sections — under reflected light microscope «Neophot» with devices for photographing at small enlargement. Physical and chemical studies were not conducted.

Investigated samples of pyrite were collected at the Mikhailovsky open pit of one of deposits of Kursk Magnetic Anomaly (KMA). The ore sequence is represented by hardly metamorphosed Precambrian ferruginous quartzite, which occur at a depth of about one hundred meters. The basic ore mineral is magnetite; the ore also includes hematite, quartz, chlorites, green hydromica celadonite, occasionally metacrysts of pyrite. Ferruginous quartzite is covered by Jurassic clay replaced on separate plots with limestones and, in turn, covered by Cretaceous clay and sand. Jurassic clay is hardly pyritized in separate places. As oxidizing pyrite creates an active sulfuric acid environment, the upper part of ferruginous quartzite under such plots is transformed into accumulations of so-called «ferruginous cream» — continuous masses of friable fine-crystalline hematite and quartz powder.

Plots (blocks) of the oxidation zone on the contact of ferruginous quartzite with limestone and especially along the ternary border ferruginous quartzite-limestone-clay are composed of cavernous limonite. Hollows in limonites are numerous, their size can attain tens of centimeters and more. Most of such hollows are intensively mineralized with pyrite, siderite and in immediate proximity to limestone — with calcite.

Secondary mineralization is also observed in cracks of the upper layers of ferruginous quartzite touched by oxidation.

Siderite in hollows grows on limonite as brushes and separated fine (1-2 mm) crystals of prismatic or rhombohedral habitus, and as spherocrystalline crusts with diameter of spherocrystals 3 to 5 mm in various phases of splitting. Pyrite is basically cubooctahedral, occurs as detached crystals, as crystal crusts covering in part or completely walls of cavities, forms pseudo-stalactites, growing over membrane fibers of iron oxides.

Ramified crystals and unusual for pyrite tubular and bubble forms described by B.Z. Kantor (1997) and one of authors (Slyotov, Makarenko, 2002, see Fig. 15-17 in the album) were met. As a rule, each large cavity shows a specific morphology of pyrite aggregates.

In one of large slit-like cavities about one meter long and in small cavities nearby, in limonite, numerous pyrite crystals have been detected with attributes of spiral splitting of subindividuals (Fig. 1) up to 5-6 mm in size. They grow up as groups or separately on a continuous spherocrystalline crust of siderite entirely covering walls of cavity and are considered as original germinal forms of spherocrystals of pyrite.

According to B. Popoff (1934), spherocrystals are radiate-fibrous spherical individuals formed at growth of splitting crystals. The crystal forms of siderite corresponding to various steps of formations of spherocrystals were

FIG . 1. Block-crystals of pyrite on a reniform spherocrystalline crust of siderite.
Photo of a sample sprayed-on with magnesium oxide on device FMN-2 (LOMO). The octahedron 4 mm

FIG . 2. A spherocrystalline concretion of siderite with a block-crystal of pyrite.
electronic microscopy-image in dissipated electrons. Spraying with aluminum. The edge of cube is 0.2 mm

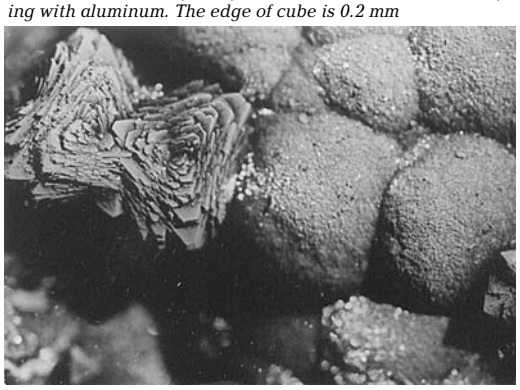

FIG . 3. Skeletal forms of block-crystals of pyrite of an octahedral habitus on a spherocrystalline crust of a siderite
electronic microscopy-IMAGE in the dissipated electrons. A rib of an octahedron of ~1.2 mm

repeatedly met a siderite crust. As shown by A.V. Shubnikov (1957) mathematically as a general case, by A.A. Godovikov (1961) for calcite and Dymkov (1984) for pitchblende, germinal forms of spherocrystals sharply differ from «mature» forms — ideal spheres with smooth or microtuberous surface (Fig. 2).

Almost all pyrite crystals have cubooctahedral habitus and rarely — octahedral (Fig. 3). With increase in crystal size, the size of cube faces increases; however, forms close to correct cubooctahedrons are rare (Fig. 4). Separate spherulites (more exactly, spherocrystals) of pyrite, covered with faces of cube, were not observed, but they sometimes meet as aggregates in reniform spherolite crusts (Fig. 5).

The edge of ideal not split octahedron with smooth brilliant faces attains 0.3-1 mm, but most likely, these are crystals of the second generation. In larger crystals, at the center of octahedron faces, germs of lamellar rosettes were observed, which at further crystal growth gradually grow almost above all the surface of octahedral face (see Fig. 3). Almost all octahedral block-crystals have apices dulled by brilliant faces of a cube. Large split octahedrons with insignificant cube faces at apices have concave subradial lamellar rosettes, growing up from the center, sometimes over the total face of octahedron (see Fig. 3 and Figs. 27, 28 in the album by Slyotov and Makarenko, 2001) and respectively, concave lamellar edges between them (skeletal growth). Rosettes, as seen in prominent parts, have lamellar form, but their structure is not precisely determined. Salient «lamellar» rosettes are appreciably twisted on different faces of octahedrons in opposite directions.

Skeletal block-crystals of octahedral habitus attain ~1.3 mm, cubooctahedral block-crystals are usually three-four times larger and skeletal octahedrons can be considered as intermediate forms of splitting cubooctahedrons. «Cubooctahedral» forms — octahedrons with essential development of cube faces — attain 5 mm by edge; wedge-shaped subindividuals growing from the center of octahedron face also terminate in cube faces. Joining along octahedron edges, they form ribbed (lamellar) slightly concave surfaces (split edges), corresponding to the position of rhombic dodecahedron faces. Apices of octahedron can also extend in the initial phase of cubooctahedral habitus formation, which can be considered as skeletal growth.

Fig. 6 shows detailed pictures of face surface morphology of cubooctahedral block-cry-

stals with spirally twisted pyramids of growing-up octahedron faces. Additional images published in works by V.A. Slyotov and V.S. Makarenko (2001, 2002) give a comprehensive impression on natural «sculpturally decorated» crystallization masterpieces.

Intermediate «transitional» forms between spherocrystalline balls and cubooctahedrons have hypertrophied faces (100) forming convex rows of stairs along directions, corresponding to cube edges. Octahedral faces of the basic individual gradually become more convex and entirely covered with fine square faces of radiantly split subindividuals. In similar forms, on covered (grown over) by subindividuals faces of octahedron remain three rectilinear seams as fine furrows on each face (Figures 1 and 5). Finally, transition occurs from a skeletal form to octahedron with insignificant development of cube faces to antiskeletal forms — to convex rounded octahedral spherocrystals entirely covered with square cube faces (Fig. 5).

Polished sections of pyrite block-crystals etched by concentrated nitric acid show a sharp anisotropy in etching of subindividuals (Fig. 7). Sections subparallel to cube faces (or these are sections of subindividuals of cubic faces?) almost do not accept etching; sections of growing over octahedral pyramid, especially on rhombic dodecahedrons (along octahedron edges) are intensively etched and show radiate-fibrous splitting. Formed textural patterns look like three-dimensional, volumetric. A little unusual chip in the cube plane helps to understand the structure of the split block-crystal. In square contours of the chip (2.5 x 2.5 mm) with rather plain surface, four smoothly extending radiate-fibrous bunches go from a dot germ at the center to angles of the square. This is presumably cross-section of lamellar rosettes on octahedron faces. It is not clear, why one angle of the square contour is truncated and poorly rounded, but practically corresponds to a cross-section of a growing up pyramid of rhombic dodecahedron face. Other radial bunches rest against right angles of the chip. In-between bunches, attributes of lamellar structure and orientation of lamellar subindividuals in parallel to radial bunches are appreciable.

As show etched polished sections, the sculpture of pyrite crystals reflects internal structure (texture) of block-crystals: each subindividual has on the surface its own apex and corresponding cut. Exclusions are accumulations of block-crystals in plots, where the second generation of pyrite — pyrite-II —

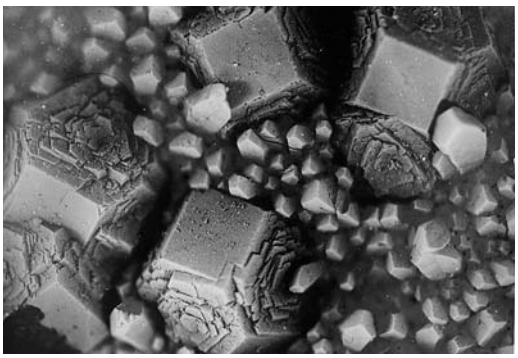

FIG . 4. Pyrite block-crystals of cubooctahedral habitus, in part grown over by a brush of calcite crystals.
Photo of a sample sprayed-on with magnesium oxide on device FMN-2 (LOMO). The cube edge is 2.5 mm

FIG . 5. Transition of a split cubooctahedron of pyrite into a spherocrystal: antiskeletal forms → initial phase of sphere formation.
Photo of a sample sprayed-on with magnesium oxide on device FMN-2 (LOMO). Magnification x10

FIG . 6. Spiral-split block-crystal of pyrite; faces of octahedron. Drawing by V.A. Slyotov and V.S. Makarenko

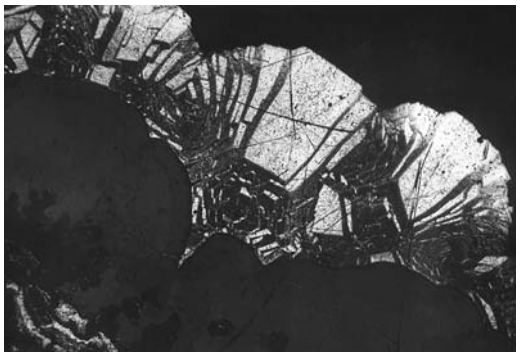

FIG . 7. Structure of crusts of split block-crystals of cubooctahedral pyrite-I on siderite, revealed by anisotropic etching of various sections of its crystals.
Microphoto of polished section after etching by nitric acid. Thickness of crust is 5—6 mm

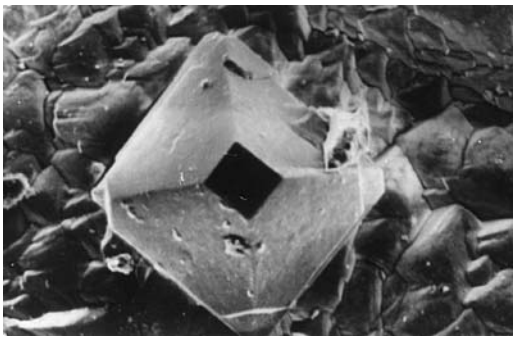

FIG . 8. Crystal of pyrite-II on the surface of siderite brush. SEM-image in dissipated electrons. Spraying with aluminum. The octahedron edge is 0.07 mm

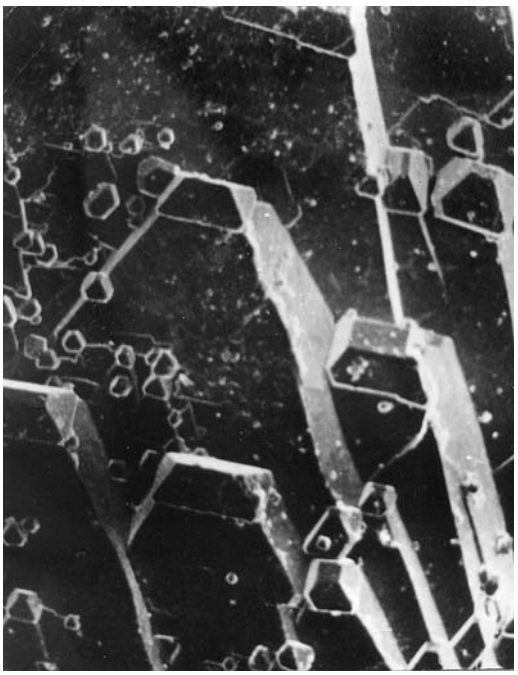

FIG. 9. Crystals of pyrite-II epitactically grown over an octahedron face of pyrite-I and covering of cube faces in apices of octahedron and «powders».
SEM-image in dissipated electrons. Spraying with aluminum. Crystals sizes in powder are ~0.04 mm

was formed. Known here two generations of pyrite can simultaneously be considered as «initiation», by the definition of D.P. Grigoriev (1949).

Pyrite of the second generations (pyrite-II) deposits as fine octahedrons or cubooctahedrons (Fig. 8) epitactically accrued on octahedron face of pyrite-I and simultaneously grows over cubic faces at apices of lamellar subindividuals (Fig. 9). Some kind of regeneration of external subindividuals occurs on block-crystals of pyrite-I. Faces of cube crowning apices of basic split block-octahedrons of pyrite-I are not entirely grown over: only a new layer appears, cut from sides by octahedron faces (Fig. 9).

Pyrite-II crystals do not bear attributes of splitting. These are fine (0.0n to 0.n millimeter in edge) independent individuals — octahedrons and cubooctahedrons — with smooth brilliant faces, epitactically accrued on octahedral faces of pyrite-I. Germinal centers of cubooctahedral crystals of pyrite-II probably had originally the form of plane-faced cube, without screw dislocations, but in cubooctahedrons of pyrite-II face (100) degenerates. This indicates the fact that simultaneously with formation of fine independent crystals on octahedrons of pyrite-I, heads of lamellar subindividuals, covered with cube faces, degenerate and acquire octahedral shape (Fig. 9).

Let's consider genetic features of described above split pyrite crystals. First of all, spirally split block-crystals of pyrite are not unique. The analogous cubooctahedral split pyrite crystals were detected in O.P. Ivanov's collection on a chalcopyrite crystal from Eghe Khiya tin deposit in Yakutia and in detail investigated crystallographically with application of goniometry and electronic microscopy by M.I. Novgorodova (1977). Her indication on analogous spiral arrangement of block subindividuals on octahedron faces and opposite directions of curling of spirals is of interest for us. At the same time, she considers that «... in spite of the fact that pyrite crystals can be qualified as split, the form and arrangement in blocks is not subject to the known scheme by Frondel estab-

lished for their varieties axially curled in directions of the ternary symmetry axes» (page 100).

Using the ontogenetic approach, we shall try to understand what germ could initiate a cubooctahedron. As noted above, at resumption of sulfide mineralogenesis, the tendency of change of crystallographic forms {100} → {111} was distinctly manifested and if we admit that germs in cubooctahedral crystals were axially curled cubic crystals characterized by C. Frondel (1936) and S.A. Borodin (1961), all would become clear. Structural memory of screw dislocation in crystals of a germinal cubic crystal on a crystallographic axis of the third order is a principal cause of splitting and formation of rosettes of subindividuals on octahedron faces. Directions of their curling entirely correspond to the C. Frondel's (1936) data. Various axially curled pyrite crystals also were indicated in works by F. Bernauer (1929), A.S. Borodin (1961, 1971), M.I. Novgorodova (1977) and in «Ontogeny of Minerals» by D.P. Grigoriev and A.G. Zhabin (1975).

In summary we shall note that curled and split pyrites, in the data of S.A. Borodin (1971), are the indicator of low temperatures and pressures of mineralogenesis.

Conclusions

1. The investigated split cubooctahedrons of pyrite are block-crystals, octahedral pyramids of grow-over in which are characterized by radial-spiral splitting.

2. The sharp anisotropy of structural etching in pyrite was established showing texture of block-crystals at impact by concentrated nitric acid. Deformation or disorder of crystal lattices of subindividuals in curled block-crystals of pyrite depend on their belonging to grow-over pyramids <100> (not etched) or to saturated with defects — <111> (etched), and also (in details) on belonging to pyrites of the first or second (no-defects) generation. Crystallographic orientation of the section probably played some role. Polished sections in planes close to cubic ~‖(100), which are almost not etched, while other, more disordered suboctahedral planes ~‖(111) are intensively etched. The prospective reason is natural deformation and disorder of the crystal lattice of pyrite during growth.

3. Sculptural elements of octahedral faces are defined by crystallization of external parts of blocks of subindividuals and epitactically grow over plane-face pyrite crystals of late initiation.

4. By the nature, the characterized pyrite block-crystals of octahedral and cubooctahedral habitus are monomineral spiral-split heterogeneous individuals being an intermediate form of evolution of spherocrystal as a ball entirely covered with square cubic faces.

5. It is supposed that formation of pyrite block-crystals is related to their growth around axially curled cubic germs at change of forms {100} → {111}.

6. Curled cuboids — germs of pyrite — existed only in the beginning of sulfide mineralogenesis at a certain object. Later generations of pyrite, including those forming autoepitactic grow-over on faces of block-crystals, are characterized by ideally smooth brilliant faces without traces of splitting or curling.

7. The considered here pyrites from KMA make a vivid example of simultaneous joint growth of grow-over pyramids of translationally deformed octahedral and disorder-free cubic faces in one crystal.

Authors are grateful to Generalov Michael Evgenievich, the employee of the Fersman Mineralogical Museum of the Russian Academy of Sciences, for valuable critical remarks.

References

Bernauer F. «Gedrillte» Cristalle. Berlin:» Gebr. Bontralger», **1929**

Borodin S.A. O skruchennykh piritakh iz Kalanguya (On curled pyrites from Kalangui) // ZVMO. **1961**. CH. 90. Issue 5. P. 578–585 (Rus.)

Borodin S.A. Skruchennye i mozaichnye kristally pirita kak indikator temperatury obrazovaniya gidrotermalnykh mestorozhdenii (Curled and mosaic pyrite crystals as the indicator of hydrothermal deposit formation temperature) // Geochemistry of hydrothermal ore formation. M.: Nauka.**1971**. P. 91-104 (Rus.)

Dymkov Yu.M. Mekhanizm rasshchepleniya kristallov kubicheskoi singonii s obrazovaniem sferokristallov (uraninit → nasturan) (Splitting mechanism of cubic crystals with formation of spherocrystals (urninite→ pitchblend) // the Mineralogichesky zhurnal. **1984**. # 1. P. 53-64 (Rus.)

Frondel C. Twisted crystals of pyrite and smoky quartz // Amer. Mus. Novitates. **1936**. N 829

Godovikov A.A. O kaltsite iz kar'era u derevni Amerovo Moskovskoi oblasti (About calcite from an open pit near the village of Amerovo of the Moscow oblast) // Proceedings of the Fersman Mineralogical Museum of the Academy of Sciences of the USSR. M.: Nauka, **1961**. Issue 12. P. 177-181 (Rus.)

Grigorev D.P. Generatsii i zarozhdeniya mineralov (Generations and initiation of minerals) // Mineral. Lvov Geological Society. **1949**. # 3 (Rus.)

Grigoriev D.P., ZHabin A.G. Ontogeniya mineralov. Individy. (Ontogeny of minerals. Individuals). M.: Nauka, **1975**.339 p. (Rus.)

Kantor B.Z. Besedy o mineralakh (Talks about minerals). M.: Astrel, **1997**.135 p. (Rus.)

Novgorodova M.I. Sluchai epitaksicheskogo narastaniya kristalla pirita na khalkopirit (Case of epitactic grow-over of a pyrite crystal on chalcopyrite) // ZVMO. **1977**. Part 106. Issue 1. P. 99-102 (Rus.)

Popoff B. Spharolithenbau und strahlungs kristallisation // Latv. Farm. Zurn. Riga, **1934**.48 s.

Shubnikov A.V. O zarodyshevykh formakh sferolitov (On germinal forms of spherulites) // Crystallography, **1957**. V. 2. Issue 5. P. 584-589 (Rus.)

Shubnikov A.V. Ob obrazovanii sferolitov (On formations of spherulites) // Crystallography, **1957**. V. 2. Issue 3. P. 424-427 (Rus.)

Slyotov V.A, Makarenko V.S. Risuya mineraly (Drawing minerals). M.: Ocean Pictures Ltd, **2001**. 24 Fig. (Rus.)

Slyotov V.A, Makarenko V.S. Risuya mineraly. Ontogeniya mineralov v risunkakh (Drawing minerals. Ontogeny of minerals in drawings. Issue II.). M.: Ocean Pictures Ltd, **2002**. 32 Fig. (Rus.)

Slyotov V.A. Risuya mineraly // Sredi mineralov (Drawing minerals // Among minerals). Almanac — **2001**. M.: Publishing house of the Fer-

Mineralogical Museums and Collections

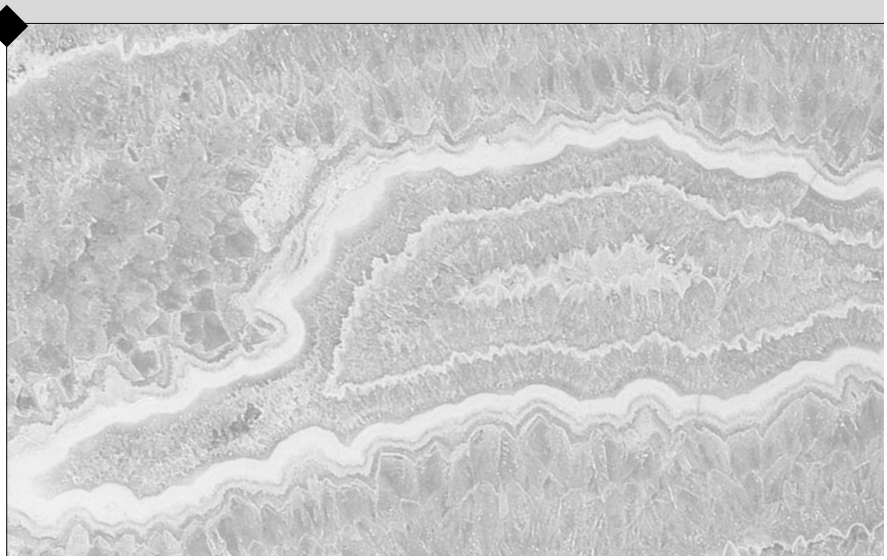

UDC 069:549

FABERGE LAPIDARY IN THE FERSMAN MINERALOGICAL MUSEUM COLLECTION

Marianna B. Chistyakova
Fersman Mineralogical Museum, RAS, Moscow mineral@fmm.ru

The Faberge collection of the Fersman Mineralogical Museum comprises a diverse group of Peter Carl Faberge masterpieces: functional items, flowers, animals, human figures, and Easter presentations.
Numerous cut gems from the Faberge lapidary workshops and others from their family collections are exhibited there.
This article describe these items.
30 color plates, 6 references.

Numerous publications describe the Faberge products. However, a great part of these deal with items now displayed outside of Russia. Collections of the Armory Chamber and State Hermitage are widely known. Items, which belong to the non-art museums are less known. Some of the collections are interesting, even unique. We believe that the Fersman Mineralogical Museum collection is one of these.

The gem and art stone collection of the Museum gained a greater part of its exhibits during the 1920s. It was a period when the state confiscated huge amounts of jewelry and pieces of art from the palaces of the tsar's family and the wealthy to transfer these, via the Museum Fund, to various museums. This was the way some lapidary masterworks were acqvired by the Mineralogical Museum. Among these were products of the famous House of Faberge. In addition, in 1926, Peter Carl's son Agafon Karlovich Faberge, a good friend of Academician A.E. Fersman, then director of the Museum, donated the remaining cut stones after the firm was closed. These were high-grade cut alexandrite, as well as variegated ornamental stones, completely representing the wide variety of gem materials the firm used. It is a known fact that the Faberge firm has been famous not just for its gold and platinum items adorned with diamonds, rubies, sapphires, and emeralds but also for its excellent works made from relatively inexpensive and common color stones (jasper, chalcedonies, garnets, malachite, lazurite, beryls, topaz, etc.)

Besides faceted gems A.K. Faberge contributed two items produced by the firm, of which one remained unfinished. His other donations were albums with photographs of Faberge workshops and some carvings, mainly flowers and animals. One album contained the sealing wax impressions of seals produced by the firm (Photo 1).

As a result of all these events, the Museum obtained about 30 masterpieces, more or less reliably attributed to Faberge.

The articles from the Museum collection fall into two groups. Items, which make the first group, are reliably attributed to Faberge. Another group comprises the items classified as the firm products just by analogy from available catalogues or by the expert judgments. More, it should be kept in mind that a good part of the objects in question had been transferred to the Museum via the Commission for Studies of the Natural Productive Forces; both A.E. Fersman and A.K. Faberge were its members. Most probably, both participated in selection and attribution of the objects for the Museum. Thus, a part of the exhibits from the Museum collection, which are not hallmarked but described by A.E. Fersman in his *Essays on the Gem History* (a section about the Faberge firm) we classify as products of the firm.

What are the minerals, which make this collection?

Cut stones make up the majority (a total of 40 minerals and varieties). These are inexpensive colored stones: garnets (pyrope and almandine), quartz (rock crystal, smoky quartz, citrine, amethyst, and chalcedony), topaz and beryl (emerald, aquamarine, and heliodor). Moonstone, tourmaline, opal, zircon, spinel, and phenacite (the mineral then unknown to non-specialists) are a smaller part of this donation. Malachite, amazonite, jasper, aventurine, and even flint represent opaque materials. Several items are made of amber and turquoise. It is interesting that they used chiastolite (an opaque variety of andalusite containing black carbonaceous impurities cut so that a section normal to the longer axis of the crystal shows a cross-like pattern); this mineral is a rarity in lapidary and jewelry.

The majority, of these are conventional gems of various colors and cuts. Along with

standard cuts, some stones present the playing card suite symbols, small shields, and other designs.

In addition to various stone products originating from the workshop of the firm, the Museum possesses a series of beautifully cut gems previously owned the Faberge family. This fact is recorded from a personal communication of V.I. Kryzhanovsky, a former director of the Museum. It comprises large greenish beryls, blue aquamarines, heliodors, topazes (blue ones from Russia and colored from Brazil), a large finely cut olivine (chrysolite), small star sapphires, rubies, opals, chrysoberyls, alexandrites, and spectacular amethysts (Photo2). This part of the collection presents unique exhibits of historical importance, as it demonstrates personal preferences of their owners. A series of Brazilian topaz comprises 12 large finely cut stones of yellow, wine, gold, orange, and violet (Photo 3). Many gemologists believe that the quality of these gems and their color range, is unique.

The statuettes in the Museum do not use a wide variety of materials. F.P. Birnbaum, a chief artist of the firm, named seven varieties of the colored stones predominately employed: jade (of six hues), rhodonite, jasper, the so-called Belorechensk quartz (aventurine bowenite, Lapis lasuli), and rock crystal. Further he reports that, along with the above, a wide variety of other stones, including the seashore pebbles and chips of simple stone pavement blocks could have been used, provided the patterns these exhibited were appropriate and artistically interesting: (Birnbaum, 1997, p. 69). This approach has been especially typical of the period after 1908, when the firm started a lapidary workshop of its own headed by P.M. Kremlev, a talented artist. Evidently, the exhibits from the Museum collection belong to that period, as evidenced by F.P. Birnbaum and indicated by the very style of the items the masters developed and cherished. F.P. Birnbaum classified the works the firm produced into two categories, those that required settings, and those, which did not. The Museum possesses items from both.

One of the best Faberge carvings in the Museum belongs to the first group. This is a low vase, with bowl and foot cut from rock crystal from Madagascar colored enamel and gems adorn the gilded silver details of this vase hallmarked by H. Vigstroem. A.K. Faberge donated this vase in 1925, and relevant facts are recorded according to his statement (Photo 4).

Other objects of the same category are a jade desk set of nine items, with the silver bearing the hallmark of A. Hallstroem (Photo 5) and an exquisite little cup made of a violet-green moss agate with a gilded silver handle having the hallmark of M. Perkhin (Photo 6).

Probably, the most exquisite Faberge masterpiece in the Museum is a bonsai tree: a tiny golden pine entwined by a blooming vine; both «grow» from a cylindrical vessel (Photo 8). The trunk of the pine and the liana are made of gold, the leaves are jade, and the vines blossoms are of greenish-gray and light grayish-violet enamel. The pine needles hide bright emerald sparkles. The vessel is cut of marble onyx, and the stand of bowenite. F.A. Afanas'yev hallmarked this composition (note that such pieces are not typical of this artist).

A massive matchbox made of coarse-grained brown aventurine, (from Shoksha, Karelia), a recent acquisition of the Museum, is a stone mushroom mounted on a silver cylindrical stand hallmarked by Yu. Rappoport (Photo 7).

However, works with no metal setting prevail in the Faberge collection. They are composite carvings of animals and people cut from colored stones great favorites of the public. Two of these are widely known due to numerous exhibitions and publications: A Reserve Regiment Soldier, 1914 (Photo 9) and An Ice Carrier (Photo 10). F.P. Birnbaum mentioned these as the best pieces of art of the type the firm produced (Birnbaum, 1997, p. 74).

Of stones used in these sculptures, F.P. Birnbaum mentioned just quartz (snow along which the ice-carrying sledge runners) and jasper (a figure of a horse). A.E. Fersman gave a detailed description of stones used in the *Ice Carrier* composition, but reported no data on the *Soldier*. The latter is listed in the Museum catalogue as a jasper item.

The results we obtained from detailed studies of the *Soldier* are as follows. His face, hands, a cap, a uniform, and a butt of his rifle are made of jasper. Flint or Jasper is the material used to make the hair. Breeches and a cauldron are green slightly patterned calcite, a bag is made of fine-grained granite; black high boots previously believed to be made of gagatite turned out to be made of fine-grained carbonate rock (black calcite). The materials of his trench coat and flask remained unrecognized. Large magnification reveals fine-grained low-porosity rock composed of colorless (quartz?) and opaque grayish-yellow grains of a soft mineral, probably, altered feldspar-quartz sandstone, a good imitation of coarse wool fabric. The belt buckle is made of gold, and silver is used for metal parts of the rifle.

Soldier is a rare signed carving: an engraving on a sole of his boot reads *Faberge 1915*.

Ice Carrier required a wider variety of stones. Along with several kinds of jasper, it employs cacholong (an apron), jade (an earflap cap) lazurite (trousers) and serpentine (a shaft-bow) from the Urals, along with bowenite. The latter has been imported from New Zealand via England. Pieces of ice are made of white quartz of various transparency, and snow is grayish-white quartz. The rein and ropes that fix the load are silver. This sculpture bears no hallmark. The Museum owns a silver copy of this composition (only snow is quartz) hallmarked by Ya. Armfel't (photo 11).

G.K. Savitsky is an author of the concept of both *Soldier* and *Ice Carrier*. In F.P. Birbaum's opinion, Savitsky «displayed here his fine taste and keenness of observation».

Three animal figures are made of pale green slightly translucent bowenite. These are a sitting lion of somewhat arrogant appearance (Photo 12), an elephant, and a baby elephant (Photo 13). The baby elephant is especially nice and funny with his raised leg and stuck out trunk. Eyes of the elephants are made of small ruby cabochons set in gold. The Museum obtained the lion's figure eyeless, and the Faberge masters could have hardly employed the material used: it is glass.

Several more small sculptures represent the animal world. A mouse that exhibits a laconic style has a smooth polished surface (Photo 14). A pair of geese, is a masterpiece of fine work: literally, all feathers are countable on their bodies (Photo 15). Natural poses of the animals are reproduced quite precisely. Light-colored material softens bulky contours of the birds. A gold chain connects flat golden rings with diamonds and rubies on the legs of the geese. Eyes of the birds are rubies framed with gold.

A snail that creeps out of its shell and an owl are both made of opaque stones. The snail shell is made of silvery obsidian, and the snail is jade. The knobby surface of the «living creature» beautifully contrasts the smoothness of its mineral «shelter». The snail raised only one of its feelers, the other remains pulled in. This small detail makes the figure lively and natural (Photo 16)

An owl is a tiny figure of fine-grained ganite that gives a fair imitation of feathers. Eyes are rubies set in gold (Photo 17).

Another spectacular carving is a spherical fluted cup with a wilted bud in it and an exquisite handle. The whole composition is cut from a single piece of agate with alternating brown and yellow layers (Photo 18).

A.E. Fersman reproduced the images of two little vases of Belorechensk quartzite (Photo 19) in his Essays on the History of the Stone when describing the Faberge products (1954, v. 1, p. 138). No other data are available on the authorship of these items. The Faberge catalogs we know of contain no descriptions of similar objects. The same situation exists with other two little flasks (presumably, glue containers), a Belorechensk quartzite apple (Photo 19) and a pear made of bowenite (Photo 20). Similar objects and their sketches are known to be produced by the firm (Tillander-Godenhielm et al, 2000); however, the attribution remains questionable. A.E. Fersman, a friend of A.K. Faberge, could have classified these items by a personal communication of the latter.

Due to the same reason we conditionally classify as Faberge works a carved bowl and a tureen made of dark gray talc-chlorite schist (Photo 21). Oriental (Siamese, according to A.E. Fersman, 1954) ornaments cover the outer surfaces of these objects totally. Faberge, via his London branch, dealt with the Far East countries, mainly with India and Siam (now Thailand). Orders from Siamese royal court were especially numerous. On invitation from Prince Tchakrobong who used to study in St. Petersburg, Peter Carl Faberge visited Siam and had been awarded a title of royal «jeweler and enamellist» (Tillander-Godenhielm et al, 2000). Jewelry prevailed in supplies to Siam, but pieces of art produced from relatively inexpensive materials are a possibility, as was the case in Russia and Europe.

A modest delicate leaf-like trough is made of dark-green, almost black jade, a material infrequently used (Photo 23). A gold inscription on its container reads: K. Werfel. The same workshop produced a large round smooth plate made of East Siberian (Onot) jade. It is not ornamented; presumably, they planned to use metal decorations.

Flowers are among the most popular Faberge articles. Their meticulous workmanship is striking. Lapidaries have been unbelievably skillful here: a dandelion with a stone stem and a realistic blossom is an example. The Museum collection has a sweet pea in a little vase (Photo 22). Petals are made of aventurine and rhodonite; a vase (with some «water» it) is rock crystal. The stem is not a commonly used copper wire wrapped in silk, but jade. F.P. Birnbaum believed that it is the same as shoeing a flea: labor consuming and impractical (Birnbaum, 1997). This object is extremely fragile and joined the collection in fragments. After restoration it became transportable (cer-

tainly, with greatest care). A jade stem is a real rarity: there is no other in Moscow.

The Museum collection has two seals, one made of lazurite (Photo 24) and another of a quartz vein in syenite (Photo 26). Some art experts who studied these items presumed that these are Faberge works. Some of them were of the opinion that in the 19th and early in the 20th centuries Faberge was the only firm that produced small-faceted rounded items resembling the seals. However, we have no direct evidences.

Small stone eggs in a special box presumably served as specimens of the Easter presents the firm was famous for (Photo 25). Every egg bears a mark made with India ink. Some eggs have bases of gold; in other cases, it is a common metal. Several eggs are made of purpurine, a special glass, developed by S.P. Petukhov, a supervisor of the St. Petersburg glass works. The process was later lost (Donova, 1973). Presumably, Faberge was the only firm that employed it. Other purpurine articles in the Museum are several small eggs (Photo 27) and a flat round plate.

A large oval-shaped fluted silver box manufactured in the Faberge workshop is interesting. It has no stone parts, but contains a dozen of glass silver-plugged tubes filled with gold sand from the Nerchinsk (the Transbaikal area) placer mines. It was a gift from the owners of the mines to crown prince (tsesarevich) Nicolas on his return from Japan via Siberia in 1891. A map of the Nerchinsk uyezd (a territorial unit) is engraved on the lid, along with a decorative metal band with inscription and the state emblem (Photo 28).

Finally, the Museum owns another remarkable article, the Tsesarevich Constellation, an unfinished Easter egg of 1917 that K. Faberge donated to the Museum. Its history is tragic. It was the last article Nicolas II ordered from Faberge as an Easter presentation for Empress Alexandra Fyodorovna.

The first of the famous Easter eggs Faberge produced for the Russian tsars was made in 1885 as a present from Alexander III to Empress Maria Fyodorovna, his wife. She liked it so much that every year Alexander III gave her as a Faberge Easter egg present a new symbol of the resurrection. Nicolas II continued this tradition and every year ordered an egg for his mother and another for his wife.

The last two eggs were ordered to be made for the Easter of 1917. These remained unfinished. In March Nicolas II gave up his crown and celebrated Easter in Tsarskoe Selo near St. Petersburg after his arrest. Chaos seized Russia. The Faberge firm was closed. F.P. Birnbaum just mentioned in his memoirs that orders remained unfinished. In his letter to Evgeny Karlovich Faberge he wrote that he knows nothing about their location.

Many years later (first in 1953, then in 1986 and 1997) the sketches of these eggs were published, preserved in an archive of T.F. Faberge, a great-granddaughter of Peter Carl Faberge (Faberge *et al.*, 1997). Still, there were no data on those eggs.

In 1925, prior to his escape from Russia, A.K. Faberge, donated to the Fersman Museum along with other articles, pieces of a composite carving: two halves of a glass egg and a cloud-like support made of the rock crystal. Orifices had been drilled in the egg and support, but other details were missing. This egg was stored in the Museum for about 80 years, until V.Yu. Voldayeva, an art expert from the Gokhran (State Storage) Museum happened to see it. At her (and our) request, T.N. Muntian, a supervisor of the Russian jewelry collection in the Armory Chamber, studied it. Subsequent events were rapid. A comparison to the published sketch (Photo 29) and F.P. Birnbaum's description demonstrated that this has been the unfinished Easter egg ordered in 1917 that had disappeared and had been considered as a loss (Muntian, 2002, 2003).

The sketch shows a cloud positioned above a rectangular jade stand (as Birnbaum described) with cherubs on it supporting a celestial sphere. Unfortunately, both cherubs and the stand either were never made, or missed being acquired by the Museum. Thus, the Museum now owns only two halves of the egg as hemispheres of dark blue cobalt glass and a rock crystal cloud. A skillfully matted rock crystal surface brings exquisite translucency and sprightliness to this cloud of stone. The upper half of the egg displays constellations of the Northern Hemisphere, and the stars on it were to be diamonds. The smallest of these remained on the glass. The largest stone was due to be in Leo: under this sign Alexei the crown prince was born, the hope of the tsar's family for continuation of the dynasty.

The egg joined the Museum collection as separate parts and could not be exhibited in public. After an appeal from the Museum, Yu.A. Ossipov, an artist and restorer of the Kremlin Art Workshop, assembled it following the original sketch (Photo 30).

The public saw it for the first time at the Faberge Easter Egg exhibition along with articles from the Armory Chamber and State Hermitage. Now it is safely back in the Museum.

Thus, the collection of the Mineralogical Museum has an almost complete range of the Faberge works which includes the mineral materials used by the firm and their spectrum of colors.

References

*Birnbaum, F.P. (***1997**) The Faberge history: lapidaries, jewelry, and silverware. In: Faberge, T.F., Gorynya, A.S., and Skurbov, V.V. Faberge i peterburgskie yuveliry [Faberge and jewelers of St, Petersburg] St. Petersburg, Neva, 703 p. (Rus.)

Donova, K.V. (**1973**) Articles from M. Perkhin's workshop. In: Materialy i issledovaniya. Gosudarstvennye muzei Moskovskogo Kremlya [Materials and research. State museums of the Moscow Kremlin] Moscow, Iskusstvo, p. 11 (Rus.)

Faberge, T., Proler, L.G., Skurlov, V.V. (**1997**) The Faberge Imperial Easter Eggs. London, 62 pp.

*Fersman, A.E. (***1954**) Ocherki po istorii kamnya [Essays on the history of stone]. Moscow, AN SSSR, V. 1, 368 pp. (Rus.)

Habsburg, G. (1986) Faberge, Hofjuwelier der Zaren.Muenchen, 95 pp.

Muntian, T.N. (**2003**) Paskhal'nye podarki Faberge [The Faberge Easter presents] Moscow, Tabu, 83 pp. (Rus.)

Muntian, T.N. Chistyakova, M.B. (**2003**) A symbol of disappearing Empire. The rediscovery of the Faberge Collection Easter Egg. Appolo, No. 1, p. 64

Snowman, A.K. (**1953**) The art of Karl Faberge, London, 1953, 355 pp.

Tillander-Godenhielm, U., Schaffer, P.L., Ilich, A.M., Schaffer, M.A. (**2000**) Golden Years of Faberge. A la Vieille Russia. Christie's, p. 14–15

UDC 549.069

CHINESE JADE DISKS FROM THE FERSMAN MINERALOGICAL MUSEUM (RAS) COLLECTION. EXPERIENCE IN ATTRIBUTION. SIGNIFICANCE AND PLACE IN CHINESE TRADITIONS

Daria D. Novgorodova
Fersman Mineralogical Museum, RAS, Moscow, daria@fmm.ru

The gem and stone art collection of Fersman Mineralogical Museum, RAS, Moscow, contains three jade disks. In 1998, these were identified as Chinese ritual *bi* disks, and their attribution begun. This paper presents the study results, along with a brief historical review of the *bi* disks as symbols inherent in Chinese cultural traditions, from the Neolithic period to present. Relevant functions and rituals are described, as well as the attribution problems associated with this jade lapidary type.
Exquisite lapidaries from Fersman Museum collection combine a great academic and aesthetical value, and Chinese jade articles are among the most interesting of these. Their historical and cultural significance in the traditional Chinese culture makes an innate part of their value as the museum exhibits.
1 table, 14 figures, 11 references.

The inventory carried out in Fersman Museum in 1998 required specification of some lapidaries. Small jade disks first listed in the first half of the 20th century were registered in the catalog as «two carved disks», and an old label specified: «two carved disks with holes at their middle parts». These items required description that is more exact. The exhibits were classified as Chinese ritual *bi* disks. Further task was to give a written depiction, obtain, and systematize data on historical and cultural significance of the *bi*.

Pieces of art as exhibits of the natural history museums are rare objects of the joint art expert and academic art history studies, whereas an adequate perception of the old natural history-oriented collections, like those of Fersman Museum, becomes a possibility in case aesthetics and science merge. Such aesthetic approach to scientific exposures and studies of the stone art artistic techniques has ever been an innate part of the classical mineralogical museum studies. The *bi* disks, like other Chinese lapidaries, present the attributes of sophisticated mythology with its hierarchy of symbols. These are outstanding pieces of the Fersman Museum collection, which make this stone art anthology valuable.

Bi disks from the Fersman Museum collection

Jade disks from the Fersman Museum collection are small carved items; two of these have a smooth edge and a shallow geometric pattern, whereas the third one is ornamented with a coiled dragon (Photos 1a, 1b, 1c). The first two disks joined the gem and stone art collection in 1923 as donations from V.I Kryzhanovsky, the then chief scholarly supervisor of the Museum (ID 2346, further Disk 1 and 2), and the last one was obtained from the State Historical Museum in 1949 (ID 4662, further Disk 3).

Disk 1 is made of pale yellow to dark brown jade; Disk 2 is straw-colored (light to medium), and Disk 3 is white. All three disks are almost ideal rounds of similar dimensions (cm): 5.6 and 0.30 to 0.41; 5.8 and 0.31 to 0.41; 5.7 and 0.22 to 0.40 (diameter and thickness of Disks 1, 2, and 3, respectively). A hole in Disk 2 is significantly off the center (about 0.2 cm).

Patterns engraved on Disks 1 and 2 are alike: one side of Disk 1 and both sides of Disk 2 exhibit belts of alternating vertical and horizontal trigrams. Four «cloud coils» occur at the center of the Disk 1 front side. Its other side is free of the trigram belt, and the «cloud coils» occupy it whole: these make four groups, each containing a rhombic latticework as a core surrounded with three coils. Disk 2 exhibits the same pattern on its both sides: a trigram belt along the edge and a four-member ornament made of short lines and curves. The meaning of the latter as a symbol is not clear. The «cloud curls» and trigrams (i.e., groups of three solid lines) symbolize skies. Further, we will see that such patterns correlate with a general symbol system traditional of Chinese jade disks.

An ornament engraved on Disk 3 portrays a fantastic beast (a coiled dragon). Despite its complexity, its contours reproduced on both sides of the disk are identical.

These items are traditional Chinese ritual disks *bi* (*pi*). *Bi* disks evolved in the Late Neolithic period as magic attributes. By majority, the *bi* disks are made of nephtite; serpentinite is a rare alternative, jadeite ancient disks are unknowns. *Bi* disks «outlived» coeval magic objects to be

preserved in Chinese material culture to present days, and their functions changed with time.

What is a bi disk?

Three major traditions were and still are the major controls of symbolic and cultural frameworks, which enable interpretation of the pieces of art: Confucianism, Taoism, and Buddhism. The pre-Confucian ancient system and the one existing now are the necessary completions. Thus, it turned out that *bi* belongs to all and every system mentioned, Buddhism excluded, being an innate element of Chinese culture.

By the 5th century B.C., a Confucian canon fixed the ritual function of a *bi* as a symbol of Skies to be sacrificed to these; due to it, the disk should be of sky-blue color. As profane items, the *bi* disks served as insignia of the fifth and fourth-rank Chinese officials; in these cases, the disks were due to carry the grain or bamboo pattern (Nott, 1977; Gump, 1962).

However, the *bi* disks were known in China since the pre-historical period, when their function in rituals had been different.

Ancient bi disks of the Late Neolithic period (5000–2200 B.C.)

The oldest Chinese jade disks (subsequently named *bi*) originate from Herneudu-Liangzhu culture; these are dated as Late Neolithic (5000–4000 B.C.), i.e., well before characters came into practice and 45 centuries before Confucius and Lao-tze (Nott, 1977; The Golden Age..., 1999). Numerous *bi* disks were found in tombs of the period, usually in combination with *ts'ung* (*cong*) tubes. *Ts'ung* is a prism, a square in its cross-section, with a cylindrical inner chamber. If viewed from top, it forms a circle inscribed into a square (Photo 2). *Bi* and *ts'ung* make a couple where *bi* serves as a lid. Researchers interpreted this as the first Chinese cosmological model comprising a square Earth and round Skies. Later this will propagate over the whole country.

The number of sepulchral jade lapidaries varied with a social position of a deceased. One tomb contained 25 *bi* disks and 33 *ts'ung* tubes (Fig. 1). Some tombs have been filled up with jade lapidaries.

Frequently, sepulchral rituals included cremation of jade lapidaries: first, these were placed into fire at the tomb, and, subsequently, the corpse was lowered into it.

In ancient China they valued jade higher than jadeite. An original explanation of the fact is that jadeite (which melting temperature is lower than that of jade), when placed into an open fire, melts to form colorless transparent beads, whereas jade gains a beautiful creamery coating, so its value grows. *Myths of the Ancient China* (He Yuan, 1987) read: «Common jadeite turned into scoria, whereas the Skies Wisdom jade remained». In Ancient China, they called the fire-treated jade «chicken bones». Such jade variety is of a special high price in the antiquity market; hence frequent falsifications. Note that no jadeite lapidaries are known to originate from Ancient China.

Written sources specify yet another function of the Neolithic jade disks. *Shuo Wкn*, the first Chinese dictionaty (*c.* 2nd century B.C.) witnesses that the *bi* disks ornamented with the coiled dragon images served as attributes of the prayer for rain ceremonies during the Shкn -nung (the Divine Husbandman) reign (Nott, 1977). What is the period in question?

Here we should address the Chinese history timeline (Table 1).

The whole history of China could be conditionally divided into two parts, a legendary period and a historical (documented) one. The Hsia dynasty (2205–1766 B.C.) is believed to be the first. However, legends, not documents make a basis for this notion, so frequently this dynasty is called legendary. For long they considered the first really historical dynasty, Shang (1766–1027 B.C.), as a legend, too, until excavations carried out as late as in the 20th century brought documentary evidences (records on the bone and bronze items used by fortune-tellers).

Legends tell that five emperors reigned prior to the Hsia dynasty.

Monarchy in China was founded by Fu Hi, a primordial ancestor of all Chinese; his reign began in 2852 B.C. Shкn -nung, the Divine Husbandman, succeeded him (2737 to 2697 B.C.) to be followed by Huang-ti, the Yellow Emperor.

Thus, the period in question is the third millennium B.C. Rituals related to prayers for rain and harvest were of major importance in Neolithic communities (Vassil'ev, 2001). These were performed by shamans (not infrequently, shamanesses). Having adorned one's garments with numerous jade items (animalistic images prevailed), such shamans went to a field, got self-entranced, and prayed to spirits and Skies for rain and harvest to be granted. Occasionally, shamans got themselves burned as a sacrifice intended to stop draught. Ancient Chinese myths frequently refer to jade decorations as attributes of such cremation ceremonies. To please the spirits of water, they threw jade lapidaries to streams.

Photo 1. Chinese ritual bi (pi) disks from the collection of the Fersman Mineralogical Museum, RAS: a,b) FMM, ID 2346; c) FMM, ID 4662

Thus, *bi* disks served not just as the sepulchral items, but as shamanic attributes as well.

Here is another interesting detail. Commentaries for *Chou Li* (the 2nd century B.C.), a book that described rituals existed during the Chou dynasty, present the first detailed record on the *bi* disk. Such disks should have a square hole at its center (i.e., a round of Skies surrounds a square Earth). However, no finds of such disks are known by now. Instead, traditional Chinese coins match this description. Due to the fact, some researchers (Lanfer, 1912) believed that these coins originated from *bi* disks used in sacrifices.

In addition to the Neolithic history of *bi*, we should mention numerous finds of these items in the Lake Baikal area. Convincing explanations of the fact remain unfound.

Neolithic ritual disks are relatively large (30 to 35 cm in diameter) and carry no ornamentations (Photos 3a, 3b). Their simplicity contrasts sharply with elaborateness of other Neolithic jade lapidaries (The Golden Age..., 1999).

Some disks have small punctures along the edge. Presumably, such disks served as shamanic attributes, not sepulchral rituals (Photo 3, in the right).

Historical China: Shang (1766–1122 B.C.), Chou (1122–255 B.C.), and Ch'in (255–207 B.C.) dynasties

During the Shang dynasty reign (1766–1122 B.C.), the jade lapidary art kept on progressing. The sepulchral jades remained mainly unchanged. In addition to the *bi-ts'ung* couple, the *kuei* ritual plaque was introduced (Fig. 2). By the middle of the next dynastic period, it replaced ts'ung to make a couple for *bi*. Subsequently, the Confucian «Book of the Rules»(Li Chi) will establish *kuei* as a symbol of East, which should be of green color.

Sepulchral *bi* disks of the Shang period remained practically the same as Neolithic: these are large and carry no ornamentations.

The **Chow** dynasty reign (1122 to 255 B.C.) was the blooming period of lapidary.

Tombs of that period contain an unbelievable *bi* variety. These differ in size; this is the period when the *bi* disks gained ornaments (Fig. 3a, 3b). The *bi* disks become applicable in areas other than funeral rituals. The earliest finds of the coiled dragon pattern engraved on the *bi* disk are dated by this period (Fig. 3b; the disk is 16 cm in diameter).

Table 1. Chinese history timeline (after Nott, 1977)

Dynasty	*Dates*
Hsia (legendary)	2205–1766 B.C.
Shang	1766–1121 B.C.
Chou	1122–255 B.C.
Ch'in	255–206 B.C.
Han	206 B.C.–A.D. 225
Three Kingdoms	A.D. 221–265
Chin	A.D. 265–420
Northern and Southern Dynasties (Nan Pei Ch'ao)	A.D. 420–589
Sui	A.D. 589–618
T'ang	A.D. 618–907
Five Dynasties (Wu Tai)	A.D. 907–960
Sung	A.D. 960–1129
Yuan (Mongolian)	A.D. 1279–1368
Ming	A.D. 1368–1644
Ch'ing (Manchu)	A.D. 1644–1911
Republic	A.D. 1911–

In compliance with Confucius, the *bi* disks were used as ceremonial decorations and just pendants (Photo 4). The *bi* disks became the components of the applied art objects (Photo 5).

During this period, jade of highest grade makes a material for decorations for living people, and not for sepulchral attributes. Another meaning of the *bi* disks assigned to these during the period was that of a good wish, unrelated to funerals or shamanism (Nott, 1977).

A short rule of the **Ch'in** dynasty (255–207 B.C.) is among the highly notable episodes of the Chinese history. Ch'in Shin Huang-ti was both a tyrant and reformer. Immortality was his dream, so innumerable missions of Taoists were sent to find and get the remedies, which would cause this effect. It was he who initiated construction of the Great Chinese Wall, and famous terracotta army guards his tomb (discovered in 1971). This emperor initiated the «cultural revolution» pattern, having ordered thousands of Confucian books to be burned in public.

Mass interest aroused by Taoists who tried to achieve immortality fed the myths related to jade properties, especially to its would-be ability to grant eternal life.

The Han dynasty (207 B.C.–A.D. 220). Sepulchral jade garments. Bi disk as a stair of the heavenly ladder

Under the influence of Taoism, a sepulchral «jade garments» became an attribute of superior nobility during the Han dynasty, 207 B.C.–A.D. 220 (Fig. 4).

Photo 7. Disk bi, the Han epoch (The golden age..., 1999)
Photo 8. A pendant of the Han epoch with the bi disks (The golden age..., 1999)
Photo 9. A dragon with the bi disk: a bucket of the Han epoch (The golden age..., 1999)

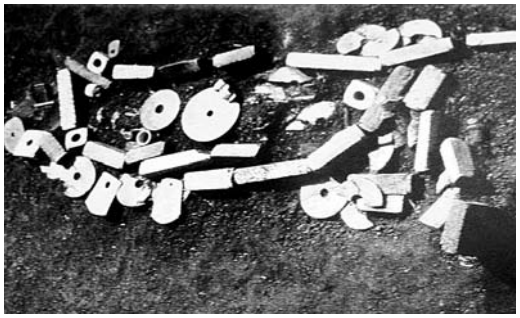

FIG. 1. Bi disks and ts'ung tubes, a burial of the Liangchu culture (3000–2000 B.C., Debain-Francfort, 2002)

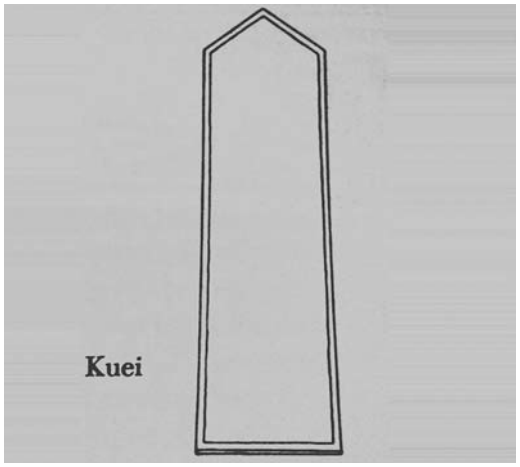

FIG. 2. Kuei, a ritual plaque (Gump, 1962)

FIG. 3a. Disks "bi" of Chou dinasty

Along with Confucian canon, a complicated series of Taoism traditions has been developing, including those Confucius rejected as superstitions: ancient shamanic rituals that employed jade, and new magic aimed at achievement of longevity and immortality, where jade, along with cinnabar, played an important role. During a century and a half, a religious branch of Taoism suppressed a philosophical one founded by Lao-tze and Chuang-tze to become a leading religious system in China (Vassil'yev, 2001).

Notions on jade as a substance that prevents a dead body from putrefaction (provided all nine natural orifices of the body closed with jade items and a cicada as a revival symbol is put into a dead person's mouth) strengthened during the Han dynasty (Nott, 1977; The golden age, 1999). *Bi* disks make an obligatory element of the sepulchral garments (Fig. 5, reproduced from The golden age..., 1999). These garments are made of jade plates connected with gold wires, and the *bi* disk is located on a sinciput. Presumably, this was done to assist the human soul, *hung*, to leave a body and ascend to heaven. *Bi* disk is a heavenly ladder.

During the Han dynasty, the jade lapidary art stood high. Shape, dimensions, and ornamentation of the *bi* disks varied widely (Photos 6, 7). Complicated sets of pendants made of small jade details, *bi* included, are typical (Photo 8). *Bi* disks became important elements of personal decoration. It played a composed role of symbol and decorative element (e.g., a bucket on Photo 9).

It has been a period when an important feature of Chinese culture revealed brightly, affection and respect to antiquities. One of the tombs contained a pre-dynastic *ts'ung* tube framed in bronze as a jewelry (probably, a family relic). First documentary descriptions described ancient bronze items and lapidaries (Debain-Francfort, 2002). Many chapters from Historical Minutes written by Syma Tsian, a prominent Chinese historian, give detailed ancient items. All that made a base for subsequent (during the Sung reign) numerous catalogues of antiquities (Debain-Francfort, 2002).

Post–Han period (A.D. 220 –): why the bi disks remained

Actually, here the historical description of the *bi* disks could be finished. Next epochs brought nothing new into their functions and patterns. However, *bi* disks have been produced in later periods, and are produced now.

In the post-Han period, jade disappears from sepulchral ceremonies. However, ceremonies practiced in Chinese imperial court

employed jade as late as 1911, i.e., by the end of the Ch'ing (Manchu) dynasty. *Bi* disks were decorative and ceremonial items. Magic and sepulchral functions of *bi* could have been preserved as parts of folk traditions, preserved and encouraged by Taoism.

Subsequent Six dynastics period (A.D. 220 – 589) has been a time of unrest in China. The lapidary art stagnated. Historians never mentioned jade lapidaries of the period. During the Tang dynasty (A.D. 589 – 906), Buddhism has come into China. New motifs in the jade lapidary of the period are benign symbols, mainly figures of animals and decorative belt buckles (Nott, 1977).

The Sung dynastical period (A.D. 960 – 1279) exhibited a general cultural rise of the nation; a new noble tradition seized the whole China: honoring and studying of antiquity.

Copying of antique items has become a tradition. Lists of items originated from the past dynasties have been issued, supplied with exquisite drawings and detailed descriptions. Collecting of old artifacts has become a conventional pastime. It turned out to be akin to archeology: the loot originated from the graveyard marauding had been described and drawn in detail.

Throughout further history of Chinese dynasties, items of newly emerging styles peacefully co-existed with originals and copies of the past periods. More, since jade lapidaries remained as everlasting traditional valuables of Chinese society, the skill of imitation and forgery here has improved for centuries and centuries. The *bi* disks have become the objects of imitation and forgery along with other jade lapidaries of the past.

In general, the jade lapidary tradition matches a general historical trend in the Chinese culture. Academician V.M. Alexeyev (1978) believes that, beginning with the times of Confucius, «unlike many other national literatures, nothing has been destroyed or terminated just for a single historical moment in Chinese literature; on the contrary, it progressed on and on... A Chinese writer, e.g., an author of the early 20th century, made a link of a continuous historical chain of literature beginning with Confucius (6th – 5th century B.C.); it would be natural for him to read verse composed by Chuang-tze, a poet and philosopher of the 4th century B.C., whose every character had been as clear to him as characters from a newspaper of the same 20th century.»

The same could be told of Chinese lapidists. Their knowledge on the art of their predecessors has been deep, being a living practice rather than abstract notion. Familiarity with cultural traditions and their preservation since

FIG. 3b. Disks "bi" of Chou dinasty

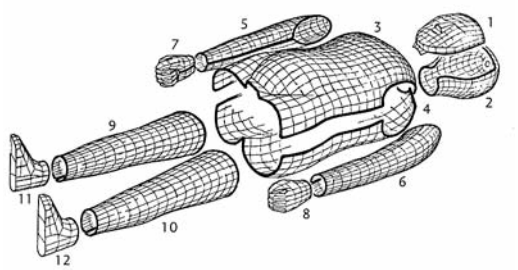

FIG .4. Jade sepulchral garment, the Han period (The golden age..., 1999)

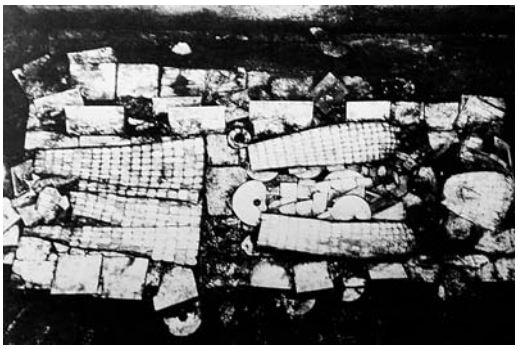

FIG. 5. Burial of the Han period. A jade garment (The golden age..., 1999)

the time of Confucius has been mandatory to the Chinese officials.

This is why the *bi* disks are on the market in modern China: real things, skillful imitations, and coarse forgery.

Problems of attribution

Jade lapidaries never carry inscriptions, which could assist in dating of an item (seals make the only exception). Everlasting turnover of patterns, motifs, and symbols inherent in Chinese jade lapidaries makes exact dating impossible in case origin of the item is unknown. In part, this is a special feature of Chinese culture. Unlike in the West, copying of predecessors is not considered as a plagiarism or annoying non-originality; on the contrary, in China this indicated good taste and high education level.

By its ornamentation, Disk 1 from the Fersman Museum collection resembles that of the Han dynasty (cf. Laufer, 1912); however, dated disks of the period carry no the trigram belts. All three disks are smaller than that of the ceremonial *bi*, which should be about 5 Chinese inches (1 Chinese inch varied from 22.5 to 33.3 mm), but the disks from the Fersman museum could have served as decorative pendants.

Disks 1 and 2 are slightly chipped along the edge; Disk 2 is slightly worn out from one side. This may be due to their usage, probably as pendants. Numerous copies of the Han jade lapidaries are known from the Ming epoch (700 to 1000 years later); later dating also is a possibility. True antiques exhibit high quality of engraving and careful finishing. Presumably, broken rhythm and displacements in the pattern, along with inaccurate cut of the lines notable at Disk 2 indicate the mass production of jade lapidaries that occurred in the end of the Ch'ing dynasty (the 19^{th} century).

Thus, Disks 1 and 2 could have been manufactured in China in the period beginning with the Ming (Disk 1) through the Ch'ing dynasty (Disk 2).

Disk 3 that displays a coiled dragon could be dated from the end of the Ming and to the early days of the Ch'ing dynasty (i.e., the second half of the 17^{th} century and later). Similar disks are recorded as the Chou items (Chinese sources mention such disks used in the third millennium B.C.). However, good preservation, smaller size relative to known ancient analogs, and, especially, the material Disk 3 is made of, i.e., high-grade white jade typical of the beginning of the Ch'ing (Manchu) dynasty (Nott, 1977) indicate that this disk is no older than the $17^{th} - 18^{th}$ century.

The 1900s make the upper age limit of these three disks: these have been listed in the Fersman Museum in 1923. The jade lapidary traditions last from ancient times, so a skilled lapidist could have produced a precise imitation of an old masterpiece.

In China, antiquities has ever been valued immeasurably higher that the modern things. High value of jade is a national Chinese tradition. Thus, a skill of imitation and forgery of jade lapidaries has a polish of ages. More, the age of some old forgeries makes these highly valuable.

Conclusions

Jade *bi* disks absorbed a multitude of myths and amazing stories. Books may be written about them. However, any kind of Chinese lapidary is like it. Uniqueness of Chinese culture that counts several millennia combined with a very special attitude of Chinese to lapidaries and, first, jade lapidaries bring these items some supernatural properties.

In modern China, where they produce imitations jade per se, as well as copies of jade lapidary antiquities, this material remains in demand, being valued high as before. Why — this is the question. Many minerals and rocks are believed to be of brighter color and more exquisite than jade. But since the days of old and to these days Chinese keep on saying: «Anything can be valued, but jade remains priceless».

References

Alexeyev, V.M. (**1978**) Kitaiskaya literatura [Chinese literature], Moscow, Vostochnaya literatura, 595 pp. (Rus.)

Debain-Francfort, K. (**2002**) Drevniy Kitai [Ancient China], Moscow, Astrel, 160 pp. (Rus.)

Desautels, P.E. (**1986**) The Jade Kingdom, NY, Van Nostrand Reinhold, 118 pp.

Gump, R. (**1962**) Jade: stone of heaven. NY, Doubleday, 260 pp.

Khe Yuan (**1987**) Mify drevnego Kitaya [Myths of the Ancient China], Moscow, Vostochnaya literatura, 527 pp. (Rus.)

Laufer, B. Jade: a Study of Chinese Archeology and Religion. Chicago, 370 pp.

Lubo-Lesnichenko, E.I. Kitai na shelkovom puti [China on the Silk Way] Moscow, Vostochnaya literatura, 394 pp. (Rus.)

Nott, St. Ch. (**1977**) Chinese jade throughout the age. Tokyo, Charles E. Tuttle, 193 pp.

Pope-Hennessy, D.U. (**1923**) Ancient China Simplified. London, Benn, 148 pp.

The golden age of Chinese archeology (**1999**) Washington, National Gallery of Art, 584 pp.

Vassil'yev, L.S. (**2001**) Kul'ty, religii, traditsii v Kitae [Cults, religions, and traditions in China], Moscow, Vostochnaya literatura, 488 pp. (Rus.)

UDK 549:069

NEW ACQUISITIONS TO THE FERSMAN MINERALOGICAL MUSEUM, RUSSIAN ACADEMY OF SCIENCES. 2002–2003

Dmitriy I. Belakovskiy,
Fersman Mineralogical Museum, RAS, e-mail: dmz@fmm.ru; website: http://www.fmm.ru

A total of 1,356 new mineral specimens were cataloged into the Fersman Mineralogical Museum main collections during the period 2002 to 2003. These specimens represent 640 different mineral species from 62 countries. Among these, 285 are new species for the Museum, including 10 species that were discovered by Museum staff members and 40 species that were discovered during this period by others. Of the minerals obtained, 54 are either type specimens or fragments of type specimens or cotypes. By the end of 2003 the number of valid mineral species in the Museum reached 2,910. Of the newly acquired items, approximately 51% were donated by 138 people and by 8 institutions, 18% were purchased, 15% specimens were collected by the Museum staff, 12% were exchanged with collectors and other museums, 3% were acquired as type specimens and 1% obtained in other ways. A review of the new acquisitions is presented by mineral species, geography, acquisition type, and source. The review is accompanied by a list of new species for the Museum along with a list of species that the Museum desires to obtain.

A total of 1356 specimens were cataloged into the Museum's five main collections[1] in the years 2002−2003. The cataloged material was separated as follows: 944 specimens were assigned to the systematic collection, 83 to the deposits collection, 230 to the crystal collection, 78 to the collection of mineral formation and transformation, and 21 specimens were catalogued into the gem collection.

About 65% of cataloged items were actually acquired in 2002−2003. The rest related to previously collected but uncataloged material. The processing of these materials could not be finished previously because of the huge volume of specimens collected. Additionally, some of the material from actively working mines, such as the iron sedimentary deposits near Kertch, Crimea, Ukraine or the Inder boron deposit in Kazakhstan was reserved (conserved) for a while to wait for possible new acquisitions with better or more representative specimens. Now those mines have stopped their operations, allowing the Museum curators to make a final selection of specimens from those deposits to either be cataloged to the main Museum collections or assigned to the exchange fund.

More than a half of acquisitions, about 51%, were donated to the Museum. Another 3% contributed as type specimens of newly discovered minerals also could be considered as donations. About 18% of the acquired items were purchased, 15% were collected by the Museum staff, 12% were obtained as an exchange with other museums and private collectors in Russia and abroad. The residual 1% came from other types of acquisitions.

This review only includes data on those specimens that were logged into the inventory of the Museum's major collections in years 2002 and 2003. Specimens that had not, at that time, been fully processed and catalogued, as well as specimens assigned to the exchange or research collections, are not included in this review.

New Acquisitions as Classified by Mineral Species

Specimens catalogued in 2002−2003 represent 640 mineral species, 285 of which are new species for the Museum. (See the list of these species given in Appendix 1). This number includes 54 species represented by type specimens, their fragments, or cotypes. 40 of the cataloged species were approved by the Commission on New Minerals and Mineral Names of the International Mineralogical Association, (IMA), since 2002, out of approximately 120 new mineral species approved for this period. 36 of those 40 species are represented by type specimens. Ten of these species were discovered and described by the Museum staff or in collaboration with the Museum staff. As of December 31, 2003 the number of valid mineral species in Fersman Museum collection totaled 2,910.

Of the 640 recently acquired mineral species, the majority, 443, are represented by only a single specimen. Another 98 are represented by 2 specimens; 3 to 5 specimens represent each of 70 species; 12 species are represented by 6 to 10 specimens and 14 species are represented by more than 10 specimens. (See Table #1 below).

Quartz and calcite are usually on the top of this list. During this period, the number of calcite specimens (34 specimens from 16 locali-

[1] The principles of subdividing Museum fund to different collections and criteria of assigning mineral specimens to those collections are given in previous new acquisition review (New data on minerals v.38, 2003).

Table 1 Mineral species by the number of specimens acquired. (for more than 5 specimens).

1.	Calcite	34	14.	Fluorapatite	10
2.	Quartz	31	15.	Xonotlite	9
3.	Vivianite	29	16.	Opal	8
4.	Hematite	24	17.	Beryl	8
5.	Sulphur	20	18.	Holfertite	8
6.	Barite	15	19.	Rutile	7
7.	Grossular	15	20.	Anapaite	7
8.	Orthoclase	14	21.	Galena	7
9.	Rhodochrosite	14	22.	Dioptase	7
10.	Hydroboracite	12	23.	Gypsum	6
11.	Corundum	11	24.	Titanite	6
12.	Pyrite	10	25.	Tsumoite	6
13.	Siderite	10	26.	Schorl	6

ties) is a bit more than for quartz and its varieties (31 specimens from 18 localities).

A considerable part of the calcite specimens are «glendonite», a calcite pseudomorph after ikaite, from Olenitsa village, Kola Peninsula. Some were collected by Museum employee A.Nikiforov and some were donated by A.Zakharov, M.Anosov and V.Levitskiy. Additional specimens came from the Bol'shaya Balakhnya river valley, Taimyr Peninsula, and were donated by D. Sulerzhitskiy. This grouping is a logical addition to a very comprehensive collection of «glendonite» from different localities around the world. A few decent druzes of scalenohedral calcite crystals recently mined in Dashkesan, Azerbaijan were purchased along with twinned, (by 120), loose calcite crystals up to 11cm from Argentina. A few other calcite druzes are from Dal'negorsk, Primorskiy Kray, Russia. These were donated by V.Ponomarenko and represent a combination of fully faced, splitted, and dendritic crystals. Calcite crystals of unusual morphology from the Korshunovskoe iron deposit, Irkutskaya Oblast' were donated by M.Moiseev. The most interesting crystal is about 3 cm in size and has pseudooctahedral shape created by combination of rhombohedra and pinacoid [www2]. Of special mention is an aggregate of blocky sphere crystals of calcite from Herja, Romania, which has a black color due to jamesonite inclusions. This aggregate was donated by N.Mozgova.

Among the quartz specimens, one of the best is a druze of pinkish-orange obelisk-shaped crystals up to 4 cm long. It is colored by hematite inclusions along one of growth zone, (Photo 1). This type of material appeared relatively recently from the 2nd Sovetskiy mine, Dal'negorsk, Primorskiy Kray. It was represented in the Museum previously by just a few middle quality specimens. Another attractive specimen is a druze of rock crystal donated by D. Abramov with a large, about 15 cm, Japanese type twin from the Astaf'evskoe deposit, South Ural [www]. A.Agafonov donated several tabular shaped smoky quartz crystals from, 10 to 13 cm, sprinkled with muscovite on one of prism faces [www]. This material was collected by the «Stone Flower» company at the Akzhailyau, East Kazakhstan in cavities under the quartz core of a pegmatite vein. A few Brazilian type twined morion crystals 8 to 11 cm in size were obtained from the Shibanovskiy massif, Primorskiy Kray. Another morion with translucent amethyst sectors was received from the Bikchiyulskoe occurence, Khabarovskiy Kray.

Among the cryptocrystalline quartz varieties are two nice cabochons of landscape moss agate with dendrites of manganese oxides from the Pstan deposit, Kazakhstan. These cabochons were donated by V.Grechin for the Museum gem collection [www]. A nice concretion of snow white cacholong from the Taskazgan, Kyzylkumy Desert, Uzbekistan, was donated by A.Agaphonov.

Finishing the review of quartz acquisitions, I would like to mention a set of 30 specimens of synthetic quartz represented by different shapes, colors, zonal or sectorial crystals grown mostly in Alexandrov City. Among these synthetic quartzes are several very interesting clusters of 2 or 3 crystals grown together looking very similar to the natural «Herkimer Diamond» from the Herkimer Dololmite deposit in New York state, USA.

Next by the number of specimens is vivianite, (29). The vivianite was mostly collected by Museum expeditions during 1986–1988, (D.Abramov). All this material is from a mined out and recultivated sedimentary iron deposit near Kertch, Crimea Peninsula, Ukraine. The specimens are different by their morphology, associations and degree of iron oxidation. Their appearance is as blue powdery earthy aggregates or green to black fascicles of crystals and radiating clusters in oolitic iron ore. There are specimens of vivianite crystals on barite spherulites, inside sea shells and even vivianite pseudomorphs after these shells. The majority of the barite specimens, (#6, Table #1), were also collected at this locality. Among them are several items of perfectly shaped yellowish spherulites and spheroidolites up to 3 cm and barite (with vivianite) pseudomorphs after wood and shells. Rhodochrosite specimens, (#9, Table #1), are mostly represented by pseudomorphs of a Ca-rich rhodochrosite variety after sea shells and were acquired from the same deposits. The

[2] The images of specimens marked with www are posted at the Museum website http://www.fmm.ru under new acquisition subdivision.

locality is the same also for siderite (#13, Table #1) and for anapaite (#20, Table #1), except for several specimens from the anapaite type locality on cape Zhelezniy Rog, Taman' Peninsula near Anapa City. This occurrence is quite similar to those in the vicinity of Kertch. Anapaite specimens from Anapa vicinities were donated by Vs. Aristov and the «Stone Flower» company. They are largest anapaite crystals in Museum (up to 1.5 cm). Together, with earlier acquisitions, these specimens are probably the world's best collection of this type of deposit mineralogy.

Hematite is fourth by quantity of specimens, (24). Most of them are new material from Pathagony, Argentina, collected at the end of 2002, and are represented by hematite pseudomorphs after spectacular skeletal magnetite crystals. In some specimens the magnetite is only partly substituted and the crystal forms are different. Most of the skeletal crystals are developed mainly along the 4-fold symmetry axis. There are some individuals with skeletal sections growing along the 3- and 2-fold axis. One of the big crystals was donated by W.Larson, USA, (Photos 2 and 3). This hematite was collected from gas caverns in an acid lava, but the exact locality is still unknown. Similar material was found on the Payun Matru Volcano, Mendoza, Argentina, however the original mineral collector contends that his occurrence is more than 1000 km distant from the Payun Matru Volcano.

Several other hematite specimens of volcanic origin are from the Tolbachik, Kamchatka and the Kudriaviy, Iturup Iisland, volcanoes. They were donated by E. Bykova and I. Chaplygin. The nice hematite crystal, with a complicated combination of rhombohedras, about 6 cm in size, was obtained from a location in Minas Gerais, Brazil.

Among the native sulfur specimens, (20), is an interesting one which consists of a solidified fragment of melted sulfur from the Golovin Volcano, Kunashir Island of the Kurilian chain. This specimen was donated by V.Znamenskiy for a new Museum exhibit entitled «Mineralogy of Volcanoes». A few honey-yellow and lemon-yellow transparent sulfur crystals were collected recently on the dump of the mined out sulfur deposit Vodino near Samara City, Volga River Region. The crystals fill nearly the entirely cavities which are also encrusted with calcite in limestone.

Eleven out of 15 catalogued grossular crystals show a morphological diversity from skeletal crystals to crystals distorted up to a pseudoorthorhombic shape [www]. The green crystals are up to 5 cm in size and were collected on the Viluy River near the Chernyshevskiy Village, Sakha-Yakutia Republic. Very nice colorless to pinkish-brown hessonite druzes with crystals up to 0.7 cm from the Bazhenovskoe Asbestos Deposit, Asbest, Ural, were donated by A.Zadov.

Among the orthoclase acquisitions the most interesting are gray semi-transparent, sometimes pinkish crystals up to 8 cm from Udacha, about 80 km east of the famous Konder alkaline-ultramafic massif. The crystals are good examples of complex twinning, Baveno type combined with one or several other kinds of twin types. Several orthoclase specimens showing perfect sun stone patterns were added to the gem collection. One is from Burma, a W.Larson, USA, donation, and another from India, location unknown.

A significant number of hydroboracite specimens were catalogued after finishing the diagnostics and specimen preparation of material collected during the Museum expedition in 1986, (D. Abramov, D. Romanov, A. Nikiforov), from the Inder Borate Deposit, Kazakhstan. The most spectacular specimens of this lot are fragments of thick (up to 10 cm) parallel-columnar veinlets of yellow with pearly luster hydroboracite. They also found hydroboracite crystals up to 2 cm by size. Other material collected on that trip is best represented by perfect colorless to yellowish-brown, partly transparent goergeyite crystals up to 15 cm, colorless transparent sulfoborite crystals up to 2 cm, extremely large, up to 3 cm, colorless transparent fragments of kaliborite crystals, and also boracite, colemanite and other boron containing sedimentary deposit type minerals. The Inder Borate Deposit was not operating for many years and unlikely will be open for work in the near future. So, now we may establish the Inder Borate Deposit collection as the best specimens for the locality and one of the best for boron containing sedimentary type mineral deposits rivaling the great deposits in the Mojave Desert of California, USA.

Corundum acquisitions include a set of synthetic crystals, grown by various methods in different labs. Only the one natural corundum is remarkable, large red crystal from Mysor, India.

Among the pyrite specimens are flattened spheroidal concretions from Liu Zhu, Guansi County, China, and a strange binocular-shaped concretion from the Ulianovsk district, donated by A. Natarius.

Several very interesting apatite specimens were catalogued. First of all is a druze of color changing apatite crystals, pink under red

incandescent light and greenish under natural or fluorescent light, with muscovite quartz and feldspar from pegmatite #66, Akzhailyau, northwest of Tarbagatay, East Kazakhstan, (Photo 4). This deposit was formerly worked for piezo-electric quartz. No such kind specimens were distributed during this mine commercial exploration. A portion of that stuff was collected a few years ago. Dark-green fluorapatite crystals in phlogopite or vermiculite are also a new material from area of Snezhinsk, formerly forbidden city in Chelyabinsk region of South Ural. By color these crystals reminds one of diopside or forsterite and according to the name («liar» in Greek) bewilder even experienced mineralogists and collectors. A good-shaped prismatic crystal up to 11 cm was obtained by Museum (photo 5). Among other apatite goodies we would note several obtained and exchanged greenish-brown apatite crystals in pink calciphyre from Yates mine, Otter lake, Quebec, Canada.

There are several remarkable xonotlite specimens among recent acquisition. They look as radiating fascicles of white needle-shaped crystals and were found in Oktiabrskiy mine, Noril'sk district (donated by E. Spiridonov). Massive pinkish xonotlite aggregate from new place of its occurrence in rodingites of Bazhenovskoe deposit, Asbest city, Urals was donated by A. Zadov.

New Acquisitions classified by Geography

Specimens catalogued in 2002–2003 were collected in 62 countries, and also in Antarctica and ocean bottom (tab. #2).

Russia

Kola Peninsula: Most of the acquisitions from Russia are traditionally from this region. This material is represented by 155 specimens, 109 mineral species, among them 53 are from Kovdor, 47 from Lovozero, and 39 from the Khibiny massifs.

Quite a representative collection of the Kovdor Massif minerals was gathered, including high quality specimens of minerals, recently discovered in this location. There are nicely shaped, up to 2 cm, feklichevite crystals [www], radiating-tabular bakhchisaraitsevite, large flakes of greenish glagolevite, colorless crystals of labuntsovite-(Mg), and golden-yellow plates of nabalamprophyllite. The Museum's list of mineral species found in the Kovdor Massif increased by the acquisition of tochilinite, lueshite, perovskite, rhabdophane-(Ce) and more than 10 other mineral species. A lot of Kovdor minerals, such as kovdorskite, rimkorolgite and some others were acquired as specimens of much higher quality as well. M.Moiseev donated most of those acquisitions.

Really splendid acquisitions also came from the Lovozero Massif. This is material from the Palitra, «Palette», pegmatite, which was exposed in the summer of 2002 during underground mining at Kedykverpakhk Mountain. This pegmatite received its name due to the spectacular colorful combination of its minerals. First of all, we were amazed with unprecedented size, up to 18 cm, of colorless pearly natrosilite in cleaved monocrystals. Natrosilite is surrounded by purple ussingite and associated with yellow vuonnemite, red villiaumite, orange serandite, white analcime and other minerals [www]. Manaksite crystals fragments should be thought of as gigantic, up to 13 cm [www]. Previously collected manaksite was represented by grains not more than 0.5 cm. In several specimens manaksite is partly replaced with yellowish zakharovite. There are several new, for the Museum, mineral species from this association including, nalipoite, white prismatic crystal up to 3 mm, formerly discovered in pegmatites at Mont Saint-Hilaire, Canada, and also barioolgite, kapustinite, K-arfvedsonite, recently discovered in this pegmatite. Several other mineral species are in the process of CNMMN IMA approval and hopefully will appear in the next review. All the specimens from the Palitra pegmatite were donated by I. Pekov and V. Grishin. A number of new, for the Museum mineral species, are type specimens from other places of the Lovozero Massif, and were donated by A. Khomyakov and N. Chukanov, including gmelinite-K, ikranite, raslakite, tsepinite-K, parakuzmenkoite-Fe, paratsepinite-Ba.

The most interesting acquisitions from the Khibiny Massif are fragment of sodalite, variety hackmanite, rhombododecahedron crystals to about 12 cm from the Koashva Mine [www] and labuntsovite-Fe druzes of small orange-red crystals up to 1 mm from the Kirovskiy Mine. The Museum collection of Khibiny mineral species was replenished by new, for the Museum, mineral species from this locality, including cerite-(Ce), cerite-(La), crichtonite, karupmollerite, takanelite, and ferroceladonite, and type specimens recently discovered in the Khibiny mineral species, including bussenite, gutkovaite-Mn, clinobarylite, kukharenkoite-(La), labuntsovite-Fe, megakalsiite, paravinogradovite, paratsepinite-Ba, thomsonite-Sr, tsepinite-Ca, shirokshinite, and eveslogite. Faceted natrolite was catalogued into

the gemstone collection. Most of the Khibiny Massif specimens were donated by I. Pekov and A. Khomyakov.

Ural Mountains: Acquisitions from the Ural Mountains are on the second place by specimen quantity. There are 86 items, among them 41 ones are from South Urals, 38 from the Middle Urals and 7 from the Polar and Subpolar Urals. They are represented by 67 mineral species.

Besides the above-mentioned Japanese twin of quartz from the Astaf'evskoe Deposit and grossular and xonotlite from Bazhenovskoe Deposit, a number of specimens from Saranovskoe chromite Deposit are remarkable. This series includes not only the typical for the deposit Cr-amesite, Cr-diaspor, Cr-titanite, Cr-clinochlore, and millerite but also new, for the Museum, material. There are brown rutile pseudomorphs after perovskite cubic crystals, a chalcopyrite crystal up to 1.2 cm in fibrous tremolite on an albite druze, a rare, for this deposit, chalcocite crystal, and green kassite plates replacing Cr-titanite crystals [www].

Among the material from South Urals must be mentioned the ilmenite crystal from the Vishnevie Mountains, anorthoclase with both sunstone and moonstone simultaneous effects, and several minerals from the Uchaly Deposit, including magnesio-axinite, tinzenite, pumpellyite-Fe''. These specimens were donated by E. Spiridonov. Type specimens of new minerals from the Urals are represented by bushmakinite and magnesiotantalite. Polyakovite-(Ce) from type locality was donated by one of describers, L. Pautov. Faceted bromellite, 7x5x4 mm, from the Emerald Mines was added to the gemstone collection.

Kamchatka and Kurilian Islands: 45 specimens were obtained from Kamchatka and 13 from the Kudriaviy Volcano, Iturup Island of Kurilian Island chain. Most of them are minerals of volcanic sublimates. The best ever specimens of cannizzarite, a new find on the Kudriaviy volcano, were donated by I.Chaplygin and M. Yudovskaya. This material excels by quality specimens from known locations such as Vucano Island, Italy. It is represented by rosette-like aggregates or separate greyish-black lustrous thin leaf-like crystals up to 0.8 cm on fracture surfaces in andesite [www]. From the same source, both location and donators, the Museum has received natural rhenium sulfide, molibdenite, grinocite, molybdite, and hematite. All have a fumarolic origin.

Another set of sublimates was acquired from the Tolbachik Volcano. These are rather big hand specimens of chalcocyanite, melanothallite, lesukite, euchlorine, fedotovite, klyuchevskite, alumoklyuchevskite, sofiite, kamchatkite and others. The individual minerals are well recognized by the naked eye in most cases. Only some mineral species are are represented by small grains, including vergasovaite, leningradite and a few others. These species were never found in better quality. Noteworthy is a druze of tenorite crystals up to 1 cm in size [www]. This piece is probably one of the best tenorite specimens. It was donated by E.Bykova, who also donated a number of other specimens from Tolbachik as well. The material described above formed the basis for our recently created Museum exposition on volcano mineralogy by O.Sveshnikova. Mineral specimens for this exposition were also donated by M.Murashko, A.Babansiy, R.Vinogradova, V.Ladygin, and O.Vlodavets.

Table 2. Countries by the number of specimens acquired

1. Russia	544	34. Azerbaijan	4
2. USA	98	35. Georgia	4
3. Ukraine	96	36. Denmark	4
4. Kazakhstan	80	37. Congo	4
5. Italia	35	38. Mozambique	4
6. Czech Republic	32	39. Republic of South Africa	4
7. Madagascar	29	40. Japan	4
8. Canada	27	41. Serbia	4
9. Argentina	25	42. Slovakia	3
10. Kirghizia	22	43. Switzerland	3
11. China	22	44. Antarctica	2
12. Norway	21	45. Hungary	2
13. Great Britain	20	46. Greece	2
14. Germany	18	47. M'janma	3
15. Uzbekistan	13	48. Namibia	2
16. Sweden	13	49. Romania	2
17. Brazil	12	50. Uganda	2
18. Tanzania	11	51. Algeria	1
19. India	10	52. Belgium	1
20. Mexico	10	53. Bosnia	1
21. France	10	54. Gabon	1
22. Tajikistan	9	55. Israel	1
23. Chile	9	56. Iceland	1
24. Australia	8	57. North Korea	1
25. Zaire	8	58. Kenya	1
26. Mongolia	8	59. Macedonia	1
27. Armenia	7	60. Oman	1
28. Afghanistan	7	61. Pakistan	1
29. Bulgaria	7	62. Poland	1
30. Bolivia	7	63. Portugal	1
31. Turkmenistan	7	64. Ocean bottom	1
32. Austria	6		
33. Morocco	6		

54 specimens are synthetic or from unknown localities.

Primorskiy Kray and Khabarovskiy Kray: The equal number, 21, of specimens came from each of those two regions. The first group is represented mostly by the above mentioned material from Dal'negorsk. From the second

group of interest are anatase crystals up to 8 mm sitting on nicely shaped twined orthoclase crystals and druzes of such crystals. This material came from the location called Udacha, «Luck», near the Konder Massif. Part of these specimens were purchased and the rest were donated by A.Stupachenko. A.Stupachenko also donated some specimens from the Konder Massif, including big montichellite crystals, lamprophyllite, arfvedsonite, and others. Among the rare species, we need to mention the yakhontovite donated by V.Postnikova.

Sakha-Yakutia: Most of the 24 Yakutian specimens, mentioned above, are grossulars from the Viluy River. Also from this place are «akhtaragdite» samples.

Baikal area, Irkutskaya oblast', Transbaikal: Among the 47 specimens from these territories we have already described above the pseudooctahedral calcite from Korshunovskoe deposit. From the rest we would like to highlight material from the Yoko-Dovyrenskiy Massif in the North Baikal area, which includes foshagite, hillebrandite, cuspidine and others donated by N.Pertsev and A.Zadov. Among more rare minerals are a type specimen of vanadiumdravite, donated by L.Reznitskiy, and also volkovskite, tantalowoginite, kilchoanite, kirschsteinite, caminite, ingodite and others.

Krasnoyarskiy Kray: Most of the 25 specimens aquired from this region are from the Norilsk group of deposits. Among them are xonotlite, see above, valleriite, sperrylite and others.

Commonwealth of Independent States (Former Soviet Union Republics)

Ukraine: (96) The biggest part of the Ukranian acquisitions werre collected during older Museum expeditions to the sedimentary iron deposits near Kertch. This material is described above. Other than these, only few native sulfur crystals from the Yazovskoe deposit, L'vov Area and a siderite crystal from the granitic pegmatite of the Volodarsk Volynskiy, Zhitomir Area were cataloged.

Kazakhstan: (80) More than a third, 36, of the cataloged items from this republic are from the Inder Borate Deposit, (see above). Also mentioned above are fluorapatite and smoky quartz from Akzhailyau and moss agate from Pstan. Among others we would like to mention a new material including cranked twins of rutile found near the Ak-Koshker Village, Turgayskaya Oblast' of north Kazakhstan, donated by R.Yashkin and A.Ivonin. Newly collected specimens are copper dendrites from the Itauz Mine, Dzhezkazgan, donated by M.Kelisuly. Also from this deposit cuprite crystals have been catalogued. Among the rare mineral species are type specimens of niksergievite, donated by G.Bekenova, and tellurides, hessite, petzite, sylvanite, and frohbergite, from the Zhana-Tube Deposit.

Kyrgyzia: (22) Nearly all of this material was collected recently by Museum employees L.Pautov, A.Agakhanov, V.Karpenko, and T.Dikaya at the Khaidarkan Mercury Deposit, khaidarkanite; at the pegmatite field Kyrk-Bulak, sinkankasite; on the Zardalek Massif, thorutite amd brannerite; and at Kara-Chagyr, rare phosphates and vanadates, including nickelalumite, hammerite, minyulite, and tangeite. Discovered by this group of collectors is the new mineral ankinovichite.

Uzbekistan: (13) Besides the cacholong mentioned above, some tellurides are of interest, including joseite-A from Ustarasay and altaite from the Koch-Bulak Deposit.

Tajikistan: (9) Most of the catalogued specimens were collected 9 or more years ago at the Dara-i-Pioz massif. These include the recently discovered (in old specimens) mineral species moskvinite-(Y), surkhobite, and maleevite.

Turkmenistan: (7) Previously collected gypsum crystals and native sulfur from sulfur mines near Gaurdak were catalogued.

Armenia: (7) Some tellurides from the Zod Deposit were aquired, including rucklidgeite, melonite, and tellurobismutite. There was no newly collected material.

Azerbaijan: (4) All obtained specimens are from the Dashkesan Iron Deposit including the above mentioned calcite crystals.

Georgia: (4) Newly collected rutile and brukite from the Verkhnyaya Racha, Rioni River Valley were donated by A.Agafonov.

Other countries:

United States of America (USA): By the quantity of specimens acquired by the Museum the USA is the second on the list. A total of 98 specimens are represented by 67 mineral species from 18 States. The majority of these specimens came from California (26), Utah (25), and North Carolina (10). Nearly equal parts of these acquisitions were donations, purchases and specimens collected by the Museum staff. The most interesting part of the obtained material includes several rare mineral species, including 2 new minerals discovered in Utah by Russian researchers. These species are larisaite and holfertite. Holfertite was described from Searl (Starvation) Canyon, Thomas Range, Delta, Utah. It is represented by small, but nice, specimens with yellow nee-

dles of holfertite in association with red beryl, smoky topaz, bixbyite and others, (Photo 6).

Added to the Museum collection from the Boron, California deposit was inderite, veatchite-p, big kurnakovite crystals and other boron minerals donated by J.Watson. Rather large, up to 2.5 cm, well shaped sulphohalite crystals from Searls Lake, California were exchanged. A pale kunzite crystal, 8.5 cm size, from the BeeBe Hole pocket on the Pack Rat Claim, Jacumba and some other specimens from southern California pegmatites were donated by J.Patterson. A small collection of specimens, representing mineralogy of emerald from alpine type veins near Hiddenite, North Carolina, was collected thanks to permission of J.Hill. J.Hill also donated a few specimens including hiddenite itself.

Among 35 specimens from **Italy,** 22 are new for the Museum mineral species from different Italian localities mostly obtained by exchange. The same situation occurred with specimens from the **Czech Republi**c, including 32 specimens, of which 17 are new for the Museum mineral species. The same was for **Germany** (18/13) and **Sweden** (13/9). New acquisitions from **Canada** are represented by minerals from the Mt. Saint-Hilaire Alkaline Massif, some good betafite crystals from Silver Crater, Ontario and by the above mentioned fluorapatite. Hematite and calcite crystals from **Argentina** (25) were also already noted.

From **China** (22) a nice spessartite on quartz and feldspar from Fujian Province and and inesite with new mineral hubeite from Da Ye mine, Hubei Province were obtained.

The series of rare minerals from **South Norway** (21) obtained as an exchange and as donations of I.Pekov and E.Semenov.

The most interesting piece from **Great Britain** (20) is a geode with unusually large, up to 1 cm, crystals of hilgardite-1A, colored pinkish by thin hematite inclusions, (Photo #7), from salt layers of the Boulby Mine, North Yorkshire. There are a few more higardite-1A smaller crystals associated with blue boracite. A few decent druzes of green fluorite [www] came from the Rogerley Mine, Weardale thanks to J.Fisher and C.Graeber of UK Mining Ventures. A few unusual zeolite specimens were donated by D.Mc Callum. Among the **Brazilian** (12) material is a great piece with crust of well shaped kosnarite crystals, up to 2 mm, on elbaite from Limoeiro, Minas Gerais and a small milarite crystal on cleavelandite from Jaguaracu, Minas Gerais. **Tanzania** (11) is represented this time by crystal fragments of brown gem quality enstatite. **France, India** and **Mexico** supplied us with 10 specimens each. There are big grains of recently discovered lulzacite from Saint-Aubin-des Chateaux, Loire-Atlantique, France, donated by Y.Moelo; a large spherulite of dark blue cavansite [www] and powellite crystals on colorless apophyllite both from Poona, India; and aggregates of creedite [www] as radiated crystals from the Navidad Mine, Durango, Mexico.

Among other foreign specimens are dark blue translucent spindle shape afganite crystals [www], to 2 cm in size, on marble matrix and a sodalite crystal [www], about 5 cm, with hackmanite areas from Sar-e-Sang, Badakhshan, **Afganistan**.

The types and sources of acquisitions

As we noted before, about 54 % of acquisitions made up donations from 138 private persons and 8 organizations. 116 donators are citizens of Russia and 22 donators are foreign citizens (including 5 citizens of CIS). Most part of foreign donators (11) are citizens of the USA. The museum expresses sincere gratitude to everyone who has donated specimens or contributed to Museum collection any other way.

The most active donator was I.Pekov who contributed the total of 104 specimens. They are mainly from the Khibiny and Lovozero Alkaline Massifs, Kola Peninsula, and some foreign alkaline massifs. Among them are 14 type specimens of new mineral species. M. Moiseev donated 39 specimens mostly from the Kovdor Massif. 29 specimens were donated by E. Spiridonov. Other donators were: L. Bulgak (25), V. Levitskiy (18), D. Belakovskiy (17), M. Anosov (13), N. Mozgova (12). More than 5 specimens were presented by A. Agakhanov, L. Pautov, N. Chukanov, N. Pertsev, A. Khomyakov, I. Chaplygin, M. Yudovskaya, A. Agafonov, A. Stupachenko, E. Bykova, M. Generalov, A. Zakharov, A. Zadov, A. Nikiforov, P. Pletnev, E. Semenov, S. Samoilovich and foreign donators — J. Watson and W. Pinch. Under 5 specimens were donated by C&J. Farmer, G. Ito, E. Grew, P. Haynes, J. Hill, A. Kidwell, W. Larson, D. McCallum, Y. Moelo, J. Patterson, R. Ramdor, K. Walenta, R.Withmore, D.Abramov, A.Akilin, S. Aleksandrov, V. Apollonov, Vs. Aristov, A. Babanskiy, V. Baskina, G. Bekenova, S. Belyh, S. Belyakov, E. Bologova, A. Bul'enkov, B. ayntroub, R. Vinogradova, O. Vlodavets, A. Voloshin, A. Vradiy, V. Grechin, V. Grishin, D. Davydov, R. Jenchuraeva, T. Dikaya, M. Dorfman, V. Dusmatov, I. Dusmatov, A.Ekimov, V.Zagorsiy, G.Zadorin, T.Zdorik, V.Znamenskiy, A.Ivonin, A.Izergin, A.Ilglyavichens, A.Kanonerov, B.Kantor, V.Karpenko, P. Kartashev, M.Kelisuby, D.Kleymenov, K.Klo-

potov, I. Klochkov, V. Kongarov, A. Konev, V. Korolev, S. Kravchenko, M. Kurilovich, V. Kushnarev, V. Ladygin, V. Lennyh, R. Liferovich, A. Malyanov, N. Manaev, O. Melnikov, L. Memetova, M. Murashko, A. Natarius, E. Pankratova, I. Peretyazhko, S. Petrusenko, L. Pozharitskaya, O. Polyakova, A. Ponomarenko, V. Ponomarenko, V. Postnikova, L. Reznitskiy, D. Savelyev, M. Samoylovich, V. Sapegin, E. Saratova, O. Sveshnikova, E. Sereda, M. Seredkin, G. Skublov, T. Soboleva, V. Starostin, V.K. Stepanov, D. Sulerzhitskiy, I. Tkachenko, A. Tourchkova, A. Ust'ev, V. Ushakovskiy, A. Fedorov, A. Haugen, P. Hvorov, A. Hohlov, E. Cheremnyh, A. Cherkasov, B. Cesnokov, L. Shabynin, A. Shevnin, B. Shkurskiy, Z. Shlyukova, V. Sreyn, G. Yuhtanov, R. Yashkin.

Six organisations donated 32 specimens to the Museum. All-Russian Institute for Synthetic Minerals (VNIISIMS) contributed a half of them, a collection of synthetic quartz crystals. Great donations were also made by the Institute of Geology and Geophysics Siberian Branch of RAS, Novosibirsk, the Moscow State Regional University, the petrography chair of the Moscow State University, Ore-Petrographic Museum IGEM RAS, joint-stock company «Inagli», and the «Stone Flower: company.

More than 200 out of 1,356 spesimens catalogued during the period 2002—2003 were collected by 11 people of the Museum staff. The largest part were collected by D. Abramov (111), A. Nikiforov (43) and D. Romanow (37). D. Belakovskiy collected 57 specimens, L. Pautov, F. Agakhanov, V. Karpenko and T. Dikaya collected 16 specimens, N. Pekova collected 6, A. Ponomarenko collected 5, and M. Generalov collected 1 specimen. Expeditions were sponsored partly by the Museum and partly from other sources.

The Museum want list as of the end of May 2004 is in appendix №2. Besides the mineral species no yet included in the Museum collections, there are some species listed which the Museum would like to obtain in better quality or for scientific research programs.

The author thanks I. Pekov, E.Sokolova, J.Patterson, N. Pekova, A. Evseev, for discussions and significant help in preparation of this article.

The list of photos for a review of new acquisitions to Fersman Mineralogical Museum Russian Academy of Sciences for 2002—2003.

Appendix 1

The list of mineral species new for Museum which were catalogued to Museum in 2002-2003

In bold are the mineral species discovered and published for that period

* — Mineral species represented by type specimens or it's fragments or cotypes

** — Mineral species which were discovered for that period by museum stuff or in colaboration with museum stuff

Aciculite
Agrinierite
Akrochordite
*Alsakharovaite-Zn**
Alumotungstite
Androsite-(La)
*Ankinovichite***
Anorthominasragrite
Arsendescloizite
Arseniopleite
Arsenoclasite
Arsenolamprite
Arsentsumebite
Baghdadite
Bakhchisaraitsevite
Banalsite
*Barioolgite**
Bartonite
Bassetite
Biraite-(Ce)*
Borocookeite*
Braitschite-(Ce)
Brianyoungite
Bulachite
Bursaite
Bushmakinite**
Bussenite*
Calcioancylite-(Nd)
Calciobetafite
Caminite
Caresite
Cejkaite
Cerchiaraite
Cerite-(La)*
Cervandonite-(Ce)
Chabazite-Ca
Chabazite-Na
Chabazite-Sr*
Chalcocyanite
Christelite
Cianciulliite
Claraite
Clinoatacamite
Clinobarylite*
Clinochalcomenite
Clinotyrolite
Cobaltpentlandite
Cobalttsumcorite
Colquiriite
Coombsite
Crichtonite
Cyanophyllite
Daqingshanite-(Ce)
Decrespignyite-(Y)
Dissakisite-(Ce)
Dwornikite
Ecandrewsite
Eclarite
Eveslogite
Feclichevite*
Fedotovite
Ferriallanite-(Ce)*
Ferriannite
Ferritaramite
Ferritschermakite
Ferroceladonite
Ferroedenite
Ferroleakeite
Ferrorichterite
Ferrosaponite*
Fettelite
Florencite-(La)
Florencite-(Nd)
Fluellite
Fluocerite-(Ce)
Foordite
Freudenbergite
Geigerite
Gjerdingenite-Fe
Glagolevite**
Gmelinite-K*
Gottlobite
Grumiplucite
Guarinoite
Guettardite
Gugiaite
Gutkovaite-Mn*
Hainite
Hakite
Hannayite
Hartite
Hatchite
Hechtsbergite
Henmilite
Heulandite-Sr
Hidalgoite
Hingganite-(Ce)
Hodgkinsonite
Hodrushite
Hohmannite
Holdawayite
Holfertite
Hubeite
Humberstonite
Hummerite
Ikranite*
Iltisite
Imiterite
Indialite
Irarsite
Jaskolskiite
Johillerite
Jungite
Jurbanite
Kaatialaite
Kamchatkite
Kamotoite-(Y)
Kampfite
Kamphaugite-(Y)
Karupmollerite-Ca*
Kassite
Kastningite
Katoptrite
Kawazulite
Kentbrooksite
Khademite
Kimrobinsonite
Kirschsteinite
Kladnoite
Klyuchevskite
Kombatite
Konderite
Kosnarite
Krasnovite*
Krettnichite
Kristiansenite
Krutaite
*Kukharenkoite-(La)**
Kurumsakite
Kuzmenkoite-Zn
Lammerite
Larisaite*
Lemanskiite
Leningradite
Lepkhenelmite-Zn*
Lulzacite
Magnesioaxinite
Magnesiotantalite*
Mahlmoodite
Maleevite**
Malladrite
Mandarinoite
Manganvesuvianite
Mattagamite
Medaite
Megakalsilite*
Melanothallite
Melonjosephite*
Metahewettite
Metaschoderite
Metavanuralite
Metazeunerite
Meurigite
Micheelsenite-(Y)
Millosevichite
Minasgeraisite-(Y)*
Minyulite
Molybdofornacite
Monazite-(La)
Montbrayite
Montdorite
Montesommaite
Moskvinite-(Y)**
Mottanaite-(Ce)
Mundite
*Nabalamprophyllite***
Nabesite
Nabiasite
Nalipoite
Natroglaucocerinite
Natrolemoynite
Neskevaaraite-Fe*
Neustadtelite
Nezhilovite
Nickelalumite
Nikischerite
Niksergievite*
Norrishite
Orthopinakiolite
Oxammite
*Parakuzmenkoite-Fe**
Paraniite-(Y)
Paratsepinite-Ba*
Paratsepinite-Na*
Paravinogradovite*
Pengzhizhongite-6H
Pentahydrite
Perhamite*
Petitjeanite
Petterdite
Phillipsite-Na
Poldervaartite
Polyakovite-(Ce)**
*Potassic chloropargasite***
Potassicpargasite
Pretulite
Pseudojohannite*
Pumpellyite-Fe''
Pumpellyite-Mg
Pushcharovskite
Quadridavyne
Rabejacite
Rappoldite
Raslakite*
Rastsvetaevaite*
Reppiaite
Ribbeite
Rickardite
Rittmannite
Roselite-betta
Rosenbergite
Rouvilleite
Sabelliite
Scainite
Scandiobabingtonite
Schultenite
Schwertmannite
Seeligerite
Serrabrancaite
Shannonite
Shirokshinite

Sinkankasite
Skippenite
Sodium boltwoodite
Soucekite
Sphaerobertrandite••
Spheniscidite
Stoppaniite
Studtite
Suredaite
Surkhobite••
Swamboite
Synadelphite
Tantalowoginite
Taramite
Teepleite
Tegengrenite•
Ternesite
Tetrarooseveltite
Thometzekite
Thomsonite-Sr•
Thorutite
Threadgoldite
Tinnunkulite &techn
Tintinaite
Tinzenite
Tolbachite
Trattnerite
Trechmannite
Trilithionite
Tsepinite-Ca•
Tsepinite-K•
Tuzlaite
Tveitite-(Y)•
Uranopolycrase
Vanadiumdravite•
Vanoxite
Vantasselite
Vaterite
Vertumnite
Vinciennite
Vitimite•
Voglite
Vrbaite
Wallkilldellite-(Fe)
Wattersite
Wawayandaite
Weddellite
Wendwilsonite
Wilkinsonite
Wroewolfeite
Yeatmanite
Yecoraite
Yeelimite
Zdenekite

Appendix #2

Fersman mineralogical museum want list of mineral species as for May 31 2004

More desirable species are in bold

Abelsonite
Abenakiite-(Ce)
Abswurmbachite
Admontite
Aerugite
Akimotoite
Acuminite
Albrechtschraufite
Althupite
Alforsite
Aluminobarroisite
Aluminocopiapite
Amminite
Ammonioborite
Ammonioleucite
Amstallite
Angelellite
Anhydrokainite
Andremeyerite
Anduoite
Antarcticite
Anthonyite
Antimonselite
Aplowite
Arakiite
Aravaipaite
Arcubisite
Ardaite
Ardealite
Argutite
Aristarainite
Armalcolite
Armangite
Arsenbrackebuschite
Arsenoflorencite-(Ce)
Arsenoflorencite-(La)
Arsenoflorencite-(Nd)
Arsenogorceixite
Arsenogoyazite
Arsenuranospathite
Artroeite
Artsmithite
Arzakite
Ashoverite
Asisite
Aspidolite
Asselbornite
Astrocyanite-(Ce)
Aurivilliusite
Baileychlore
Baiyuneboite-(Ce)
Balavinskite
Balipholite
Bamfordite
Bararite
Barberiite
Bariomicrolite
Bariorthojoaquinite
Bariosincosite
Barquillite
Barringerite
Barringtonite
Barstowite
Bartelkeite
Batiferrite
Baumstarkite
Bayankhanite
Baylissite
Bearthite
Bechererite
Bederite
Belendorffite
Bellbergite
Bellidoite
Bellite
Benauite
Berdesinskiite
Bernalite
Bernardite
Berndtite
Bideauxite
Bigcreekite
Bijvoetite-(Y)
Bismutostibiconite
Bleasdaleite
Blossite
Bobjonesite
Bobkingite
Bobtraillite
Bogvadite
Boldyrevite
Bonaccordite
Boralsilite
Borishanskiite
Bornhardtite
Bostwickite
Bottinoite
Bracewellite
Bradleyite
Brandholzite
Brendelite
Brianroulstonite
Brinrobertsite
Brodtkorbite
Brokenhillite
Brongniardite
Buchwaldite
Buckhornite
Bunsenite
Bursaite
Burtite
Butschliite
Cabalzarite
Cadwaladerite
Calcioancylite-(Nd)
Calcioaravaipaite
Calcioburbankite
Calciocopiapite
Calciogadolinite
Calciopetersite
Calcjarlite
Calclacite
Calderonite
Cameronite
Camgasite
Canaphite
Caoxite
Capgaronnite
Carboborite
Carlinite
Carlosruizite
Carlsbergite
Carmichaelite
Carobbiite
Carraraite
Cascandite
Cassedanneite
Cassidyite
Caswellsilverite
Catalanoite
Cavoite
Cebaite-(Ce)
Cebaite-(Nd)
Ceriopyrochlore-(Ce)
Cervelleite
Cesanite
Chadwickite
Chaidamuite
Chameanite
Changbaiite
Changchengite
Changoite
Chantalite
Chaoite
Charmarite
Chavesite
Chenite
Cheremnykhite
Chessexite
Chestermanite
Chillagite
Chiluite
Chladniite
Chloraluminite
Chlormanganokalite
Chlorocalcite
Choloalite
Chrisstanleyite
Chromatite
Chrombismite
Chvaleticeite
Clairite
Clearcreekite
Clerite
Cleusonite
Clinocervantite
Clinoferrosilite
Clinomimetite
Clinorhabdophane-(Ce)
Clinoungemachite
Cobaltarthurite
Cobaltkieserite
Cobaltneustadtelite
Cobaltpentlandite
Cobaltzippeite
Cochromite
Comancheite
Combeite
Comblainite
Compreignacite
Congolite
Coskrenite-(Ce)
Costibite
Cousinite
Coyoteite
Crerarite
Criddleite
Cualstibite
Cuboargyrite
Cupalite
Cupriauride
Cupromakovickite
Cuprorivaite
Cyanochroite
Cyanophane
Damaraite
Damiaoite
Danbaite
Danielsite
D'Ansite
Daomanite
Deanesmithite
Deliensite
Deloryite
Derriksite
Dervillite
Despujolsite
Dessauite
Diaoyudaoite
Dickthomssenite
Dienerite
Dietzeite
Dinite
Diomignite
Dittmarite
Dixenite
Donharrisite
Dorallcharite
Douglasite
Downeyite
Doyleite
Dozyite
Dreyerite
Drobecite
Drugmanite
Drysdallite
Dukeite
Duttonite
Earlandite
Eastonite
Ecandrewsite
Edenharterite
Effenbergerite
Ehrleite
Ekatite
Ellinite
Emilite
Ercitite
Erlianite
Ernienickelite
Ernigglilite
Ertixiite
Esperanzaite
Eugsterite
Eveite
Fabianite
Faheyite
Fahleite
Fairchildite
Fangite
Feinglosite
Felbertalite
Fencooperite
Ferrarisite
Ferriclinoferroholmquistite
Ferriferropedrizite
Ferrikinoshitalite
Ferrilotharmeyerite
Ferriottolinite
Ferripedrizite
Ferrisurite
Ferriwhittakerite
Ferrokentbrooksite
Ferrokesterite
Ferrokinoshitalite
Ferropyrosmalite
Ferrorichterite
Ferrotitanowodginite
Ferrowodginite
Ferruccite
Fetiasite
Fianellite
Fiedlerite-1A
Fingerite
Fischesserite
Flagstaffite
Fletcherite
Flinkite
Florenskyite
Fluorbritholite-(Ce)
Fluoronyboite
Flurite
Fontanite
Francoanellite
Francoisite-(Nd)
Frankhawthorneite
Franklinfurnaceite
Franklinphillite
Fransoletite
Freboldite
Freedite
Fritzscheite
Fuenzalidaite
Fukalite
Fukuchilite
Furongite
Furutobeite
Gabrielite
Gabrielsonite
Gainesite
Gaitite
Galgenbergite
Galileiite
Gallobeudantite
Gananite
Ganterite
Gaotaiite
Garavellite
Garrelsite
Garyansellite
Gatehouseite
Gatelite-(Ce)
Gaultite
Gebhardite
Gengenbachite
Georgeericksenite
Gerdtremmelite
Gerenite-(Y)
Gerstmannite
Gianellaite
Giannetite
Giniite
Giraudite
Girdite
Giuseppettite
Glushinskite
Goldquarryite
Gortdrumite
Gottardiite
Graemite
Graeserite
Gramaccioliite-(Y)
Grandreefite
Grantsite
Grattarolaite
Graulichite-(Ce)
Gravegliaite
Grayite
Griceite
Grimaldiite
Grimselite
Grossite
Guangnanite
Guanine
Guggenheimite
Guildite
Gupeiite
Gysinite-(Nd)
Haapalaite
Hafnon
Haggertyite
Haigerachite
Halagurite
Hallimondite
Hanawaltite
Harrisonite
Hashemite
Hastite
Hatrurite
Hawthorneite
Haxonite
Haycockite
Hectorfloresite
Heideite
Heidornite
Hellandite-(Ce)
Helmutwinklerite
Hemloite
Hendersonite
Heneuite
Hennomartinite
Henryite
Hentschelite
Hexatestibiopani-ckelite
Hiarneite
Hieratite
Hoganite
Honessite
Hongquiite
Horsfordite
Howardevansite
Huangite
Hugelite
Hungchaoite
Hydroastrophyllite
Hydrobasaluminite
Hydrochlorborite
Hydrodresserite
Hydrombobomkulite
Hydromolysite
Hydrophilite
Hydroromarchite
Hydroscarbroite
Hydrowoodwardite
Hydroxylbastnaesite-(Ce)
Hydroxylbastnaesite-(La)
Hydroxylbastnaesite-(Nd)
Hydroxylpyromorphite
Hydroxyuvite
Hyttsjoite
Imhofite
Ingersonite
Iridarsenite
Itoigawaite
Itoite
Jachymovite
Jagueite
Jaipurite
Jamesite
Janggunite
Jankovicite
Jarosewichite
Jeffreyite
Jensenite
Jentschite
Jerrygibbsite
Jervisite
Jianshuiite
Jixianite
Johachidolite
Johninnesite
Johnsomervilleite
Johntomaite
Johnwalkite
Joliotite
Jolliffeite
Jorgensenite
Juabite
Julienite
Junoite
Jusite
Kadyrelite
Kahlerite
Kalicinite
Kamaishilite
Kamitugaite
Katoite
Keilite
Kempite
Kenhsuite
Keyite
Keystoneite
Khademite
Khatyrkite
Khomyakovite
Kieftite
Killalaite
Kinichilite
Kintoreite
Kirkiite
Kitaibelite
Kitkaite
Kittatinnyite
Kivuite
Kleemanite
Kochite
Konyaite

Koritnigite
Kornite
Koutekite
Kozoite-(La)
Kribergite
Krieselite
Krinovite
Kuannersuite-(Ce)
Kulkeite
Kullerudite
Kupcikite
Kusachiite
Kutinaite
Kuzelite
Kuzminite
Laflammeite
Laforetite
Lalondeite
Langisite
Lanmuchangite
Laphamite
Larosite
Larsenite
Launayite
Laurelite
Lausenite
Lautenthalite
Lawrencite
Lawsonbauerite
Leakeite
Lecontite
Lehnerite
Leisingite
Lepersonnite-(Gd)
Levinsonite-(Y)
Levyclaudite
Lewisite
Liebauite
Liebenbergite
Lindqvistite
Lindsleyite
Lisetite
Lishizhenite
Lonecreekite
Loranskite-(Y)
Loseyite
Loveringite
Luberoite
Lubtheenite
Lucasite-(Ce)
Lukenchangite-(Ce)
Lukrahnite
Lunijianlaite
Lyonsite
Macaulayite
Macedonite
Machatschkiite
Macphersonite
Macquartite
Maghagendorfite
Magnesiodumortierite
Magnesiosadanagaite
Magnesiosadanagaite
Magnesiostaurolite
Magnesiumchloro-p
hoenicite
Magnesiumzinnwaldite
Magnesiumzippeite
Magnolite
Mahnertite
Majorite
Makinenite
Makovickyite
Mallestigite
Manganarsite
Manganeseshadlunite
Mangangordonite
Manganilvaite
Manganochromite
Manganocummingtonite
Manganogrunerite
Manganokukisvumite

Manganolangbeinite
Manganolotharmeyerite
Manganostibite
Manganotapiolite
Mantienneite
Marecotite
Marinellite
Marshite
Martinite
Marumoite
Mathewrogersite
Mathiasite
Matsubaraite
Mattagamite
Matteuccite
Mattheddleite
Matveevite
Maufite
Mayingite
Mbobomkulite
Mcalpineite
Mcauslanite
Mcbirneyite
Mccrillisite
Medenbachite
Melanostibite
Mengxianminite
Mereheadite
Mereiterite
Metaalunogen
Metaankoleite
Metadelrioite
Metakahlerite
Metakirchheimerite
Metakoettigite
Metalodevite
Metasaleeite
Metaschoepite
Metastudtite
Metauranospinite
Metavandendriesscheite
Metavanmeersscheite
Metazellerite
Mikasaite
Minehillite
Mitscherlichite
Modderite
Moeloite
Mohrite
Monazite-(Nd)
Monazite-(Sm)
Monimolite
Moreauite
Morelandite
Morimotoite
Morozeviczite
Moschelite
Mountkeithite
Moydite-(Y)
Mozartite
Mozgovaite
Mroseite
Muchuanite
Muckeite
Mummeite
Mundrabillaite
Munirite
Muskoxite
Muthmannite
Mutinaite
Nagashimalite
Nagelschmidtite
Nahpoite
Nanlingite
Nasinite
Nasledovite
Natrodufrenite
Natrofairchildite
Natrolemoynite
Natroniobite
Natrotantite
Nchwaningite

Nevadaite
Niahite
Nichromite
Nickelbischofite
Nickenichite
Niedermayerite
Nielsbohrite
Niigataite
Nioboaeschynite-(Nd)
Niobokupletskite
Nisbite
Noelbensonite
Nowackiite
Nullaginite
Nyboeite
Obertiite 98-046
Oboyerite
O'Danielite
Odinite
Oenite
Okayamalite
Omeiite
Ominellite
Oneillite
Oosterboschite
Orebroite
Orickite
Orlymanite
Orpheite
Orschallite
Orthojoaquinite-(Ce)
Orthojoaquinite-(La)
Orthowalpurgite
Osarsite
Osbornite
Oswaldpeetersite
Otjisumeite
Ottemannite
Oursinite
Overite
Owensite
Paarite
Paceite
Paderaite
Paganoite
Pahasapaite
Painite
Palladoarsenide
Palladobismutharsenide
Palladseite
Palmierite
Pampalargaite
Panasqueiraite
Panethite
Panunzite
Paraarsenolamprite
Parabariomicrolite
Parabrandtite
Paracoquimbite
Paracostibite
Paradocrasite
Parafransoleite
Parajamesonite
Parakhinite
Paralstonite
Paramontroseite
Paraniite-(Y)
Pararobertsite
Paraschoepite
Parascorodite
Parisite-(Nd)
Parkinsonite
Parwelite
Paulkellerite
Paulmooreite
Pehrmanite-9R
Peisleyite
Pellouxite
Penobsquisite
Percleveite-(Ce)
Permanganogrunerite
Perryite

Pertsevite
Petedunnite
Peterbaylissite
Petewilliamsite
Petrovskaite
Petrukite
Philipsbornite
Philolithite
Phosphammite
Phosphofibrite
Phosphogartrellite
Phosphorroesslerite
Phosphovanadylite
Phosphowalpurgite
Phyllotungstite
Pillaite
Pinalite
Pinchite
Pingguite
Piretite
Pirquitasite
Pitiglianoite
Pizgrishite
Platarsite
Playfairite
Plumalsite
Plumbobetafite
Plumbotsumite
Polkovicite
Potassiccarpholite
Potosiite
Poubaite
Poudretteite
Schoellhornite
Schreyerite
Schwertmannite
Sclarite
Protoanthophyllite
Proudite
Przhevalskite
Pseudocotunnite
Pseudograndreefite
Pseudorutile
Pseudosinhalite
Putzite
Qandilite
Qilianshanite
Qingheiite
Qitianlingite
Raadeite
Rabbittite
Rabejacite
Radovanite
Radtkeite
Rambergite
Rameauite
Rankachite
Ransomite
Rayite
Redingtonite
Reederite-(Y)
Refikite
Reidite
Reinerite
Rengeite
Retzian-(Ce)
Retzian-(La)
Retzian-(Nd)
Rhabdophane-(Nd)
Rhodarsenide
Rhodplumsite
Richetite
Rilandite
Ringwoodite
Rinmanite
Riomarinaite
Roaldite
Rodolicoite
Rohaite
Rollandite
Rondorfite
Ronneburgite
Rooseveltite

Rossmanite
Rouaite
Roubaultite
Rouseite
Routhierite
Rouxelite
Ruarsite
Rubicline
Ruitenbergite
Ruthenarsenite
Sabatierite
Sabelliite
Sabieite
Sadanagaite
Sailaufite
Saliotite
Salzburgite
Samfowlerite
Samuelsonite
Sanderite
Santanaite
Santite
Sarmientite
Sasaite
Sayrite
Scacchite
Schafarzikite
Schaferite
Schertelite
Scheteligite
Schiavinatoite
Schieffelinite
Schoellhornite
Schreyerite
Schwertmannite
Sclarite
Scotlandite
Sederholmite
Seelite
Selwynite
Sesquiterpenelactonite
Sewardite
Shabaite-(Nd)
Shakhovite
Shandite
Sharpite
Sheldrickite
Sherwoodite
Shirozulite
Shuangfengite
Sicherite
Sidpietersite
Sidwillite
Sieleckiite
Sigismundite
Silhydrite
Silinaite
Simmonsite
Simonellite
Simonite
Simplotite
Sinjarite
Sinnerite
Sinoite
Slawsonite
Sphaerobismoite
Spodiosite
Spriggite
Springcreekite
Srilankite
Stalderite
Stanekite
Stanfieldite
Stanleyite
Stenhuggarite
Stercorite
Sterlinghillite
Stibiobetafite
Stillwaterite
Stoiberite
Strontiochevkinite
Strontioginorite

Strontiomelane
Strontiomicrolite
Stumpflite
Suessite
Sundiusite
Surite
Susannite
Suzukiite
Sveite
Svenekite
Sverigeite
Swaknoite
Swartzite
Sweetite
Symesite
Synchysite-(Nd)
Szymanskiite
Takedaite
Takeuchiite
Tamaite
Tantalaeschynite-(Y)
Tarkianite
Taseqite
Tedhadleyite
Teineite
Tellurohauchecornite
Telluronevskite
Temagamite
Tengchongite
Terranovaite
Teschemacherite
Testibiopalladite
Thadeuite
Theoparcelsite
Theresemagnanite
Thomasclarkite-(Y)
Thornasite
Tillmansite
Tischendorfite
Tivanite
Tlalocite
Tobelite
Tomichite
Tongbaite
Tongxinite
Tooeleite
Torreyite
Toyohaite
Trabzonite
Tranquillityite
Treasurite
Trembathite
Trigonite
Trikalsilite
Trimounsite-(Y)
Trippkeite
Tristramite
Trogtalite
Trustedtite
Tschortnerite
Tsugaruite
Tsumgallite
Tuite
Tundrite-(Nd)
Tungstibite
Turtmannite
Tweddillite
Uchucchacuaite
Uhligite
Ungarettiite
Ungemachite
Uramphite
Urancalcarite
Uranosilite
Uranotungstite
Uricite
Utahite
Vanadomalayaite
Vanmeersscheite
Vanuranylite
Varulite
Vastmalandite-(Ce)

Vatatsumite
Vaughanite
Veenite
Verbeekite
Viaeneite
Viitaniemiite
Vincentite
Virgilite
Vochtenite
Voggite
Vonbezingite
Vozhminite
Vulcanite
Vuorelainenite
Wadalite
Wadsleyite
Wakefieldite-(Y)
Walfordite
Walkerite
Wallkilldellite-(Fe)
Wallkilldellite-(Mn)
Walthierite
Wardsmithite
Warikahnite
Watanabeite
Watkinsonite
Wattevillite
Weishanite
Welinite
Werdingite
Wesselsite
Wheatleyite
Whiteite-(CaMnMg)
Widenmannite
Wilcoxite
Wilhelmkleinite
Wilkmanite
Wiserite
Woodallite
Wooldridgeite
Wupatkiite
Wyartite
Wycheproofite
Xanthiosite
Xenotime-(Yb)
Xiangjiangite
Xifengite
Xilingolite
Ximengite
Xingzhongite
Xitieshanite
Yagiite
Yanomamite
Yedlinite
Yimengite
Yingjiangite
Yixunite
Yoshiokaite
Yuanjiangite
Yvonite
Zabuyelite
Zaccagnaite
Zaherite
Zairite
Zellerite
Zenzenite
Zhanghengite
Zhongshangonite
Ziesite
Zincalstibite
Zincgartrellite
Zincohoegbomite
Zincostaurolite
Zincovoltaite
Zincrosasite
Zincroselite
Zinczippeite
Zircophyllite
Zirklerite
Zodacite
Zoubekite
Zugshunstite-(Ce)

Mineralogical Notes

UDC 548.3

ON THE MALACHITE SPIRAL CRYSTALS

Boris Z. Kantor
Moscow, AG@compas88.ru

The main reason for spiral bending of malachite crystals from *Tyrol* is probably the zinc admixture. The admixture entails formation of thermodynamically stable «sandwich» structures and their curling under mechanical tension due to non-coincidence of element sizes in adjacent layers.

The finds in Tyrol, Austria, of spiral and curl-like crystals (Fig. 1) diagnosed as malachite are repeatedly mentioned in publications (Meixner, Paar, 1975; Brandstä tter, Seemann, 1984; Jahn, 1997). The reasons for formation of exotic forms have been discussed (Jahn, 1997; Wight, 1998), but were not cleared up completely.

The reference to dislocation mechanism of growth convincingly explains the extended form of crystals (Wight, 1998). As to the curling of crystals, «environmental conditions of growth ..., in particular, unequal growth rate of fibers in a malachite bunch» (Brandstä tter, Seemann, 1984), surface tension of mineral forming environment and mechanical tension near the dislocation axis (Wight, 1998), and even spiral character of dislocation growth (Jahn, 1997) were mentioned among the reasons. However, thin needles and fibers of «normal» malachite also grow under the dislocation mechanism, but do not curl. So, the dislocation growth mechanism cannot be asknowledged to be the single or main reason of the discussed phenomenon. «Unequal growth rate of fibers», in our opinion, also cannot be an explanation as it proceeds from notorious existence of a bunch of fibers (really notable in illustrations to quoted articles), which in itself requires a substantiation.

What is noticeable, that is the bluish and rather pale coloring of crystals usually indicating zinc admixture in malachite (at adequate, as a whole, color rendition in illustrations to publications by S. Jahn and Q. Wight). Really, the connect of 2.7% zinc is mentioned, which is abnormally much for malachite and twice above that in normal green malachite from the same deposit. The last circumstance suggests that curling of crystals is related to this feature of their composition. S. Jahn considers the zinc admixture as a reason for dislocations (Jahn, 1997). More general assumption of the important role of zinc «inclusions» is stated by Q. Wight (1998).

The discussed phenomenon becomes understandable if one considers the crystal structure of discussed «malachite» to consist of «copper» and «zinc» (or mixed) elements of somehow different sizes and configuration. Lattice cells of malachite $Cu_2[(OH)_2|CO_3]$ and rosasite $(Zn,Cu)_2[(OH)_2|CO_3]$ really differ from each other in linear dimensions by 0.64 — 4.7 % in different directions while angle β in rosasite accepts various values (Strunz, 1982), depending probably on Zn/Cu ratio.

Similar mixed structures are more stable when provided with the distant order in them, characterized by ordered arrangement of elements of one type between elements of another type, for example, separately in different layers. As is known, these «sandwich» structures have ability to bent spontaneously and even to roll into rolls. The chrysotile structure is a classical example of «sandwich» structure.

Simplifying extremely the picture, let us imagine a two-dimensional crystal structure of a mixed crystal consisting of rectangular elements of greater A x B and smaller a x b sizes, located separately in adjacent layers of a two-layer package (Fig. 2*a*). This combination of elements of different sizes in one structure results in elastic straining — rectangles turn into slanting trapezes (marked by crosses of diagonals), which is equivalent to essential increment of free energy.

Obviously, this condition of a fragment is unstable and, owing to the elastic character of deformation conditioned by forces of chemical bond, it would bent on an arch (Fig. 2*b*) until the sum of deformations would reaches the possible minimum at this combination of elements. As a result, elements would take the form of equal, in each layer, isosceles trapeziums, in a maximum degree reduced to rectangles. The free energy would reach the possible at this conditions minimum and a fragment, having accepted an arched form, would pass into equilibrium state.

The said above is confirmed by calculations. The degree of deformation and free energy are determined by the sum of areas of shaded plots of deformations (Fig. 2*a*).

The area of i (from the middle) deformed plot in the first option is equal to the strained area $S_i = B\, d_{i_1}/2 + b d_{i_2}/2$,

where d_{i_1} and d_{i_2} — displacements of borders of big and small elements along their common border.

As in isomorphism conditions these elements only slightly differ in sizes, it is possible to accept to be

$d_{i_1} \approx d_{i_2} = i(A\text{-}a)/2$,

and then

$S_i = i/4 \cdot (B+b)(A\text{-}a)$,

while the total area of n strained plots is

$$S_{total} = 1/4 \cdot (B+b)(A\text{-}a) \sum_{i=1}^{n} i = 1/8 \cdot n\,(n+1)(B+b)(A\text{-}a)$$

In the arched structure all shaded areas are equal and the total area of n strained plots is

$$S'_{total} = n/2\,(B+b)(A\text{-}a)$$

The ratio of areas expressing the deformation degree of the structure is

$S_{total} : S'_{total} = (n+1)/4$

S'_{total} is i.e. always less than S_{total},

as expected.

It is easy to see that other ratio of element numbers (for example, as in the considered case, 2.7 % of «zinc» elements) would not change the picture, but only increase the curvature radius.

Thus, sorting of elements during the growth enables, under other conditions being equal, decrease of free energy, whereas chaotic arrangement of elements excludes this possibility. Hence, sorting of elements is motivated and is ruled by a natural process towards the decrease of free energy.

Passing from a two-layer package to a structure of a set of packages, where elements of both types are separately packed, it is necessary to assume the origination of tangential shift tension accompanying bending between packages of layers. It is these tensions that cause the longitudinal splitting of a growing crystal into fibers, but also support the process of their curling. The stated reasons also remain in force for more realistic model of structure of unequal thtee-dimensional monoclinic elements, as lattice cells of malachite and rosasite actually are. This model results in crystal curling by a spiral, which really occurs.

Summarizing, it is necessary to draw a conclusion that origination of sandwich structures is a necessary and sufficient condition for minimization of that part of free energy, which is conditioned by the presence of two types of elements, and curling of a crystal is nothing other than a method and morphological expression of free energy minimization. The curled form of «malachite» from Tyrol is paradoxically closer to equilibrium than hypothetical flat-face form of the same mineral. At the same time, on the background of the considered main reason, it is natural to assume the influence of other factors — unequal growth rates at different sides of a crystal, as at growth of gypsum antolites (Maleev, 1971), the surface phenomena, tension near the axis of dislocation, etc.

Analogous ordering of structure probably explains the origination of curled and curved forms of other mixed crystals, for example, manganous calcite from Dalnegorsk (Fig. 3).

References

Brandstä tter F., Seemann R. Die Malachite Spirale von Schwaz, Tirol // Magma. **1984.** Nr. 3. SS. 52—53

Jahn, S. Neue Malachite in Spiral und Lockenform vom Bergbau Schwaz-Brixlegg, Tirol // Mineralien Welt. **1997.** Nr. 6. SS. 20—26

Maleev M.N. Svoistva i genezis prirodnykh nitevidnykh kristallov i ikh aggregatov (Properties and genesis of natural thread-like crystals and their aggregates). M., Nauka, **1971**.199 p. (Rus.)

Meixner, H., Paar, W. Neue Untersuchungen am «Lockenmineral» von Brixlegg, Tirol // Der Karinthin. **1975.** Nr. 72/73. SS. 175—181

Strunz, H. Mineralogische Tabellen. Leipzig, Akademische Verlaggesellschaft. 1982. 621 S.

Wight, Q. The Curly Malachite of Schwaz-Brixlegg, Tyrol, Austria // Rocks and Minerals. **1998.** Vol. 73. No. 5. Pp. 314—318

UDC 549.091

DIAMOND IMAGES ON THE POSTAL STAMPS OF THE WORLD

Vyatcheslav D. Dusmatov
Fersman Mineralogical Museum, RAS, Moscow, dusmatov@fmm.ru

Igor V. Dusmatov
Ordzhonikidze Moscow State Geological Prospecting University, Moscow.

«One can hardly tell what exactly attracts people to this stone. Naturally, it catches your eyes with its extraordinary bright luster and a color play of rays it reflects. Numerous are other beautiful gems, but this one has gained its supremacy due to other reason. It has been its unusual hardness that counted. Hence its name diamond — diamant — diamas, i.e., utterly unyielding».

A.E. Fersman. Stories about Gems.

Existing bibliography on diamonds is unbelievably vast. Any kind of information is available on the mineral, from its formative conditions to structural features and techniques to produce artificial crystals. The following text is a compilation that employs data from various publications, occasionally with no proper references.

A legend related to the Pentateuch tells that God in the evening dusk of the sixth Creation day made ten things, and *shamir* (diamond in Hebrew) had been among them. It had been as large as a barley grain, and its single touch could crash a stone and burst an iron rod. This had been the stone Moses used to cut twelve names of the sons of Israel on the stone tablets and on the ephod fastenings (Bobylev, 2000).

Golkonda, India, has been the first place of the diamond mining. Mahabharata and Veda scripts of the 10th century B.C. refer to this stone as *waira*. Legends of the 12th century B.C. mention diamond as an adornment. The oldest diamond-related artifact is believed to be a Greek bronze statuette dated as 480 a. B.C., which eyes are diamonds of Indian origin.

Bobylev (2000) reported that it was Afanassiy Nikitin, a merchant from Tver, who managed to visit India in the 15th century, coined («imported») the existing Russian name of the mineral, *almaz*.

By the first half of the 20th century, major producers of diamonds were Angola, Australia, Botswana, Zaire, Namibia, and RSA; in the 1950s Russia joined this highly privileged "diamond club" to become its seventh member. Now 20 and more countries of the world mine diamonds, mainly from kimberlites and placers. Over 1000 diamondiferous kimberlite bodies are known in the world. A promising diamondiferous kimberlite pipe costs 5 to 6 billion USD. The mining output of diamonds per year is about 100 M ct (about 20 metric tons). A total amount of diamonds the mankind mined during its history is estimated as 3600 M ct (720 t); provided the mining rate remains, the explored reserves will last for three decades. The world production of synthetic diamonds is *c.* 450 M ct per year, what totally covers the existing demand.

About 60% of the mined natural diamonds are the jewelry and collection stones, and their considerable part is stored as the currency reserves. Diamond is the gem the jewelers value and adore. It combines magnificence, strength, and originality. Hardness and purity inherent in diamond symbolize the best human qualities and unbending nature of the Power. It is not by chance diamonds are the key adornments of the national regalia. Another unique property of the diamond is that it burns down leaving no residue like love, like passion. Maybe, that is why diamonds and brilliants are able to trap and enslave human souls entirely (Pelekhova, 2002).

Frequently unique diamonds are exposures of the state-owned or private museum collections. Some diamonds are historical relics. However, a vast majority of living people is deprived of the chance to feel the whole charm of this gem. Instead, most postal agencies of the diamond-mining countries issue stamps portraying minerals, diamond included. Countries where diamonds are cut into brilliants do the same. In our earlier publication we reported on the minerals, which images are reproduced on stamps (Dusmatov, 2001): diamonds adorn stamps issued in more than 20 countries.

First of all, we should mention a stamp with A.E. Fersman's portrait: he was the first Russian scientist who studied morphology of the dia-

mond crystals in detail. The stamp issued in the USSR in 1971 shows the Shah, a diamond of dramatic history described by Fersman and stored now in the national Diamond Fond. A stamp issued in the USSR in 1968 due to the 8th International mineral processing congress displays the Gornyak (Miner) a 44.6-ct diamond, also stored in the Diamond Fond.

Golkonda, South India, was the finding place of the Koh-i-noor, or Mountain of Light (Urdu), originally 800 ct. After the first cut (rose-not-brilliant-cut) it weighed 191 ct; in 1852 it was re-cut into a stellar (oval) 108.9-ct brilliant. Queen Victoria used to wear it as a brooch; later the diamond was mounted on the cross at the top of the crown of Queen Elizabeth. A stamp issued in Belize portrays this crown.

The Cullinan (named after Thomas Cullinan, a president of the diamond mining company) is an undisputable leader among diamonds portrayed at the postal emissions. When found in South Africa, it weighed 3106 ct. A Cambodian postal block presents its view. In 1907, they presented the diamond to King Edward VII. Later on, nine large and 96 smaller brilliants were made of it; the total weight of the brilliants was 1063.65 ct (65.75% lost). The largest of these, Cullinan I, or the Star of Africa (516.5 ct), adorned the Sovereign's Royal Scepter. The Cullinan II, an elongated brilliant of 309.33 ct, became a part of the Imperial State Crown of Great Britain. The Minor African Stars aka the Cullinan III and IV are among the Crown Jewels. The Cullinan III (92 ct) is mounted in the finial of Queen Mary's Crown and can form an ensemble with the Cullinan IV (62 ct) thus to be converted into a pendant-brooch. The Cullinan V a 18.5-ct heart-shaped diamond, adorns a circlet of Queen Mary's crown. The Cullinan VI (11.55 ct), a marquise-cut stone, is a drop on a diamond-and-emerald necklace of the Crown Jewels. The Cullinan VII (8.7 ct, marquise-cut) and the Cullinan VIII (6.7 ct), an elongated stone, are parts of an all-diamond brooch (see the Cambodian postal block). The Cullinan IX (4.4 ct) is set in a ring, and 96 smaller diamonds (a total of 7.55 ct) are mounted in the Imperial State Crown. A postal block issued in Guinea-Bissau demonstrates all regalia of Queen Elizabeth II. Postal emissions of twenty and more countries display the Crown Jewels with brilliants made of the Cullinan fragments. South Africa issued stamps and an envelope with the Cillinan 1 and II images.

Diamonds are shown on Botswanian stamps. One of these shows diamonds of variegated color mined in the country: colorless, blue, greenish, yellowish, and pale lilac. A series of diamond-shaped stamps demonstrates diamond mining and processing, as well as diamond jewelries.

Sierra Leone issued a wide variety of diamond-related stamps. These vary in shape and contain information on weight of natural and cut stones. A stamp from Niuafoou shows a kimberlite pipe, kimberlite that hosts a diamond, and a brilliant. Ghana issued a stamp with a diamond against the background of the open-pit mine. Diamond images adorn the stamps of Tanzania, Congo, Angola, Australia, Lesotho, Afghanistan, and Somalia; in the latter case the stamp demonstrates both a mineral and its crystalline structure.

References

Bobylev, V.V. (**2000**) *Istoricheskaya gemmologiya* [Historical gemology], Moscow, VNIGNI, 180 pp. (Rus.)

Dusmatov, V.D., Dusmatov, I.V. (**2001**). Mineralogical Museum as displayed at the stamps of the world. In: *Sredi mineralov* [Among the minerals] (an almanac), Moscow, Ecost, p. 189–192 (Rus.)

Fersman, A.E. Rasskazy o samotsvetakh [Stories about gems] Moscow, Nauka, **1974**, 254 pp. (Rus.)

Pelekhova, Yu. (**2002**) Where the diamonds are? *Versiya (weekly)*, August 5–11 (Rus.)

In memoriam: Vyacheslav Dzhuraevich Dusmatov

A short fatal disease carried away from us Vyacheslav Dzhuraevich Dusmatov (16.03.1936 – 27.05.2004), Cand. Sci. (Geol., Mineral.), senior research associate of the Fersman Mineralogical Museum, RAS, and a talented geologist and mineralogist who studied natural mineral resources of Tajikistan.

V.D. Dusmatov was born in Garm, Tajikistan. In 1959 he graduated from the Geological Department of Tajik State University in Dushanbe. His career followed from senior technician in the Geological Institute of the Tajik Academy of Sciences to Director of Geological Museum of the Tajik AS and a project leader in the Soyuzkvartzsamitsvety Association. In 1994, he accepted a position of a director of the Tajik State Research Institute for Mineral Deposits, and later during the same year he became a chief gemologist of the Rukhom National Enterprise. In 2001 Vyacheslav Dusmatov joined a staff of the Fersman Mineralogical Museum, RAS, where he took up studies of Academician A.E. Fersman's archive.

A scope of his scientific interests was quite wide, from mineralogy and petrology of alkalic rocks of Middle Asia to economic geology of gemstone. He worked much to promote biological aspects of mineralogy, especially those related to mumiyo. His studies of historical mineralogy in Tajikistan acknowledging Al Berouni and Avicenna as founders of mineralogy became widely known. The museum-related activities played an important part in Dusmatov's studies. During the course of his work in the Tajik Institute of Geology (1959 – 1994), he collected and several thematic series of the rock and mineral samples, which characterized the largest mineral deposits of the Pamirs. These collections made a basis of geological museum organized at this institute. He was not just a curator: he designed and manufactured many windows and racks in the museum. Mineralogical projects carried out under his leadership were attractive for young researchers.

Vyacheslav Dusmatov was fond of nature and flowers; he was deeply interested in history of religion. His deepest passions were badges and stamps. He collected stamps all his life, and mineralogy part is widely known among the collectors. This collection reflected his academic interests and love to the minerals.

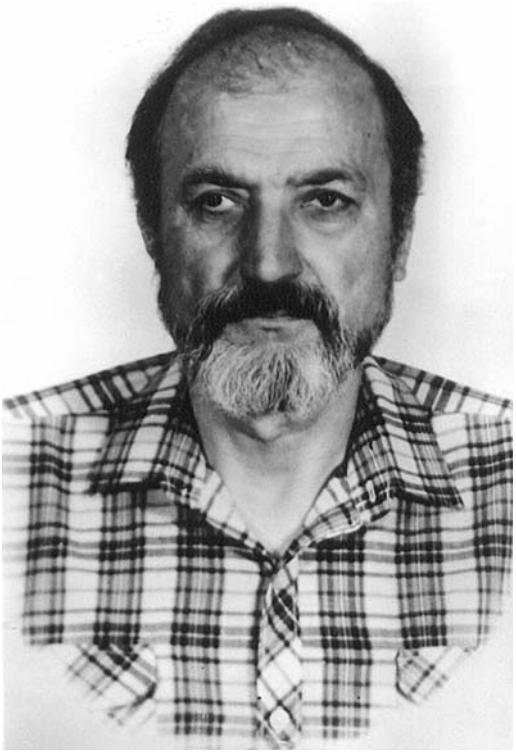

When studying alkalic rocks and related pegmatites, Vyacheslav Dusmatov, an experienced field geologist and mineralogist, visited numerous plutons in Gissar and Alay. It was Dara-i-Pioz, a unique alkaline pluton located at the south slopes of the Alay Ridge, that became a key object of his studies. Early in the 1960's, detailed studies were carried out here to estimate this pluton as a source of alumina. The conclusion on nepheline rocks of the pluton has been negative, but the researchers found a noteworthy rare metal mineralization. In 1960, V.D. Dusmatov began his studies of alkalic rocks exposed at the south slope of the Alay Ridge. In the upper part of the Dara-i-Pioz River basin, he established an original rare metal-TR-U mineralization. This mineral assemblage has not been observed elsewhere since then. The first publications on mineralogy of the area written by V.D. Dusmatov and E.I. Semyonov in 1963 deals with Y-Be datolite («calcibeboronsilite»). The same authors have published a series of papers on ekanite, U-thorite, rinkolite, and agrellite during the period from 1965 through 1989. V.D. Dusmatov, E.I. Semyonov, and

A.P. Khomyakov discovered new minerals: baratovite, darapiosite, and zirsilite. Later on, V.D. Dusmatov and A.F. Efimov discovered a series of new minerals: cesium kupletskite, tajikite, tienshanite, sogdianite, and surkhobide.

V.D. Dusmatov first described endogenous reedmergnerite. He was the person who first found stillwellite-Ce (a green variety of leucosphenite) at the territory of the USSR. In co-authorship with A.S. Povarennykh he obtained IR spectra of the minerals discovered or first found in this pluton. An extended series of papers he wrote in co-authorship with F.N. Abdusalomov described amphiboles, pyroxenes, and micas.

V.D. Dusmatov continued his studies of geology, geochemistry, and mineralogy of the Dara-i-Pios pluton till 1991. Using an air photo base map, he compiled a geological map of the upper part of the Dara-i-Pios river basin on 1:25,000-scale with all rock varieties contoured on it.

Another area V.D. Dusmatov was interested in was geology of gems: exploration, reserve estimation, and mineralogy.

To honor his achievements in this area, Leonid A. Pautov and Atali A. Agakhanov named a new mineral they discovered dusmatovite (Vestnik MGU, 1996, Ser. Geol., No. 2, p. 54–60).

Having joined the RAS Mineralogical Museum, V.D. Dusmatov undertook studies of Academician Fersman's archive. He browsed a lot of typewritten materials, manuscripts, photos, and newspaper clips of the period. All these materials have been thoroughly studied, sorted, and prepared for publication, what resulted in a book titled *Unknown Fersman* issued by the Museum in 2003 to celebrate the 120th birthday of A.E. Fersman. Vyacheslav Dusmatov always remained energetic and optimistic in his plans for the future. His devotedness to work inspired his coworkers. Kind, responding, and modest, he gained love and gratitude from his colleagues.

V.D. Dusmatov published 200 and more publications, including 3 monographs. Some of these are listed below:

Dusmatov, V.D., Efimov, A.F., Semyonov, E.I. (1963) First finds of stillwellite in the USSR. Doklady AN SSSR, 153, No. 4: 913–915. (in Rus.)

Dusmatov, V.D. (1969) Alkalic rocks of Central Tajikistan: State of the art. Izvestiya AN Tajik SSR, otd. fiz-mat. i geol.-khim. nauk, No. 2 (32): 97–102. (in Rus.)

Dusmatov, V.D. (1970) Mineralogy and geochemistry of alkalic and granite rocks from the upper part of the Dara-i-Pios River basin, South Alay. In: Voprosy geologii Tadzhikistana (Problems of Tajik geology), Dushanbe. (in Rus.)

Efimov, A.F., Dusmatov, V.D., Alkhazov, V.Yu. et al (1970) Tajikite, a new TR boron silicate, the hellandite group. Doklady AS USSR, v. 195, No. 5: 1190–1193. (in Rus.)

Klimov, G.K., Akramov, M.B., and Dusmatov, V.D. (1991) Classification of intrusive rock series of Tajikistan. In: New data on Tajik geology, Dushanbe. (in Rus.)

Dusmatov, V.D. (1997) Marble onyx from Middle Asia (in Chinese).

Vyacheslav Dzhuraevich Dusmatov will remain as a prominent figure among Russian and Tajik mineralogists

Staff Members of the Fersman Museum

In memoriam: Alexander Kanonerov

Untimely left us Alexander Kanonerov (b. February 27, 1955, d. September 27, 2003), an outstanding Uralian amateur mineralogist, a talented researcher of the regional natural history, one of the top Russian collectors, and an active member of the All-Russia Mineralogical Society. He lived in Nizhny Taghil and was a staff member of the Uralian Mining Preserve-Museum. Anybody who encountered this bright person would not forget his sparkling energy and unusual enthusiasm he emanated in every matter he took up. It was Alexander Kanonerov who a decade ago initiated detailed mineralogical studies of the Murzinka pegmatite fields famous for their gems and ore deposits of the Nizhny Taghil surroundings; he was tireless in inspiring this work and was its immediate part. During the last eight years he prepared more than 20 papers, both solely and as a co-author. These are detailed mineralogical descriptions of the Nizhny Taghil area, monographs on the Alabashka pegmatite field, one of the best-known mineralogical objects of the Urals. The most significant of these publications are *Mineralogy of the Kazennitsa pegmatite vein, Middle Urals* (Popov *et al.*, 1996), *Murzinka gem mines — A mineralogical guide and cadastre* (Kanonerov and Chudinova, 1998), *Cr-bearing kassite from Saranovskoe deposit: first find in the Urals* (Popova *et al.*, 1998), *Minerals of the Nizhny Taghil area* (Kanonerov, 1999), *Mineralogy of granite pegmatite: the Alabashka field of the Uralian Gem Belt* (Popova *et al.*, 1999), *Murzinka: Alabashka Pegmatite Field* (Popova, Popov, Kanonerov, 2002) and the Russian version of the latter, *Abandoned Ag-Pb mines at the Taghil River* (Kanonerov, Radostev, 2002), *Be-bearing cordierite from desilicated Lipovka pegmatites, Middle Urals, and specialties of its crystalline structure* (Pekov *et al.*, 2003), *New data on mineralogy of the Gorno-Anatolsky silver mine, Middle Urals* (Popov, Kanonerov, 2003), and *Massive sulfide copper deposits of the Taghil area: a chronicle of discoveries (1640—1968)* (Kanonerov, 2003).

He was a person of detailed knowledge of mineralogy and mining of the region; ever thirsty for new data, he not just managed to extract these from archives and old publications, but pinpointed abandoned mine workings to make excavation and cleaning with his own hands dreaming of the time when these will become the outdoor museum items.

Since his childhood Alexander Kanonerov has been interested in minerals, and his collection comprises ten thousand samples and more. Along with its systematic part, it comprises complete and variegated selections on individual local objects of the Middle and South Urals, these real masterpieces of a high professional. Formally, a geological college limited his edu-

cation; nevertheless, he was a member of the Uralian Academy of Mineralogy. Alexander was a proved connoisseur of practical mineralogy. AS a staff member of the Mining museum, he prepared from his personal collection a vast mineralogical exhibition, as well as selections on history of mineralogical studies and mining in the Nizhny Taghil area. Thousands (!) of samples he collected joined the museum collections over the whole Russia. Alexander's generosity matched his energy. Nobody recalls a case when an interested visitor left his home with no gift. He was an active and unselfish volunteer in organization of the student training courses, mineralogical excursions, visits to hardly accessible mines; weeks and weeks of his unpaid time were spent for that. Alexander thoroughly prepared rich mineral sample selections for further thematic studies of mineralogical problems to be carried out by narrow academic specialists.

He was a unique in fieldwork with his huge experience and deeply developed intuition. Alexander amazed his colleagues by his ability to unmistakably pinpoint old pits, tiny rock exposures, and hardly recognizable mounds of mine dumps abandoned a century and a half ago, be it located in a dense forest or in a town outskirt. He was a real mineral hound: minerals used to come to him in localities where our great-granddads lost hope to find them. His field work geography during the 1970's — 1980's is quite impressive: hundreds of objects over the Soviet Union, from Carpathians and Kola Peninsula to Tien Shan and Russian Far East. Naturally, he considered Middle Urals, his home place, as a key region, so during the last decade he focused his efforts here. Along with Nizhny Taghil and Murzinka, he was highly interested in Lipovka, Potanya Hills, Berezovskoe, and a series of other Middle Ural mineralogical localities. He knew no season breaks in his field work, and samples he collected had been invariably interesting.

A classical old hand of a Uralian digger peacefully co-existed in his personality with a seeking researcher and collector; a Uralian dialect word *khitnic*, what can be invariably imperfectly mirrored in English as mineral predator, adds some color to Alexander's portrait. This component of his personality made him an unforgettable companion: with his outstanding appearance, juicy humor, powerful efficiency, and deep knowledge of Uralian nature, history, and traditions, Alexander effortlessly was becoming a leader in any relevant discussion. Along with it, he was always keen to information provided by his counterparts, asking for new publications and studying these meticulously. We know not of other amateur mineralogist in Russia comparable to Alexander by his sparkling energy and results achieved during the course of a period so short. And how vast were his plans for future! Alexander's heart has ever been at the heart of his matter, and once it failed...

Visible memory about this outstanding person remains in his papers and books, in collections and exhibitions he prepared, and, certainly, in mineral kanonerovite, the only natural triphosphate, which Alexander found in the Alabashka pegmatite field he loved so dearly.

Igor V. Pekov, Valentina I. Popova,

Mineralogical Almanac

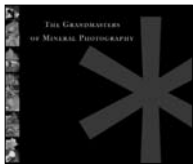

The Grandmasters of Mineral Photography Mineralogical Almanac Special Issue.
136 pages, 117 color plates, 13 b/w photos, soft cover.
This special issue features 14 expert mineral and gem photographers Roberto Appiani (Italy), Nelly Bariand (France), Louis-Dominique Bayle (France), Rainer Bode (Germany), Michael A. Bogomolov (Russia), Hidemichi Hori (Japan), Terry E. Huizing (USA), Michael B. Leibov (Russia), Olaf Medenbach (Germany), Harold and Erica Van Pelt (USA), Jeffrey A. Scovil (USA), Stefan Weiss (Germany), Wendell E. Wilson (USA) whose work is well known to collectors and mineralogists throughout the world. For the past 30 years, thousands of their mineral photographs have been published in numerous scientific and popular science books, as well as in every periodical for collectors

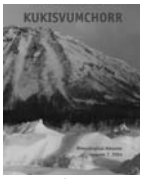

Mineralogical Almanac vol. 7. Famous Russia Mineral Localities Series. Kukisvumchorr Deposit (Kola Peninsula): Mineralogy of Alkaline Pegmatites and Hydrothermalites. by I.V. Pekov and A.S. Podlesnyi. 168 pp., soft cover. 312 chemical analyses of 165 minerals and 163 references.
Kukisvumchorr deposit is actively operated since 1929 by Kirovskii Mine, the first mine at Kola Peninsula. A complex of alkaline pegmatites and hydrothermalites of the Kukisvumchorr stands out even against a background of mineralogically unique Khibiny massif. It is real reserve of rare minerals; many of them occur here as nice large crystals. All 212 present-day known mineral species and more than 20 pegmatites have been described, 111 color plates, 110 b/w photos, 125 crystal drawings, geological schemes and pegmatite sections are given.

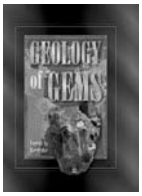

Geology of Gems *by Eugenii Kievlenko*. Edited by Dr. Art Soregaroli. First English Edition.
468 pages. 136 color plates, 128 b/w drawings, hard cover. Price: US$98
The book contains detailed and comprehensive information about gem localities over the world, and their geological setting. The book is full of geological illustrations, which make the text easily understandable. In addition we included 136 color photographs of all the main gems, mentioned in the book, taken by the best mineral photographers of the world. The book is of great value both for collectors and professionals.

Back issues

MA vol. 6. Crystal Growth & Development: Interpreted From a Mineral's Present Form *by Boris Z. Kantor, 2003*. pp. 128, full color, color plates – 142, b & w drawings – 72.
This volume devoted to basic ideas of mineral ontogeny, which is a branch of Mineralogy dealing with mineral forms, their origination and transformation. This book is for those mineral collectors and amateurs who seek a deeper knowledge of minerals and want to learn about mineral structure, origin, and history from a mineral's crystal form. More than one hundred color photos of minerals together with numerous sketches give the reader a lot of new information.

MA vol. 5 Famous Russia Mineral Localities Series. Murzinka: Alabashka Pegmatites Field
by V.I. Popova, V.A. Popov, A. A. Kanonerov, 2002, pp. 136, full color, softbound. Color plates – 108, b/w and drawings – 181.
The issue contains most complete and updated description of geological setting of Alabashka pegmatites field in general and each productive pegmatite vein in particular. Mineralogy of the region is described on the basis of all data accessible to the moment, including recent investigations of the authors.

Next coming

Minerals of the Kerch iron-ore basin at Eastern Crimea *by Nikita Chukanov*. **Mineralogical Almanac,** vol. 8. **Famous Russia Mineral Localities Series.** *2005*. pp. 128, full color, soft cover.
The Kerch iron-ore deposits which were discovered at the end of 19th century are famous among collectors of the world for beatuful inique clusters and druses of of vivianite, anapaite, rhodochrosite, barite and other minerals, present in many mineralogical collections and museums of the world. The fact that the Kerch basin has also a significant mineral variety is less known: now about 100 mineral species are known within it, most interesting of which are phosphate minerals. Two minerals (anapaite and mitridatite) have been first discovered in this formation and rather recently a number of new for Kerch minerals have been found, distinguished by rarity, singularity or beauty of specimens.

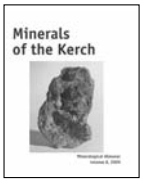

Publication of Fersman Mineralogical Museum (RAS)

Natural Mineral Forms. The book involves systematization and description of various mineral forms known in the nature. This is the first published well-illustrated course that tracks the evolution of the crystal perfectness over the wide range of mineralization conditions. It proceeds from almost ideal crystals to highly defective ones, which can be rightly identified as both individual forms and aggregates. Regularly and irregularly formed aggregates of minerals are also considered. The comparison the mineral forms crystallizing in fluid (gas, liquid), viscous (melt), and solid (rock) media is of great interest.

Order from web-site www.minbook.com or by e-mail minbooks@online.ru

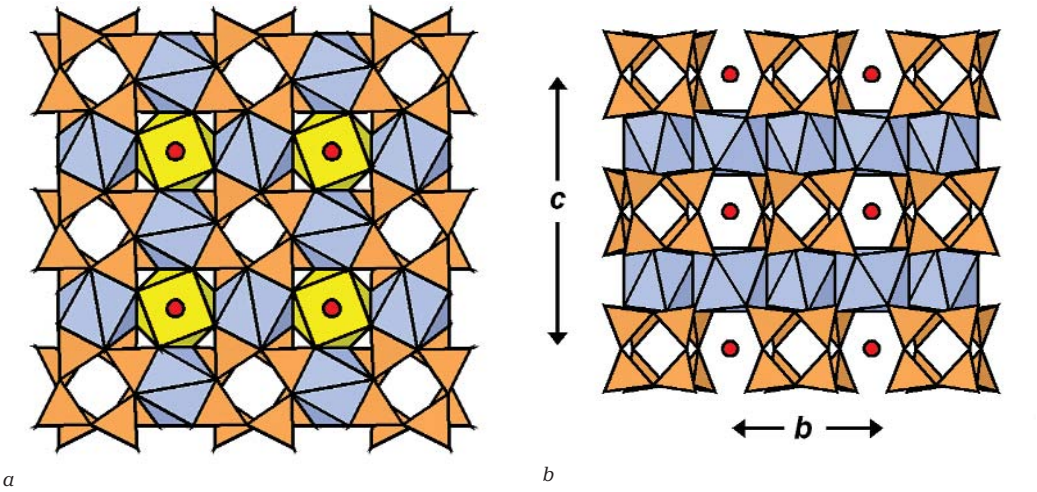

FIG. 3. Crystal structure of arapovite: a) projection on (001); b) projection on (100). Si tetrahedra are orange, A and B [8]-coordinated polyhedra are yellow and blue correspondingly, C atoms are shown as red circles

ions with smaller valence (Pb, REE), and B-site is occupied not only by calcium but also sodium. It isn't excluded that the presence in the nature of the end member with formula $UCa_2Si_8O_{20}$ is possible, however it isn't clear that this phase will have the crystal structure of arapovite or turkestanite type. The possibility of the presence in the nature the vacancy-dominant phase by C-site is confirmed by finding of «uranium hydrate variety of ekanite» (Semenov, Dusmatov, 1975), which chemical composition can be recalculated on following formula (Si = 8): $(U_{0.85}Th_{0.21})_{1.06}(Ca_{1.47}Na_{0.23})_{1.70}(\square_{0.68}K_{0.32})_{1.00}Si_8(O,OH)_{20}\cdot nH_2O$. Unfortunately, this phase remains while structurally unstudied.

The sample with arapovite was given to the Fersman Mineralogical Museum RAS (Moscow).

Acknowledgments

The authors thank Pavel V. Khvorov for help in carrying out of field works at the moraine of Dara-i-Pioz glacier and in laboratory studies and Igor V. Pekov for valuable advices.

References

Dusmatov V.D. To mineralogy of one of the alkaline rocks massifs. //In book: Alkaline Rocks of Kirgizia and Kazakhstan. (Shchelochnye Porody Kirgizii i Kazakhstana). Frunze. *1968.* P. 134–135. (Rus.)

Dusmatov V.D. Mineralogy of Dara-i-Pioz Alkaline Massive (South Tyan-Shan). (Mineralogiya Shchelochnogo Massiva Dara-i-Pioz (Yuzhnyi Tyan'-Shan')). PhD Thesis. M. **1971.** 18 p. (Rus.)

Ginzburg I.V., Semenov E.I., Leonova L.L., Sidorenko G.A., Dusmatov V.D. Alkali-enriched crystalline ekanite from Middle Asia. // Trudy Mineralogicheskogo Muzeya AN SSSR. **1965.** N. 16. P. 57–72. (Rus.)

Kabalov Yu.A., Sokolova E.V., Pautov L.A., Schneider J. Crystal structure of the new mineral, turkestanite, calcium analogue of steacyite. // Krystallografiya. **1998.** V. 43. № 4. P. 632–636. (Rus.)

Pautov L.A., Agakhanov A.A., Sokolova E.V., Kabalov Yu.K. Turkestanite, $Th(Ca,Na)_2(K_{1-x}\square_x)Si_8O_{20}\cdot nH_2O$, new mineral with twinned fourfold silica-oxide rings. //ZVMO. **1997.** № 6. P. 45–55. (Rus.)

Richard P, Perrault G. Structure crystalline de l'ekanite de St-Hilaire, P.Q. // Acta Crystallogr.1972. B. 24. P. **1994–1999**

Semenov E.I., Dusmatov V.D. To mineralogy of Dara-i-Pioz alkaline massive. // Doklady AN Tajik. SSR **1975.** V. 18. № 11. P. 39–41. (Rus.)

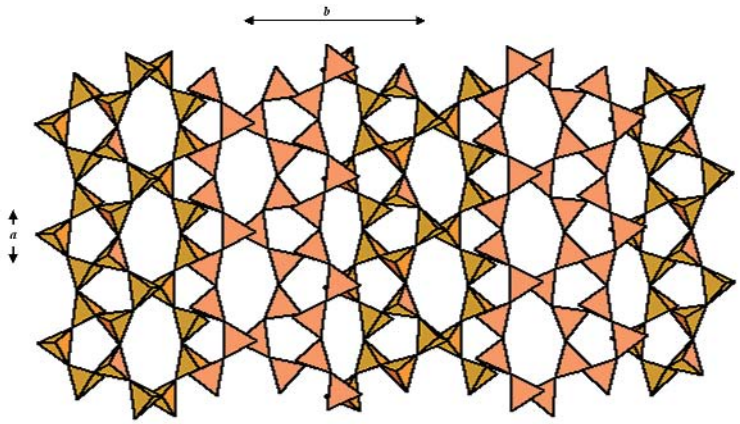

FIG. 1. Silica-oxide layers $\{Si_{18}O_{45}\}^{18}$ in the crystal structure of zeravshanite

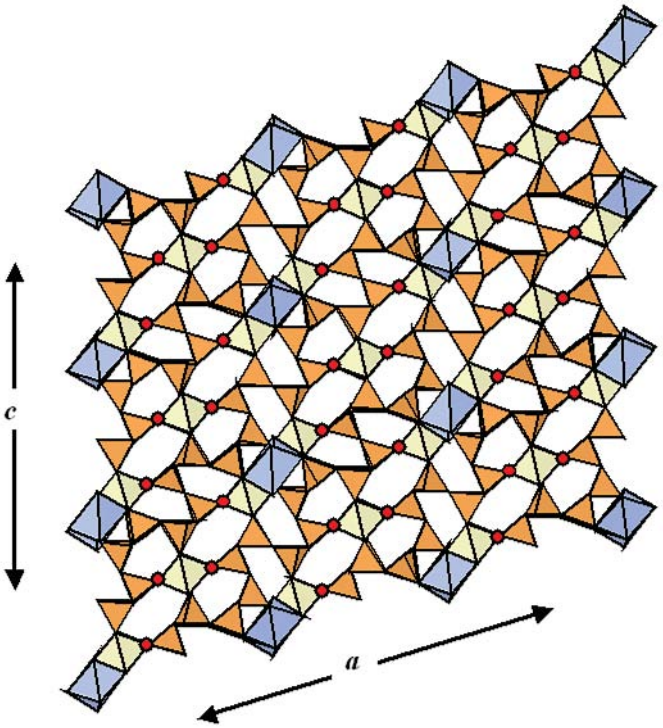

FIG. 2. The crystal structure of zeravshanite projected on (010).
Si-tetrahedra are orange,
M-octahedra are yellow,
Na-polyhedra are blue,
A atoms are shown as red circles

Photo 1. A typical view on vanadium-bearing shists. Kara-Chagyr deposit. Photo by V.Yu. Karpenko

Photo 2. Vanadium-bearing nickelalumite spherolites with volborthite, Kara-Chagyr.
a) № 5439 (4x6 mm) (there is a bluish ankinovichite core on allophane in front of the picture);*
b) № 5341 (3x4 mm).
Photo: Natalia A. Pekova

Photo 3. Vanadium-bearing nickelalumite spherolites, Kara-Chagyr. № 5345 (4x6 mm).
Photo: Natalia A. Pekova

Photo 4. Two generations of volborthite (dark-green sceleton tabular crystals (1) and light-green acicular ones (2)), growing upon nickelalumite spherolites. Kara-Chagyr — a) № 5339 (10x6 mm); b) № 5444 (5x3 mm). Photo: Natalia A. Pekova

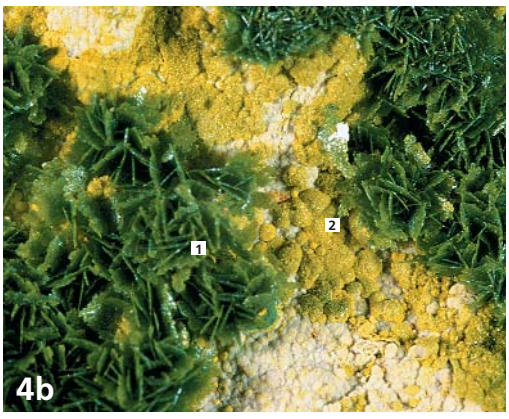

* *here and further size of a image size is given*

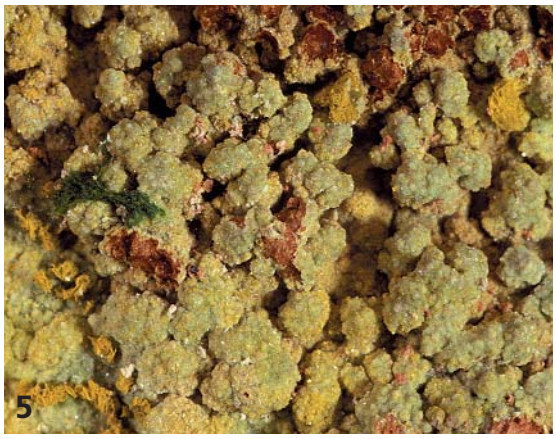

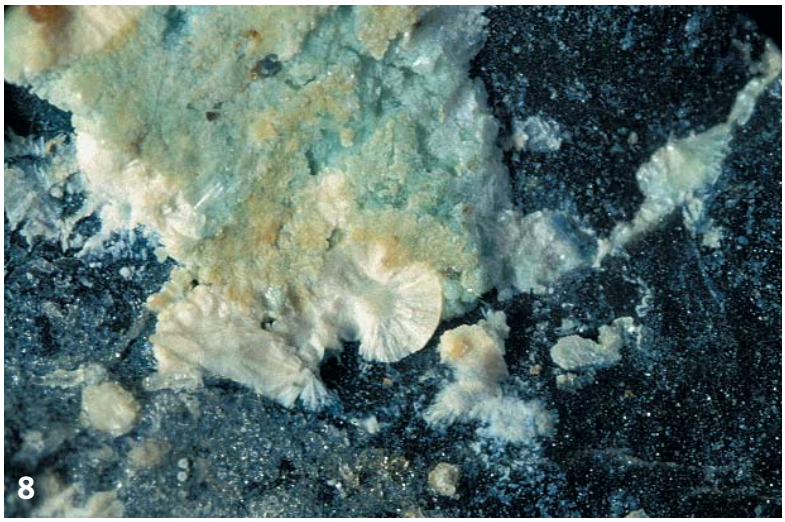

Photo 5. A small-grained ankinovichite core, grown upon nickelalumite spherolites. Yellow crystals belongs to tyuyamunite and brownish core — to allophane. Kara-Chagyr. № 5448 (6x10 mm). Photo: Natalia A. Pekova

Photo 6. Nickelalumite spherolites, covered with a core of ankinovichite acicular crystals, Kara-Chagyr. № 5445 (6x9 mm). Photo: Natalia A. Pekova

Photo 7. Tyuyamunite tabular yellow crystals and volborthite dark-green ones, grown on ankinovichite spherolites. Kara-Chagyr. № 5443 (5x8 mm). Photo: Natalia A. Pekova

Photo 8. A bluish core of a zincian nickelalumite. Spherolite in the center belongs to allophane pseudomorphose upon nickelalumite. Kara-Tangi. № 5360 (3x4 mm). Photo: Natalia A. Pekova

Photo 1. Schrö ckingeritev crystals from the Komsomolskoye deposit. Photo M.B. Leibov

Photo 2. Monomineral segregation of schrö ckingeritev. Size of segregation 2 x 1 cm. Komsomolskoye deposit. Sample of the Fersman Mineralogical Museum. Photo M.B. Leibov

Photo 3. Crystal of green beryl from schist, site #2. Size of crystal 9 x 5 mm. Specimen from A.A. Chernikov's collection. Photo M.B. Leibov

Photo 4. Emerald in quartz.
a) Size 3 x 2 cm. Sample of M.D. Dorfman's collection.
b) Size 6 x 4 cm. Sample #3533 of V.I. Stepanov's collection in the Fersman Mineralogical Museum. Photo M.B. Leibov

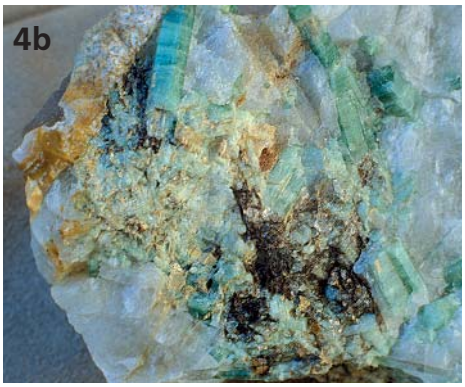

Photo 5. Change of color in emerald along the crystal. Crystal length 1.5 cm. Sample ? 3533 of V.I. Stepanov's collection of the Fersman Mineralogical Museum. Photo M.B. Leibov

Photo 6. Green beryl with change of transparency from opaque through translucent to transparent emerald green color. A.A. Chernikov's samples.
a) Crystal of beryl is crushed and healed by quartz. Length of crystal 1,6 cm
b) Crystals are crushed. Photo M.B. Leibov

Photo 7. Phenakite crystal. Size 0,9 x 0,8 cm. Site # 2 in the endocontact of Kuu granite massif. A.A. Chernikov's sample. Photo M.R. Kalamkarov

Photo 8. Phenakite replaced by bertrandite. Size 1 x 0,8 cm. Site # 2. Sample from A.A. Chernikov's collection. Photo M.R. Kalamkarov

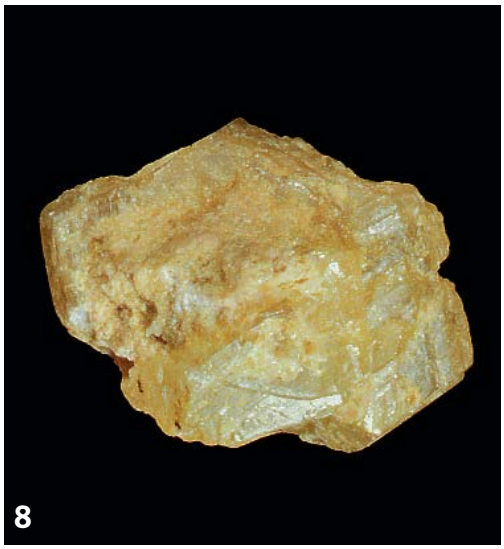

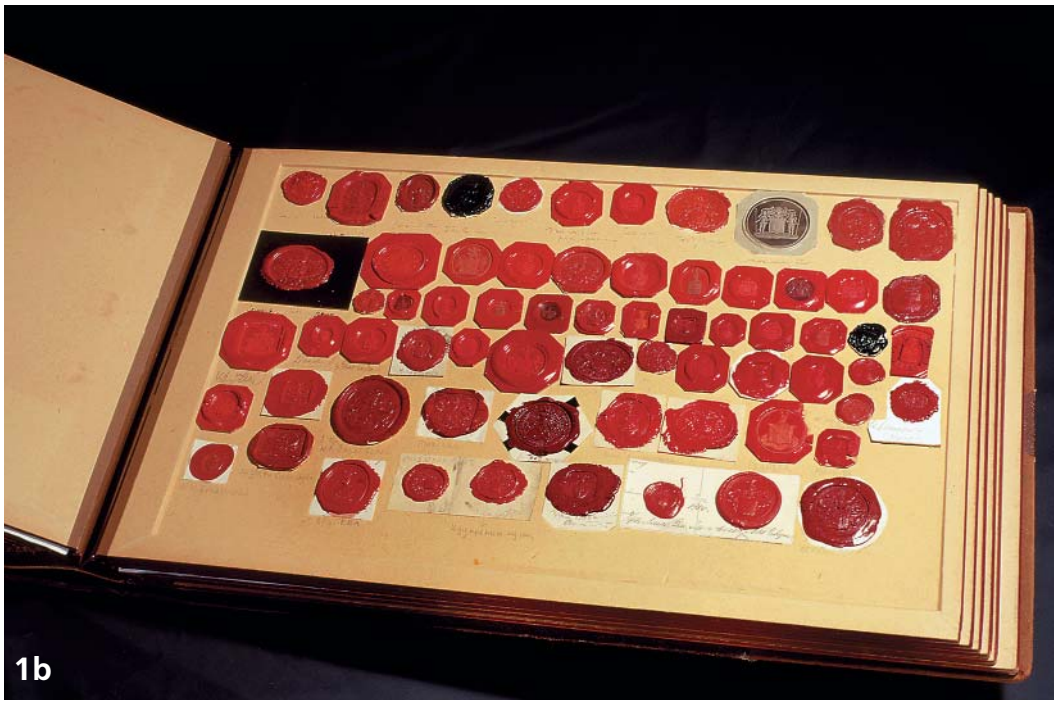

Photo 1(a, b). An album with the Faberge seal offprints. FMM.
Photo Michael A. Kalamkarov

Photo 2. Faberge cut gems. FMM.
Photo Michael A. Kalamkarov

Photo 3. Cut topazes, Faberge. FMM.
Photo Michael A. Kalamkarov

4

5

Photo 4. A vase a la Renaissance. Rock crystal, gilded silver, enamel, and garnets. Hallmark: H. Vigsrtoem. Height 20 cm. FMM, ID 2724. Photo Michael Leibov

Photo 5. A writing set (jade and silver). Hallmark: A. Hallstroem. FMM, ID 2300—2308. Photo Michael A. Kalamkarov

Photo 6. A liana-wound pine (jade, marble onyx, bowenite, emeralds, gold, enamel). Hallmark: F. Afanassiev. Height 11.5 cm. FMM, ID 2406. Photo Michael A. Kalamkarov

Photo 7. A mushroom (a matchbox) (belorechensk quartzite, silver). Hallmark: Yu. Rappoport. Size 17×17×17 cm. FMM, ID 7785. Photo Michael A. Kalamkarov

Photo 8. A cup (moss agate, gilded silver). Hallmark: M. Perkhin. FMM, ID 1756. Photo Michael A. Kalamkarov

Photo 9. A reserve regiment soldier, 1914. Jasper, calcite, flint, silver. Designed by G.K. Savitsky, performed by P.M. Kremlyov (1915). Height 15 cm. FMM, ID 2571. Photo Michael A. Kalamkarov

Photo 10. An ice carrier. Jasper, cacholong, jade, lazurite, serpentinite, quartz, and silver. Designed by G.K. Savitsky. Height 18 cm. FMM, ID 2570. Photo Michael A. Kalamkarov

Photo 11. An ice carrier. Quartz and silver. Hallmark: Ya. Armfelt. Height 18 cm. FMM, ID 7782 Photo Michael A. Kalamkarov

Photo 12. A lion. Bowenite (New Zealand). Height 21 cm. FMM, ID 1616. Photo Michael A. Kalamkarov

Photo 13. A baby elephant and his mother. Bowenite (New Zealand), rubies, and gold. Height 2.5 and 7.5 cm. IDs 1762 and 1761. Photo Michael A. Kalamkarov

11

12

13

Photo 14. A mouse. Rock crystal, rubies, and gold. Height 4.5 cm. FMM, ID 1757. Photo Michael A. Leibov

Photo 15. Geese. Rock crystal, diamonds, rubies, and gold. Height 8 cm. FMM, ID 1617. Photo Michael A. Leibov

Photo 16. A snail. Jade and obsidian. Dimensions 5×3 cm. FMM, ID 1748. Photo Michael A. Leibov

Photo 17. An owl. Granite 2.5 cm. FMM, ID 1602. Photo Michael A. Kalamkarov

Photo 18. A cup. Agate (Saxony). Diameter 10 cm. FMM, ID 1524. Photo Jeff Scovill

16

17

18

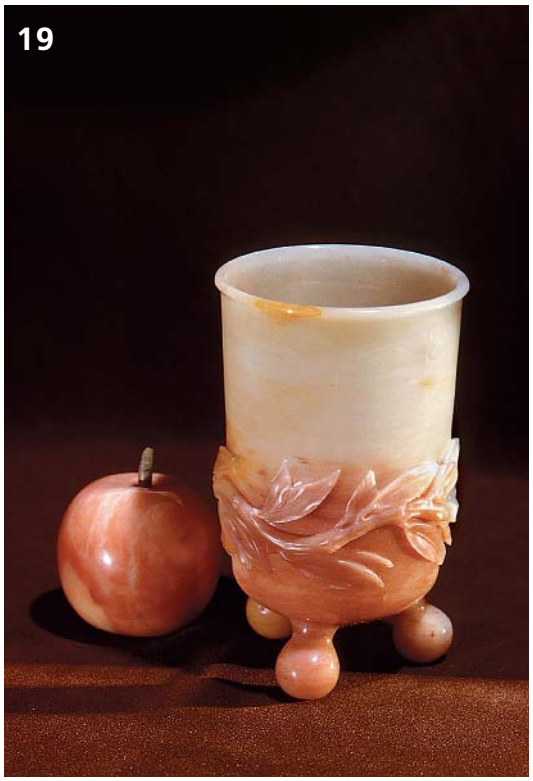

19

20

21

Photo 19. A vase and an apple. Belorechensk quartzite (Altai, Russia). IDs 1776 and 1777. Photo Michael A. Kalamkarov

Photo 20. A peach (a flask for glue). Bowenite (New Zealand). Height 10 cm. FMM, ID 1584. Photo Michael A. Kalamkarov

Photo 21. A bowl and a turret (Siamese) Chlorite schist. Diameter 18 cm. FMM, ID 1614. Photo Michael A. Kalamkarov

Photo 22. Sweet peas in a vase. Rhodonite, Belorechensk quartzite, jade, rock crystal. Height 19 cm. FMM, ID 2354 and 2530. Photo Michael A. Leibov

Photo 23. A little trough. Black jade, K. Werfel's workshop. Size 10×10 cm. FMM, ID 1744. Photo Michael A. Leibov

Photo 24. A seal. Lazurite. Height 8.5 cm. FMM, ID 4153. Photo Michael A. Leibov

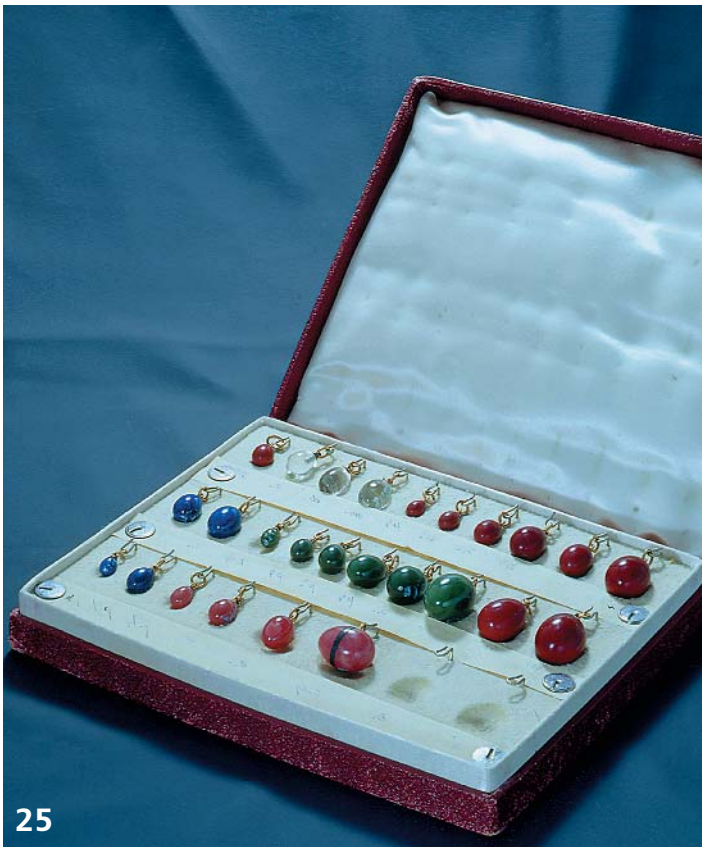

Photo 25. Easter eggs. Purpurine, rock crystal, lazurite, and rhodonite. Dimensions vary from 0.8 to 1.6 cm. FMM, ID 3728. Photo Michael A. Kalamkarov

Photo 26. A seal. Vein quartz/syenite. Height 8.5 cm. FMM, ID 4169. Photo Michael A. Kalamkarov

Photo 27. A plate and eggs. Purpurine. Eggs size 0.8—1.6 cm. FMM. Photo Michael A. Kalamkarov

Photo 28. A box with the gold sand samples from the Nerchinsk placer mines (1881). Dimensions 36x30x6 cm. a) Fragment of top cover; FMM, ID 7827. Photo Michael A. Leibov

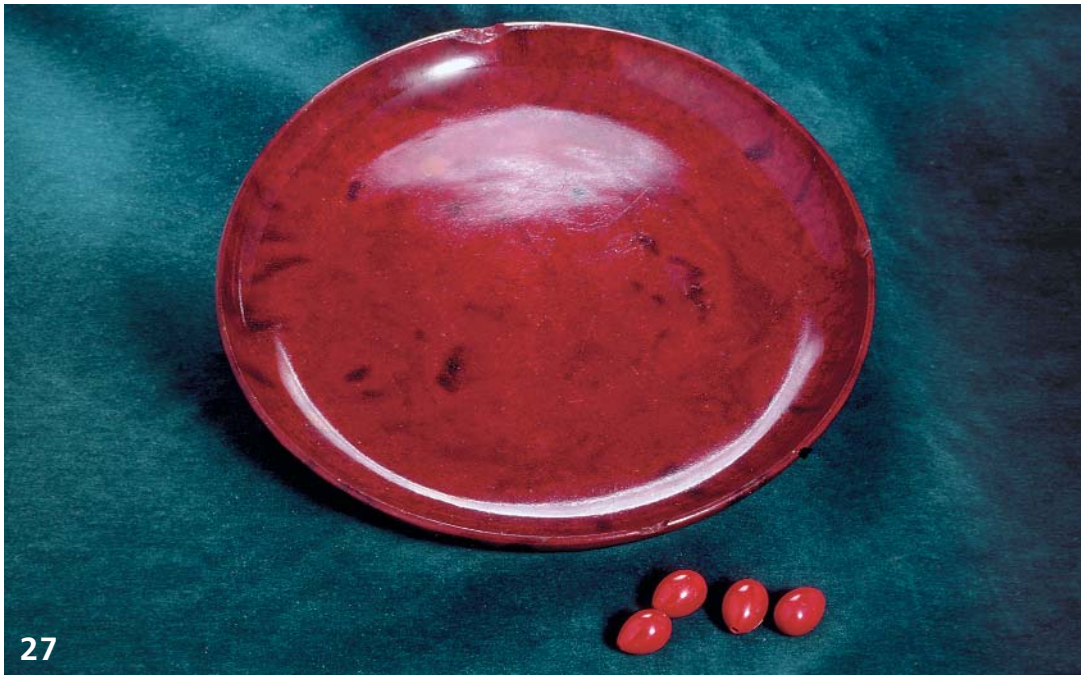

28

28a

Photo 29. A sketch of an Easter egg (1917). T.F. Faberge's archive

Photo 30. Tsesarevich (crown prince) Alexei: an Easter egg (1917). Rock crystal and glass. Height 18 cm. FMM, ID 2723. Photo Michael A. Leibov


1a


1b


1c

Photo 2. Ts'ung (cong) tubes (Debain-Francfort, 2002)

Photo 3. Neolithic bi disks. Massive jade of uneven color. Punctures are discernible at the top (Laufer, 1912)

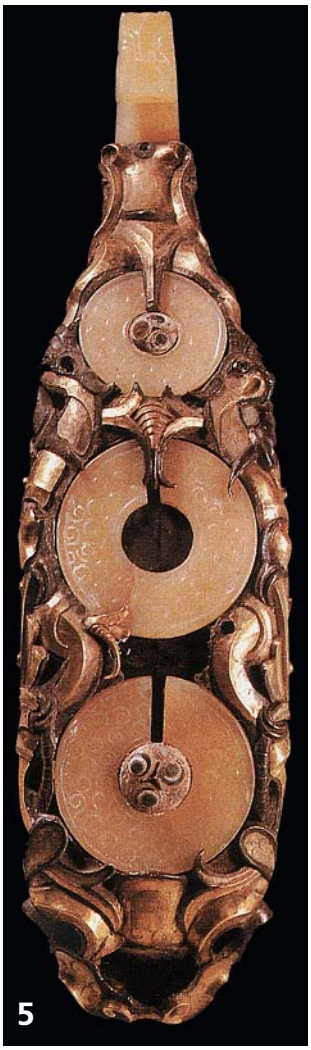

Photo 4. Chou dynasty: bi disks as ceremonial articles. A pendant with the bi disks (Debain-Francfort, 2002)

Photo 5. A buckle adorned with the bi disks. The Chou dynasty (Debain-Francfort, 2002)

Photo 6. Disk bi, the Han epoch (The golden age..., 1999)


7


8


9

1. *Quartz. The druze of crystals about 4 cm long colored by hematite inclusions. 2-nd Sovetskiy mine, Dal'negorsk, Primorskiy Kray, Russia. Purchase. Size 13 cm. FMM, #90050.*

2. *Hematite. A Pseudomorph after skeletal crystal of magnetite. Patagonia, Agentina. W. Larson donation. Size 7 cm. FMM, #90857.*

3. *Hematite. Pseudomorph after skeletal crystal of magnetite. Patagonia, Agentina. Purchase. Size 9 cm. FMM, #91086.*

Photo Natalia Pekova

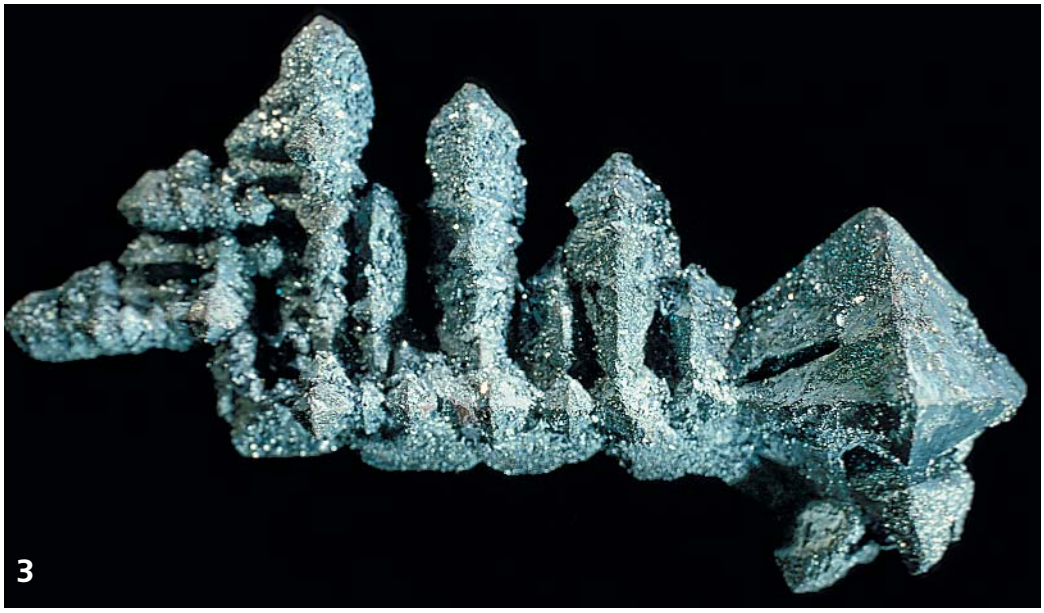

4. *Fluorapatite. Pegmatite #66, Akzhailyau, Tarbagatai, East Kazakhstan. Purchase. Size 9 cm. FMM, #91406.*
5. *Fluorapatite. Snezhinsk, Chelyabinskaya oblast', South Urals, Russia. Purchase. Size 11 cm. FMM, #91379.*
6. *Holfertite. Yellow needle pierced through red beryl crystal (bixbite). With hematite on riolite. Starvation Canyon, Thomas Range, Utah, USA. Collected by Museum staff. Beryl crystal size is about 0.5 cm. FMM, #91372.*
7. *Hilgardite-1A. Geode with crystals up to 1 cm.*
   a) Fragment with crystals
   b) Common view
   Boulby mine, North Yorkshire, Great Britain. Exchange. Size 11 cm. FMM, #91148.

Photo Natalia Pekova

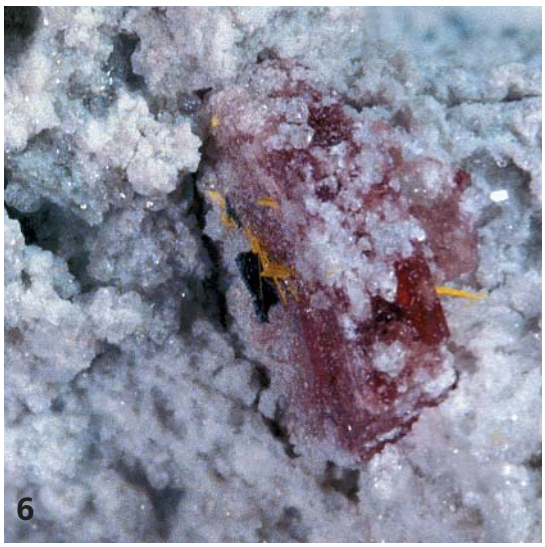

FIG. 1. Spiral crystal of malachite. Tirol, Austria. Photo Rainer Bode. Under the permission of «Mineralien Welt»

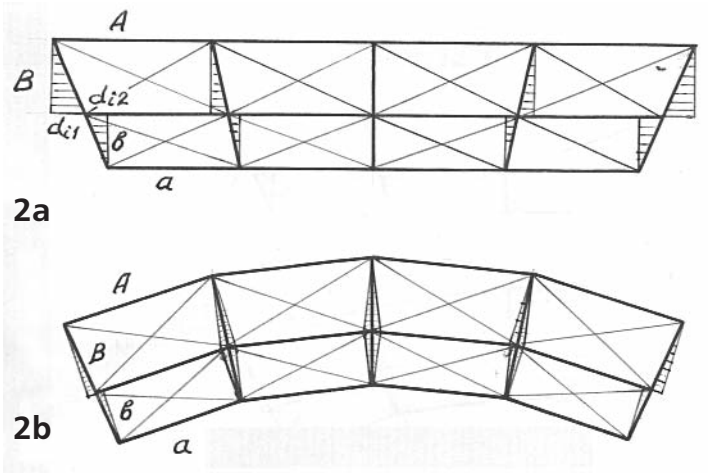

FIG. 2. Fragment of mixed crystal structure (explanation in text)

FIG . 3. Crystal of the manganous calcite, width 12 cm; Dalnegorsk, Primorski Krai. Photo of the author


AFS
10000
AFGHAN POST 1999

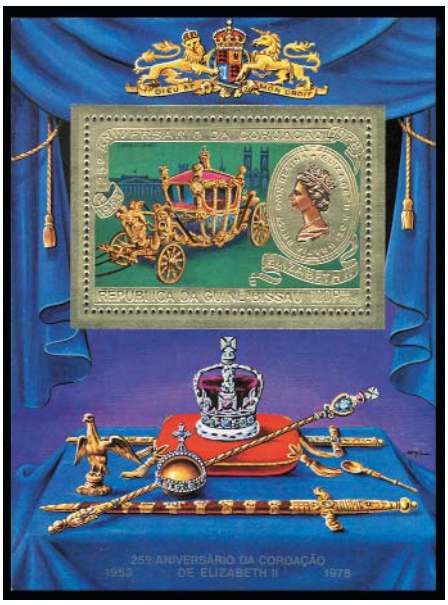
REPUBLICA DA GUINE-BISSAU
25º ANIVERSÁRIO DA CORÔAÇÃO
DE ELIZABETH II
1953
1978


500Sh.So. SOMALI REPUBLIC
POST 1997
Diamond


ประเทศไทย THAILAND
DIAMOND


3.00
DIAMONDS יהלומים
MILLENNIUM
ISRAEL
AIR MAIL · EXPORT
ישראל


BELGIË · BELGIQUE
3F + 1F


4d
GHANA


Sierra Leone
LAND OF
IRON & DIAMONDS
POSTAGE
5c


ANGOLA
CORREIOS
1980
DIAMANTE
16.00


Minerals of Tanzania
Diamonds
40/-
Tanzania


St. Christopher
Nevis
Anguilla
55c
THE HEAD OF SCEPTRE WITH CROSS
SILVER JUBILEE

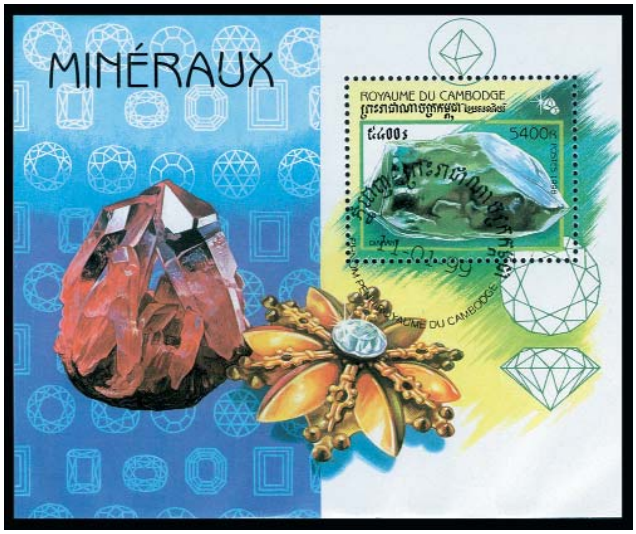
MINÉRAUX
ROYAUME DU CAMBODGE
5400R


BELIZE
E R
$5


1961
1966
REPUBLIC OF
SOUTH AFRICA
1c


REPUBLIQUE FRANÇAISE
70
CHARTE EUROPEENNE DE L'EAU

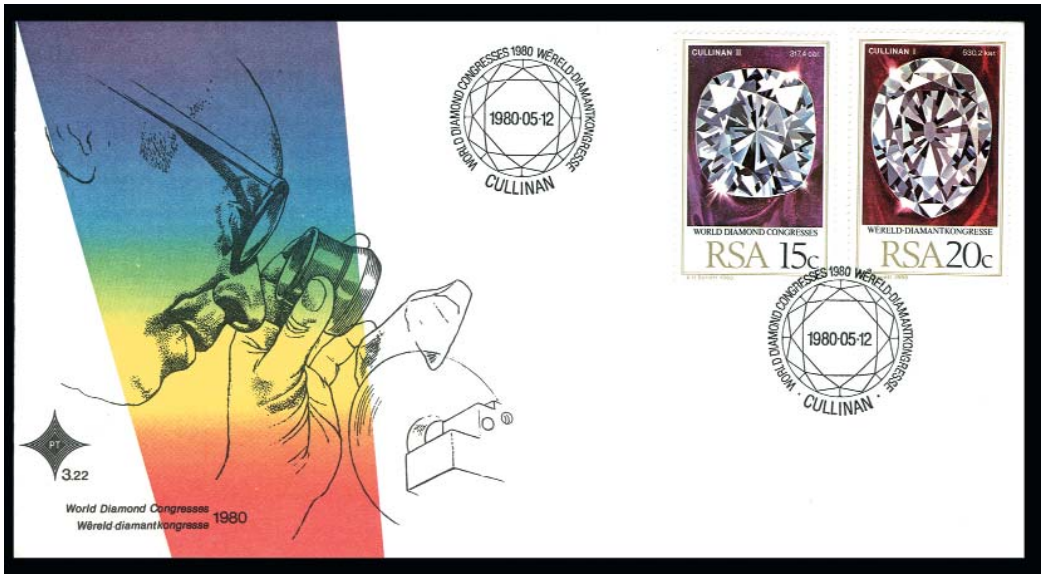
WORLD DIAMOND CONGRESSES 1980 WERELD-DIAMANTKONGRESSE
1980-05-12
CULLINAN
CULLINAN II
CULLINAN I
WORLD DIAMOND CONGRESSES
WERELD-DIAMANTKONGRESSE
RSA 15c
RSA 20c
3.22
World Diamond Congresses
Wereld diamantkongresse 1980


МЕЖДУНАРОДНЫЙ КОНГРЕСС ПО ОБОГАЩЕНИЮ ПОЛЕЗНЫХ ИСКОПАЕМЫХ
VIII
ЛЕНИНГРАД-1968
ПОЧТА
6к СССР


SIERRA LEONE
Land of Iron & Diamonds
POSTAGE
3½c
MORE GREAT GEM DIAMONDS ARE FOUND IN SIERRA LEONE THAN ANY OTHER COUNTRY


LESOTHO BROWN DIAMOND
Lesotho
5c

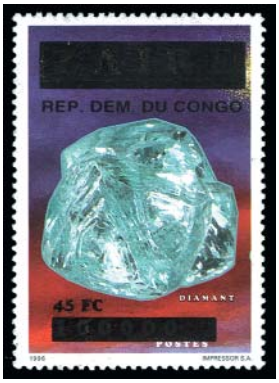
REP. DEM. DU CONGO
45 FC
DIAMANT
POSTES


GIBRALTAR
E R
International Youth Year
20p


PILIPINAS
U.P.
DIAMOND
JUBILEE
YEAR
1983
P1.20


АЛМАЗНЫЙ ФОНД СССР
БРОШЬ «РОЗА»
1971
ПОЧТА СССР
20к


АЛМАЗНЫЙ ФОНД СССР
АЛМАЗ «ШАХ»
1971
ПОЧТА СССР
10к


АЛМАЗНЫЙ ФОНД СССР
БУКЕТ НАРЦИССОВ
1971
ПОЧТА СССР
10к